REMARKS

No claims are being amended, added or cancelled. Claims 1-2, 4-11, 14-19, 21-22 and 27-28 are pending in this application.

Electrochemical cell or fuel cell background

A fuel cell catalytically converts the chemical energy of a supplied fuel and a supplied oxidizer into electrical energy. As discussed in Applicants' paragraph 2 one common type of fuel cell is a proton exchange membrane (PEM) fuel cell. The PEM fuel cell contains a membrane electrode assembly (MEA) provided between two flow field or bipolar plates. Gaskets are used between the bipolar plates and the MEA to provide seals thereat. Fuel cells include catalysts to facilitate the conversion of chemical energy into electrical energy. Since an individual PEM fuel cell typically provides relatively low voltage or power, multiple PEM fuel cells are stacked to increase the overall electrical output of the resulting fuel cell assembly. Sealing is also required between the individual PEM fuel cells in the stack.

Fuel cell performance and life can be degraded by a variety of contaminants. Some contaminants can substantially degrade fuel cell performance at part per billion impurity levels.[1] Fuel cell contaminants can come from the fuel or oxidant supply; from corrosion products of metal fuel cell components; and from the non-metallic gaskets and materials used between fuel cell components to seal the cells. Contamination and subsequent fuel cell degradation has been a problem for many years and continues to be a problem at the present time.[2] There are ongoing studies to find and eliminate sources of fuel cell contamination.[3]

---

[1] Garzon, F.H. et al; *The impact of impurities on long term PEMFC performance*; presentation preprint for 216th ECS Meeting, Vienna Austria, (October 2009).

[2] The attached exhibits all discuss fuel cell contamination and span the time frame from 2001 to 2009. Cheng, X. et al; *A review of PEM hydrogen fuel cell contamination, . . .*; Journal of Power Sources; 165, 2, 739-756, (March 2007) states that over 150 articles on the subject of fuel cell contamination were reviewed.

[3] Molter, Trent M.; *The effects of impurities on fuel cell performance and durability*; (May 2007). *Effects of fuel and air impurities on PEM fuel cell performance*; 2008 DOE

Some known contaminants include silicon[4], inorganic and metallic cations[5,6,7,8,9] sulfur[10], ammonia[11] and amines[12,13,14]. Fuel cell gaskets[15] and seals[16] have been found to be a source of fuel cell contaminants.

Fuel cells remain expensive to buy and replace and have too short a working life to be practical for widespread energy generation. Contamination of fuel cells shortens their life and requires premature replacement or repair of the cells, thereby raising the cost of using the cells. Thus, any steps to control fuel cell contamination and extend fuel cell life are very desirable and the goal of ongoing research.

Hydrogen Program Review; presented by Fernando Garzon, Los Alamos National Laboratory, (June 2008).

[4] Schulze, M. et al; *Degradation of Sealings for PEFC test cells . . .*; Journal of Power Sources; 127, 222-229 (2004).

[5] St-Pierre, Jean, et al.; *Successful Demonstration of Ballard PEMFCS . . .*; Journal of New Materials for Electrochemical Systems; 5, 263-271 (2002).

[6] Kelly, M.J. et al; *Conductivity of polymer electrolyte membranes . . .*; Solid State Ionics; 176, 25-28, 2111-2114 (August 2005).

[7] Cheng, X. et al; *A review of PEM hydrogen fuel cell contamination, . . .*; Journal of Power Sources; 165, 2, 739-756, (March 2007).

[8] Molter, Trent M.; *The effects of impurities on fuel cell performance and durability*; (May 2007).

[9] Wu, J. et al; A review of PEM fuel cell durability: . . .; Journal of Power Sources; 184, 105-119, 107, (June 2008).

[10] Molter, Trent M.; *The effects of impurities on fuel cell performance and durability*; (May 2007).

[11] Zhang, X. et al; *Contamination of membrane-electrode assemblies by ammonia . . .*; presentation preprint for 216th ECS Meeting, Vienna Austria, (October 2009).

[12] Privette, R.M. et al; *2.5 MW PEM fuel cell system for Navy ship service power*; paper presented at the 1999 Review Conference on Fuel Cell Technology (1999).

[13] Hoffman, Donald; *Marine Fuel Cells*; Marine Vessel and Air Quality Conference; February (2001).

[14] WO 02/084099; *Filter Assemblies and Systems for Intake Air for Fuel Cells*; pp. 25, lines 6-9, (October 2002).

[15] Cleghorn, S.J.C. et al; *A polymer electrolyte fuel cell life test . . .*; Journal of Power Sources; 158, 446-454, 453 (2006).

1. **Applicant's response to the rejection of claims 1-2, 4-11, 17, 21-22 and 27-28 under 35 U.S.C. §103(a).**

Claims 1-2, 4-11, 17, 21-22 and 27-28 were rejected under 35 U.S.C. §103(a) as allegedly being unpatentable over U.S. Patent No. 6,080,503 to Schmid et al. in view of U.S. Patent Publication No. 2003/0199652 to Deviny et al for the reasons given in Point 3.

a) **The rejection is improper as it lacks the predictability and reasonable expectation of success required for a prima facie obviousness rejection.**

In discussing predictability, the courts have recognized the general unpredictability of the chemical arts. "In the field of chemistry generally, there may be times when the well-known unpredictability of chemical reactions will alone be enough to create reasonable doubt as to the accuracy of a particularly broad statement put forward as enabling support for a claim. In re Marzocchi, 169 USPQ 367, 368-370 (CCPA 1971). The principle applies most often to the less predictable fields, such as chemistry, where minor changes in a product or process may yield substantially different results. In re Soni, 54 F.3d 746, 750 (Fed. Cir. 1995).

"To the extent an art is unpredictable, as the chemical arts often are, KSR's focus on these "identified, predictable solutions" may present a difficult hurdle because potential solutions are less likely to be genuinely predictable." Eisai Co. v. Dr. Reddy's Labs., Ltd, 533 F.3d 1353 (Fed. Cir. 2008). The prior art can be modified or combined to reject claims as *prima facie* obvious as long as there is a reasonable expectation of success. MPEP §2143.02. Predictability of results in combining references to arrive at a solution, and therefore a reasonable expectation of success in achieving those results, is one important requirement for a prima facie obviousness rejection. This requirement is mandated by both the Courts and by the Patent Office.

---

[16] Schulze, M. et al; *Degradation of Sealings for PEFC test cells . . .*; Journal of Power Sources; 127, 222-229 (2004).

At the time of Applicants' invention contamination of fuel cells was a known problem. At the time of Applicants' invention some known fuel cell contaminants included metal cations and ammonium compounds. Multiple references teach that amines are known or suspected fuel cell contaminants. See Privette, R.M. et al; *2.5 MW PEM fuel cell system for Navy ship service power*; Hoffman, Donald; *Marine Fuel Cells*; and WO 02/084099; *Filter Assemblies and Systems for Intake Air for Fuel Cells*, pp. 25, lines 6-9. However, as discussed above there are continuing long term studies by Universities and U.S. Government laboratories to research the effects of contaminants in fuel cells, identify fuel cell contaminants and find the sources of those contaminants. Thus, at the time of Applicants' invention the existence of the fuel cell contamination problem was known and some contaminants, such as amines, and some contamination sources, such as seals, were identified; but a complete understanding of the identity and sources of fuel cell contamination was not known.

Deviny teaches the use of complexed initiator systems including a complexed initiator component and a carboxylic acid decomplexer. (abstract) The "initiator component" typically comprises an organoborane amine complex and an optional diluent. When mixed with the polymerizable composition, the decomplexer in the polymerizable composition liberates the initiator (e.g., organoborane) from the complexer (e.g., amine), enabling polymerization of the monomer to be initiated. (0041) The decomplexer is "capable of" forming an ionic bond with the amine cation of the organoborane amine complex during liberation. (0047) There is no teaching or suggestion that all of the liberated amine cations are ionically bonded to the complexer. There is no teaching or suggestion that the weak ionic bond between the decomplexer and amine cation is permanent in the wet environment of a fuel cell (the waste products of a fuel cell are water) or that the weakly ionically bonded amine complex will not poison a fuel cell catalyst or contaminate a fuel cell.

A skilled person at the time of Applicants invention would know that fuel cells are expensive and would strive to maximize the life of a fuel cell. This would

12

include avoiding use of materials, such as amines, known or suspected to contaminate fuel cells and shorten their life. Fuel cell seals were also a known source of fuel cell contaminants. A skilled person at the time of Applicants' invention would have no expectation of success in maximizing fuel cell life by using amines, including the liberated amine cations and amine salts of the Deviny boron initiators, as a component of the fuel cell seal. Claims 1-2, 4-11, 17, 21-22 and 27-28 are not obvious and are patentable for at least this reason.

b) There is no motivation to modify the references as proposed in the rejection.

Thus, in cases involving new chemical compounds, it remains necessary to identify some reason that would have led a chemist to modify a known compound in a particular manner to establish prima facie obviousness of a new claimed compound. Takeda Chem. Indus. v. Alphapharm Pty., Ltd., 492 F.3d 1350, 1356 (Fed. Cir. 2007). "In the same way, when the prior art teaches away from the claimed solution as presented here . . ., obviousness cannot be proved merely by showing that a known composition could have been modified by routine experimentation or solely on the expectation of success; it must be shown that those of ordinary skill in the art would have had some apparent reason to modify the known composition in a way that would result in the claimed composition." Ex parte Whalen II, pp. 16, appeal 2007-4423 (BPAI 2008). "The [KSR] Court did not, however, discard the TSM test completely; it noted that its precedents show the invention 'composed of several elements is not proved obvious merely by demonstrating that each of its elements was, independently, known in the prior art.'" Ex parte Whalen II, pp. 15, appeal 2007-4423 (BPAI 2008)

As discussed above at the time of Applicants' invention the existence of the fuel cell contamination problem was known and some contaminants (such as metal cations, ammonium compounds and amines) and some contamination sources (such as seals) were identified; but a complete understanding of the identity and sources of fuel cell contamination was not known.

As discussed above Deviny teaches the use of complexed amine-organoborane initiator systems wherein the organoborane portion of the complex must be liberated from the amine portion of the complex to allow the freed organoborane to initiate polymerization.

A skilled person at the time of Applicants invention would know that fuel cells are expensive and would strive to maximize the life of a fuel cell. This would include avoiding use of materials, such as amines, known or suspected to contaminate fuel cells and shorten their life. Fuel cell seals were also a known source of fuel cell contaminants. A skilled person at the time of Applicants' invention would have no motivation to use materials that are known fuel cell contaminants (liberated amine cations and weakly bonded amine complexes) in a fuel cell location known to be a source of contamination (seals). Claims 1-2, 4-11, 17, 21-22 and 27-28 are not obvious and are patentable for at least this reason.

c) The art teaches away from the proposed combination.

A "reference will teach away if it suggests that the line of development flowing from the reference's disclosure is unlikely to be productive of the result sought by the Applicant." Winner v. Wang, 202 F.3d 1340 (Fed Cir. 2000) citing Gurley at 553. "One important indicium of nonobviousness is 'teaching away' from the claimed invention by the prior art." In re Braat, 16 USPQ2d 1813, 1814 (Fed. Cir. 1990). We have noted . . . as a useful general rule that references that teach away cannot serve to create a prima facie case of obviousness. McGinley v. Franklin Sports, Inc., 262 F.3d 1339 (Fed. Cir. 2001). A prima facie case of obviousness can be rebutted if the applicant . . . can show that the art taught away from the claimed invention in any material respect. In re Haruna, 249 F.3d 1327 (Fed. Cir. 2001). A reference that teaches away from a claimed invention does not provide the suggestion or motivation needed to anticipate or make obvious a claimed invention. In fact, the courts have stated that a reference that teaches away from a claimed invention is an indication of

14

the nonobviousness of that invention.

The rejection proposes using the Deviny organoborane complexes as a reaction initiator. As discussed above Deviny teaches the use of complexed amine-organoborane initiator systems wherein the organoborane portion of the complex must be liberated from the amine portion of the complex to allow the freed organoborane to initiate polymerization.

At the time of Applicants' invention fuel cells are expensive and maximizing fuel cell life is, and continues to be, a desirable objective. The art generally teaches that fuel cell contaminants undesirably shorten fuel cell life and should be avoided in fuel cell use. Multiple references teach that amines are actual or suspected fuel cell contaminants that can shorten fuel cell life. The art teaches against use of materials that are known fuel cell contaminants (liberated amine cations and weakly bonded amine complexes) in a fuel cell location known to be a source of contamination (seals). Claims 1-2, 4-11, 17, 21-22 and 27-28 are not obvious and are patentable for at least this reason.

2. Applicant's response to the rejection of claims 14-16 under 35 U.S.C. §103(a).

Claims 14-16 were rejected under 35 U.S.C. §103(a) as allegedly being unpatentable over Schmid et al. in view of Deviny et al. as applied to claims 1-2, 4-11, 17, 21-22 and 27-28 and in further view of European Patent No. 1201722 to Kneafsey et al for the reasons given in point 4. Schmid, directed to fuel cell sealants, does not teach or suggest boron initiators. Deviny and Kneafsey do not teach or suggest use of organoborane initiators in fuel cells.

a) Applicants' claims 14-16

Applicants' claims 14-16 depend from claim 1. Claim 1 recites the presence of a cured sealant composition comprising the reaction products of a

15

polymerizable component and a boron-containing initiator. Claim 14 recites that the boron-containing initiator comprises an alkyl borohydride. Claim 15 recites that the boron-containing initiator comprises specific alkyl borohydrides having a specific structure and including M^+. M^+ is a metal ion, an alkyloxy metal ion, an alkali metal ion, a quaternary ammonium cation, and combinations thereof. Claim 16 recites that the boron-containing initiator comprises specific alkyl borohydrides having a specific structure and including M. M is a M is a Group IA metal, Group IIA metal, ammonium, tetraalkylammonium, phosphonium, or metal complex.

b) The rejection is improper as it lacks the predictability and reasonable expectation of success required for a prima facie obviousness rejection.

At the time of Applicants' invention contamination of fuel cells was a known problem. At the time of Applicants' invention multiple references taught that metal cations and ammonia were known or suspected fuel cell contaminants. See St-Pierre, Jean, et al.; *Successful Demonstration of Ballard PEMFCS . . .*; Kelly, M.J. et al; *Conductivity of polymer electrolyte membranes . . .*; Cheng, X. et al; *A review of PEM hydrogen fuel cell contamination, . . .*; Molter, Trent M.; *The effects of impurities on fuel cell performance and durability*; Wu, J. et al; *A review of PEM fuel cell durability: . .* ; Zhang, X. et al; *Contamination of membrane-electrode assemblies by ammonia . . .* As discussed above amines were known or suspected fuel cell contaminants.

However, as discussed above there were, and still are, continuing long term studies by Universities and U.S. Government laboratories to research the effects of contaminants in fuel cells, identify fuel cell contaminants and find the sources of those contaminants. Thus, at the time of Applicants' invention the existence of the fuel cell contamination problem was known and some contaminants, such as metal cations, ammonia and amines, and some contamination sources, such as seals, were identified; but a complete understanding of the identity and sources of fuel cell contamination was not known.

As discussed above Deviny teaches the use of complexed amine-organoborane initiator systems wherein the organoborane portion of the complex must be liberated from the amine portion of the complex to allow the freed organoborane to initiate polymerization. Kneafsey teaches use of metal alkyl borohydrides (abstract).

A skilled person at the time of Applicants invention would know that fuel cells are expensive and would strive to maximize the life of a fuel cell. This would include avoiding use of materials, such as metal cations, amines and ammonia, known or suspected to contaminate fuel cells and shorten their life. A skilled person at the time of Applicants' invention would have no expectation of success in maximizing fuel cell life by using metal cations, amines and ammonia as a component of the fuel cell seal. Claims 14-16 are not obvious and are patentable for at least this reason.

c) **There is no motivation to modify the references as proposed in the rejection.**

As discussed above at the time of Applicants' invention the existence of the fuel cell contamination problem was known and some contaminants (such as metal cations, ammonium compounds and amines) and some contamination sources (such as seals) were identified; but a complete understanding of the identity and sources of fuel cell contamination was not known.

As discussed above Deviny teaches the use of complexed amine-organoborane initiator systems wherein the organoborane portion of the complex must be liberated from the amine portion of the complex to allow the freed organoborane to initiate polymerization. Kneafsey teaches use of metal alkyl borohydrides (abstract).

A skilled person at the time of Applicants invention would know that fuel cells are expensive and would strive to maximize the life of a fuel cell. This would include avoiding use of materials, such as metal cations, amines and ammonia, known or suspected to contaminate fuel cells and shorten their life. A skilled person at the time

17

of Applicants' invention would have no motivation to use metal cations, amines and ammonia in a fuel cell and especially in a fuel cell location known to be a source of contamination (seals). Claims 14-16 are not obvious and are patentable for at least this reason.

d) The art teaches away from the proposed combination.

As discussed above Deviny teaches the use of complexed amine-organoborane initiator systems wherein the organoborane portion of the complex must be liberated from the amine portion of the complex to allow the freed organoborane to initiate polymerization. Kneafsey teaches use of metal alkyl borohydrides (abstract).

At the time of Applicants' invention fuel cells are expensive and maximizing fuel cell life is, and continues to be, a desirable objective. The art generally teaches that fuel cell contaminants undesirably shorten fuel cell life and should be avoided in fuel cell use. Multiple references teach that metal cations, amines and ammonia are actual or suspected fuel cell contaminants that can shorten fuel cell life. The art teaches against use of materials that are known fuel cell contaminants (metal cations, amines and ammonia) in a fuel cell location known to be a source of contamination (seals). Claims 14-16 are not obvious and are patentable for at least this reason.

3. Applicant's response to the rejection of claim 18 under 35 U.S.C. §103(a).

Claim 18 was rejected under 35 U.S.C. §103(a) as allegedly being unpatentable over Schmid et al. in view of Deviny et al. as applied to claims 1-2, 4-11, 17, 21-22 and 27-28 and in further view of U.S. Patent Publication No. 2004/0010099 to Kneafsey et al for the reasons given in point 5. Schmid, directed to fuel cell sealants, does not teach or suggest boron initiators. Deviny and Kneafsey do not teach or suggest use of organoborane initiators in fuel cells.

a) Applicants' claim 18

Applicants' claim 18 depends from claim 1. Claim 1 recites the presence of a cured sealant composition comprising the reaction products of a polymerizable component and a boron-containing initiator. Claim 18 recites that the boron-containing initiator comprises a complex of an organoborane and polyaziridine having a specific structure.

b) The rejection is improper as it lacks the predictability and reasonable expectation of success required for a prima facie obviousness rejection.

At the time of Applicants' invention contamination of fuel cells was a known problem. At the time of Applicants' invention multiple references taught that inorganic and metal cations, ammonia and amines were known or suspected fuel cell contaminants. However, there were, and still are, continuing long term studies by Universities and U.S. Government laboratories to research the effects of contaminants in fuel cells, identify fuel cell contaminants and find the sources of those contaminants. Thus, at the time of Applicants' invention the existence of the fuel cell contamination problem was known and some contaminants, such as inorganic and metal cations, ammonia and amines, and some contamination sources, such as seals, were identified; but a complete understanding of the identity and sources of fuel cell contamination was not known.

As discussed above Deviny teaches the use of complexed amine-organoborane initiator systems wherein the organoborane portion of the complex must be liberated from the amine portion of the complex to allow the freed organoborane to initiate polymerization. Kneafsey teaches use of complexed organoborane-polyaziridine initiators (abstract). The polyaziridine cation must be liberated from the complex to allow the freed organoborane to initiate polymerization.

A skilled person at the time of Applicants invention would know that fuel cells are expensive and would strive to maximize the life of a fuel cell. This would

include avoiding use of materials, such as metal cations, amines, ammonia and chemically similar N atom containing cations, known or suspected to contaminate fuel cells and shorten their life. A skilled person at the time of Applicants' invention would have no expectation of success in maximizing fuel cell life by using metal cations, amines, ammonia and chemically similar N atom containing cations as a component of the fuel cell seal. Claim 18 is not obvious and patentable for at least this reason.

c) There is no motivation to modify the references as proposed in the rejection.

As discussed above at the time of Applicants' invention the existence of the fuel cell contamination problem was known and some contaminants (such as inorganic and metal cations, amines, ammonia and chemically similar N atom containing cations) and some contamination sources (such as seals) were identified; but a complete understanding of the identity and sources of fuel cell contamination was not known.

As discussed above Deviny teaches the use of complexed amine-organoborane initiator systems wherein the organoborane portion of the complex must be liberated from the amine portion of the complex to allow the freed organoborane to initiate polymerization. Kneafsey teaches use of complexed organoborane-polyaziridine initiators (abstract). The polyaziridine cation must be liberated from the complex to allow the freed organoborane to initiate polymerization.

A skilled person at the time of Applicants invention would know that fuel cells are expensive and would strive to maximize the life of a fuel cell. This would include avoiding use of materials, such as inorganic and metal cations, amines, ammonia and chemically similar N atom containing cations, known or suspected to contaminate fuel cells and shorten their life. A skilled person at the time of Applicants' invention would have no motivation to use inorganic and metal cations, amines, ammonia and chemically similar N atom containing cations in a fuel cell and especially

20

in a fuel cell location known to be a source of contamination (seals). Claim 18 is not obvious and patentable for at least this reason.

d) The art teaches away from the proposed combination.

As discussed above Deviny teaches the use of complexed amine-organoborane initiator systems wherein the organoborane portion of the complex must be liberated from the amine portion of the complex to allow the freed organoborane to initiate polymerization. Kneafsey teaches use of complexed organoborane-polyaziridine initiators (abstract). The polyaziridine cation must be liberated from the complex to allow the freed organoborane to initiate polymerization.

At the time of Applicants' invention fuel cells are expensive and maximizing fuel cell life is, and continues to be, a desirable objective. The art generally teaches that fuel cell contaminants undesirably shorten fuel cell life and should be avoided in fuel cell use. Multiple references teach that inorganic and metal cations, amines, ammonia and chemically similar N atom containing cations are actual or suspected fuel cell contaminants that can shorten fuel cell life. The art teaches against use of materials that are known fuel cell contaminants (inorganic and metal cations, amines, ammonia and chemically similar N atom containing cations) in a fuel cell location known to be a source of contamination (seals). Claim 18 is not obvious and patentable for at least this reason.

4. Applicant's response to the rejection of claim 19 under 35 U.S.C. §103(a).

Claim 19 was rejected under 35 U.S.C. §103(a) as allegedly being unpatentable over Schmid et al. in view of Deviny et al. as applied to claims 1-2, 4-11, 17, 21-22 and 27-28 and in further view of U.S. Patent No. 6,806,330 to Sonnenschein et al for the reasons given in point 6.

Applicants presume that the reference to U.S. Patent No. 6,803,330 in the rejection is a mistake and the correct Patent No. for Sonnenschein et al is 6,806,330.

a) Applicants' claim 19

Applicants' claim 19 depends from claim 1. Claim 1 recites the presence of a cured sealant composition comprising the reaction products of a polymerizable component and a boron-containing initiator. Claim 19 recites that the boron-containing initiator is a complex of trialkyl borane or alkyl cycloalkyl borane and an amine compound.

b) The rejection is improper as it lacks the predictability and reasonable expectation of success required for a prima facie obviousness rejection.

At the time of Applicants' invention contamination of fuel cells was a known problem. At the time of Applicants' invention some known fuel cell contaminants included metal cations and ammonium compounds. Multiple references teach that amines also known or suspected fuel cell contaminants. However, as discussed above there are continuing long term studies by Universities and U.S. Government laboratories to research the effects of contaminants in fuel cells, identify fuel cell contaminants and find the sources of those contaminants. Thus, at the time of Applicants' invention the existence of the fuel cell contamination problem was known and some contaminants, such as amines, and some contamination sources, such as seals, were identified; but a complete understanding of the identity and sources of fuel cell contamination was not known.

As discussed above Deviny teaches the use of complexed amine-organoborane initiator systems wherein the organoborane portion of the complex must be liberated from the amine portion of the complex to allow the freed organoborane to initiate polymerization. Sonnenschein teaches use of amine-organoborane complexes as polymerization initiators (abstract). The complexes dissociate when heated or decomplexed to provide organoborane and amine or ionically bonded amine-decomplexer salt. (Col. 3, Lines 12-27).

A skilled person at the time of Applicants' invention would know that fuel cells are expensive and would strive to maximize the life of a fuel cell. This would include avoiding use of materials, such as amines, known or suspected to contaminate fuel cells and shorten their life. Fuel cell seals were also a known source of fuel cell contaminants. A skilled person at the time of Applicants' invention would have no expectation of success in maximizing fuel cell life by using amines, including the liberated amine cations and weakly complexed amines of the Sonnenschein boron initiators, as a component of the fuel cell seal. Claim 19 is not obvious and is patentable for at least this reason.

c) There is no motivation to modify the references as proposed in the rejection.

As discussed above at the time of Applicants' invention the existence of the fuel cell contamination problem was known and some contaminants (such as metal cations, ammonium compounds and amines) and some contamination sources (such as seals) were identified; but a complete understanding of the identity and sources of fuel cell contamination was not known.

As discussed above Deviny teaches the use of complexed amine-organoborane initiator systems wherein the organoborane portion of the complex must be liberated from the amine portion of the complex to allow the freed organoborane to initiate polymerization. Sonnenschein teaches use of amine-organoborane complexes as polymerization initiators. The complexes dissociate when heated or decomplexed to provide organoborane and amine or ionically bonded amine-decomplexer salt.

A skilled person at the time of Applicants invention would know that fuel cells are expensive and would strive to maximize the life of a fuel cell. This would include avoiding use of materials, such as amines, known or suspected to contaminate fuel cells and shorten their life. Fuel cell seals were also a known source of fuel cell contaminants. A skilled person at the time of Applicants' invention would have no

23

motivation to use materials that are known fuel cell contaminants (amine cations) in a fuel cell location known to be a source of contamination (seals). Claim 19 is not obvious and patentable for at least this reason.

d) The art teaches away from the proposed combination.

The rejection proposes using the Sonnenschein organoborane complexes as a reaction initiator. As discussed above, Sonnenschein teaches use of amine-organoborane complexes as polymerization initiators. The complexes dissociate when heated or decomplexed to provide organoborane and amine or weakly, ionically bonded amine complex.

At the time of Applicants' invention fuel cells are expensive and maximizing fuel cell life is, and continues to be, a desirable objective. The art generally teaches that fuel cell contaminants undesirably shorten fuel cell life and should be avoided in fuel cell use. Multiple references teach that amines are actual or suspected fuel cell contaminants that can shorten fuel cell life. The art teaches against use of materials that are known fuel cell contaminants (amine cations) in a fuel cell location known to be a source of contamination (seals). Claim 19 is not obvious and patentable for at least this reason.

Space intentionally blank.

In summary, Applicant has addressed each of the rejections in the present Office Action. It is believed the application now stands in condition for allowance, and prompt favorable action thereon is respectfully solicited.

The Examiner is invited to contact Applicant's attorney if a conversation will hasten prosecution of this application. Applicant's undersigned attorney may be reached by telephone at (860) 571-2501, by facsimile at (860) 571-5028 or by email at james.piotrowski@us.henkel.com. All postal correspondence should be directed to the address given below.

Respectfully submitted,

Matthew P. Burdzy

Date: _August 24, 2009_
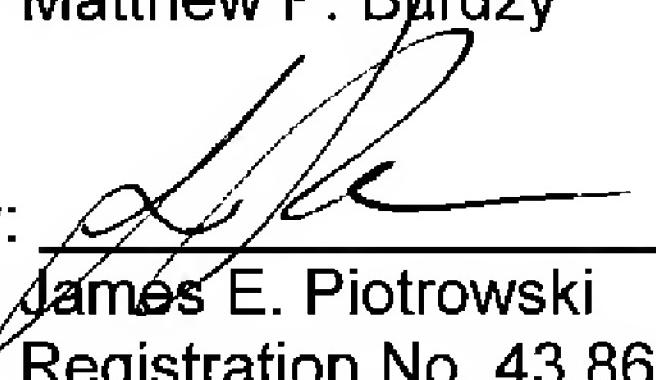
By: _____
James E. Piotrowski
Registration No. 43,860
Attorney for Applicant

HENKEL CORPORATION
Legal Department
One Henkel Way
Rocky Hill, CT 06067
860.571.2501 (Office)
860.571.5028 (Fax)

G:\Legal\Patents\LC Cases\LC-519-PCT-US\0809_Amendment.doc

25

Exhibits:

- Privette, R.M. et al; *2.5 MW PEM fuel cell system for Navy ship service power*, paper presented at the 1999 Review Conference on Fuel Cell Technology (1999).
- Hoffman, Donald; *Marine Fuel Cells*; Marine Vessel and Air Quality Conference; February (2001).
- WO 02/084099; *Filter Assemblies and Systems for Intake Air for Fuel Cells*; (October 2002).
- St-Pierre, Jean, et al.; *Successful Demonstration of Ballard PEMFCS . . .*; Journal of New Materials for Electrochemical Systems; 5, 263-271 (2002).
- Schulze, M. et al; *Degradation of Sealings for PEFC test cells . . .*; Journal of Power Sources; 127, 222-229 (2004).
- Kelly, M.J. et al; *Conductivity of polymer electrolyte membranes . . .*; Solid State Ionics; 176, 25-28, 2111-2114 (August 2005).
- Cleghorn, S.J.C. et al; *A polymer electrolyte fuel cell life test . . .*; Journal of Power Sources; 158, 446-454 (2006).
- Cheng, X. et al; *A review of PEM hydrogen fuel cell contamination, . . .*; Journal of Power Sources; 165, 2, 739-756, (March 2007).
- Molter, Trent M.; *The effects of impurities on fuel cell performance and durability*; (May 2007).
- Wu, J. et al; A review of PEM fuel cell durability: . . .; Journal of Power Sources; 184, 105-119, 107, (June 2008).
- *Effects of fuel and air impurities on PEM fuel cell performance*; 2008 DOE Hydrogen Program Review; presented by Fernando Garzon, Los Alamos National Laboratory, (June 2008).
- Zhang, X. et al; *Contamination of membrane-electrode assemblies by ammonia . . .*; presentation preprint for 216th ECS Meeting, Vienna Austria, (October 2009).
- Garzon, F.H. et al; *The impact of impurities on long term PEMFC performance*; presentation preprint for 216th ECS Meeting, Vienna Austria, (October 2009).
- *Fuel cell basics*; http://www.fctec.com/fctec_basics.asp (August 2009)

- Privette, R.M. et al; *2.5 MW PEM fuel cell system for Navy ship service power*, paper presented at the 1999 Review Conference on Fuel Cell Technology (1999).

2.5 MW PEM Fuel Cell System for Navy Ship Service Power

R. M. Privette, T. A. Flynn, M. A. Perna
McDermott Technology, Inc.

R. Holland, S. Rahmani, C. Woodburn
Ballard Power Systems

S. W. Scoles, R. C. Watson
BWX Technologies, Inc.

In 1997, the Office of Naval Research (ONR) initiated an advanced development program to demonstrate a ship service fuel cell power generation module. The ship service generator supplies the electrical power requirements of the ship. When completed, this program will provide the basis for new fuel cell-based ship service power system designs that will be a viable and attractive option for future U.S. Navy surface ships.

A ship service fuel cell (SSFC) power generation module possesses attractive characteristics for U.S. Navy and other marine vessels. Chief among them is a high system level efficiency that is achieved through the direct electrochemical conversion of fuel. The low acoustic and thermal signatures expected from these systems are also attractive benefits. Simplicity of design adds some additional benefit. Maintenance costs are expected to be low. The fuel cells and stacks themselves have no moving parts and require little or no maintenance. The system "balance-of-plant" which manages fuel, air, and exhaust has few moving parts and contributes to reduced maintenance resulting in cost savings to the Navy and enhanced ship effectiveness. Reduction of power system emissions has become an issue in many harbors throughout the world. Emissions of NOx, CO, and unburned hydrocarbon pollutants from the SSFC generator are reduced up to 95% compared to gas turbines or diesel engines. Finally, fuel cells are inherently modular and can be distributed throughout the ship in a configuration compatible with all-electric ship concepts, and enhanced survivability designs.

The ONR advanced development program currently consists of two phases. During Phase 1, competitive conceptual designs of 2.5 MW SSFC power plants are being prepared, along with critical component demonstrations designed to reduce development risk. The critical demonstrations include testing fuel cell cathode tolerance to salt laden air, military shock and vibration tests of cell hardware, and demonstration of reforming and fuel desulfurization technology using Navy logistic fuel. Phase 1 will be completed in 1999. Phase 2 of the development program, scheduled for completion in 2002, will result in a nominal 500 kW fuel cell ship service generator demonstration module to be constructed and tested in a laboratory setting.

This paper summarizes some of the Phase 1 efforts of a team consisting of McDermott Technology Inc., BWX Technologies, Ballard Power Systems, and Gibbs & Cox. Conceptual design and critical component testing activities are described for a 2.5 MW Proton Exchange Membrane (PEM) SSFC system.

The 2.5 MW SSFC system conceptual design criteria were as follows:

- provide 2.5 MW net electrical power at 450 VAC, 3 phase, 60 Hz;
- run on naval distillate fuel (NATO F-76);
- achieve minimum system level efficiency of 40% (based on lower heating value) at 50% of rated load;
- achieve system size and weight goals of 57 l/kW and 18 kg/kW, respectively;

- achieve estimated cost in production of $1500/kW;
- be developed using commercial or near-commercial technologies;
- be highly reliable and maintainable; and
- be self-contained with respect to water balance and energy balance.

These criteria were addressed through a conceptual design process consisting of trade-off studies, control system development, system layout, and other system level evaluations.

The baseline system concept is shown schematically in Figure 1. This system concept uses an autothermal reformer (ATR) based conceptually on a Defense Advanced Research Projects Agency (DARPA) and U.S. Army Research Office-funded, logistic fueled, adiabatic reformer designed and built by International Fuel Cells [1]. Downstream of the ATR is a series of components that clean up the reformate gas (remove CO and H_2S) before the hydrogen rich gas is sent to the fuel cell. The sulfur cleanup is accomplished by use of a set of cycling regenerable sorbent beds followed by a polishing sulfur sorbent bed. This desulfurization system is able to achieve 1 ppm of sulfur in the reformate gas. The CO is removed by water-gas shift in high and low temperature shift reactors followed by selective oxidation of CO over a precious metal catalyst. The spent fuel and air from the fuel cell are mixed and burned to drive a turbocompressor and recover compression work. The extensive heat exchanger network required to achieve system-wide water and energy balance is not shown in Figure 1.
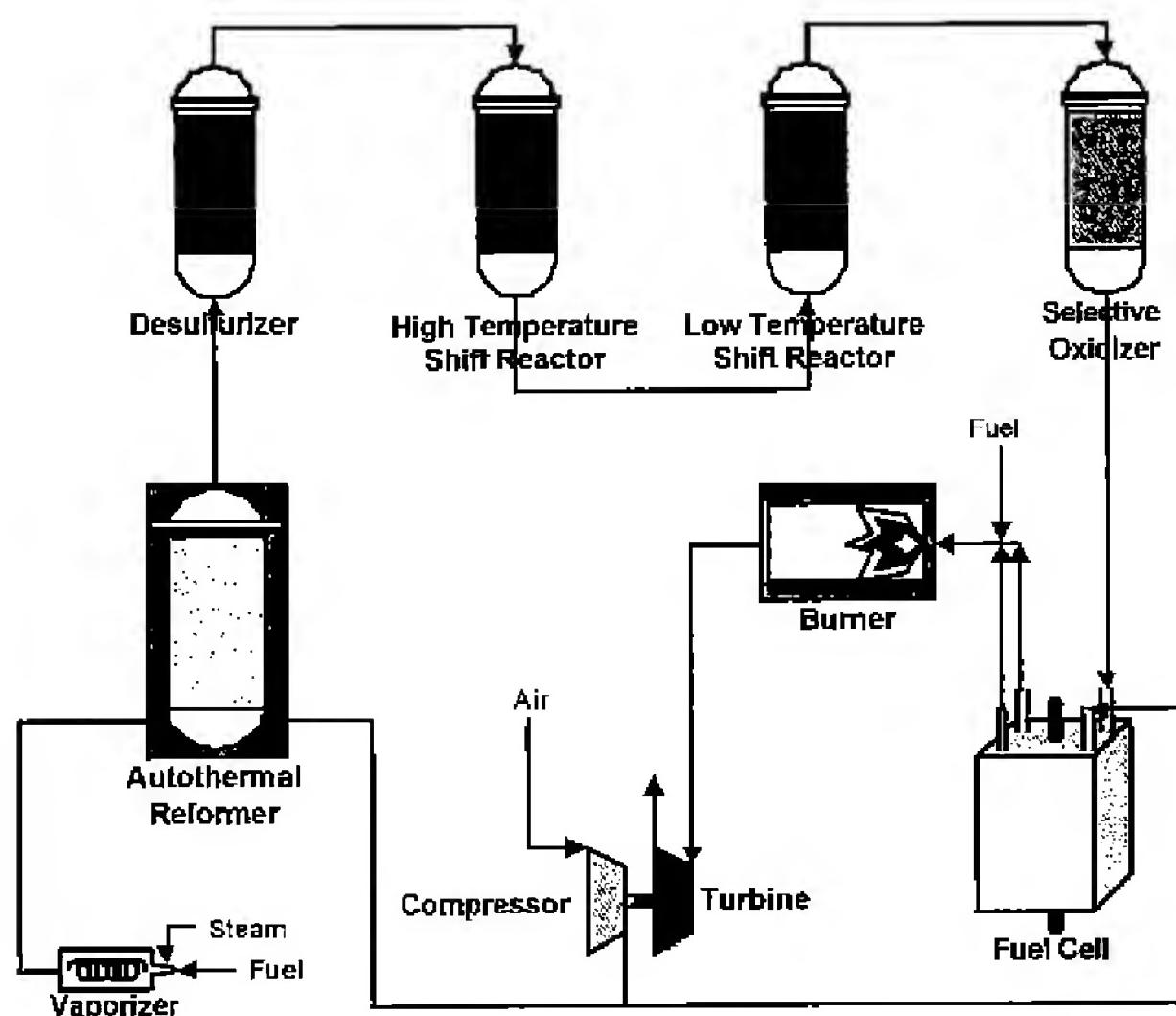
Figure 1. Simplified Process Diagram for the Baseline 2.5 MW Ship Service Fuel Cell Generator.

System physical layout began with the development of a system piping and instrumentation diagram. The component sizing information from the trade-off analyses was used to assemble a three dimensional representation of the system. The layout considered grouping of hot components, minimization of piping runs, and accessibility to equipment for maintenance. The layout, with structural components removed for clarity, is shown in Figure 2.

[1] International Fuel Cells; Fuel Cell Technology for Prototype Logistic Fuel Mobile Systems, Final Report; FCR 14968A; 10/98.
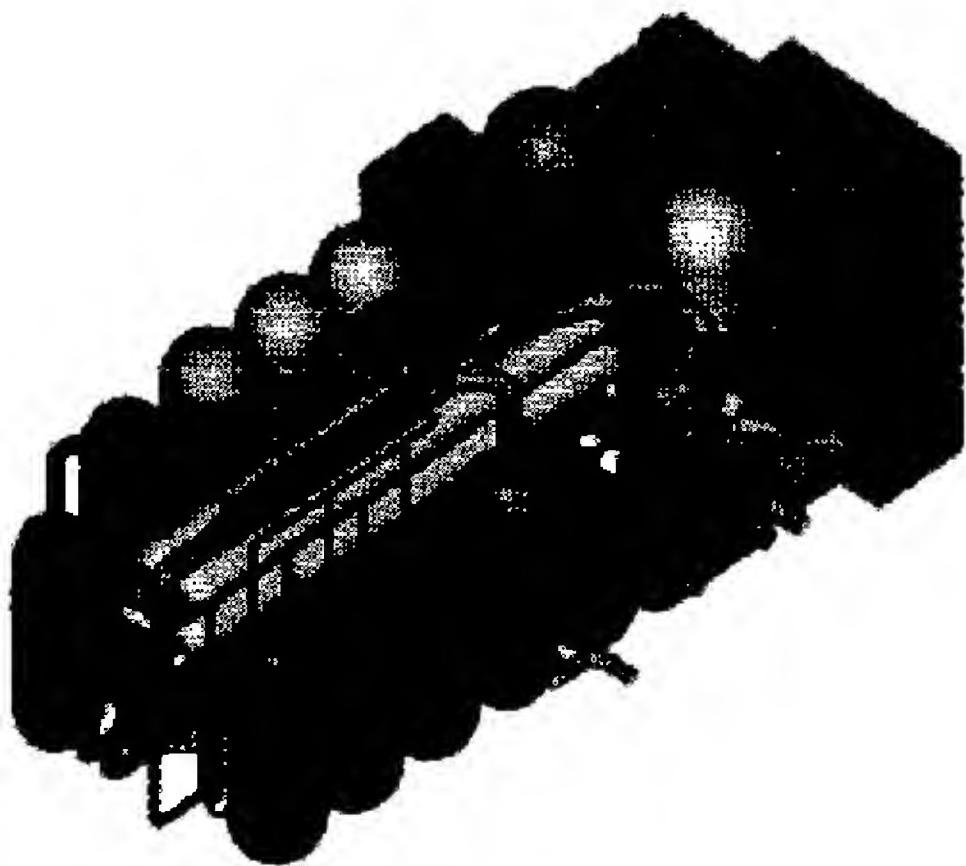
Figure 2. Physical Layout of Baseline 2.5 MW Ship Service Fuel Cell Generator Conceptual Design

The SSFC conceptual design achieves all of the stated design objectives. Further work is required to ensure that the design can meet all of the Navy's requirements in all system operating modes.

A major portion of Phase 1 of the SSFC program focused on demonstrating the suitability of PEM fuel cells for marine application. The focus of this effort was four-fold: assess the effect of salt air on PEM fuel cell operation; qualify the PEM fuel cell to U.S. military shock and vibration standards (MIL-S-901, Grade A and MIL-STD-167-1); characterize the fuel cell stack performance with simulated diesel reformate; and quantify the effect of ammonia and amines (potential contaminants from the fuel processor) on fuel cell performance. Results from the salt air and shock and vibration tests are reported here.

Figure 3 shows a summary of the 50-ppm salt air trial conducted by Ballard Power Systems using a 10-cell PEM fuel cell stack. The plot shows four polarization curves from a single stack operated with different air inlet conditions. Stack performance with ambient air, prior to salt injection is shown ("No Salt"). Polarization data taken at the start of a test run with 50-ppm salt in the inlet air stream is also shown and is almost indistinguishable from the "No Salt" line. It is evident that there is no immediate loss of power due to the introduction of salt at this highest level.

The stack was operated for over ten hours under the 50-ppm salt air condition. Polarization performance was once again recorded after completing ten hours of operation. Even after ten hours of continuous operation under these conditions, the stack does not show any consistent drop in performance. After stopping salt introduction, stack polarization performance was again recorded. This data showed an insignificant difference in the stack power output before the 50-ppm salt air trial and after.

Short term fuel cell stack testing under simulated marine air conditions has not revealed any adverse effects of salt-laden air on fuel cell performance. This result holds even for extremely high levels of salt seen in rough sea states with no other means of protection against salt contamination (i.e. salt filters or louvers). Additional long term salt air testing is planned for late 1999 to assess lifetime effects.

The shock and vibration testing was performed at the National Engineering and Test Establishment in Montreal, Canada. The fuel cell stack tested showed no performance degradation in the shock (MIL-S-901D) and vibration (MIL-STD-167-1) environments. PEM fuel cell technology is thus qualified for marine service as both critical and ancillary equipment either with or without shock mitigation (i.e. dampeners) in place.

SSFC Contract MK700 10-Cell Test
Stack Performance under 50 ppm Salt Air Conditions (SN: 689)
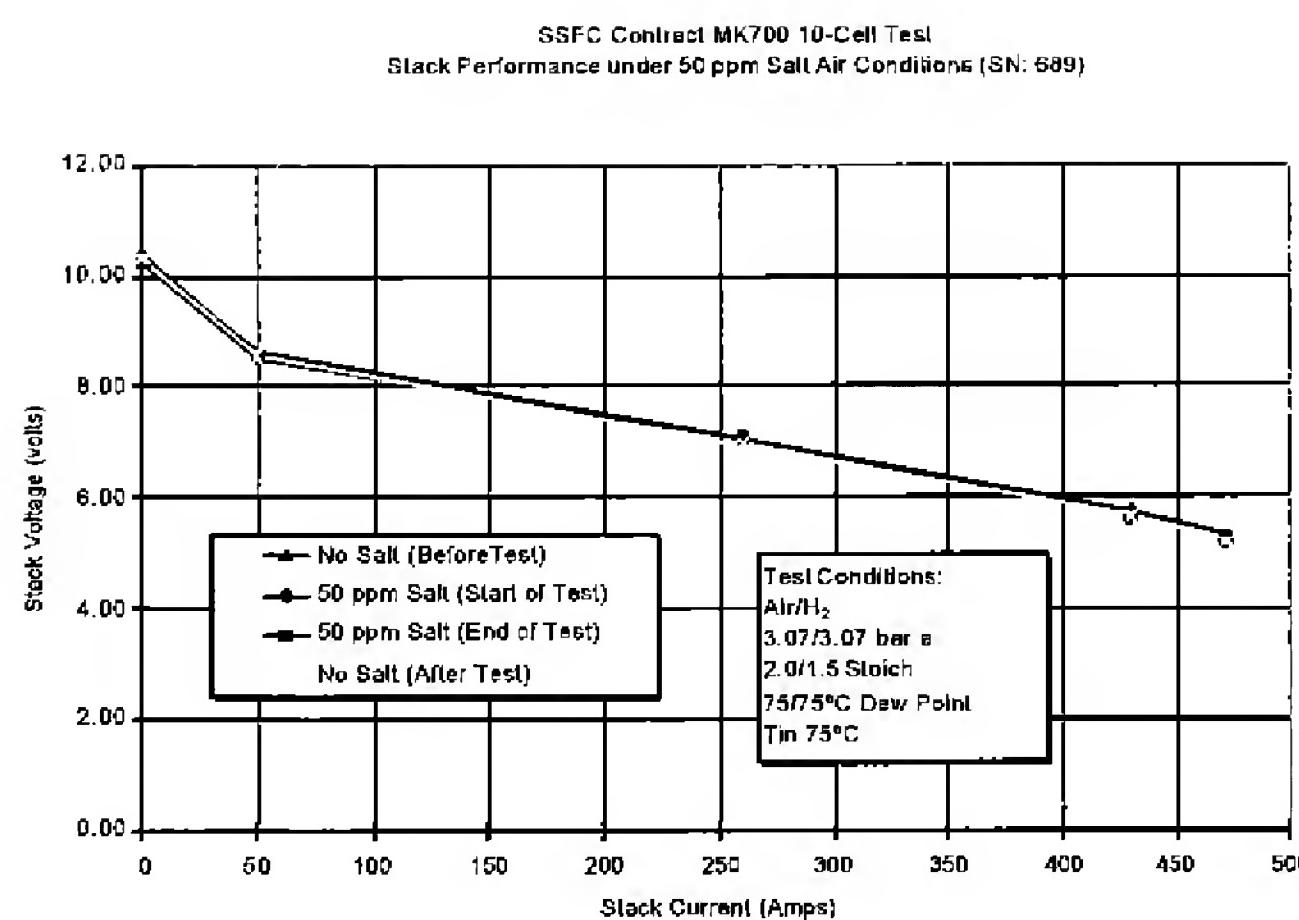
Figure 3 PEM Fuel Cell Response to Salt Air Conditions

The successful fuel cell demonstrations under salt-air, shock and vibration conditions prove the suitability of PEM fuel cells in these naval marine environments. The test conditions were more severe than any expected shipboard conditions. PEM fuel cells should, therefore, be applicable to a variety of shipboard applications.

The SSFC generator fuel processor converts naval distillate fuel (NATO F-76) to a gas acceptable for use by the PEM fuel cell stack. During Phase 1, the critical components of the fuel processor, including the reformer and regenerable desulfurizer, were demonstrated. A 20 kW Phase 1 demonstration scale was chosen to allow economical verification of the technology while providing reasonable scale-up to a 500 kW subsystem during Phase 2. The demonstration fuel processor included an air heater, catalytic autothermal reformer, desulfurizer and carbon monoxide clean up. A photo of the fuel processor test facility at the McDermott Technology, Inc. - Alliance (Ohio) Research Center is shown in Figure 4. The gas clean-up components were sized for a 10-kWe gas capacity to support parametric testing of catalyst breakthrough and to evaluate space velocity design considerations.
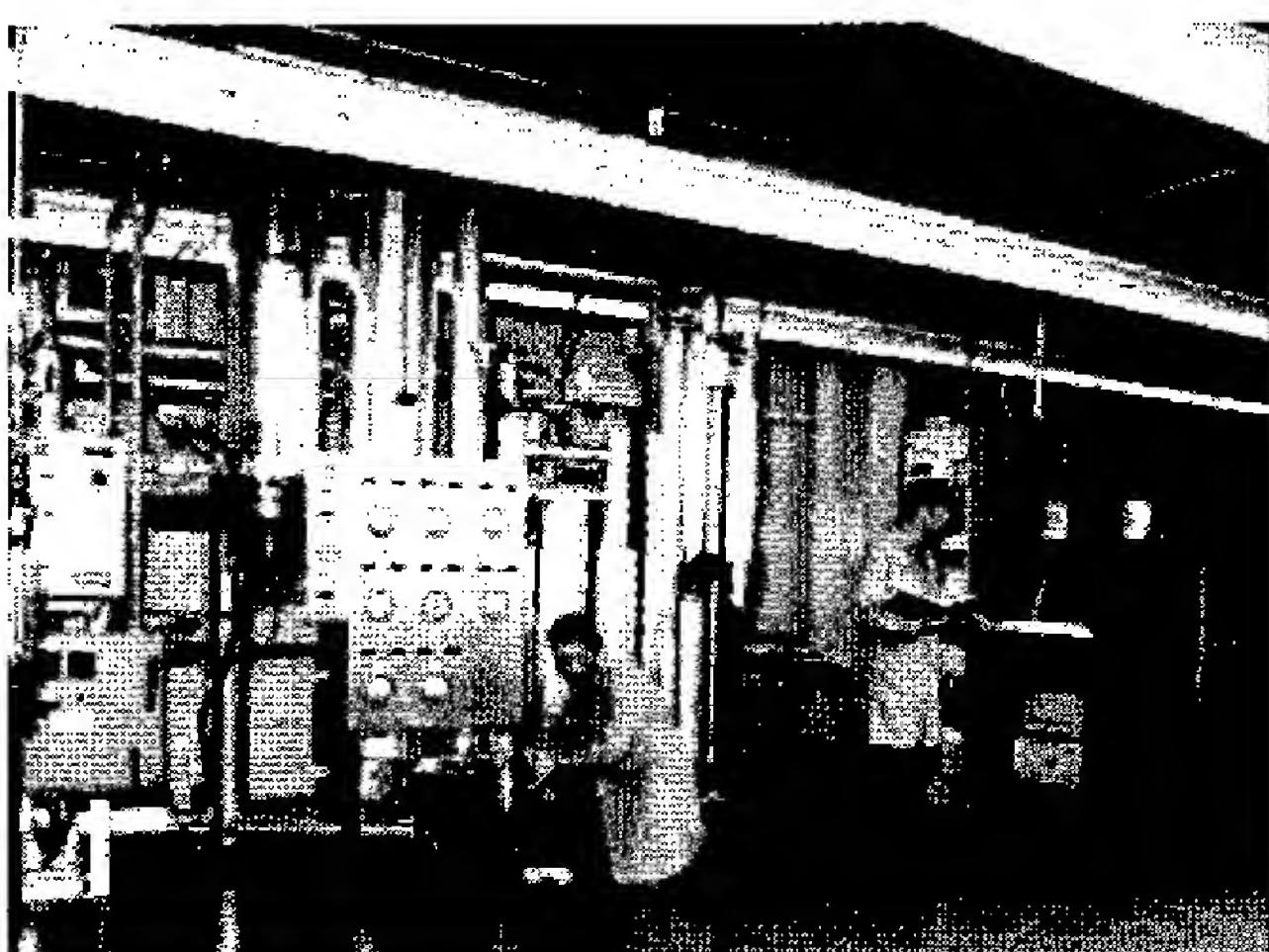
Figure 4. SSFC Fuel Processor Test Facility at McDermott Technology, Inc. - Alliance (OH) Research Center

The SSFC fuel processor test matrix included tests designed to prove the capabilities of the reformer and the desulfurizer. Testing started with operating conditions for which there was previous data. Following these verification tests, operating conditions typical for the SSFC conceptual design as well as conditions intended to define the operability limits of the reformer were evaluated.

Results from testing of the autothermal reformer are shown in Figure 5. The plot shows cold gas efficiency[2] as a function of operating pressure. Test data includes operation at fuel flow rates of 5 and 10 lbm/hr, steam-to-carbon molar ratio of 3.5, and fuel equivalence ratio[3] of 4.2. Reformer efficiency exceeded the target level of 95% for all test conditions. Efficiency calculations result in values greater than 100 percent since they exclude incoming thermal energy in the preheated air and steam (which is converted to chemical energy in the exiting reformate gas). Another important measure of reformer performance is the percent conversion of F-76 fuel to light gases (CH_4, CO_2, and CO). Reformate gas analysis showed that nearly 100 percent of the F-76 fuel was successfully converted to these light gases.
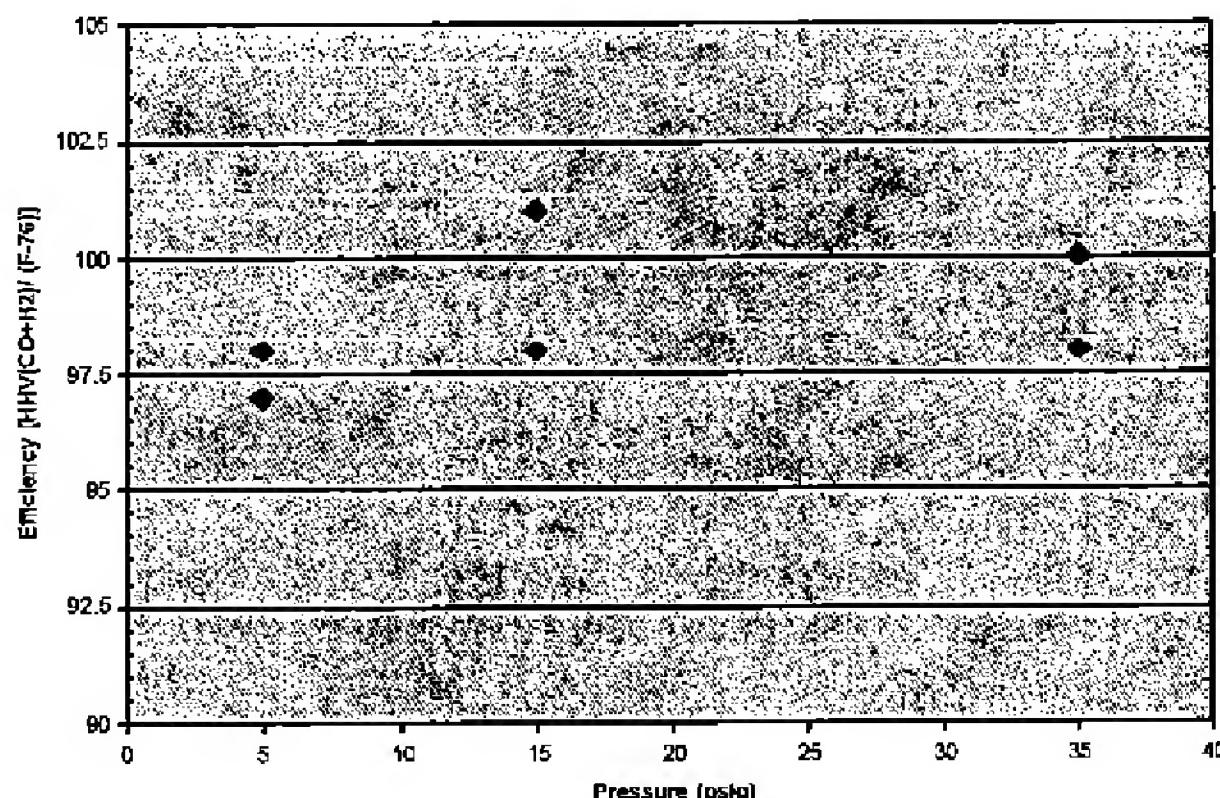
Figure 5. SSFC Fuel Processor Autothermal Reformer Efficiency.

The results described here from the Ship Service Fuel Cell Phase 1 Concept Design and Critical Technology Evaluation confirm the *potential* suitability of a PEM fuel cell-based electrical generator for use in Navy shipboard applications. The system conceptual design presents a compact, efficient generator with high reliability and acceptable cost. The reduced scale demonstrations of critical fuel cell and fuel processor components were successfully completed.

ACKNOWLEDGEMENTS

---

[2] Cold Gas Efficiency = Higher Heating Value [(H2 + CO)] / [NATO F-76 fuel]
[3] Fuel Equivalence Ratio = Actual Air-to-fuel ratio / Stoichiometric Air-to-fuel ratio

- Hoffman, Donald; *Marine Fuel Cells*; Marine Vessel and Air Quality Conference; February (2001).

Marine Fuel Cells

Marine Vessel and Air Quality Conference
1-2 February 2001
Hyatt Regency Hotel
San Francisco, CA

Donald Hoffman
Technical Manager, 824
Naval Sea Systems Command
Philadelphia

---

What is a Fuel Cell

A Fuel Cell operates likes a battery. It supplies electricity by combining hydrogen and oxygen electrochemically without combustion. Unlike a battery, it does not run down or require recharging and will produce electricity, heat and water as long as fuel is supplied.

Fuel Cell Operation

Fuel Reforming
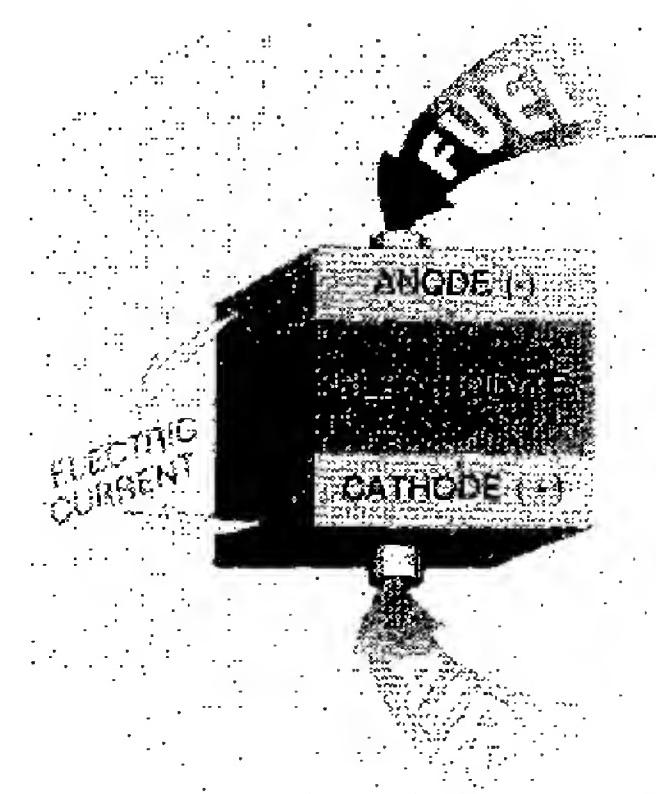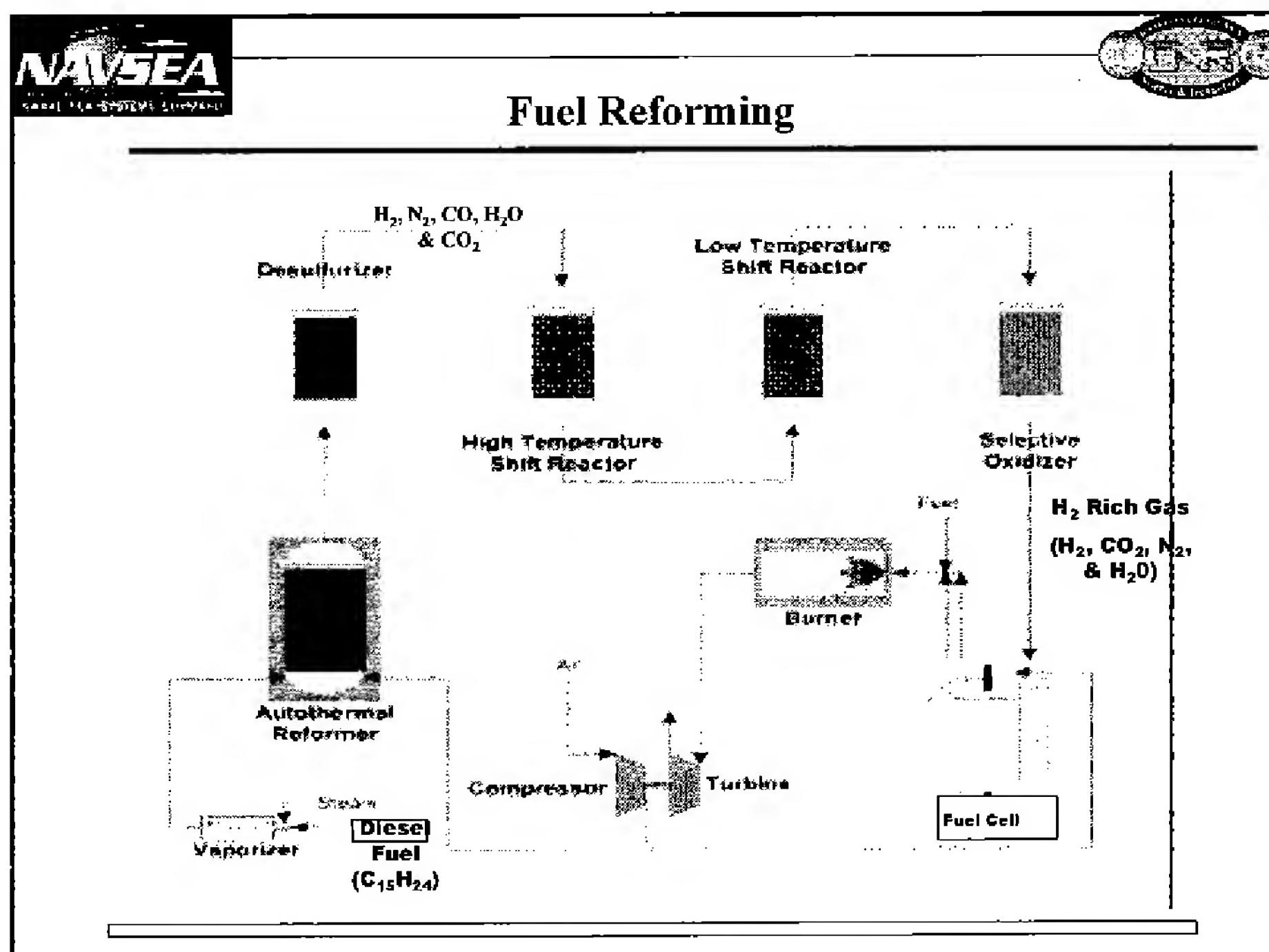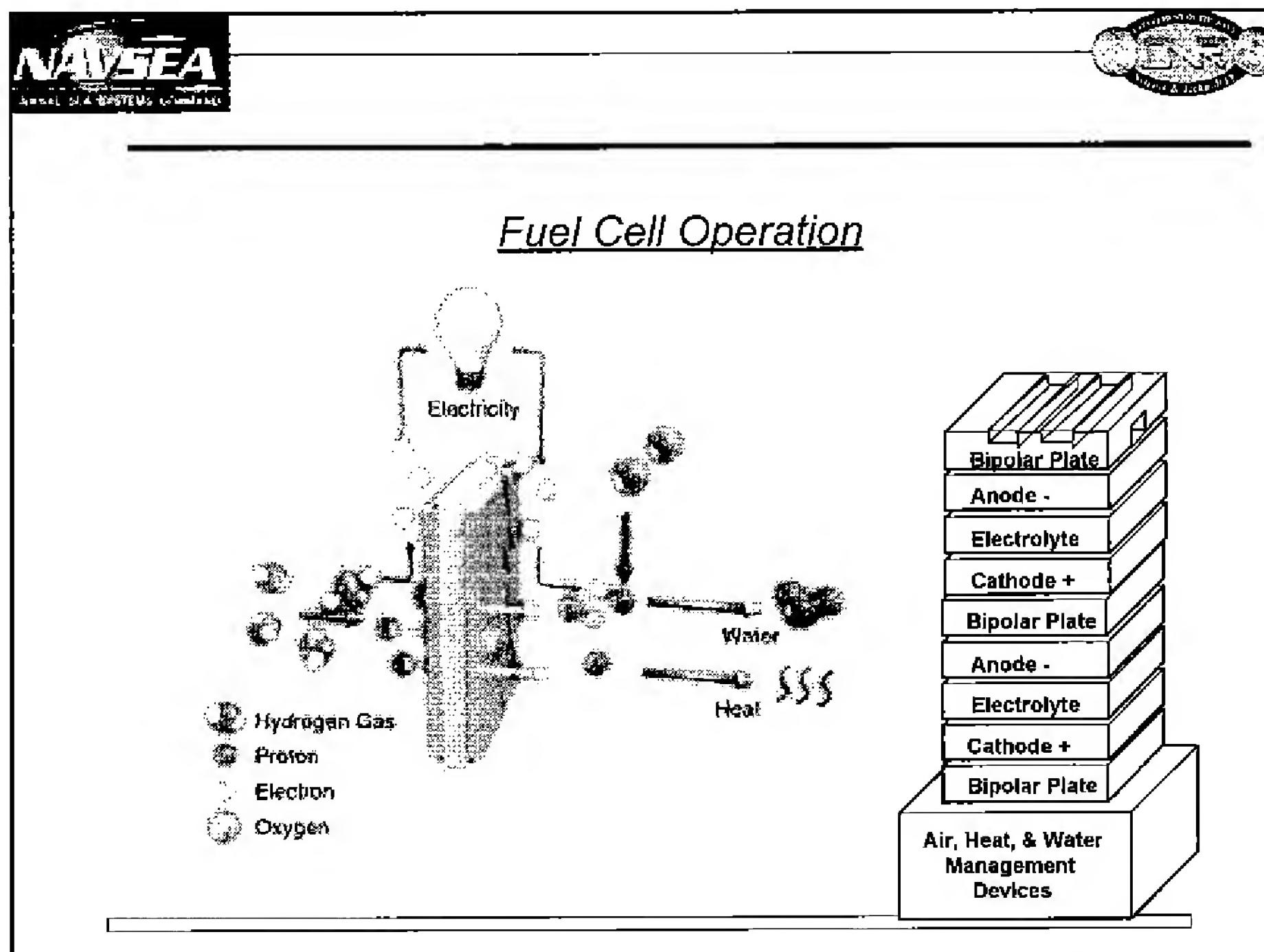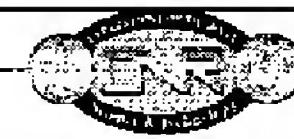
Fuel Cell Types

	Electrolyte	Cell Temp (°F)	Lifetime Projected (Hrs)	Cell Contaminant	Single-Cycle Electrical Efficiency (%)
Proton Exchange Membrane (PEM)	Polymer Membrane (Solid)	180	40,000	S, CO	35-40
Alkaline (AFC)	Potassium Hydroxide (Solid)	200	10,000	CO, CO2	<40
Phosphoric Acid (PA)	Phosphoric Acid (Liquid)	450	40,000	S,CO	35-40
Molten Carbonate (MC)	Potassium Lithium Carbonate (Liquid)	1200	40,000	S	45-55
Solid Oxide (SO) [Tubular, planar, monolithic]	Zirconium Dioxide Ceramic (Solid)	1800	40,000	S	45-60

Fuel Cell Manufacturers

	PA	PEM	MC	SOFC
Ballard		X		
DAIS Analytic		X		
Fuel Cell Energy			X	
H Power		X		
Honeywell		X		X
International Fuel Cells	X	X		
Plug Power		X		
Siemens Westinghouse				X
Technology Management Inc				X
Ztek				X

Fuel Cell Markets

Fuel cell power system markets could soon exceed $3 billion worldwide*

UUV/MCM

10^0 10^1 10^2 10^3 10^4 10^5 10^6 10^7

Power (Watts)

MEMS

"BA5590"

Home Electricity

UAV

Stationary Power

*Arthur D. Little, Inc, Cambridge, MA, reference #44335.

Shipboard Market

- Marine Market Surveys for fuel cell power sources by MTI for PEM systems and FCE for MC systems conclude:
  - Ship Service fuel cell generators for both commercially and Military Marine Markets compete economically with small turbines and marine diesels in terms of life cycle costing.

  - Diesel-fueled fuel cell ship service generator system for commercial marine applications will be in the 200 kW to 1 Mw range; military applications in the 500 kW to 2.5 Mw range.

  - Military represents only 1% of total marine FC market.

- Independent USCG marine market survey validates conclusions.

- DOE/Industry also project future new concept higher power, ultra-high efficiency fuel cell power systems adaptable for marine high power propulsion applications

Diesel-fueled commercial and military surface ship markets represents a significant potential market; circa 2005.

COMPARISON OF EFFICIENCIES FOR ELECTRIC POWER PLANTS
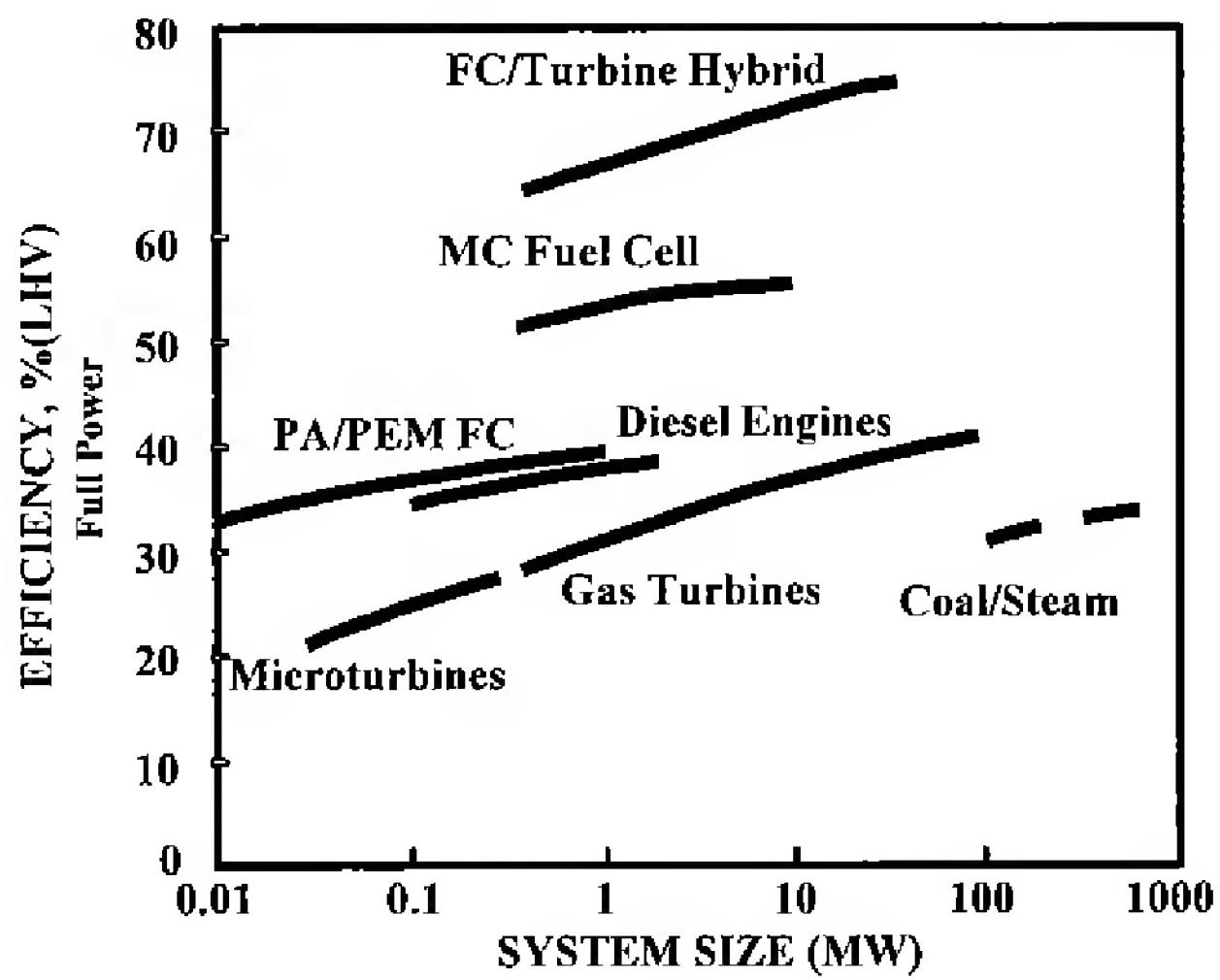
Annual Fuel Consumption
(3,000 Operating Hours)

Gas Turbine Generator Set		641,465 Gallons
		$628,636
Diesel Generator Set		321,703 Gallons
		$315,268
Fuel Cell Generator Set		214,315 Gallons
		$210,028

= 50,000 gallons; ($.98/gallon)

Annual Maintenance

NAVSEA

Gas Turbine Generator Set	[figures representing maintenance hours]	1,050 Hrs
Diesel Generator Set	[figures representing maintenance hours]	1,031 Hrs
Fuel Cell Generator Set	[figures representing maintenance hours]	739 Hrs (Present Technology)

[figure] = 100 hours of maintenance

EMISSION COMPARISON
(gm/HP Hr @ 100% Power)

NAVSEA

[Bar chart with three groupings: CO_2, NO_x, SO_x]

CO_2			NO_x			SO_x		
SSFC	501K GTG	3608 SSDG	SSFC (~.0004)	501K GTG	3608 SSDG	SSFC*	501K GTG	3608 SSDG

* With Desulfurizer Regeneration

Fuel Cell Design Comparison

Design Issues	Ships	Cars Trucks	Utility
Power Density	High	High	Low
Fuel Type	Navy Distillate/ Marine Diesel	Gasoline/H2/ Methanol/Diesel	Natural Gas/ Coal Derived
Life, MTBO	40,000 Hrs	10,000 Hrs	40,000 Hrs
Dynamic Response	Fast	Fast	Slow
Operating Environment	Severe	Moderate	Benign

Navy Shipboard Fuel Cell Program

Program Summary

Objective: Develop shipboard fuel cell power systems with acquisition cost, weight, and volume comparable to other market options, for future Navy ships and craft.

State of the Art: Industry is developing fuel cell technology for stationary and non-marine transportation applications operating on non-logistics fuels. Commercial units expected between 2001 and 2005, with stationary systems available before automotive systems. Little effort in diesel reformation.

Approach: Develop fuel cell power systems and components to enable commercial fuel cell equipment to be used in the unique Naval shipboard environment.

Navy Technical Challenges

- Fuel Type
  - ✓ Logistic Fuel reforming

- Power Density, Cost & System Efficiency

- Reliability and Maintainability

- Duty Cycle/Transient Response

- Marine Environment
  - ✓ Cell Life
  - ✓ Environmental Contaminants
 - ✓ Shock & Vibration
  - ✓ Ship Motions

Goals/Metrics

	DDG-51 GTG	AOE-6 SSDG	SSFC Goals 2005	HPFC Goals 2010
Unit Volume (ft3/kW)	1.1	2.84	2	TBD
Unit Weight (lb/kW)	27.2	36.4	40	TBD
Fuel Efficiency (at 50% load)	16%	37%	40%	70%
Acquisition Cost ($/kW)	1600	480	1500	1200
Scalable to: (MW)	-	-	3	20

SSFC: Ship Service Fuel Cell Program
HPFC: High Performance Fuel Cell Program

Navy Shipboard Fuel Cell Program

Program Timeline/Transition

FY	00	01	02	03	04	05	06	07	08	09	10	11

Fleet Introduction
Ship Platform Managers

IPS Transition Full Scale
Design, Fabrication, Operation and Testing of Full Scale Ship Service Fuel Cell

ONR/NAVSEA Advanced Technology Development
- 500KW IFP Design
- Fabrication, and Testing of 500KW ATR Integrated Fuel Processor
- Design, Fabrication, and Testing of 625KW MCFC Demonstrator
- At Sea Evaluation 625KW Demonstrator
- Design, Fabrication, and Testing of HPFC Demonstrator
- SSFC Concept Design, Risk Reduction Testing

Legend
- ☐ Planned
- ☐ Proposed
- △ Decision Point

ONR Applied Research
High Performance Fuel Cell Program
(Adv. Reform, FC Hybrid Model, Sulfur Tolerance, High Temp FC Marinization)

Navy Shipboard Fuel Cell Program

Ship Service Fuel Cell Program Demonstration

Controller — Fuel Cell Stacks — Exhaust — Air Intake — DC/AC Converter — Fresh/Seawater Heat Exchanger
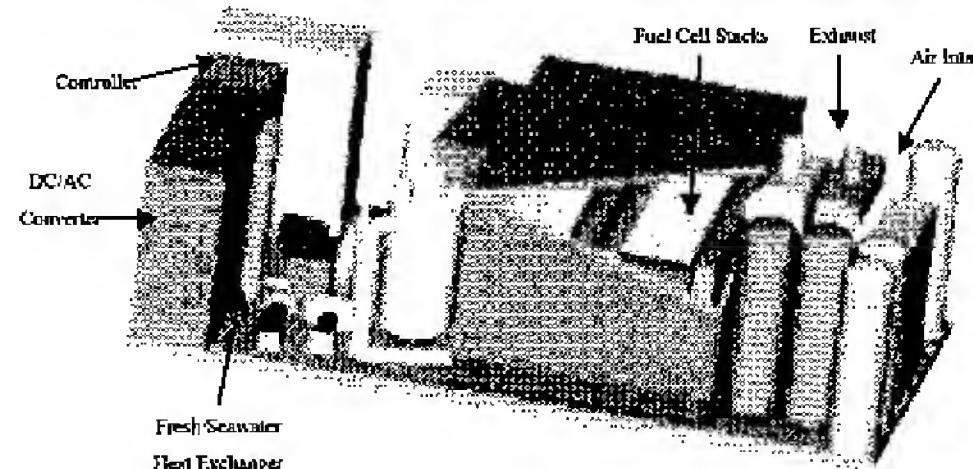
FuelCell Energy 625kW 450V, 3φ, 60 HZ, 50% Efficient MC SSFC Power Module Concept

PHASE I: Complete ($4.6M) FY00
- 2.5 MW SSFC Conceptual Design
- Sub-scale risk reduction demonstrations
  - Cell salt air tolerance
  - NATO F-76 diesel fuel reforming
  - Fuel contaminant removal and cell sensitivity (sulfur)
  - Cell shock and vibration
- Analytical model
- Marine/Navy market surveys

PHASE II: (36 month, $12.6M ONR cost shared contract awarded May 00 to FCE, Inc.)
- 625kW SSFC module detailed design
- 625kW SSFC module fabrication
- Factory testing
- Dynamic simulation model
- IPS program transition planned – ship impact/cost studies underway
- LABEVAL (FY04)

PHASE III:
- At-Sea demonstration (FY05)

625 kW MODULE INTERNAL ARRANGEMENT

FuelCell Energy

S-D1607

Ship Service Fuel Cell Program Demonstration

McDermott Technology

500kW SSFC Autothermal Reformer (ATR) based NATO F76 Diesel Integrated Fuel Processor (IFP)

PHASE I: Completed ($ 4.5 M) FY00
- 2.5 MW *PEM SSFC* Conceptual Design
- Sub-scale risk reduction demonstrations
  - Cell salt air tolerance
  - NATO F-76 diesel fuel reforming
  - Fuel contaminant removal and cell sensitivity (sulfur, CO, ammonia, amines)
  - Cell shock and vibration
- Analytical performance model
- Marine/Navy market surveys

PHASE II: (36 month, $16.5M 50% cost shared ONR program.
- Initial $3.8M ONR contract award July 00 to MTI)
- 500kW IFP preliminary design
- 500kW IFP detailed design
- 500kW IFP fabrication
- 500kW IFP factory testing
- Dynamic simulation model

NAVSEA

HPFC S&T Development
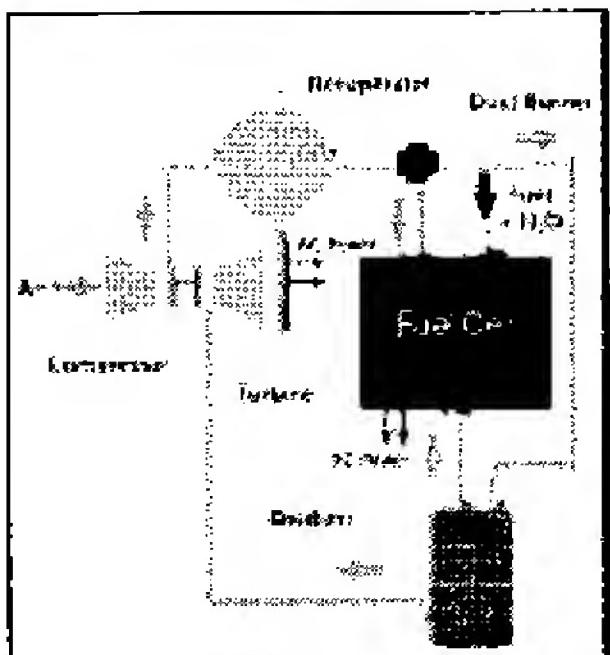
Solid Oxide Fuel Cell coupled to a gas turbine generator to provide a 70% efficient power source scaleable to 20MW.

- Advanced Fuel Reforming
- Sulfur Tolerance
- HPFC Design & Trade Off
- SOFC/GT Hybrid Modeling
- SOFC Marinization
- Multistage FC

NAVSEA

Interagency Working Group

U.S. COAST GUARD

RADM John T. Tozzi
Assistant Commandant for Systems

RADM G. Gaffney, II
Chief of Naval Research

NAVSEA

RADM M.T. Coyle
Deputy Commander for Engineering

Mission Statement

- Foster the use of Fuel Cells for ship applications utilizing diesel fuels to fulfill national transportation needs.

- Transfer the technology to the public.

- Actively involve industry in the development efforts.

- Reduce duplicative efforts – coordinate/cooperate on marine fuel cell requirements.

- Demonstrate the effectiveness of focused interagency partnership.

Diane H. Josephson
Deputy Undersecretary for Oceans Management & Atmosphere

John E. Graykowski
Maritime Administration

R.S. Begura
Director, Office of Fossil Energy

Fenton Carey
Associate Administration for Research, Technology & Analysis

Original Signatories to MOU Approved 2 February 1998

Foreign Marine Fuel Cell Interest

- **Canada:** Ballard developing 200 kW methanol/LOX fuel cell for military submarines.

- **Germany:**
  - Siemens Power Generations Group recently delivered 300 kW PEM fuel cell for Class 212 submarines.
  - HDW has tested 2 Ballard 80 kW PEM power plants for submarine service.

- **UK:** UK is interested in jointly developing a 1.5 MW ship service PEM fuel cell.

- **French & Netherlands** Navies are investigating marine fuel cell applications.

- **Japan:** Evaluating fuel cells for marine applications.

- **Italian Navy:** Proposed 1MW MC FC system for surface ship applications.

- **4 NATO Countries** supporting diesel fuel reforming (100 KW) demonstrations.

Summary

- High efficiency fuel cell systems provide the potential for substantial payoff with reduced production of overall emissions in commercial and military applications.

- ONR/NAVSEA program underway to demonstrate Fuel Cell Power Systems for future naval combatants and other craft.

- Navy Shipboard Fuel Cell Program is developing technology to overcome unique Navy technical challenges while leveraging commercial fuel cell advancements.

Appl. No.: 10/597,180
Attorney Docket: LC-519/PCT/US

29

- WO 02/084099; *Filter Assemblies and Systems for Intake Air for Fuel Cells*; (October 2002).

(51) **International Patent Classification**[7]: **F02M 35/14**, H01M 8/04, 8/06, B01D 53/04

(21) **International Application Number:** PCT/US02/11443

(22) **International Filing Date:** 11 April 2002 (11.04.2002)

(25) **Filing Language:** English

(26) **Publication Language:** English

(30) **Priority Data:**

09/832,715	11 April 2001 (11.04.2001)	US
09/879,441	12 June 2001 (12.06.2001)	US
10/122,647	10 April 2002 (10.04.2002)	US

(63) **Related by continuation (CON) or continuation-in-part (CIP) to earlier applications:**

US	10/122,647 (CON)
Filed on	10 April 2002 (10.04.2002)
US	09/832,715 (CIP)
Filed on	11 April 2001 (11.04.2001)
US	09/879,441 (CIP)
Filed on	12 June 2001 (12.06.2001)

(71) **Applicant** *(for all designated States except US)*: DONALDSON COMPANY, INC. [US/US]; 1400 West 94th Street, Minneapolis, MN 55440-1299 (US).

(72) **Inventors; and**

(75) **Inventors/Applicants** *(for US only)*: STENERSEN, Eivind [NO/US]; N8811 - 1047 Street, River Falls, WI 54022 (US). NYMAN, William, Michael [US/US]; 865 Trotters Ridge, Eagan, MN 55123 (US). CANEPA, Richard, Thomas [US/US]; 4965 Rosewood Lane North, Plymouth, MN 55442 (US).

(74) **Agent:** BRUESS, Steven, C.; Merchant & Gould P.C., P.O. Box 2903, Minneapolis, MN 55402-0903 (US).

(81) **Designated States** *(national)*: AE, AG, AL, AM, AT, AU, AZ, BA, BB, BG, BR, BY, BZ, CA, CH, CN, CO, CR, CU, CZ, DE, DK, DM, DZ, EC, EE, ES, FI, GB, GD, GE, GH, GM, HR, HU, ID, IL, IN, IS, JP, KE, KG, KP, KR, KZ, LC, LK, LR, LS, LT, LU, LV, MA, MD, MG, MK, MN, MW, MX, MZ, NO, NZ, OM, PH, PL, PT, RO, RU, SD, SE, SG, SI, SK, SL, TJ, TM, TN, TR, TT, TZ, UA, UG, US, UZ, VN, YU, ZA, ZM, ZW.

(84) **Designated States** *(regional)*: ARIPO patent (GH, GM, KE, LS, MW, MZ, SD, SL, SZ, TZ, UG, ZM, ZW),

[Continued on next page]

(54) **Title:** FILTER ASSEMBLIES AND SYSTEMS FOR INTAKE AIR FOR FUEL CELLS
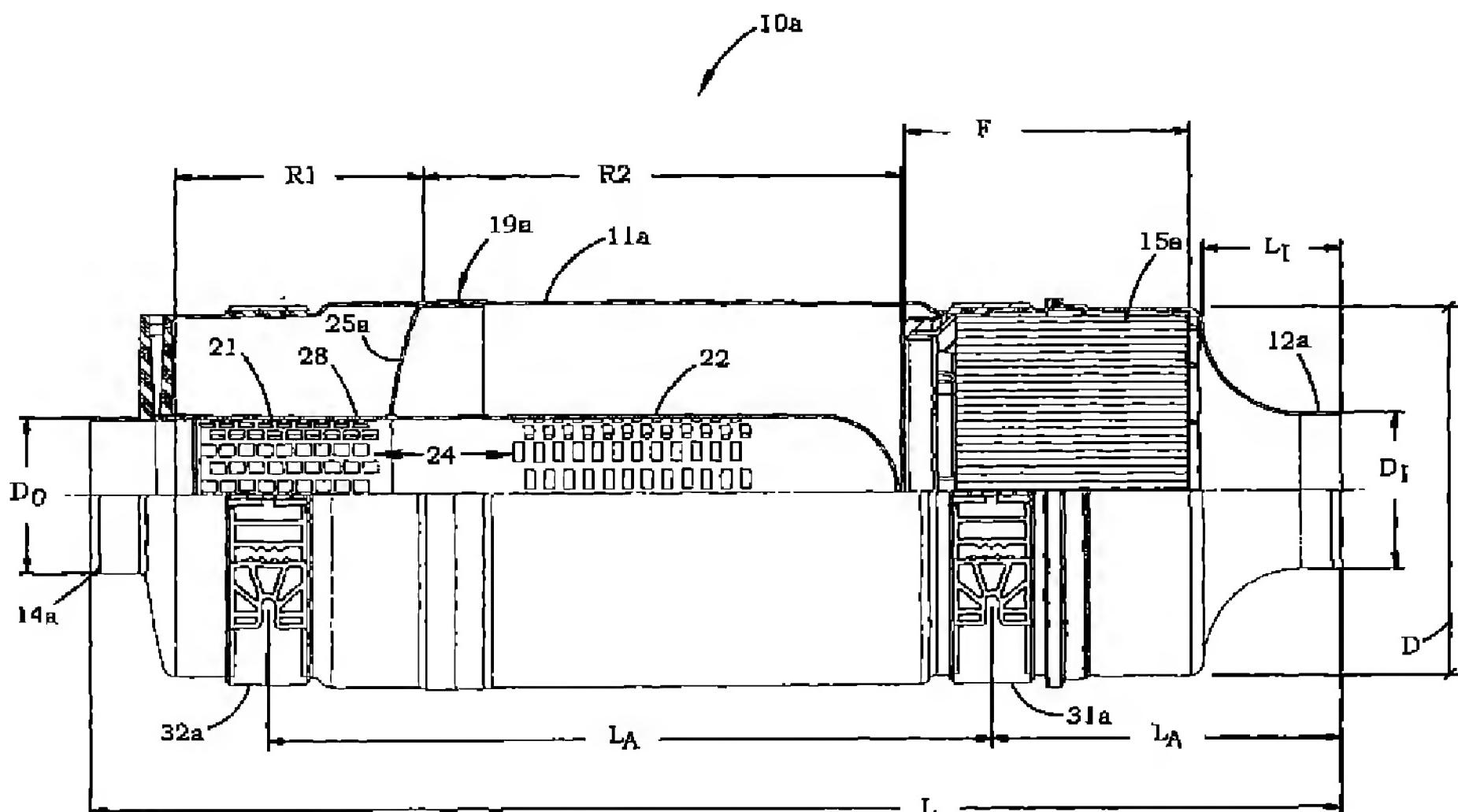
(57) **Abstract:** A filter assembly for removing particulate contaminants and chemical contaminants from an incoming dirty air stream for a fuel cell. The filter assembly also includes a noise suppression element that reduces sound waves or noise emanating from any equipment, such as a compressor. The filter assembly can include a particulate filter portion for removing physical or particulate contaminants, a chemical filter portion for removing chemical contaminants, or can have both portions.

WO 02/084099 A1

this can be done, for example, by coating or impregnating the carrier material with the acidic or basic material.

Examples of acidic compounds that are often present in atmospheric air and are considered as contaminants for fuel cells include, for example, sulfur oxides,

5   nitrogen oxides, hydrogen sulfide, hydrogen chloride, and volatile organic acids and nonvolatile organic acids. Examples of basic compounds that are often present in atmospheric air and are considered as contaminants for fuel cells include, for example, ammonia, amines, amides, sodium hydroxides, lithium hydroxides, potassium hydroxides, volatile organic bases and nonvolatile organic bases.

10   For PEM fuel cells, the cathodic reaction occurs under acidic conditions, thus, it is undesirable to have basic contaminants present. An example of a preferred material for removing basic contaminants, such as ammonia, is activated carbon impregnated or coated with citric acid.

A first embodiment of a filter element 15 (Figure 1) having both the

15   physical or particulate removal portion and a chemical removal portion is shown in Figure 9 as filter element 15c. Filter element 15c is similar to filter element 15a of Figure 7 in that filter element 15c has filter construction 100 (shown in phantom in Figure 9) with first flow face 105 and second flow face 110, support band 162, frame 200, and sealing system 60. Filter element 15c further includes an adsorbent element

20   300, such as shaped activated carbon. Adsorbent element 300 is positioned on frame 200 within frame 200 and sealing system 60. The compressible sealing system 60 frictionally retains adsorbent element 300 in the desired position, but can be deformed to release adsorbent element 300 for replacement when the adsorbent is spent.

In a preferred embodiment, adsorbent element 300 is a shaped mass of

25   activated carbon material held together by a thermoplastic binder. A preferred adsorbent element 300 includes activated carbon material, sieve size 12x20 or 8x16, molded with a level of 8% ethylene-vinyl acetate binder. Such a preferred adsorbent element 300 can be made in accordance with the teachings of U.S. Patent Nos. 5,189,092 (Koslow) or 5,331,037 (Koslow). In another preferred embodiment,

30   adsorbent element 300 is made from layers (not shown) of carbon material available from Hollingsworth & Vose of East Walpole, MA (also known as H&V).

- St-Pierre, Jean, et al.; *Successful Demonstration of Ballard PEMFCS . . .*; Journal of New Materials for Electrochemical Systems; 5, 263-271 (2002).

Successful Demonstration of Ballard PEMFCS for Space Shuttle Applications

Jean St-Pierre*, Nengyou Jia

Ballard Power Systems
9000 Glenlyon Parkway
Burnaby, BC, Canada, V5J 5J9

Abstract: *An 11,000 hours PEMFC lifetest (8 cells Mk513 stack) was conducted using oxygen and hydrogen feed streams which demonstrated a very low degradation rate (< 2 $\mu V \cdot h^{-1}$) without the formation of external leaks and leaks between cathode and anode compartments. Degradation mechanisms included mass transport related voltage losses due to a change in hydrophilicity of the catalyst substrate and seal oxidation. The results met NASA's requirement of a 10,000 hour life and demonstrate a significant step towards reducing costs of the present AFC flight system which currently lasts between 1,000 and 2,600 hours. Recommendations for a subsequent test program are also provided.*

1. INTRODUCTION

Polymer electrolyte membrane fuel cells (PEMFCs) were first used for space applications during the Gemini program (1962-1966) and subsequently for the Biosatellite 2 program (1967) [1,2]. However, at the end of this period, the power density could no longer rival the performance of the emerging alkaline fuel cells (AFCs). As a result, the PEMFC technology was subsequently abandoned in favor of the alkaline fuel cell for Apollo missions (1968-1972). Today, alkaline fuel cells are still used to power the Space Shuttle missions.

However, the development of PEMFCs for terrestrial applications (micro power, portable, motive and stationary) which has benefited from substantial investments during the last few years has resulted in increased performance, long lifetimes and reduced costs surpassing the alkaline fuel cell characteristics. Also, requirements for space applications have evolved and are presently more stringent [3]. In particular, significantly smaller life cycle costs are necessary to achieve future objectives. This

requirement as well as others for the Space Shuttle include a 10,000 hour life system (compared to the current 12 kW alkaline fuel cell system life of approximately 1,000-2,600 hours [3-4]) producing 20 kW at a nominal 28 V dc packaged in a volume comparable to the current alkaline fuel cell power plant.

The capability and feasibility of meeting life requirements are being demonstrated with one of Ballard's commercially developed PEMFC stacks. Successful demonstration of this capability would significantly reduce the cost, schedule and technical risks of developing the flight system. Advanced commercial hardware development promises additional improvements in terms of performance and cost.

2. EXPERIMENTAL

2.1 Stack configuration

A modified Ballard 8 cells Mk513 stack with an internal humidification section was used for all tests. Since the Mk513 design was originally developed for air operation, a modification was required to allow relatively pure oxygen operation at low stoichiometries with the objective of avoiding water management

---

*To whom correspondence should be addressed:
Email: jean.st-pierre@ballard.com

issues due to lower pressure drops induced by reduced gas flow rates. In addition, the stack and test station materials were not altered and therefore another objective of the program was to determine their behaviour under relatively pure oxygen service (> 99.8 %).

The membrane/electrode assemblies were made by hot pressing together a Dow membrane manufactured by Dupont, an anode made from a Toray carbon fiber paper onto which a catalyst layer (Pt/Rh mixture with 4 mg Pt·cm^{-2} and 1.4 mg Rh·cm^{-2}) and a Nafion ionomer layer were deposited, and, a cathode also made from a Toray carbon fiber paper onto which a carbon layer, a catalyst layer (4 mg Pt·cm^{-2}) and a Nafion ionomer layer were deposited.

After the lifetest was completed, a membrane/electrode assembly (cell 7, counted from the negative bus plate), was delaminated and samples were cut from the anode, cathode and membrane, near the oxidant inlet port, near the fuel inlet port, in the center, near the oxidant outlet port, and near the fuel outlet port (Figure 1). In addition, humidifier membrane samples from both oxidant and fuel subsections were analyzed. The samples were analyzed by ICP-MS to determine the levels of twelve different potential contaminants (Mg, Al, Si, K, Ca, Cr, Mn, Fe, Ni, Cu, Zn, Mo). The contaminant selection is representative of stack and test station construction materials (stainless steel, brass, contaminants from carbon plates).
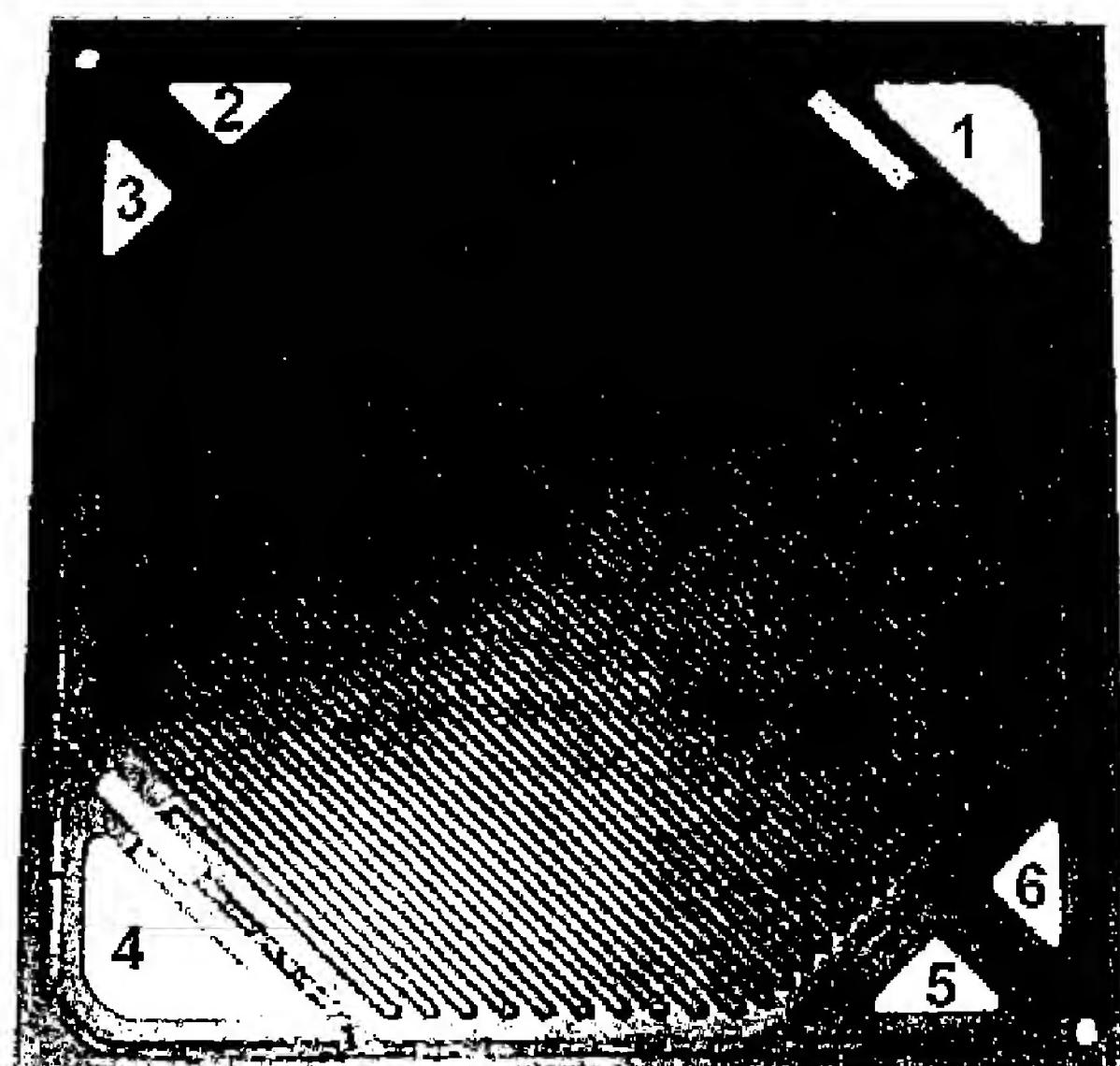
Figure 1: Modified oxidant flow field plate illustrating the internal ports and serpentine flow field (1: oxidant inlet, 2: fuel inlet, 3: coolant inlet, 4: oxidant outlet, 5: coolant outlet, 6: fuel outlet).

Seal sample (from both active and humidification sections) analyses by FTIR were completed after the lifetest was completed.

2.2 Test station configuration

The test station coolant loop was equipped with a filter unit (1.4 l packed bed containing in a 1:1:1 volume ratio activated carbon, an anion exchange resin and a cation exchange resin) to minimize the risk that the coolant water, which also acted as the humidification water and was in physical contact with the membrane/electrode assemblies, transmitted contaminants which have a detrimental effect on cell performance. The filter unit state was constantly monitored by measuring three different parameters related to the outlet water. For the conductivity and pH measurements, commercially available meters were used (YSI model 35 conductance meter, Accumet 950 pH/ion meter) with water samples which were agitated and cooled to room temperature. Organic contaminants also need to be eliminated from the coolant water but are not detected by the water conductivity and pH measurements. Instead, chemical oxidation of the water samples followed by titration was used to determine the organic content of the coolant loop [5]. Humidification membrane and membrane/electrode assembly degradation was monitored by measuring the fluoride content of water samples (ion chromatography) used to determine the filter unit state.

Relatively pure oxygen (> 99.8 %) and hydrogen (> 99.9 %) were used to meet Ballard's specifications. The stack inlet and outlet gases were analyzed using commercial residual gas analysis equipment (Spectrum Research model QMS300) to first ensure that the specifications were met, but also to determine whether or not contaminants were released or generated within the stack during operation.

2.3 Test procedure

The stack was operated continuously, except to perform diagnostics. Initially, the lifetest was operated at 0.538 A·cm^{-2}. However, after approximately 1,000 hours, the current density was increased to 0.861 A·cm^{-2} to test the hardware limits. Measurements at the lower current density value of 0.538 A·cm^{-2} were still obtained after this change but only accounted for a few hours of operation per week. Since voltage data were obtained at two current densities, it allowed the definition and determination of two performance degradation rates. Different current densities may lead to different degradation rates since controlling mechanisms (kinetic, ohmic or mass transport) may differ and be differently affected over life.

A summary of the diagnostics performed during stack operation, which were designed to extract the maximum information from both fuel cell stack and test system (for fuel cell system input), is provided in Table 1. Other diagnostics were also performed at the end of the lifetest to determine whether any material degradation occurred. On a daily basis, cell voltages as well

as cell resistances (using a commercial milliohmmeter Hewlett-Packard model 4328A operating a 1 kHz) were measured, while the operational conditions were monitored and adjusted, if required, to the desirable values. On a weekly basis, leak rates from the stack were measured (from the anode compartment to the cathode compartment, from the anode and cathode compartments to the ambient atmosphere, and from the anode and cathode compartments to the coolant compartment) and water samples were taken from the anode and cathode knockout drums, and from the filtering unit loop to determine their conductivity and pH. In addition, after the decision was made to increase the current density to 0.861 A·cm^{-2}, the cell voltage was also measured on a weekly basis at 0.538 A·cm^{-2}. Every 1,000 hours, a polarization was performed by repeatedly changing the current density and waiting for a few minutes before recording the steady state voltage. Finally, other tests were performed on an irregular basis which include determination of the total organic and fluoride content of different water samples (from the same sources as for the determination of water conductivity and pH), leak rate measurements after unscheduled shutdowns and residual gas analysis of the reactant streams.

Table 1: Summary of the tests performed during the lifetest

Test Frequency	Test Performed
Daily	• Cell voltage at 0.538 A·cm^{-2} (< 1,000 h) and at 0.861 A·cm^{-2} (> 1,000 h) • Cell resistance • Operational conditions verification
Weekly	• Water conductivity • Water pH • Leak rates • Cell voltage at 0.538 A·cm^{-2} (> 1,000 h)
Every 1000 h	• Polarization
Infrequently	• Total organic carbon • Fluoride content of water samples • Residual gas analysis of reactant streams • Leak rates after unscheduled shutdown • Humidification membrane and membrane/electrode assembly sample examination • Seal sample examination

At the end of the lifetest, samples were taken from humidification membranes, membrane/electrode assemblies and seals, and analyzed by the methods given in section 2.1.

3. RESULTS AND DISCUSSION

3.1 Beginning of life stack performance

Polymer electrolyte membrane fuel cells polarization curves are easily discussed using simple parametric relationships such as [6]:

$$V = E^r - b\log\left(\frac{i}{i_o}\right) - Ri - m\exp ni \qquad (1)$$

where the cell voltage V is in Volts, the reversible cell voltage E^r is in Volts, the Tafel slope b is in V/decade, the current density i is in A·cm^{-2}, the exchange current density i_0 is in A·cm^{-2}, the cell resistance R is in ohm·cm^2, and m and n are parameters characterizing mass transport effects. Equation 1 includes all the performance losses of interest (kinetic, ohmic, mass transport). Other similar relationships, which contain additional mass transport related parameters, have also been derived and could equally be used to discuss performance losses [7-11]. With pure reactants, mass transport losses are largely minimised. For this specific case, all relationships [6-11] are simplified to the same equation (equation 1 without the last term on the right hand side).

The beginning of life polarization curve is illustrated in Figure 2 and is represented by the fitted simplified equation 1 (noting that E^r + blog(i_0) is a constant) which assumes that kinetic and ohmic performance losses are the only important terms:

$$V = 0.872 - 0.068\log(i) - 0.111i \qquad (2)$$

where V is in Volts and i is in A·cm^{-2}. Since the stack had 8 cells, it was possible to compute the cell performance standard deviation (voltage measurements for the 8 cells at a given time, Figure 3). Generally, the standard deviation increases with current density because more sources of variation are present. In the present case, at low current densities only electrode kinetics (mostly the oxygen reduction reaction) are important. At larger current densities, ohmic losses associated with the membrane and mass transport losses are becoming more important. Even if the standard deviation increases with current density, values are relatively low which indicates good reproducibility of the membrane/electrode assembly and stack components manufacturing processes. In addition, it is noted that the standard deviation increases under open circuit conditions. Again, the reason for this is the presence of additional sources of cell performance variation, such as the formation of a mixed potential (Pt oxidation, oxygen reduction).

Average cell resistance values at the beginning of life are given in Figure 2 and are fairly constant over the current density range investigated. It is also observed that the average cell resistance values obtained with the milliohmmeter (0.31-0.35 mΩ) are smaller than the value derived from Equation 2 (0.111 Ωcm^2 / 294.4 cm^2 cell active surface area for the Mk513 design = 0.38 mΩ). The milliohmmeter operates at a frequency of 1 kHz which is sufficiently large to ensure that the measured values do not include mass transport related effects. Therefore, the ohmic region of the polarization curve is really pseudo-
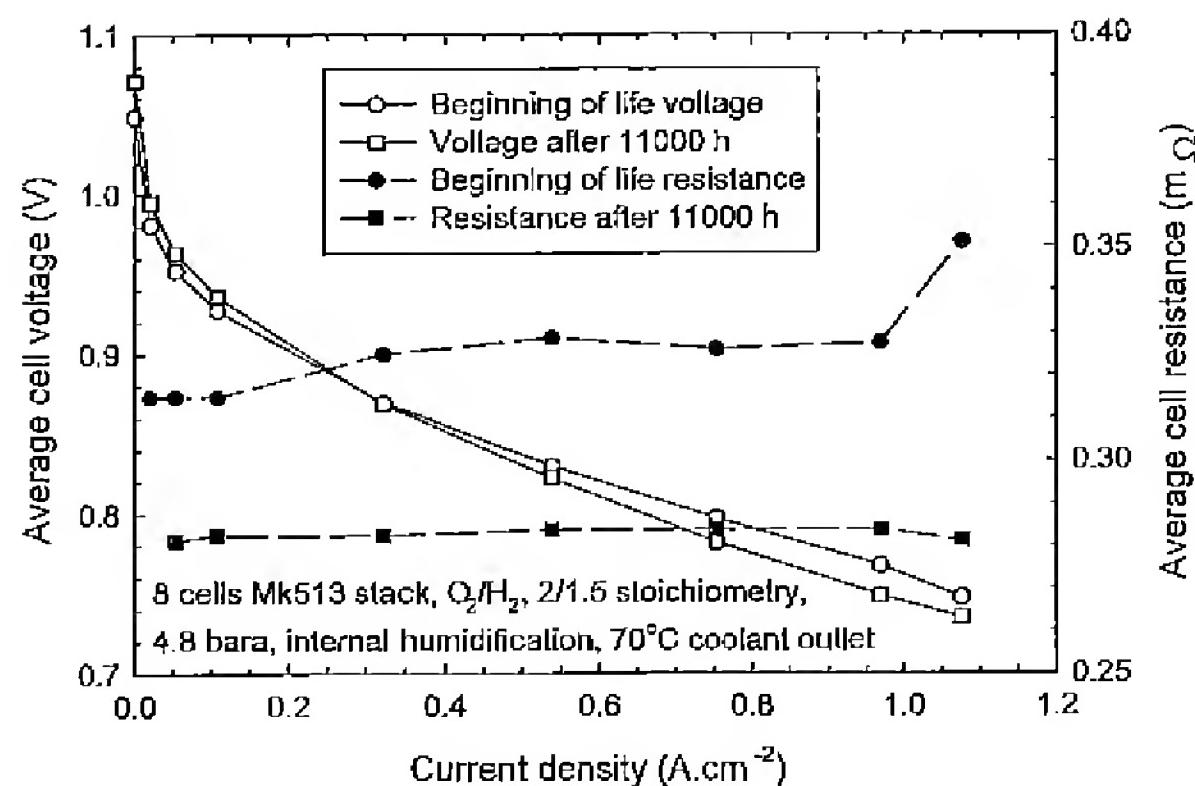
Figure 2: Polarization curves and average cell resistances obtained at the beginning of life and after more than 11,000 hours of operation.

Figure 3: Cell voltage and resistance standard deviations obtained at the beginning of life and after more than 11,000 hours of operation.

ohmic in character (ohmic behaviour but not ohmic origin), comprising both ohmic and mass transport contributions.

The average cell power generated at the beginning of life is derived from Equation 2:

$$P = (0.872 - 0.068 \log(i) - 0.111i)i \qquad (3)$$

where P is the power generated in $W \cdot cm^{-2}$. The peak power is found by solving equation $dP/di = 0$ using Equation 3. The peak power is 1.57 $W \cdot cm^{-2}$ at a current density of 3.62 $A \cdot cm^{-2}$. This is substantially higher than the maximum experimental value derived from Figure 2 (0.81 $W \cdot cm^{-2}$ at 1.08 $A \cdot cm^{-2}$) which offer the possibility of further enhancements to the stack characteristics (volume and weight). However, it is necessary to point out that other performance limiting mechanisms will occur at such high current densities (mass transport) which will further limit the peak power achievable. Therefore, the theoretical peak power computed here only represents an upper limit.

The preceding results allow the computation of the power density, size and weight of an hypothetical and desirable 20 kW system (gross power, which means that parasitic losses, which were not measured or calculated in this study, need to be taken into account to compute the net power) operated at a current density of 0.861 $A \cdot cm^{-2}$. The results show that the Mk513 based system fits into the space shuttle volume allocation (112 vs 166 l) but its weight is substantially larger than the allocation (468 vs 119 kg). Other more advanced and higher gravimetric power density stack architectures, such as the Mk7 and Mk9 (both volume and weight targets are met with these designs), should therefore be considered for subsequent develop-

ment phases. It should also be noted that other specifications will need to be met such as output voltage, heat rejection and ability to operate with lower grade reactants.

It is difficult to eliminate heat in space since radiative heat transfer is largely dominant. Therefore, it is important that the amount of heat generated by the fuel cell is predictable and that heat removal mechanisms are known. The coolant heat dissipation at the beginning of life is given in Figure 4. The measured values are also favorably compared to a theoretical expression which indicates that the main heat removal mechanism is mainly due to the coolant flow [12]:

$$Q = iA \left(\frac{\Delta H}{nF} - V \right) \qquad (4)$$

where Q represents the heat dissipated in W, i the current density in $A \cdot cm^{-2}$, A the total active surface area in cm^2, $\Delta H/nF$ the thermoneutral voltage (higher heating value, 1.564 V) and V the cell voltage in Volts. Equation 2 is used to represent the V term in equation 4. The thermoneutral voltage under the present test conditions was determined by first computing the thermodynamic efficiency at the cell temperature ($\Delta G/\Delta H$ [13]) followed by the computation of $\Delta G/nF$ using the Nernst equation.

3.2 Stack performance over time

The polarization completed after more than 11,000 hours of operation illustrated in Figure 2 is represented by the following equation similar to Equation 2:

$$V = 0.883 - 0.068 \log(i) - 0.14i \qquad (5)$$
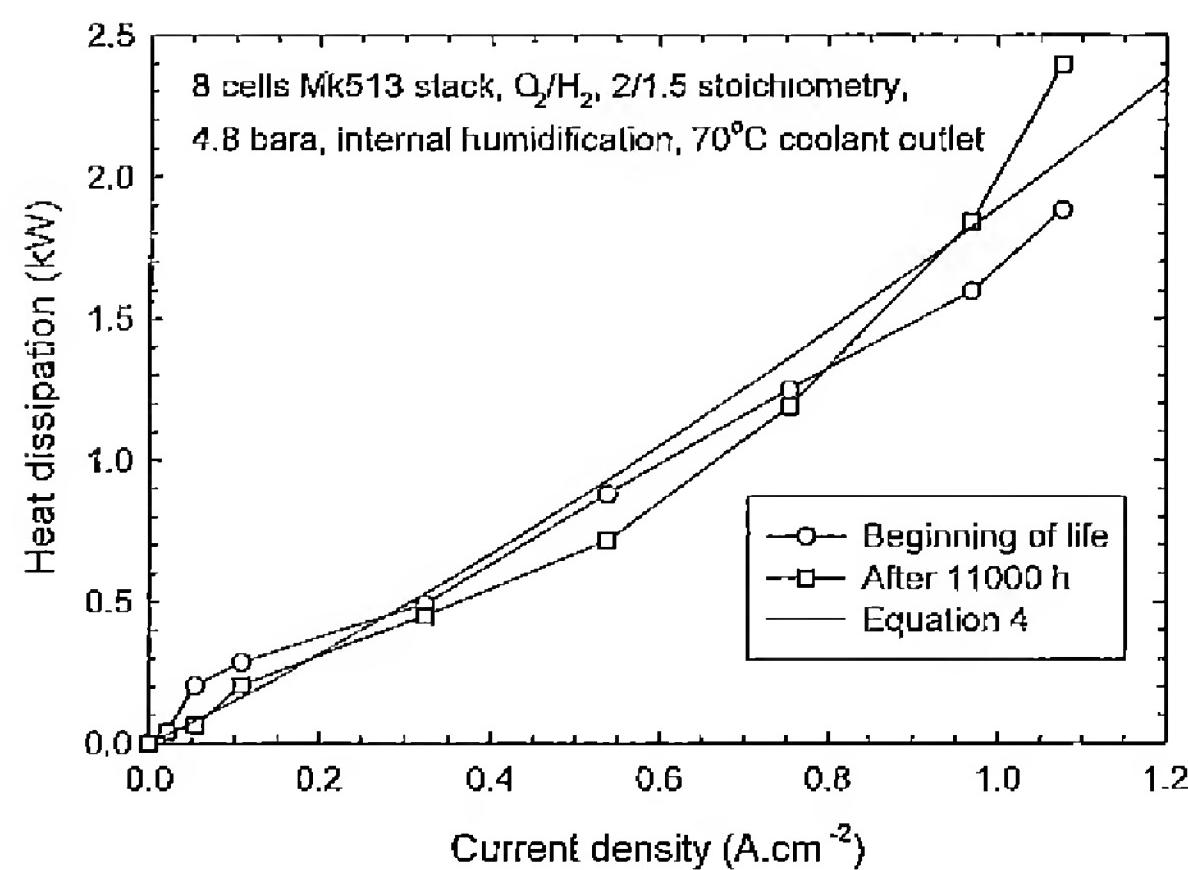
Figure 4: Comparison between the theoretical coolant heat dissipation and measured values obtained at the beginning of life and after more than 11,000 hours of operation.

A comparison between the beginning of life (Equation 2) and after more than 11,000 hours of operation data (Equation 5) reveals the appearance of a slight kinetic gain of 9 mV (an analysis of variance showed significance at the 1 % significance level between the beginning of life and after more than 11,000 hours of operation data when the error term was obtained by pooling all interaction terms). This is likely due to the presence of contaminants deposited on catalysts during the membrane/electrode assembly processing and subsequently oxidized during stack operation. It is also likely due to slow equilibrium processes occurring at the catalyst surfaces and in the membrane. In addition, a slightly larger ohmic resistance is observed (an increase from 0.111 to 0.14 Ωcm^2). This increase in resistance is not supported by the milliohmmeter measurements as will be discussed. At 0.538 and 0.861 A·cm^{-2}, the change in ohmic resistance respectively represents a 16 and 25 mV loss. A net performance loss of 7 and 16 mV supported by the polarization plots (the ohmic loss added to the 9 mV kinetic gain) at respectively 0.538 and 0.861 A·cm^{-2} is computed and will be used for comparison purposes with the cell voltage values recorded during the lifetest duration.

The cell performance standard deviation was not affected by operation even after 11,000 hours (Figure 3) which is partly indicative of the absence of significant new sources of variation associated with operation time. Low standard deviations lead to increased reliability by decreasing, for example, the likeliness of cell reversal during operational condition upsets or during dynamic operation.

Figure 5 show average cell voltages measured during the lifetest duration. Very low average degradation rates of -1.4 and -1.3 μV·h^{-1} were obtained at respectively 0.538 and

0.861 A·cm^{-2}. The cell performance loss during the lifetest is computed using these degradation rates and results in values of 16 and 14 mV at respectively 0.538 and 0.861 A·cm^{-2} after 11,072 hours. These values are consistent, within experimental error, with those deduced from the polarization curves (Figure 2). Published work for PEMFCs ([14-15]) using alternate membranes (Raipore R-1010 and R-4010, poly(tetrafluoroethylene-co-hexafluoropropylene) grafted with polystyrene sulfonic acid) showed significantly larger degradation rates which are mostly attributable to the membrane instability (for example, up to 50-250 μV·h^{-1}, [14]). The degradation rates obtained here for the PEMFC are also smaller by an order of magnitude than those published for the AFC (-20 μV·h^{-1}, [16]).
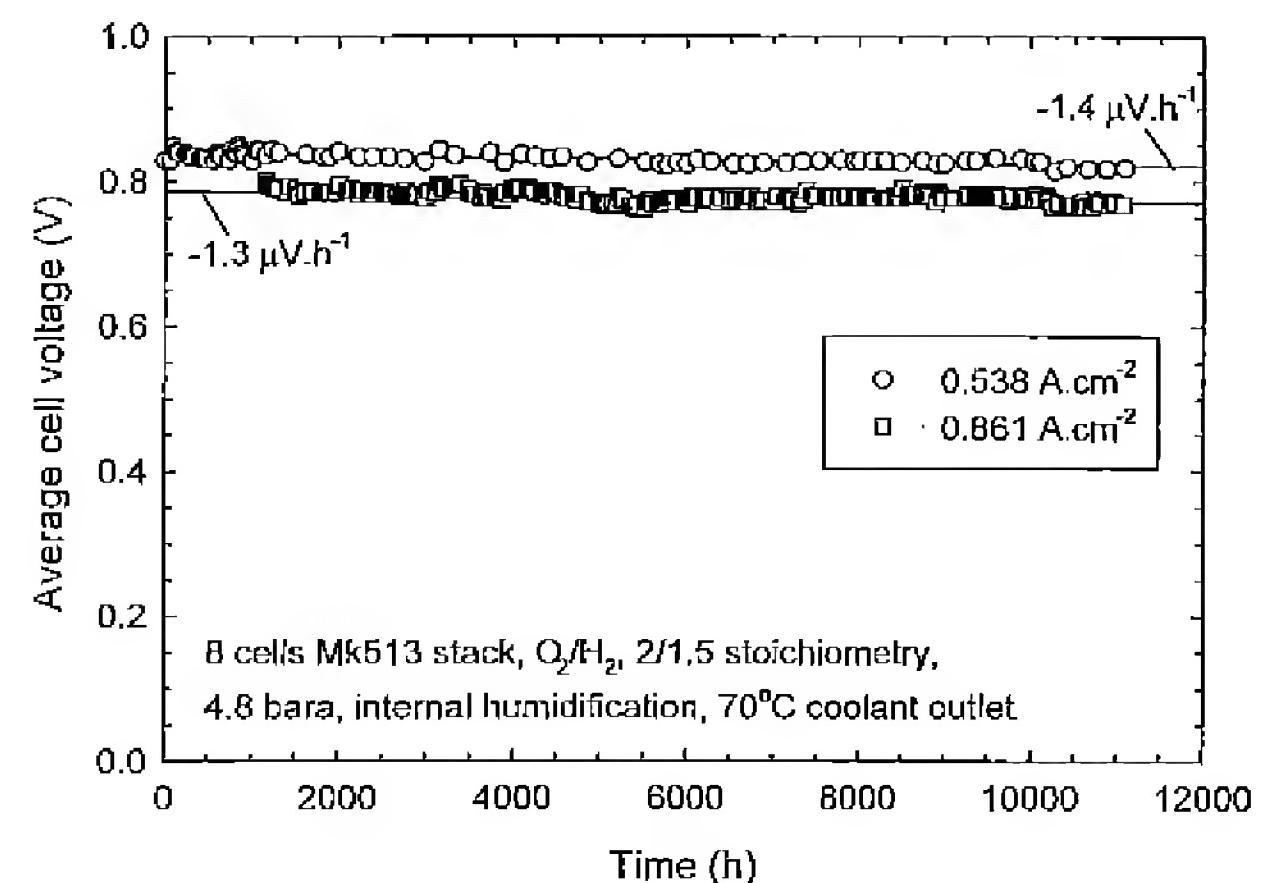

Figure 5: Average cell voltage at two current densities as a function of time.

The cell resistance was also measured during the lifetest duration and measured values appear in Figure 6 (the event at approximately 5000 hours was due to a change in the milliohmmeter unit used to take the measurements). Generally, the current density did not have any effect on the measured values, but an apparent decrease was observed over the lifetest duration (-2.8 and -2.2 nΩ·h^{-1} at respectively 0.538 and 0.861 A·cm^{-2}), which at first appears inconsistent with the increase deduced from the polarization curves. It should be noted again that the milliohmmeter operates at a frequency of 1 kHz which is sufficiently large to ensure that the measured values do not include mass transport related effects. Therefore, the ohmic region of the polarization curves is really pseudo-ohmic in character, comprising both ohmic and mass transport contributions (the only remaining cause of degradation besides kinetic and ohmic factors). The evidence suggests that there is an increase in mass transport losses partly compensated by a decrease in ohmic losses. This ohmic loss could be due to compression resulting in a slow reduction in membrane thickness over long

periods of time. Further evidence supporting these degradation mechanisms will be presented in the next section.
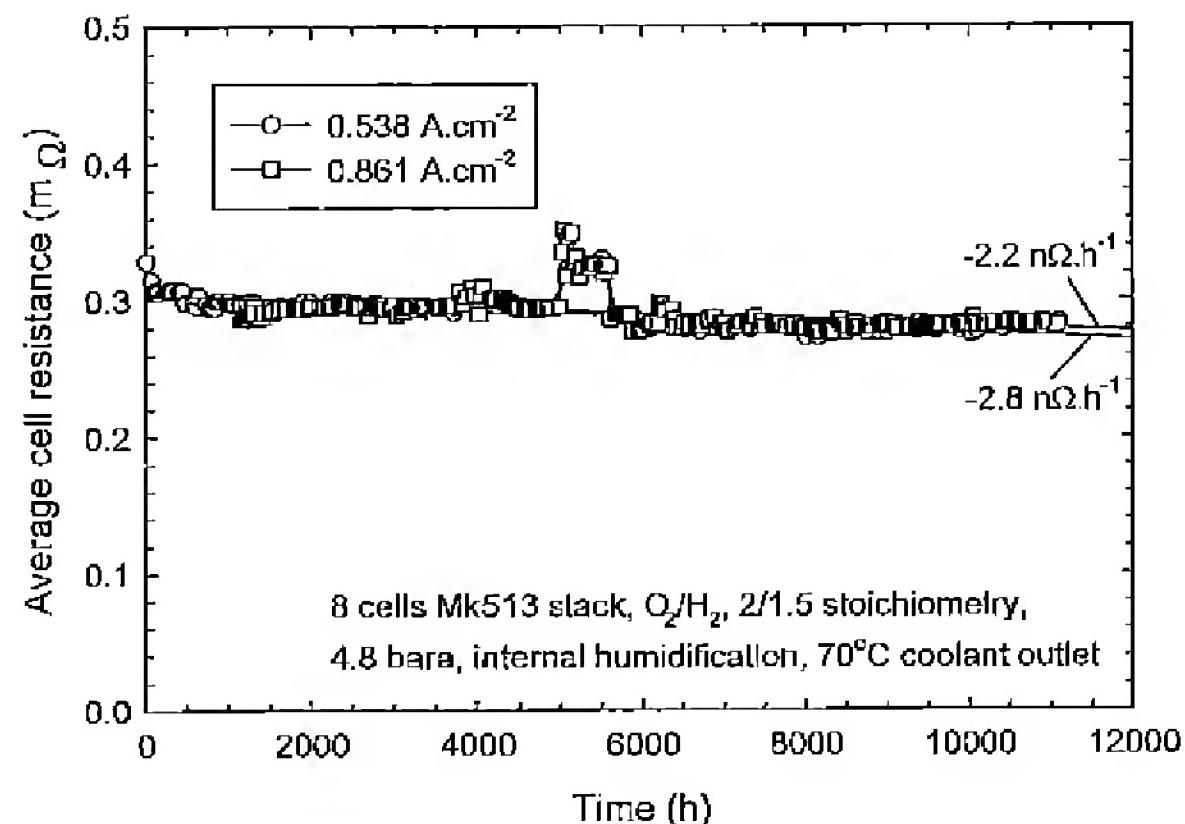

Figure 6: Average cell resistance at two current densities as a function of time.

The cell performance degradation rate had only a small negative impact on the power delivered by the stack (less than 3 % change in voltage at 1 A·cm^{-2} using equations 2 and 5) which could in practice be easily circumvented by slightly increasing the current density as long as the voltage stays within the allocated range. This strategy would also slightly and negatively affect system efficiency (increased heat rejection) while increasing reactant consumption. The coolant heat dissipation, related to cell performance, was unaffected by operation as shown in Figure 4. The variations are likely due to daily and seasonal changes in laboratory temperature which affect to a small extent the heat dissipated by natural convection.

3.3 Stack and test station component analysis

Although several types of analysis were carried out on many of the stack and test station components, a substantial proportion of the analyses did not reveal important or critical issues related to stack reliability. This is to a large extent due to the almost maintenance free operation and low cell performance degradation observed during the entire lifetest duration. The only significant material degradation mechanism identified was seal oxidation whereas the cell performance loss was due to a change in catalyst substrate hydrophilicity. External leaks and leaks between cathode and anode compartments were not detected during the entire lifetest duration.

Figures 7 and 8 show some of the water sample characteristic values obtained during the duration of the lifetest. With a filter unit, the water conductivity was kept at a low level of approximately 2 μS·cm^{-1}which resulted in minimal contamination problems. The filter unit needs to be repacked when the

conductivity value increases or when the pH decreases, indicating that one or both of the ion exchange resins is saturated with ionic contaminants. The filter unit needed to be repacked twice during the lifetest (at 4076 and 8513 hours) which lead to a deduced lifetime in the present test configuration of approximately 5,000 hours. The large water conductivity values obtained at the beginning and near the end of the lifetest were due to substantial periods of test station inactivity. During these periods, contamination of the water by test station, stack and membrane/electrode assembly materials was still occurring while the filter unit was inactive, resulting in increased water conductivity values and decreased water pH values when the tests were resumed and the test station was active. The results also reveal that conductivity is a more sensitive parameter to establish the need for filter maintenance. Table 2 reports the measured total organic carbon values for different samples. The total organic carbon values were always low during the entire duration of the lifetest, which means that the activated carbon bed was never saturated before the ion exchange resins needed replacement. As a consequence, its size could be reduced to save space. Also, little contamination occurred after the water was transferred to the reactant gases as evidenced by the low total organic carbon content values of the water condensed from the stack outlets. The fluoride content of water samples (same sources as indicated in Table 2) was determined and always revealed values below the detection limit (0.05 mg·l^{-1}). These results (Figures 7 and 8, Table 2) indicate that the water produced was significantly pure and possibly potable (further specific tests, such as bacterial count, are required to confirm this suggestion).

Table 2: Water sample total organic carbon values measured during the PEMFC lifetest

Time (h)	Anode Condenser (ppm)	Cathode Condenser (ppm)	Coolant/Humidification Circuit (ppm)
115	5.1	1	Not measured
475	2.9	1.1	Not measured
2997	1	1.6	Not measured
6020	1.8	1.2	< 1
7018	1.8	1.1	1.2
8010	< 1	< 1	< 1
9100	< 1	< 1	< 1
10027	1.1	< 1	< 1
11072	2.1	< 1	1.2

The residual gas analyzer data revealed that nothing was detected beyond 50 atomic mass units up to the instrument limit of 300 atomic mass units. It was concluded that the inlet gases contain small amounts of contaminants (H_2O, N_2, Ar, O_2, CO, CH_4 for hydrogen, and H_2O, N_2, Ar, H_2, CO, CH_4 for oxygen) which correspond to those described in the specifications. There
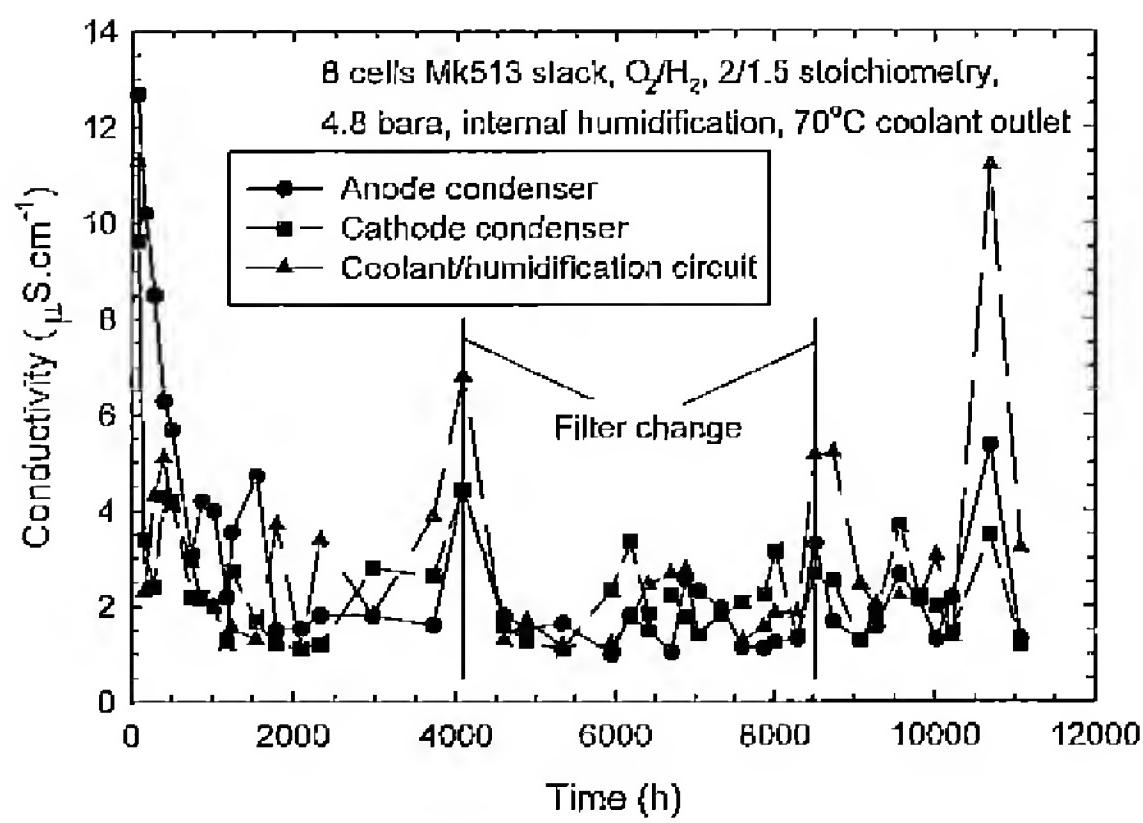
Figure 7: Water sample conductivity values as a function of time.
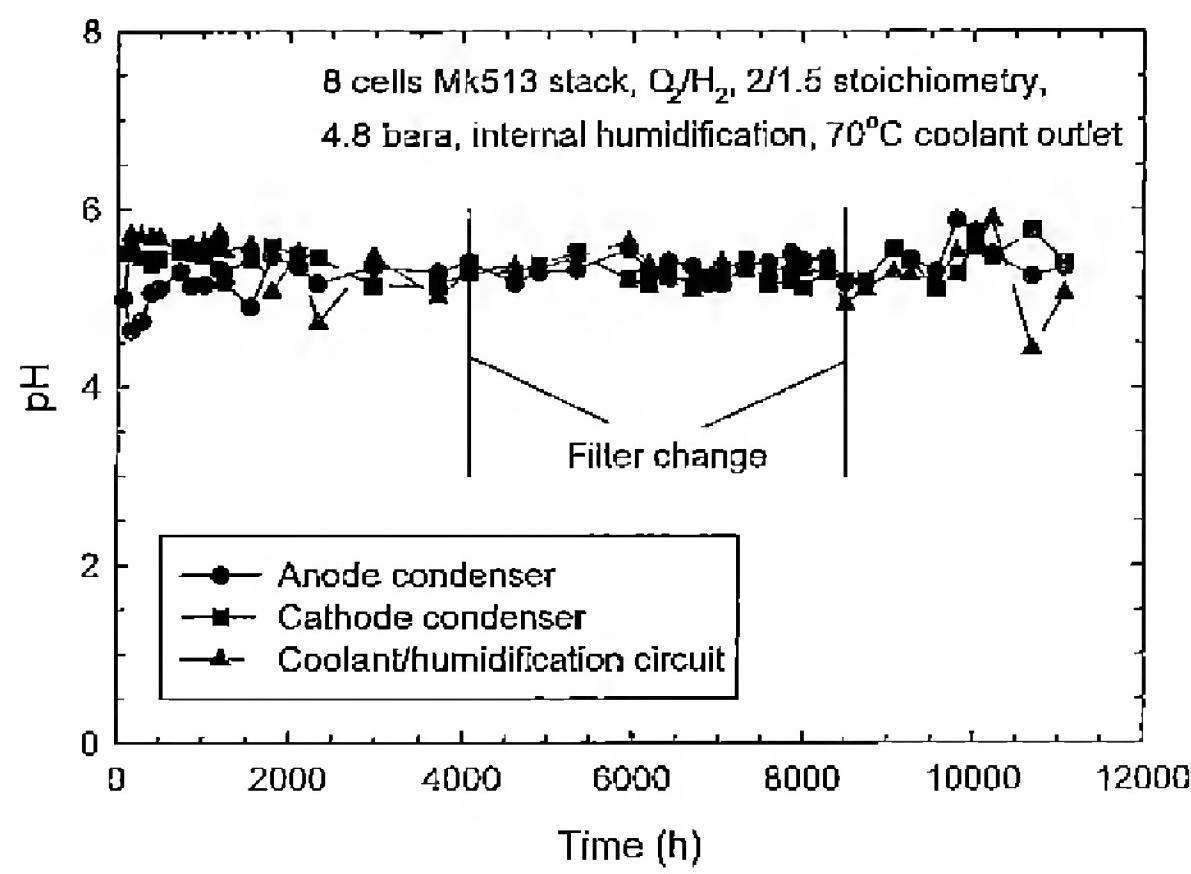

Figure 8: Water sample pH values as a function of time.

was no evidence that inlet gases were modified by addition or formation of contaminants within the stack.

Generally, more contaminants were found in the humidification membrane than in the delaminated membrane/electrode assembly samples. This is expected because humidification membranes are in direct contact with the largest carrier/source of ionic contaminants (coolant/humification water). Some contaminants may escape through the membrane and find their way to the membrane/electrode assembly. For all samples, the contaminants levels are low even after more than 11,000 hours of operation and did not affect the cell performance. Contaminants can increase kinetic losses by adsorption on catalyst surfaces and ohmic losses by ion exchange (H^+ displacement by other cations) [17]. However, such trends were not experimen-

tally observed (the increase in pseudo-resistance is due to mass transport).

There is indication that the membranes did not sustain any significant chemical modification during the lifetest duration (polarization, resistance, fluoride loss, membrane composition). The observed decrease in ohmic resistance was due to the appearance of a mass transport loss (pseudo-ohmic resistance). Figure 9 illustrates the cathode side of membrane/electrode assembly 8. It is observed that the flow field is clearly visible on the carbon fiber paper. The areas corresponding to the channels are more hydrophilic than those located below the flow field landings. This is the characteristic that makes the flow field appear so clearly when the membrane/electrode assembly is slightly wet. This is explained by either a change in the carbon fiber paper Teflon content, a change in carbon surface groups, a change in effective porosity (possibly due to long term mechanical compression) or a localized accumulation (near the carbon fiber paper/flow field interface) of hydrophilic impurities which may lead to mass transport problems if water accumulates, thus making oxygen diffusion towards the catalyst layer more difficult.
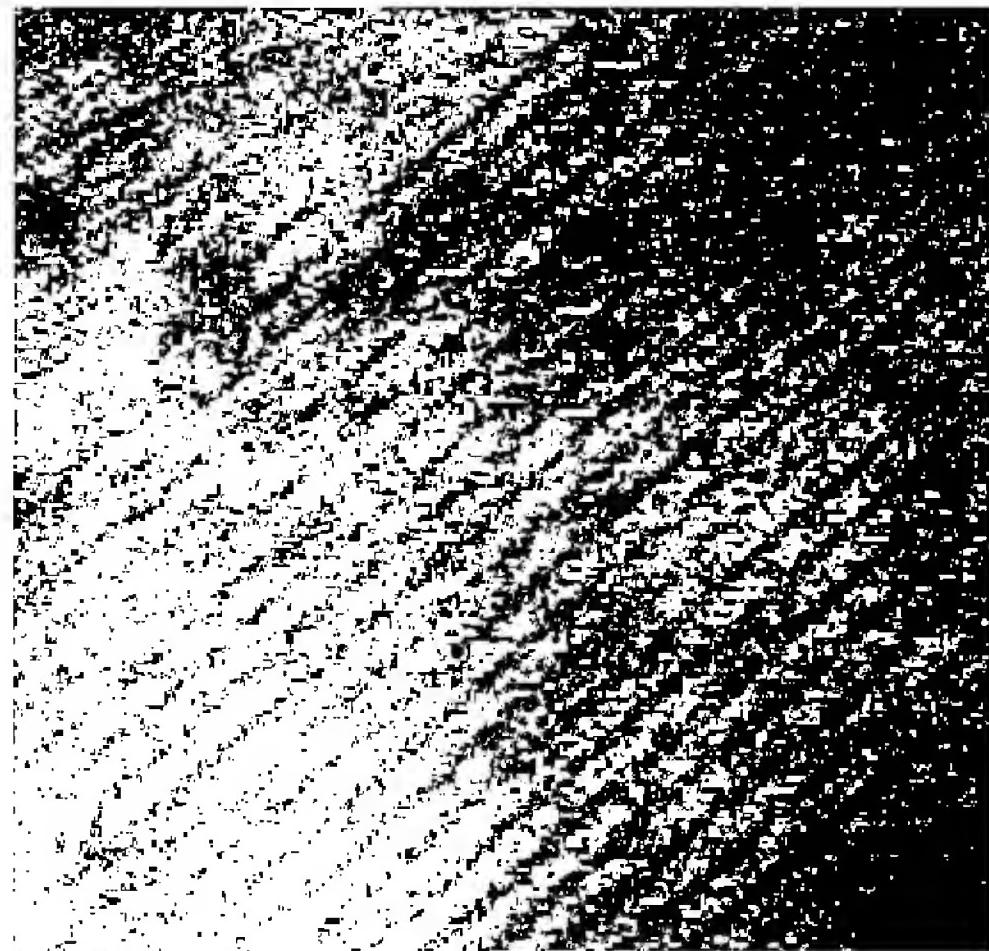

Figure 9: Cathode side of membrane/electrode assembly 8 after more than 11,000 hours of operation

Although no leaks related to seal failures were detected during the entire lifetest duration, seals were affected by long exposure to the stack operating conditions. Sample analyses revealed that oxidation has taken place and that it was more extensive in the humidifier than in the active section of the stack. These results indicate that further work is necessary to improve seal resistance. Test station materials were visually examined after the lifetest was completed, but no abnormalities were detected. However, it is still possible that the materials were affected (for example, hydrogen embrittlement) and further tests will be required to confirm this hypothesis.

4. CONCLUSION

Under the direction of NASA, a PEMFC lifetest was completed to determine degradation mechanisms. The lifetest was carried out for more than 11,000 hours and demonstrated very low performance degradation ($< 2 \ \mu V \cdot h^{-1}$). Interestingly, the lifetest was not terminated by a technical deficiency but rather by the fact that the desired 10,000 hours requirement was achieved. The PEMFC also exhibited some other desirable characteristics such as the possibility that the water produced is potable, low cell performance standard deviations indicative of the reproducibility of the membrane/electrode assembly and stack manufacturing processes, and the possibility to increase system power density and/or decrease system size. Other stack designs now available from Ballard would meet the space shuttle weight constraint of a desirable 20 kW system.

The lifetest results also indicate that the cell performance is affected over long periods of operation by one possible mechanism. There is a slight increase in mass transport loss which is consistent with previous reports [17]. From a mechanical point of view, the weakest stack component appears to be the seal which is subjected to oxidation. Further cell performance and reliability improvements of PEMFCs operated with oxygen and hydrogen reactants will require work in these key areas.

On the basis of the present work, which successfully demonstrated critical NASA requirements and identified the PEMFC as an excellent candidate for future space applications, the following recommendations are made, which could form the basis of a subsequent test program:

- Increase cell performance to allow operation at high current densities and high power densities without compromising heat rejection requirements

- Investigate other more advanced stack hardware to ensure that the weight requirement is met

- Confirm by more appropriate tests the product water potability

- Confirm the cause of the performance mass transport loss and develop associated mitigation strategies

- Identify and test more durable seal compositions

- Consider new modes of operation (dead end, recirculation)

- Determine the effects of lower purity fuel and oxidant reactants

- Design, build and test a complete 20 kW ground demonstration system

5. ACKNOWLEDGMENTS

REFERENCES

[1] G. Halpert, H. Frank, S. Surampudi, Interface, **8**, 25 (Fall 1999).

[2] M. Warshay, P. R. Procopius, J. Power Sources, **29**, 193 (1990).

[3] M. Warshay, P. Procopius, M. Le, G. Voecks in "Proceedings of the 1997 32nd Intersociety Energy Conversion Engineering Conference", Part 1 of 4, paper 97294, IEEE, Piscataway, NJ, USA, 1997, page 228.

[4] G. Suljak in "1994 Fuel Cell Seminar Program and Abstracts", Courtesy Associates, Washington DC, 1994, page 412.

[5] "Standard Methods for the Examination of Water and Wastewater", 17th and 19th editions, edited by M. A. H. Franson, American Public Health Association, Washington DC, 1989 and 1995.

[6] J. Kim, S.-M. Lee, S. Srinivasan, C. E. Chamberlin, J. Electrochem. Soc., **142**, 2670 (1995).

[7] J. Lee, T. Lalk, A. Appleby, J. Power Sources, **70**, 258 (1998).

[8] G. Squadrito, G. Maggio, E. Passalacqua, F. Lufrano, A. Patti, J. Appl. Electrochem., **29**, 1449 (1999).

[9] D. Chu, R. Jiang, C. Walker, J. Appl. Electrochem., **30**, 365 (2000).

[10] E. Passalacqua, F. Lufrano, G. Squadrito, A. Patti, L. Giorgi, Electrochim. Acta, **46**, 799 (2001).

[11] L. Pisani, G. Murgia, M. Valentini, B. D'Aguanno, J. Power Sources, **108**, 192 (2002).

[12] K. Scott, "Electrochemical Reaction Engineering", Academic Press, New York, 1991.

[13] K. Kordesch, G. Simader, "Fuel Cells and their Applications", VCH, Weinheim, 1996.

[14] H. Wang, G. A. Capuano, J. Electrochem. Soc., **145**, 780 (1998).

[15] F. N. Büchi, B. Gupta, O. Haas, G. G. Scherer, Electrochim. Acta, **40**, 345 (1995).

[16] "Fuel Cell Handbook", 5th edition, Department of Energy, Morgantown, West Virginia, 2000.

[17] J. St-Pierre, D. P. Wilkinson, S. Knights, M. Bos, J. New
     Mat. Electrochem. Systems, **3**, 99 (2000).

- Schulze, M. et al; *Degradation of Sealings for PEFC test cells . . .*; Journal of Power Sources; 127, 222-229 (2004).

Degradation of sealings for PEFC test cells during fuel cell operation

M. Schulze [a,*], T. Knöri [a], A. Schneider [b], E. Gülzow [a]

[a] Institut für Technische Thermodynamik, Deutsches Zentrum für Luft-und Raumfahrt, D-70569 Stuttgart, Germany
[b] Adam Opel AG, GAPC, IPC 81-90, 65423 Rüsselsheim, Germany

Abstract

For long-term operation of fuel cells the stability of all components is needed under extreme conditions. Especially the components in polymer electrolyte fuel cells (PEFCs) may show corrosion problems caused by the acid character of the solid electrolyte. One of the parts, which is commonly neglected, is the sealing material. Sealings are necessary for separating the gas compartments from the each other in order to avoid mixing of hydrogen and oxygen. A typical sealing material is silicone.

Fuel cell components are characterized after operation in single cells under typical fuel cell conditions. After fuel cell operation frequently an alteration is visible on the sealing and the membrane parts which were in direct contact with each other. Those parts of the membrane, which were in contact with the sealing surface, became colored. Motivated by this observation membranes and sealings were investigated by scanning electron microscopy (SEM) and energy dispersive X-ray analysis (EDX). In addition, electrodes and backings were investigated by X-ray photoelectron spectroscopy (XPS).

With the XPS measurements of the electrodes operated in a silicone sealed cell, residues of the silicone were detected on its surface. This indicates that the decomposition products of the silicone seals have a high mobility. In SEM/EDX mappings, an enrichment of silicone residues on the platinum was observed. Therefore, the decomposition products may contribute to a poisoning of the catalysts and may also change the hydrophilic/hydrophobic characteristic of the electrodes.
© 2003 Elsevier B.V. All rights reserved.

Keywords: PEFC; Silicone; Sealing; Degradation; Scanning electron microscopy; Energy dispersive X-ray analysis; X-ray photoelectron spectroscopy

1. Introduction

In the last decade worldwide energy consumption continued to climb. It increased in the last decade by some 10% up to approximately 3.6×10^{20} J in the year 1999. According to the International Energy Agency's (IEA) World Energy Outlook, the global demand for primary energy will increase by 57% (corresponding to 2% a year) from 1997 to 2020 at an annual economic growth of roughly 3%. The IEA anticipates an annual rise in global CO_2 emissions between 1997 and 2020 of almost 14 billion tons. This corresponds to a total increase of 63% or 2.1% a year [1,2]. If this increase of consumption is maintained, fossil energy resources will be spent within a few generations and the problem of environmental pollution will become a key issue for the future of mankind. Therefore, the future of energy supply lies in renewable energy sources and developing new energy conversion technologies such as fuel cells. Due to their potential in converting chemical energy with high efficiency directly into electrical energy and their environmen-

tally friendly character, fuel cells and especially the polymer electrolyte fuel cell (PEFC) have the chance to become a sustainable, resource-saving energy source for diverse applications, e.g. for the mobile sector [3].

The modular design of a PEFC suggests that manufacturing will in future will be of low-cost and permits mass production. Recent improvements in fuel cell technology have led to a degree in development, which allows to envisage commercial fields. Within the next decades a successive replacement of conventional energy conversion technologies is likely, even if certain technical obstacles remain still to be overcome. For long-term operation of fuel cells stability of all components is needed. At present, the status of fuel cell development can not guarantee sufficient life times of several thousands of hours for mobile or portable applications and several ten thousands of hours for stationary applications. Therefore, the investigation of degradation mechanisms is a main topic in fuel cell research [4]. However, only a few publications exist concerning the investigation of degradation effects of polymer electrolyte membrane fuel cells [5–16].

One component commonly neglected in the research of degradation effects is the sealing material. In a PEFC sealings are necessary to separate the gas compartments from

* Corresponding author. Tel.: +49-711-6862-456;
fax: +49-711-6862-747.
E-mail address: mathias.schulze@dlr.de (M. Schulze).

the each other and to avoid mixing of hydrogen and oxygen respectively. A faulty or inappropriate sealing leads to fuel losses and reduced voltage due to the formation of a mixed potential at the electrodes. Usually the resulting gas mixture can explode if the ratio of oxygen and hydrogen lies in a certain range. In a fuel cell, the hazard of an explosion is improbable due to the presence of the noble metal platinum. Platinum acts as a catalyst and stimulates the reaction of the fuel and the oxidant gas. But the heat of reaction of this catalytic combustion generates hot spots in the MEA. Thus, temperature rises until the membrane will be destroyed. The resulting holes enhance mixing of the gases that finally may lead to an open fire. Besides these safety aspects, it is also necessary from the manufacturer's point of view that the sealing materials should be easy to handle, low priced and chemically inert, even under the corrosive environment caused by the acid electrolyte and the chemical conditions. Typical sealing materials are fluorine caoutchouc, EPDM and silicone.

2. Experimental

2.1. Sample preparation

For the experiments membrane–electrode assemblies (MEAs) with two different types of electrodes were used. The first one contains commercial electrodes purchased from E-TEK with 20 wt.%. Pt/C and a Pt-loading of $0.4\,mg/cm^2$. The second one was a proprietary development prepared with the DLR dry spraying technique. In contrast to typically used preparation methods for commercial electrodes from a catalyst-containing suspension, the DLR manufacturing way is a dry process avoiding solvents and complicated process steps and can fit to a fully automated mass production [17–22]. It is a consequent further development of the manufacturing technique for alkaline fuel cell electrodes [23–30], with a new deposition type of the powder mixture for the reaction layer. The resulting electrodes contained 20 wt.% Pt/C and a Pt-loading of $0.2\,mg/cm^2$ on each electrode. On each electrode E-TEK single sided backings were used as gas diffusion layers. In both cases the MEAs were prepared by hot pressing the electrodes (1.6 MPa, 2 min, 160 °C) onto a Nafion® membrane (purchased from DuPont). The active area of each MEA was $4.8 \times 4.8\,cm^2$.

2.2. Electrochemical experiments

All electrochemical experiments were carried out in a $23\,cm^2$ single cell. On the cathode side, a stainless steel electrode holder with moulded meander structures was used as gas distributor. The current collector on the anode had a flow-field with a chocolate wafer structure which was divided into 4×4 quadratic segments of stainless steel. By means of this device, the value of the current which is generated in a certain region of the membrane electrode assembly

was recorded separately for each segment, so that the MEAs can be characterized by V–I curves and local current densities. At DLR, the segmented cells are used for the investigation of hydrogen supplied polymer electrolyte membrane fuel cells as well as for the investigation of direct methanol fuel cells (DMFC). More details of this device can be found in [31]. Between the membrane electrode assembly and the segmented cell, a sealing of silicone-red® was used for separating the gas compartments against the environment. On both sides of the MEA, silicone sealings were used.

The cells were fixed in test setups which were developed for automatic, continuous and safety controlled operations with hydrogen and oxygen or air. These facilities allow the variation of the operating conditions in a wide range of parameters [21,31,32]. In our experiments the cells operated in the dead-end-mode at a temperature of 80 °C with pure hydrogen and oxygen (H_2 5.0 and O_2 4.8, Messer Griesheim) at 2.0 bar absolute. Both gases were not humidified. The anode side was purged by opening the outlet valve with pulses of 0.5 s every 900 s. On the cathode side, the outlet was opened for 0.5 s every 120 s at the beginning. Later on, the intervals were extended to 240 s. For the start-up, the MEAs were humidified by an injection of liquid water directly into the test-cell. The cell voltage was 500 mV. Under these conditions, the cathode became flooded over the operational time.

2.3. Physical characterization

The different fuel cell components were characterized after operation.

After preparation and electrochemical stressing by fuel cell operation, the MEAs were investigated by scanning electron microscopy (SEM) [33] combined with energy dispersive X-ray spectroscopy (EDX) [33], X-ray photoelectron spectroscopy (XPS) [33] and porosimetry (with mercury intrusion) [34,35]. For the SEM and EDX measurements, a Zeiss Gemini microscope (LEO) was used in combination with a NORAN VOYAGER 3000 EDX-detector. This SEM allows high magnification imaging at low and high beam voltages (1–30 keV). The SEM and EDX measurements were performed on the backside surface as well as on cross sections of the MEAs.

The XPS measurements were performed in a XSAM 800 (Kratos). The XPS equipment is described in more details in [36]. XPS yields information about the chemical composition of the surface and the method shows a very high surface sensitivity. In contrast, EDX has a low surface sensitivity and yields information about the bulk composition of the volume close to the surface. SEM yields information about the surface structure and gives information about the bulk character. The used XPS does not allow to investigate the samples with a high lateral resolution, the possible resolution amounts to a few mm^2; therefore, no XPS investigations on cross sections were performed, but only the electrode surfaces, reaction layers and backings, as well as the membrane surface of the MEAs.

3. Results and discussion

After an operational time of several days, a leakage test showed that the mechanical function of the silicone sealings still remain. After these tests, the fuel cells were opened and the different parts of them were examined. At first, it can be noticed that the sealings always stuck on the Nafion® membrane and an alteration of those membrane areas which were in direct contact with the sealings was visible. Those parts of the membrane surface became colored yellow, which indicates a chemical reaction of the sealing material. A thermal change of the sealing could be excluded, because their range of application was from −90 up to 250 °C according to the manufacturers specification.

Motivated by the change of the silicone appearance, the MEA was studied with different physical methods to investigate alterations in the structure and in the chemical composition. On the cathode backside, numerous particles were visible. The particles were imaged with optical and scanning electron microscopy. The particle sizes are in the range of below 1 μm to few hundred μm. Different forms of the particles were observed; compact particles, which were determined by EDX as platinum oxide shown in [37] and more structured particles.

Fig. 1 shows a photography of the MEA taken with a light microscope. The displayed area is approx. 5.5 × 3.9 mm². The bright region at the left upper corner shows the membrane, below the diagonal in the figure the cathode backing is displayed. On the cathode backing, bright domains can be observed. Thus, depositions were observed on the whole cathode backing. On the anode backing, no particles were visible by light microscopy.

Fig. 2 shows a SEM image of such a structured particle. The first explanation for particles on the cathode backside would be a kind of impurities, but the displayed particle has a form like a crumpled foil and such a form of a particle is untypical for dust, abrasion or similar impurities. Therefore, the particles were investigated by EDX. In the EDX analysis silicon and oxygen were determined as main components. Silicon oxide particles in the form of sand (crystalline structure) as well as in form of glass (amorphous structure) typically have a different particle shape. In addition, if the particles were abrasion fragments of the silicone sealing, similar particles should also be found on the anode side, which was not case. Therefore, the displayed particle seems to be a separated part of the silicone sealing or is formed by a reaction with decomposition fragments of the silicone sealing. A significant concentration of carbon and fluorine in the particles was not observed. In the carbon mapping, the structure of the carbon cloth is shadowed by the particle. From the silicon, oxygen, carbon and fluorine signal, it cannot be distinguished if the particle is a fragment of the sealing or a decomposition product. In addition to the silicon and oxygen, some platinum can be detected. The platinum in the particle is observed in the edges of the investigated particle. The platinum decoration of the edges indicates an alteration in the electrodes. The mobility of platinum and its agglomeration in PEFC electrodes is a known effect [37,38], where the platinum migrates in the direction from the anode to the cathode [37].

The particles on the cathode backing are distributed over the complete area. Consequently, the decomposition products from the silicone sealing must be mobile.

On the anode backing no particles, neither platinum oxide [37] nor the silicone-containing particles could be observed. Two different hypotheses allow to explain why no silicon is observed on the anode backing: on the one hand, the decomposition components of the silicone move in the


Fig. 1. Photography of membrane electrode assembly made by a light microscope on the cathode backing. The displayed area is 5.5 × 3.9 mm².
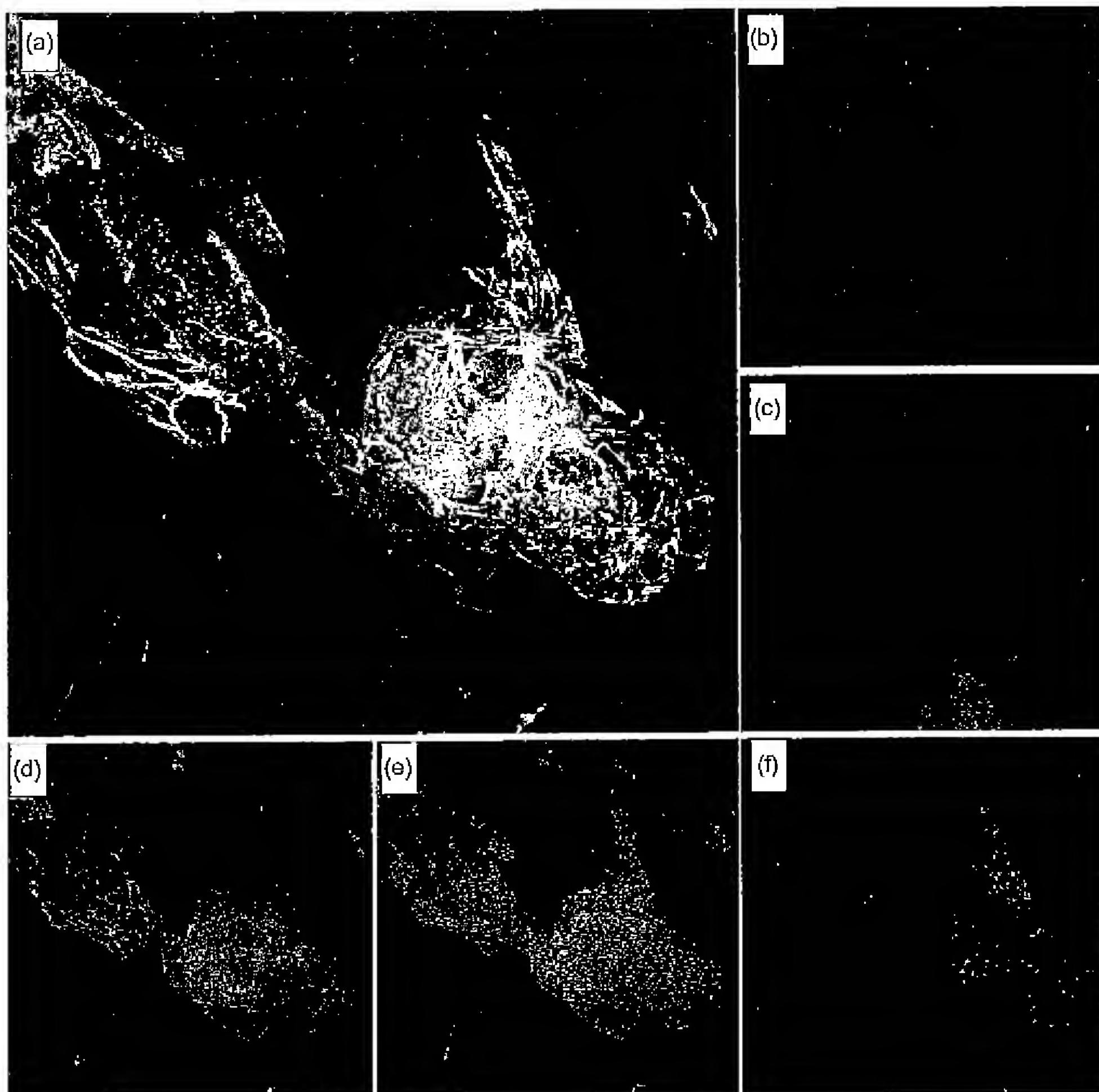
Fig. 2. SEM micrograph of a particle of the backside of the cathode backing after fuel cell operation (a) and the corresponding EDX mappings for carbon (b), fluorine (c), silicon (d), oxygen (e) and platinum (f). The imaged area is $460 \times 460\,\mu m^2$.

same direction as the platinum; possibly the driving force for the mobility is the electrical field for both. On the other hand, the reaction conditions on anode and cathode differ extremely; therefore, it is possible that the silicone sealing decomposes only on the cathode side. Which explanation is correct cannot be derived from these investigations on the reaction layer. Therefore, additional measurements are needed.

In an independent XPS investigation on the reaction layer surface of a used commercial electrode applied as anode in the reaction layer silicon was detected (Fig. 3). Also, in this case, silicone red® was used as sealing material for the cells. For the XPS analysis of used electrodes using commercial electrodes, there is the advantage that the electrodes can be better separated from the membrane electrode assemblies after operation. This is due to the preparation technique; the commercial electrodes are manufactured as self contained units; in contrast the reaction layers prepared with the DLR dry spraying technique [20,21,39] are fixed on the membrane and cannot be separated. The XP spectrum is dominated by the carbon, oxygen and fluorine signal. The platinum cata-

lyst in the commercial electrodes is covered by a polymer film [21,40]. Additionally, the signal of silicon, enlarged in Fig. 3, was observed. This is a second indicator for a high mobility of the silicone decomposition products. Combining the high mobility of the silicone decomposition fragments and the attraction between these and the platinum catalyst a poisoning of the catalyst becomes more likely.

Furthermore, the sealings have a hydrophobic character. Therefore, the decomposition products could also be hydrophobic and may change the wetting behavior of the electrodes, which is determined by the content of polytetrafluoro-ethylene PTFE [41]. The influence of the silicone decomposition fragments on the wetting behavior of the electrodes cannot be determined, because the PTFE in the electrodes is also changed by the electrochemical stressing due to fuel cell operation [42].

The silicon in the anode reaction layer is a clear indicator that the silicon decomposition fragments move in the same direction as the platinum—from the anode backing in the direction to the cathode backing. In addition, the XPS measurements show clearly that the silicone on the anode side
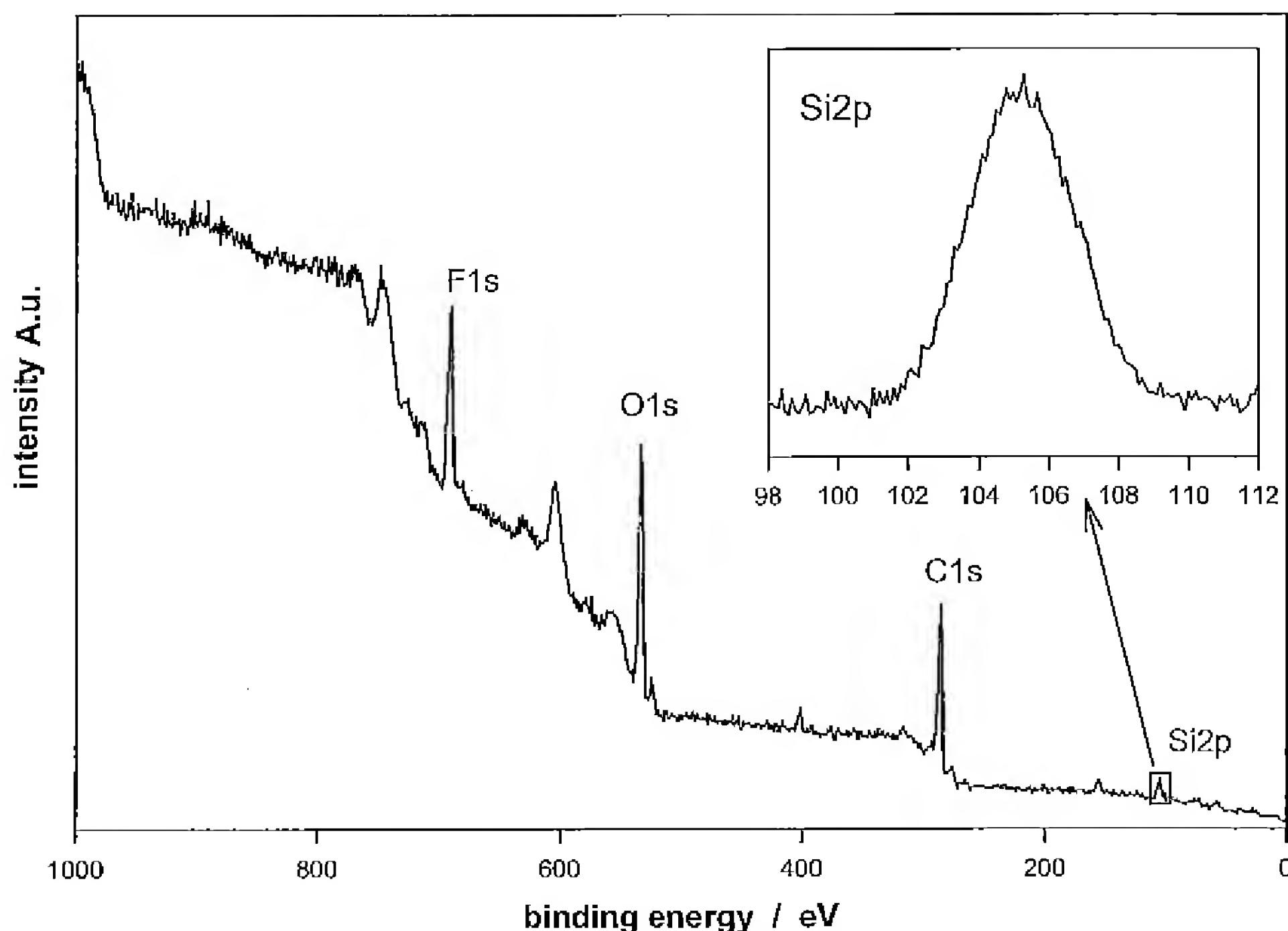
Fig. 3. XP spectrum of an used electrode (The Si2p-region is enlarged).

decomposes, too. An alternative explanation for the silicon on the anode reaction layer could be given, if the silicone decomposition products migrate from the cathode side through the membrane to the anodic reaction layer. This should be excluded because no silicon was detected on the cathodic reaction layer as well as no silicon was observed in the membrane (see below). Therefore, the silicone decomposes also on the anode side, this means, the reaction conditions are not the reason why the silicon-containing particles are only observed on the cathode backing and not on the anode backing. Therefore, it can be concluded that the movement of the silicone decomposition fragments is not induced by the different reaction conditions on anode and cathode, but is induced by a directed movement of the silicone decomposition fragments.

In order to get more information about the movement of the silicone decomposition fragments and the commonly observed platinum and silicon a cross section of the used DLR MEA operated with silicone red® as sealing material was investigated by SEM and EDX (Fig. 4). Fig. 4a and b show the SEM micrographs imaged with back-scattered electrons and with secondary electrons. Using the back-scattered electrons for the imaging, the contrast is determined by the difference in the efficiency to back-scatter electrons. Heavy elements are displayed brighter than light elements in this imaging mode. If the secondary electrons are used for the imaging, the contrast is determined by the differences in the electron work function. In addition, the secondary electrons are detected in a high angle to the sample normal, therefore, the shadowing effect yields a more steric impression. In both imaging modes, the platinum is displayed bright and

the membrane is displayed dark. The thickness of the membrane is approximately 90 μm.

In the EDX mapping, carbon is detected in the electrodes, while the carbon concentration in the membrane is significantly lower. The fluorine is bound in the polymers, PTFE and Nafion®. Consequently, the fluorine concentration is maximum in the polymer electrolyte membrane and the hydrophobic layer. The electrolyte membrane also contains a significant concentration of sulfur. The platinum is concentrated in the reaction layer as expected. Very interesting is the distribution of the silicon in the cross section. The decomposition products of the silicone sealing could only be found on the reaction layer of the anode whereas the cathode reaction layer remains silicon-free. Only particles containing silicon are found in the cathode backing.

The electrolyte membrane contains oxygen and sulfur. In addition, the oxygen of the air can oxidize the catalyst in the reaction layers after operation and separation of the membrane electrode assemblies from the fuel cell. Consequently, oxygen is found in the reaction layer and in the membrane. The oxygen concentration in the anode reaction layer is higher than in the cathode reaction layer. In addition, a high oxygen concentration is found in the silicon containing particle in the cathode backing. Both, the higher oxygen concentration in the anode reaction layer and the oxygen in the silicon particles, show that oxygen is found accompanying the silicon—this means the silicon is in an oxidized form.

In the membrane, no silicon is observed. Consequently, the transport of the silicone decomposition fragments in the membrane and in the electrode must be completely different.
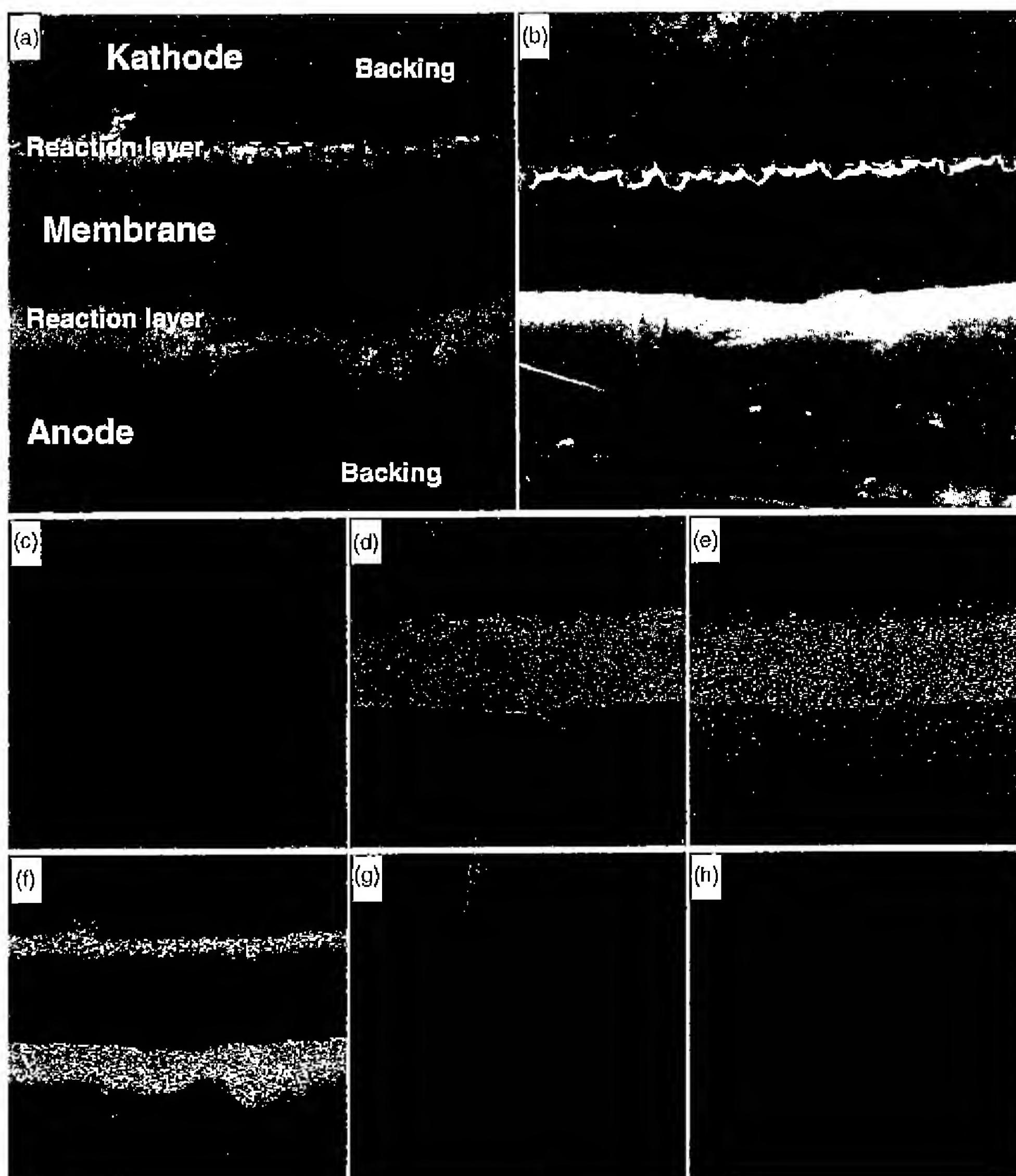
Fig. 4. SEM micrograph and EDX-mappings of a MEA cross section: (a) SEM micrograph image with back-scattered electrons; (b) imaged with the secondary electrons, (c–h) EDX mappings for the elements: (c) carbon, (d) fluorine, (e) sulfur, (f) platinum, (g) silicon and (h) oxygen. The imaged area is 190 × 190 μm².

If the transport in the membrane were to would be fast, a low silicon concentration in the membrane is possible, but in the cathode reaction layer silicon should also be observable. Therefore, the absence of the silicon in the membrane is effected by the hindering of the diffusion into the membrane from the electrode side. Consequently, it can be concluded, that the Nafion® membrane is a diffusion barrier for the silicone decomposition fragments.

The combined appearance of silicon and platinum especially in the EDX analysis of the particles on the cathode backing indicates that an attractive interaction between platinum and the silicone decomposition fragments exists. The attractive interaction could be the cause for the directed movement of the silicone decomposition fragments, because

the silicone fragments follow the moving platinum, but in this case also silicon should be detected in the cathode reaction layer. Therefore, most likely for the movement of the silicone decomposition fragments a directed driving force exists like that for the platinum migration.

A risk for fuel cells is that the probability of a poisoning of the platinum catalyst increases due to the attractive interaction. The poisoning of the catalyst is more critical in the anode than in the cathode, because for the silicone decomposition fragments the driving force yields a migration away from the cathode reaction layer.

In addition to a poisoning of the catalyst, the silicone decomposition fragments may change the wetting behavior of the electrodes. On the anode side, mainly the reaction layer

is influenced; on the cathode side, mainly the gas diffusion layer. In both electrodes, the transport processes will be influenced by the decomposition of the silicone. Caused by the barrier function of the polymer electrolyte membrane, the silicone decomposition fragments will be enriched on the interface between the membrane and the anode reaction layer. This will increase the transition resistance, whereas the problem is more critical in MEAs with self-contained electrodes assemblies than in MEAs with reaction layers directly fabricated onto the membrane, because the transition resistance between electrode and membrane is higher using self-contained electrodes and therefore, the migration of the ions in the interface zone is enhanced, which is also observed for the platinum [37]. In any case, the silicone decomposition fragments in the electrodes as well as the enrichment in the interface between membrane and anode should influence the media transport in the electrodes and should effect the behavior near the limiting current. During the operational time of the tested MEA here the electrochemical performance did not change significantly, the behavior near the limiting current was not investigated.

4. Conclusion

If sealings fabricated of silicone-red® are used for fuel cell operations, they are subjected to a degradation process. This decomposition proceeds at both electrodes. Therefore, the different conditions in the two gas compartments, the oxidizing environment at the cathode side the reducing one at the anode side of the membrane electrode assembly, cannot be the cause for that reaction. Most likely, the acid character of the polymer electrolyte membrane in combination with the thermal stressing of the sealing material induces the alteration, even if the mechanical function of silicone sealings remains. Hence, the sealings stick on both sides of the membrane which leads to the observed coloration to yellow.

The products of this reaction have a high mobility and try to move from the anode to the cathode forced by the electrical field. On the anode side, the fragments of the sealing material diffuse from the edge of the MEA to the reaction zone, on the cathode they get to the backside of the gas diffusion layer, where they are able to react with the catalyst, forming particles containing silicon, oxygen and platinum. The Nafion® membrane itself is a barrier for the different decomposition products and remains silicon-free, so that the fragments have to accumulate in the reaction layer of the fuel cell's anode.

This accumulation of silicone decomposition products may change the wetting character of the electrodes, the water balance of the cell and finally the mass transfer within both electrodes due to the wetting behavior of silicone which is different from that of electrode materials. Especially if there is an alteration of the water balance in the cathode due to silicone, this may strongly change the electrochemical behavior and requires an adaptation of the operation

conditions to the changed cathode character. Furthermore, the platinum catalyst of the anode can be poisoned due to an interaction of the noble metal to the silicone fragments. Impedance studies on MEAs have shown, that the contribution of the anode towards the total impedance usually can be neglected [43]. According to this result, a distinct change of the anode's condition should effect the behavior and the performance of the MEA close to the limiting current.

A lot of different degradation processes, agglomeration of the catalyst [37], changes of PTFE [42] and so on, proceed simultaneously. So, it is impossible to quantify the influence of the individual degradation effects separately at the present state of knowledge. Therefore, further investigations of degradation processes are necessary.

References

[1] The Federal Ministry of Economics and Technology, Germany, Energy Report: Sustainable Energy Policy to Meet the Needs of the Future, Documentation 508, June 2002, http://www.bmwi.de.
[2] IEA World Energy Outlook 2000.
[3] K. Kordesch, G. Simader, Fuel Cells and Their Applications, VCH–Verlag, Weinheim, 1996.
[4] For example: BMBF-Project: Langlebige PEFC als Voraussetzung für eine Wasserstoffenergiewirtschaft, supported by the German Bundesministerium für Bildung und Forschung.
[5] E. Gülzow, M. Schulze, N. Wagner, T. Kaz, R. Reißner, G. Steinhilber, A. Schneider, J. Power Sources 86 (2000) 352.
[6] M.S. Wilson, J.A. Valerio, S. Gottesfeld, Electrochim. Acta 40 (1995) 355.
[7] M.S. Wilson, F.H. Garzon, K.E. Sickafus, S. Gottesfeld, J. Electrochem. Soc. 140 (1993) 2872.
[8] B. Mattsson, H. Ericson, L.M. Torell, F. Sundfolm, Electrochim. Acta 45 (2000) 1405.
[9] G. Hübner, E. Roduner, J. Mater. Chem. 9 (1999) 409.
[10] M. Schulze, M. Lorenz, N. Wagner, E. Gülzow, Fresenius J. Anal. Chem. 365 (1999) 106.
[11] D.P. Davies, P.L. Adcock, M. Turpin, S.J. Rowen, J. Power Sources 86 (2000) 237.
[12] D.P. Davies, P.L. Adcock, M. Turpin, S.J. Rowen, J. Appl. Electrochem. 30 (2000) 101.
[13] P.G. Dirven, W.J. Engelen, C.J.M. Van Der Poorten, J. Appl. Electrochem. 25 (1995) 122.
[14] J.M. Rheaume, B. Müller, M. Schulze, J. Power Sources 76 (1998) 60.
[15] F.N. Büchi, B. Gupta, O. Haas, G.G. Scherer, Electrochim. Acta 40 (1995) 345.
[16] S. Gupta, D. Tryk, S.K. Zecevic, W. Aldred, D. Guo, R.F. Savinell, J. Appl. Electrochem. 28 (1998) 673.
[17] D. Bevers, E. Gülzow, A. Helmbold, B. Müller, Innovative production technique for PEFC electrodes, in: Proceedings of the Fuel Cell Seminar, Orlando, 1996, p. 668.
[18] A. Helmbold, German Patent DE 197 57 492 A 1, 1999.
[19] D. Bevers, N. Wagner, German patent DE 195 09 749 C2.

[20] E. Gülzow, et al., Fuel Cell Bull. 15 (1999) 8–12.
[21] E. Gülzow, A. Helmbold, T. Kaz, R. Reißner, M. Schulze, N. Wagner, G. Steinhilber, J. Power Sources 86 (2000) 352.
[22] E. Gülzow, T. Kaz, J. Power Sources 106 (2002) 122.
[23] H. Sauer, German patent DE 2 941 774 (CI H01M4/88).
[24] A. Winsel, German patent DE 3 342 969 (CI C25B11/06).
[25] E. Gülzow, K. Bolwin, W. Schnurnberger, Dechema-Monogr. Bd. 117 (1989) 365.
[26] E. Gülzow, W. Schnurnberger, Dechema-Monogr. Bd. 124 (1991) 675.
[27] E. Gülzow, K. Bolwin, W. Schnurnberger, Dechema-Monogr. Bd. 121 (1990) 483.
[28] E. Gülzow, B. Holzwarth, M. Schulze, N. Wagner, W. Schnurnberger, Dechema-Monogr. Bd. 125 (1992) 561.
[29] M. Schulze, E. Gülzow, G. Steinhilber, Appl. Surf. Sci. 179 (2001) 252.
[30] E. Gülzow, M. Schulze, G. Steinhilber, J. Power Sources 106 (2002) 126.
[31] E. Gülzow, T. Kaz, R. Reißner, H. Sander, L. Schilling, M.V. Bradke, J. Power Sources 105 (2002) 261.
[32] S. Weißhaar, R. Reissner, W. Schröder, E. Gülzow, J. Power Sources 118 (2003) 405.

[33] G. Ertl, J. Küppers, Low Energy Electron and Surface Spectroscopy, VCH–Verlagsgesellschaft, Weinheim, 1985.
[34] Carlo Erba Microstructure Line No. 5, 1987, p. 1.
[35] Carlo Erba Microstructure Line No. 19, 1987, p. 2.
[36] M. Schulze, E. Gülzow, K. Bolwin, W. Schnurnberger, Fresenius J. Anal. Chem. 353 (1995) 778.
[37] M. Schulze, A. Schneider, E. Gülzow, Alteration of the distribution of the platinum catalyst in membrane–electrode assemblies during PEFC operation, in: Proceedings of 8th UECT, 20–21 June 2002, Ulm, Germany.
[38] P. Staiti, A.S. Arico, V. Antonucci, S. Hocevar, J. Power Sources 70 (1998) 91.
[39] E. Gülzow, T. Kaz, J. Power Sources 106 (2002) 122.
[40] J.M. Rheaume, B. Müller, M. Schulze, J. Power Sources 76 (1998) 60.
[41] M. Schulze, M. Lorenz, T. Kaz, XPS study of electrodes formed from a mixture of carbon black and PTFE powder, Surf. Interface Anal. 34 (2002) 646.
[42] R. Reissner, B. Thoben, T. Kaz, M. Schulze, E. Gülzow, Degradation of the hydrophobicity of fuel cell electrodes, in: Proceedings of the 8th UECT, 20–21 June 2002, Ulm, Germany.
[43] N. Wagner, J. Appl. Electrochem. 32 (2002) 859.

- Kelly, M.J. et al; *Conductivity of polymer electrolyte membranes . . .*; Solid State Ionics; 176, 25-28, 2111-2114 (August 2005).

ScienceDirect
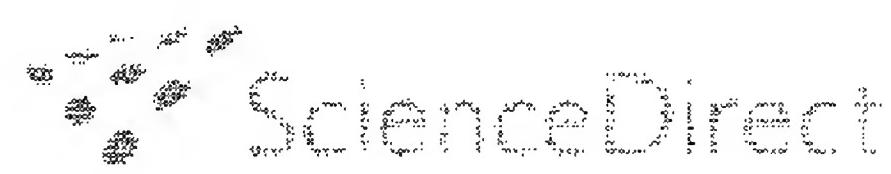
Home   Browse   Search   My Settings   Alerts   Help

Quick Search

All fields

🛈 search tips

Journal/book title

return to SCIrUS

Find more full-text articles: Your search for ""fuel cell" cation contamination " would return **754** results on ScienceDirect. View Results

▸ Abstract   Figures/Tables   Order Document

doi:10.1016/j.ssi.2004.07.071 ▸ **Article Toolbox**
⊘ Cite or Link Using DOI

Conductivity of polymer electrolyte membranes by impedance

⏱ E-mail Article
🔲 Cited By
💾 Save as Citation Alert
📡 Citation Feed

🌐 Export Citation
Add to my Quick Links
Add to ▸collab
↻ Permissions & Reprints
↺ Cited By in Scopus (6)

Related Articles in ScienceDirect
▪

spectroscopy with microelectrodes

Michael J. Kelly[a], [✎], [✉],
Bernhard Egger[a, b],
Günter Fafilek[a, b], **Jürgen O. Besenhard**[a, c],
Hermann Kronberger[a, b]
and Gerhard E. Nauer[a, d]

[a]ECHEM Center of Competence in Applied Electrochemistry, Viktor Kaplan Strasse 2, A-2700, Wiener Neustadt, Austria

[b]Institute of Chemical Technologies and Analytics, Vienna University of Technology, Getreidemarkt 9/164, A-1060, Vienna, Austria

[c]Institute for Chemical Technology of Inorganic Materials, Graz University of Technology, Stremayrgasse

Composite polymer electrolyte for Li-ion battery
Chemical Physics Letters

- Performance of a polymer electrolyte membrane fuel cell...
  Journal of Power Sources
- PVDF-HFP-based porous polymer electrolyte membranes for...
  Journal of Power Sources
- Polymer electrolyte membranes and their production
  Membrane Technology
- Polymer electrolyte membrane for electrochemical applic...
  Membrane Technology
- View More Related Articles
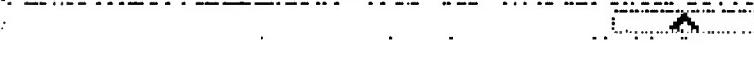
View Record in Scopus

16, A-8010, Graz, Austria

[d]Institute of Physical Chemistry, University of Vienna Währinger Straße 42, A-1090, Vienna, Austria

Abstract

The protonic conductivity of the polymer electrolyte membrane (PEM) in the PEM fuel cell is critical to the overall power density of the fuel cell system. The conductivity can be influenced by the presence of impurity cations in the membrane. By the use of electrochemical impedance spectroscopy with
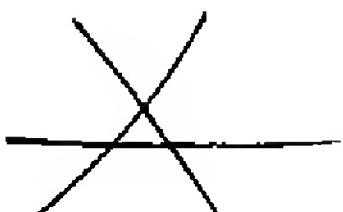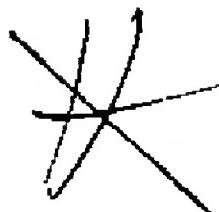
microelectrodes, the local conductivity of Nafion membranes, which had been exposed to part per million (ppm) concentrations of impurity cations, was evaluated. Inorganic impurity cations studied included Cu^{2+}, Fe^{3+}, Na^+ and Ni^{2+}. Membranes were immersed in sulphate salt solutions of these cations, prepared in distilled water. Conductivity values at 0.1, 1 and 10 ppm cation impurity level were found to vary little from values for the blank solution. However at 100 ppm, a significant decrease in conductivity was observed. At this higher concentration of impurity, the Ni^{2+} and Cu^{2+} contaminated membranes displayed lower conductivity than that contaminated by Na^+.

Meanwhile Fe^{3+} contaminated membrane had the lowest conductivity. That this decrease in conductivity was greater for cations of higher valence corresponds with the high affinity of the sulphonic acid sites in Nafion to multivalent foreign cations. The results illustrate the detrimental effect of small amounts of contaminants on conductivity in Nafion membrane.

Keywords: Conductivity; Polymer electrolyte membrane; Impedance; Microelectrode; Cation contamination

PACS: 66.10.Ed

Article Outline

1. Introduction
2. Experimental
3. Results and discussion
References

Corresponding author. Tel.: +43 2622 222 6633; fax: +43 2622 222 6650.

Home   Browse   Search   My Settings   Alerts   Help

About ScienceDirect | Contact Us | Information for Advertisers | Terms & Conditions | Privacy Policy

- Cleghorn, S.J.C. et al; *A polymer electrolyte fuel cell life test . . .*; Journal of Power Sources; 158, 446-454 (2006).

A polymer electrolyte fuel cell life test: 3 years of continuous operation

S.J.C. Cleghorn*, D.K. Mayfield, D.A. Moore, J.C. Moore, G. Rusch,
T.W. Sherman, N.T. Sisofo, U. Beuscher

W.L. Gore & Associates, Inc., 201 Airport Road, P.O. Box 1488, Elkton, MD 21922, USA

Abstract

Implementation of polymer electrolyte fuel cells (PEMFCs) for stationary power applications requires the demonstration of reliable fuel cell stack life. One of the most critical components in the stack and that most likely to ultimately dictate stack life is the membrane electrode assembly (MEA). This publication reports the results of a 26,300 h single cell life test operated with a commercial MEA at conditions relevant to stationary fuel cell applications. In this experiment, the ultimate MEA life was dictated by failure of the membrane. In addition, the performance degradation rate of the cell was determined to be between 4 and 6 $\mu V h^{-1}$, at the operating current density of 800 mA cm^{-2}. AC impedance analysis and DC electrochemical tests (cyclic voltammetry and polarization curves) were performed as diagnostics during and on completion the test, to understand materials changes occurring during the test. Post mortem analyses of the fuel cell components were also performed.
© 2005 Elsevier B.V. All rights reserved.

Keywords: Polymer electrolyte fuel cells; Life test; Stationary fuel cells; Fuel cell diagnostics; AC impedance; Cyclic voltammetry

1. Introduction

Over the last decade, polymer electrolyte membrane fuel cells (PEMFCs) have received ever growing interest resulting in significant technological advancement, especially in areas of increasing power density and decreased materials utilization, with the advent of thin membranes [1] and reduced precious metal catalyst loadings [2]. PEMFCs have gained interest for many potential power source applications, including battery replacements for portable devices, automotive traction as replacement for the internal combustion engine and in stationary power generation. The cost targets and technology requirements facing the PEMFC seem exceedingly daunting to overcome before wide spread commercial automotive markets [3] are possible. As portable power sources fuel cells need to achieve higher power density to compete as battery replacements in the most attractive high-volume consumer markets (powering devices, such as cell phones, PDA and laptops) [4]. In contrast, it has

been argued for many years that there may be fewer barriers to market entry for PEMFCs as stationary power plants [5]. For this application, systems cost targets are much less demanding than automotive, fuel is widely available (storage and infrastructure are not a problem) and typically volumetric and gravimetric constraints are not critical, allowing the fuel cell to be operated at favorable conditions.

Stationary fuel cell power plants are attractive, as they offer the potential of higher efficiency and lower greenhouse gas emissions, than available technologies and may be cost-competitive with grid power in areas where the cost of electricity is expensive relative to natural gas. Alternatively, fuel cells may be preferred where grid connection is not practical or does not offer reliable power.

The key to the commercial implementation of stationary fuel cell systems is the demonstration of reliable long life. In fact, it is generally recognized that a cost-effective stationary fuel cell power plant requires the fuel cell stack life expectancy to exceed 40,000 h. The critical component of the fuel cell, and the component that is most likely to dictate stack life, is the membrane electrode assembly (MEA). Until very recently, there was very little publicly available data demonstrating extended

---

operational life of PEMFCs, and also few publications reporting the mechanisms of MEA performance loss and failure after extended operation. This is probably because much of this activity has been confined to the industrial sector. However, in recent years, there has been a significant increase in publicly available data, as a result of increasing academic activity and an increasing willingness of industrial organization to publish. Several recent reviews have compiled many of the literature publications referencing PEMFC durability [6], and ionomer membrane degradation [7].

The longest PEMFC demonstration that we are aware of in the open literature was a 60,000 h life test reported by GE in 1979 [7–9]. This GE stack module was operated with pressurized hydrogen/oxygen and used MEAs based on NAFION[®] 120 membrane (250 μm thick). The limited post mortem data reported from this test demonstrated the tensile properties of the membranes had deteriorated, while the BET surface area of the catalyst was not changed. St-Pierre and Jia [10] more recently reported extended operation for a hydrogen/oxygen stack, with a voltage decay rate of less than $2\,\mu V\,h^{-1}$ in 11,000 h of operation without failure. Kinetic, ohmic and transport losses in the stack over its life were monitored. The diagnostics and post mortem analysis reported the primary cause for power loss was increased mass transport over-potential, this was attributed to an increased hydrophilicity of the gas diffusion media.

Within the last several years there has been a proliferation of publications reporting several thousands of hours of single cell and short stack life, presumably using much thinner membranes and lower catalyst loadings (the MEA characteristics are not always disclosed) than the early GE stack. Several notable examples include single cell demonstrations performed at Osaka gas [11], some of which have exceed 17,000 h life with voltage decay rates of less than $5\,\mu V\,h^{-1}$, operating with reformate fuel [12,13]. Fuji Electric Co. Ltd. reported 10,000 h of hydrogen operation [14] in a single cell and reported over 15,000 h, with no significant voltage decay at $0.4\,A\,cm^{-2}$ for a 45-cell stack. In addition, Wilkinson and St-Pierre of Ballard [6] have published results of a series-of-life tests operated with reformate fuel in short stacks, the longest of which has exceeded 13,000 h without failure, with a reported voltage decay rate of $0.5\,\mu V\,h^{-1}$ [15].

There is also a growing body of literature outlining various in situ electrochemical methods [16,17] and ex situ analytical techniques [18–21], which can be employed to characterize MEAs either during life testing or upon failure, to understand MEA and fuel cell degradation mechanisms. However, there are very few examples of publications that deploy the known analytical techniques to understanding changes occurring in the MEA during extended life testing. In this publication, we report results of what we believe to be the longest single cell fuel cell life test operated with a commercial MEA and the associated diagnostic results which were used to understand materials changes occurring during the test. This MEA has both membrane thickness and precious metal loading consistent with meeting the cost targets for stationary fuel cell applications.

2. Experimental

This publication focuses on the results obtained from the operation of a single cell PEMFC life test, which was operated under continuous load for 3 years (over 26,000 h), the diagnostics performed during the course of the life test, and the post mortem analysis performed on the components on completion of the test.

The life test was performed in 25-cm^2 single cell hardware (Fuel Cell Technologies, Albuquerque, NM). Anode and cathode flow fields, were both triple channel serpentine designs machined into graphite (POCCO graphite) and were assembled in co-flow orientation. The cell was assembled with a Gore PRIMEA[®] Series 5621 MEA; based on a 35 μm GORE-SELECT[®] membrane with a cathode loading of $0.6\,mg_{Pt}\,cm^{-2}$ and an anode with Pt–Ru alloy loading of $0.45\,mg\,cm^{-2}$. Gore CARBEL[™] CL gas diffusion media was used on both anode and cathode sides of the cell[1]. An incompressible silicone coated fiberglass gasket (CHR–furon) was used on either side of the membrane to provide cell sealing. A second thin incompressible gasket, referred to as a sub-gasket, was placed between the MEA and gas diffusion media to define the cell active area of 23 cm^2. The gasket arrangement was chosen and cell assembly was performed such that the average active area compression was approximately 150 psi (the assembly pressure was predetermined using PRESSSUREX pressure sensitive paper from Sensor Products, Inc., NJ). The eight lubricated bolts of the cell hardware were torqued to 45 in lbs per bolt.

Reactant humidification, gas flow rate, back-pressure and cell temperature were all controlled from a fuel cell test station (Globetec, now Electrochem, Boston, MA). During the 3 years of continuous operation of the life test, the cell temperature was controlled at 70 °C, the outlet reactant pressures were maintained at ambient pressure, reactants were stoichiometrically controlled and the reactants were saturated at cell temperature. It is very important to highlight that significant effort was given to controlling the reactant inlet relative humidity to 100% RH. To prevent liquid water from entering the fuel cell, liquid water traps were used and the reactant gas lines into the fuel cell were heated a few degrees above the cell temperature. Several times during the experiment the test was stopped and the test station re-calibrated. Current, voltage and cell resistance (by current interrupt) data were collected as a function of time, over the entire length of the test using a computer controlled Scribner electronic load (Scribner and Associates, Southern Pines, NC).

Much of the first 3000 h of this life test were performed with a simulated reformate fuel of composition: 43% nitrogen, 17% carbon dioxide, 50 ppm carbon monoxide and a balance of hydrogen. In addition 4% air bleed was used to mitigate the effects of CO poisoning. The detailed description of this data is the subject of another publication [22]. However, the remaining 23,000 h, and therefore the majority of this life test, was performed with pure hydrogen fuel (99.999% hydrogen). Filtered, compressed and dried air was used throughout the test.

---

[1] GORE, CARBEL, GORE-SELECT, PRIMEA and designs are trademarks of W.L. Gore & Associates, Inc.

The life test was operated continuously at constant current of 800 mA cm^{-2}. The life test was interrupted approximately every 500 h to perform in-cell electrochemical diagnostics in a systematic manner. To interrupt the test, the load was disconnected and reactant flows stopped. The cathode compartment of the fuel cell was switched to fully humidified nitrogen flow. Once the open cell voltage (OCV) had reached a steady-state value of less than 100 mV, cyclic voltammetry and electrochemical hydrogen cross-over measurements were performed on the cell. Once these diagnostics had been completed the cell was returned to the hydrogen/air life test operation at constant current, 800 mA cm^{-2}. After several hours operation, a polarization curve was performed under voltage control. Upon completion of the life test, more extensive in-cell diagnostics (AC impedance [23]) and out-of-cell diagnostics were performed to try to further elucidate material changes that may have occurred during the extended operation of this fuel cell.

In order to understand MEA integrity and performance decay in operating fuel cells, we have found it extremely valuable to identify and define the following terms [24]:

2.1. Reliability

MEA reliability failure is typically defined as either inability of the MEA to operate in a stack or single cell at start-up, or a short-term (less than 100 h) membrane failure. MEA reliability may be associated with the use of defective MEAs, or the result of poor cell or stack design or assembly, causing MEA shorting, puncturing or "burn-through". MEA reliability problems are addressed with attention to MEA manufacturing quality, proper handling, and effective cell or stack design, and are not the discussed in this publication.

2.2. Durability

The overall cell performance decay rates, measured during continuous and uninterrupted operation, is the sum of both stability and durability decay rates. The durability decay rate is defined as the unrecoverable portion of this total decay rate. This is measured from comparing cell performances in polarization curves as a function of time (or comparing cell performance after recovery techniques). Durability decay rate is a result of irreversible materials changes occurring in the cell (i.e. loss in electrochemical surface area or carbon corrosion, etc.).

2.3. Stability

The stability decay rate is the recoverable function of the power loss observed during continuous operation. The stability decay rate is calculated by subtracting the durability decay rate (i.e. the portion that was not recovered from performing polarization curves) from the total decay rate. MEA performance lost as a result of stability decay is typically concerned with non-steady-state behavior and is associated with sensitivity to operating conditions (water management) and reversible materials changes.

3. Results and discussion

3.1. Life test operation

The cell voltage, iR compensated cell voltage and cell resistance for the entire 26,300 h life test as a function of time on load operated at constant current, 800 mA cm^{-2} are shown in Fig. 1. The initial performance of this cell operated on hydrogen was 0.65 V at 800 mA cm^{-2}, upon completion of the test the performance had declined to approximately 0.54 V. This is a total voltage loss of 110 mV in 26,300 h and corresponds to an overall voltage decay rate of 4.2×10^{-6} V h^{-1} (or 4.2 μV h^{-1}). A linear regression fitted through the voltage data at 800 mA cm^{-2} for the hydrogen fueled operating period of the experiment (from 3000 to 26,300 h) produced an overall voltage decay rate of 6.4 μV h^{-1}. Both of these overall decay rates are examples of what we have defined as a durability decay rate, as the cell performance was periodically recovered by performing in-cell diagnostics (discussed below).

It can also be ascertained from Fig. 1 that the measured resistance for the cell is observed to undergo very little overall change during the life of the test, actually decreasing from approximately 82 mΩ cm^2 to approximately 68 mΩ cm^2 in 26,300 h.
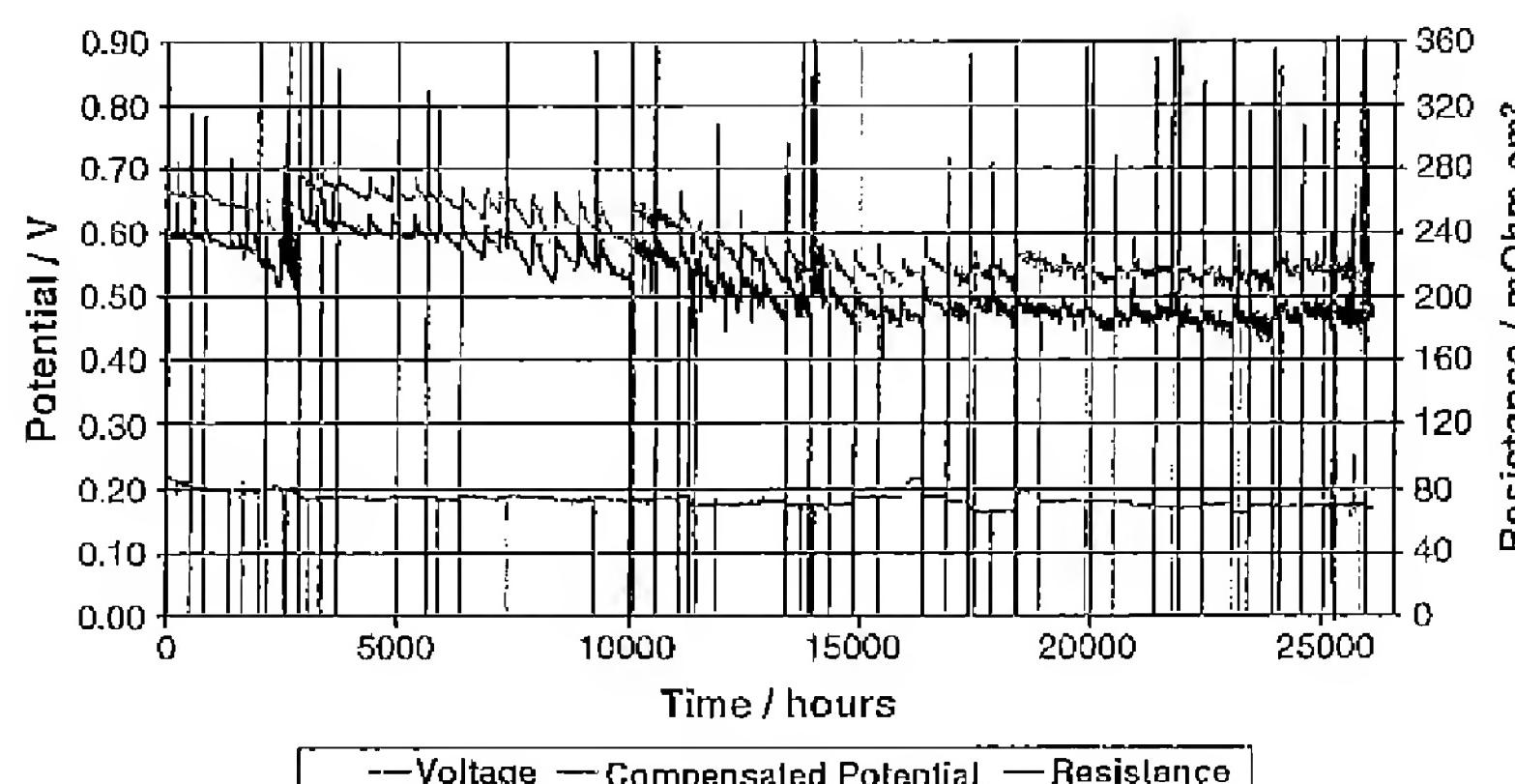

Fig. 1. Cell voltage, iR compensated cell voltage and cell resistance as a function of hours on load operated at constant current, 800 mA cm^{-2} for the entire 26,300 h life test. Cell temperature 70 °C. Air: 2.0× stoichiometry, ambient pressure, 100% RH. Hydrogen: 1.2× stoichiometry, ambient pressure and 100% RH.

This change is expected to result in an 11 mV increase in performance at 800 mA cm^{-2}. It is, therefore, evident that the source of voltage decay apparent in the test cannot be accounted for by an increase in membrane resistance. This is confirmed by the iR corrected voltage decay rate matching the decay rate of the raw voltage data (also shown in Fig. 1).

One characteristic of this test, worth further comment, is the saw-tooth behavior of the voltage trace over the length of the life test, with a typical periodicity of approximately 500 h. The peak in the saw-tooth co-insides with re-starting of the test following interruption to perform fuel cell diagnostics. This result demonstrates that interruption of the life test and performance of electrochemical diagnostics provides recovery of the cell voltage. The cell voltage again typically decays upon re-starting the fuel cell under load after completion of diagnostics. To illustrate the effect of the diagnostics typical detailed voltage/time plots at two different periods in time are shown in Fig. 2a and b. The examples demonstrate that interruption of the test to perform diagnostics recovered cell performance by approximately 80 mV (Fig. 2a, from 7300 to 9000 h) and approximately 40 mV (Fig. 2b, from 20,300 to 21,700 h). This corresponds to stability decay rates of approximately 140 and 40 µV h^{-1}, respectively. It is believed that MEA performance decay, resulting from cell instability, was typically the result of non-steady-state behavior, and therefore by definition, was fully recoverable. MEA stability is associated with the MEA's sensitivity to operating conditions (i.e. water management) or reversible material changes (such as

formation of formation of Pt oxides, adsorption of poisons or an increase in oxygen transport resistance as a result of formation of liquid water barriers). The stability decay rate between recoveries can be quite variable, and is also relatively high, compared to the reported durability decay rate. The data plotted in Fig. 2a and b also indicates that although there is a concurrent saw-tooth behavior in the measured cell resistance, it cannot account for the magnitude of the voltage changes observed.

3.2. In fuel cell diagnostics

There is always a trade-off when designing fuel cell life test experiments as to the value of operating the test with or without interruption to perform diagnostic experiments. Of course operation without periodic diagnostics is more likely to approach cell operation in the application. However, when starting this experiment, there were very few publications reporting the effects of long-term operation on the materials within the cell. Therefore, it was our philosophy in this life test to perform diagnostics in order to maximize our learning from this experiment.

3.2.1. Cyclic voltammetry

The life test was interrupted every 500 h (later in the test, the uninterrupted period of operation was increased to every 1000 h) of load operation to perform diagnostics. First cyclic voltammetry was performed with the fuel cell cathode as the working electrode. Three complete voltage scans from 10 to 1200 mV (using the hydrogen electrode as the counter and reference) were recorded at 100 mV s^{-1}, the results of the third scan at various selected periods in time are compiled in Fig. 3. The voltammetry scan at 0 h was typical of those recorded for fuel cell electrodes, and the description of the various peaks is reported elsewhere in the literature [16]. As the life test progressed, the charge associated with platinum oxide formation and reduction, was observed to decrease, while the double layer capacitance charge shows a slight increase. It is also important to comment that there is no evidence for additional or unexpected peaks developing in the
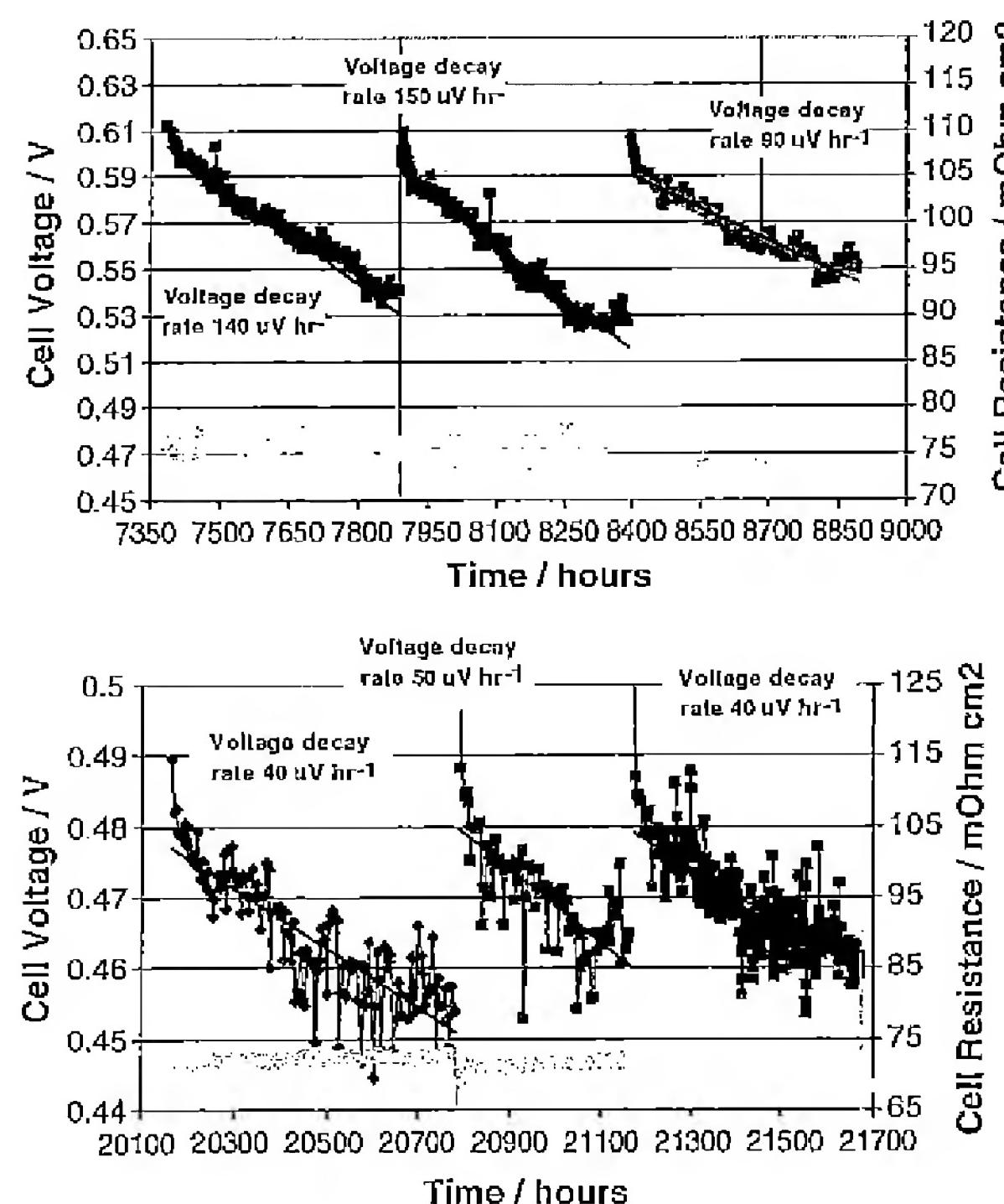

Fig. 2. Detail of cell voltage and cell resistance as a function of time on load operated at constant current of 800 mA cm^{-2} for (a) 7390–8890 h and (b) 20,170–21,670 h. Cell temperature 70 °C. Air: 2.0× stoichiometry, ambient pressure, 100% RH. Hydrogen: 1.2× stoichiometry, ambient pressure and 100% RH.
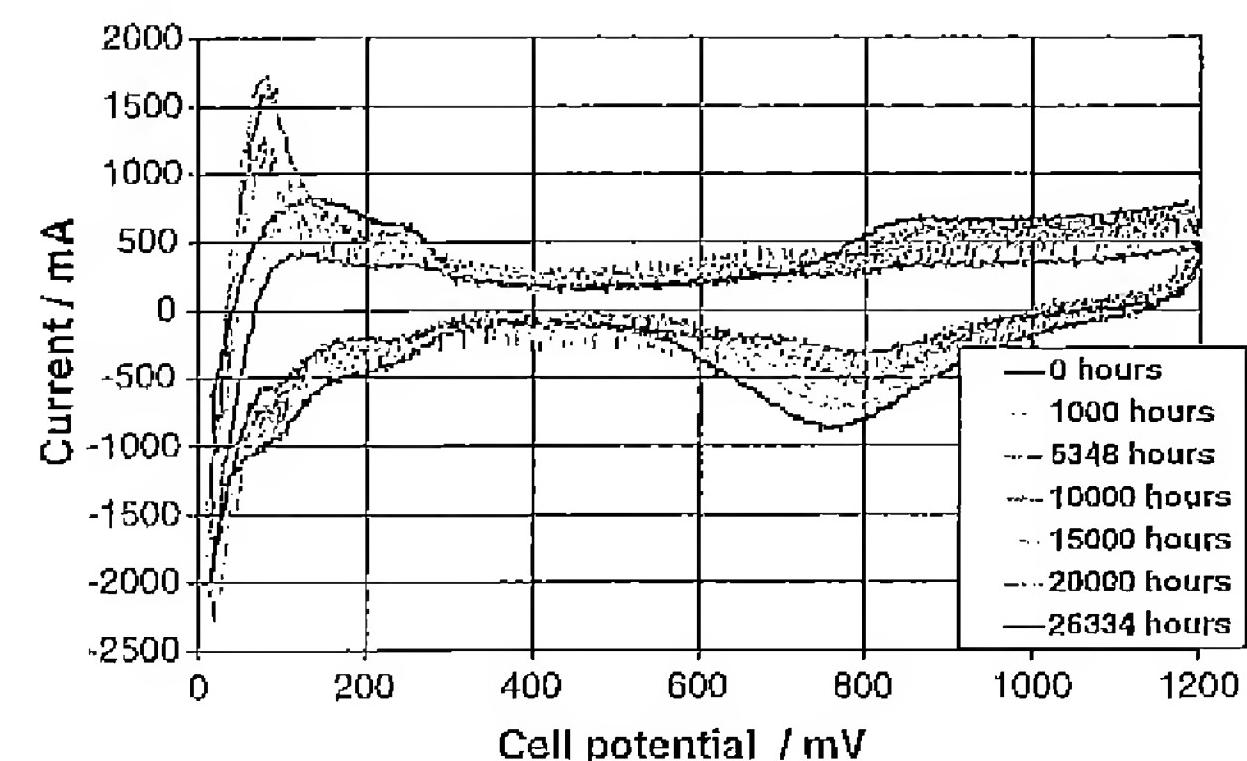

Fig. 3. Cyclic voltammetry recorded at 0, 1000, 5348, 10,000, 15,000, 20,000 and 26,334 h during the life test. Voltage scan between limits 10 and 1200 mV at a potential scan rate of 100 mV s^{-1}. Cell temperature 70 °C. Working electrode (fuel cell cathode) 50 ml min^{-1} nitrogen, ambient pressure and 100% RH. Secondary and reference electrode (fuel cell anode): 50 ml min^{-1} hydrogen, ambient pressure, 100% RH.
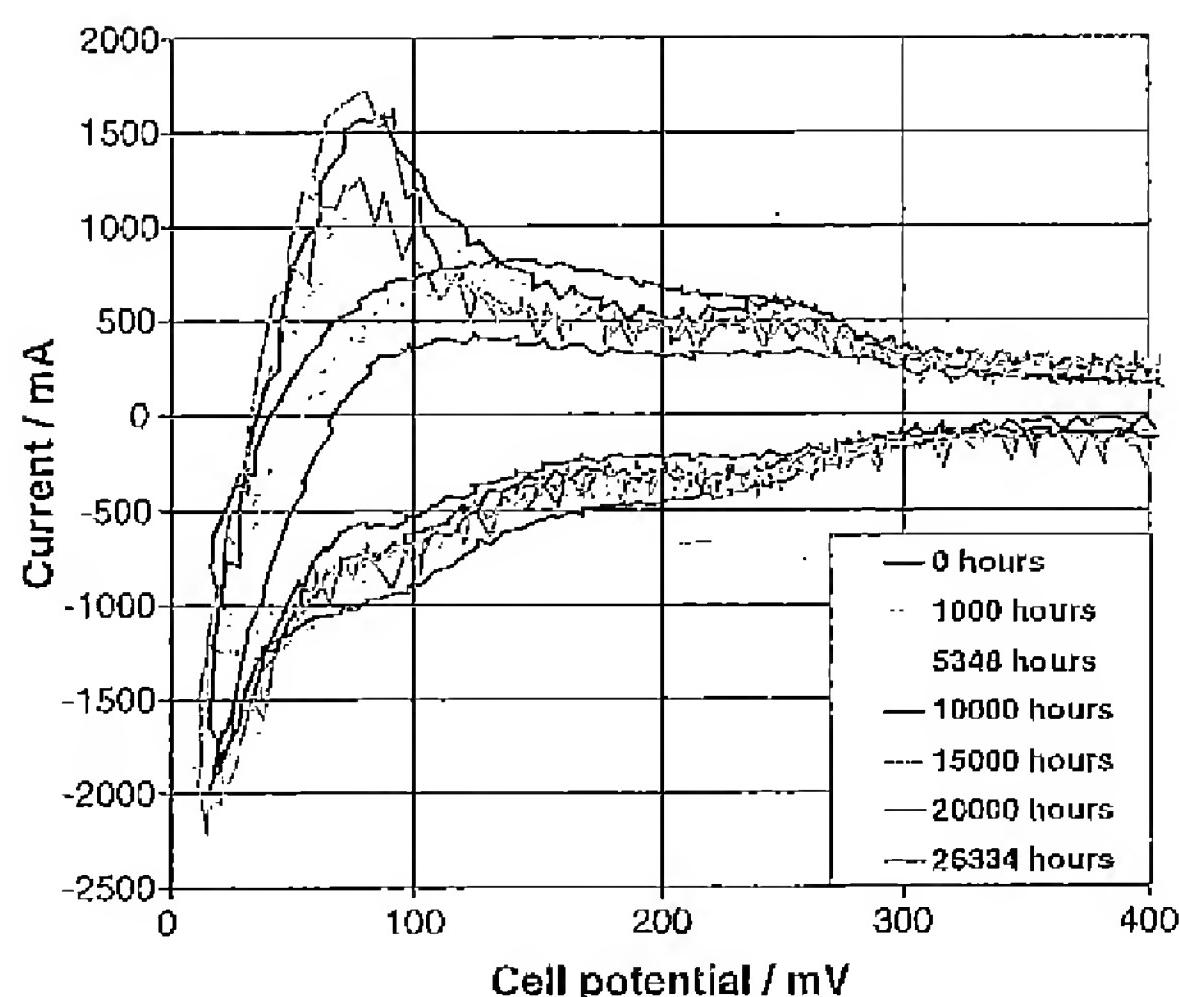
Fig. 4. Detail of cyclic voltammetry in the hydrogen region during the life test (see Fig. 5 for details).

voltammetry during the test, which might indicate the introduction of adsorbed electro-active poisons at the cathode electrode. The primary motive for performing cyclic voltammetry during this life test was to quantitatively monitor the change in electrochemically active area (ECA) of the cathode, by measuring the charge associated with hydrogen adsorption and desorption (Fig. 4). In our experiments at Gore, we have been much more successful at quantifying ECA from the hydrogen oxidation peaks of the voltammetry (compared to hydrogen desorption). In this experiment, the apparent charge associated with the hydrogen oxidation region does not significantly change throughout the 26,300 h life test (Fig. 5, total hydrogen oxidation charge). However, further analysis of the data indicates that a large oxidation peak developed at 80 mV (see scans at 5000, 10,000, 15,000 and 20,000 h in Fig. 4). This peak, at approximately 80 mV, is likely to be associated with oxidation of molecular hydrogen, formed on the reverse scan in the voltamogram. By curve fitting, the charge for molecular hydrogen oxidation was estimated in each voltammogram, and then subtracted from the total charge measured in the hydrogen region. Fig. 5 shows the total charge measured in the hydrogen region, the estimated

charge associated with molecular hydrogen oxidation and the charge calculated for oxidation of adsorbed hydrogen (or ECA) as a function of time. As commented before, the total hydrogen oxidation charge does not change significantly within the test. Interestingly, the fitted molecular hydrogen oxidation charge appears to increase to a maximum at approximately 15,000 h, after which the data becomes quite noisy. Despite this noise in the data, the calculated ECA consistently decreases throughout the life test. In total, it was estimated that approximately 66% of ECA was lost in 26,300 h of operation. Linear interpolation of the data gave a reasonably good fit, with a loss of ECA of $1 \times 10^{-6}\,\mathrm{C\,cm^{-2}\,h^{-1}}$. Using a simple Tafel kinetic calculation and assuming a Tafel slope of 70 mV per decade [25], it can be calculated that a 66% loss in ECA should result in a 34 mV loss in cell performance.

We have not been able to adequately understand the reason for the erratic behavior in formation of molecular hydrogen during this test, however, it does suggest that the working electrode was allowed to proceed to a lower potential than desirable for the ECA measurement. Two possible explanations for molecular hydrogen formation could be: (a) a shift in the reference electrode potential or (b) a change in the catalytic nature of the working electrode. It is unlikely that cell resistance change is responsible for this behavior. It was decided that we should maintain the starting potential at 10 mV, during the length of this experiment, and use regression methods to eliminate the additional charge resulting from molecular hydrogen oxidation in determination of the ECA.

3.2.2. Hydrogen cross-over

A key MEA characteristic, measured throughout the life test, was hydrogen cross-over through the ionomer membrane, which provides data on the health of the membrane. This was measured by the electrochemical technique [26], each time the cell was interrupted for diagnostics. A membrane is determined to have failed when the hydrogen cross-over current density exceeds between 10 and 15 mA cm^{-2}. (This is an arbitrary value used to provide a consistent end point to life tests, even though at this hydrogen permeation rate, no impact on cell performance is observed.) The initial (0 h) hydrogen cross-over current density was less than 1 mA cm^{-2}, no measurable change in hydrogen
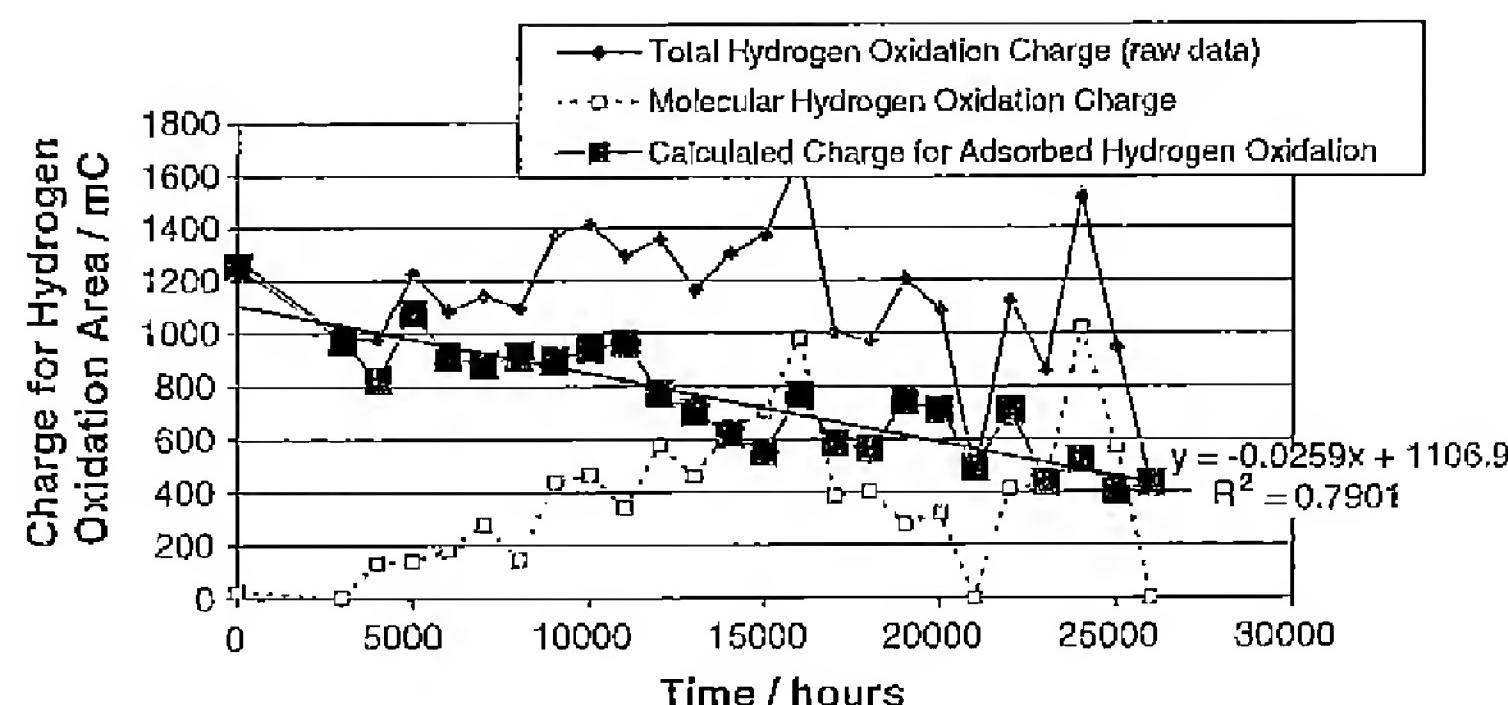

Fig. 5. Analysis of charge measured in the hydrogen oxidation region during the cyclic voltammetry experiments as a function of time over the period of the life test. Molecular hydrogen oxidation was estimated from curve fitting the voltammetric peak at 80 mV. The charge for adsorbed hydrogen (used for ECA) is calculated from total charge minus charge for molecular hydrogen oxidation.
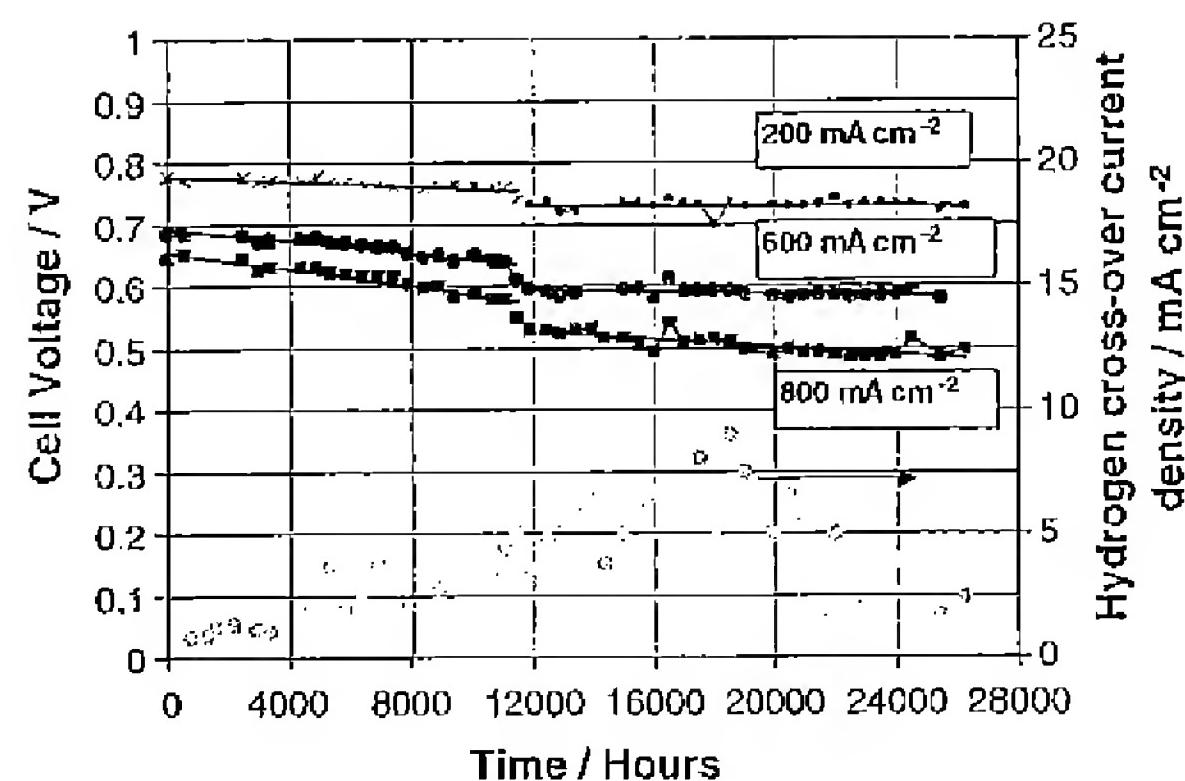
Fig. 6. Cell voltage interpolated from polarization curves at 200, 600 and 800 mA cm⁻² and hydrogen cross-over current density as a function of time measured during the life test. Cell temperature 70 °C. Air: 2.0× stoichiometry, ambient pressure, 100% RH. Hydrogen: 1.2× stoichiometry, ambient pressure and 100% RH.


Fig. 7. Polarization curves at various periods in time (0, 500, 5348, 10,100, 15,000, 20,000 and 26,330 h) during the life test. Cell temperature 70 °C. Air: 2.0× stoichiometry, ambient pressure, 100% RH. Hydrogen: 1.2× stoichiometry, ambient pressure and 100% RH.

cross-over current was apparent until at least 5000–7000 h of operation (Fig. 6). After approximately 1 year of operation, the hydrogen cross-over current density follows a slow increase to approximately 22,000 h. This data can be reasonably fitted to an exponential curve, $y = 1.33 \exp(8 \times 10^{-5}t)$. After 22,000 h operation, the measured hydrogen cross-over current density was observed to decrease to approximately 2–3 mA cm⁻². This effect was extensively investigated at the time, by varying the hydrogen overpressures, and measuring hydrogen cross-over current density cathode to anode and vice-versa. The data was found to be repeatable (Fig. 6 from 22,000 to 26,000 h). The reason for the change in behavior of the cell to the electrochemical test is not fully understood, however, it should also be pointed out that this is the first life test exceeding 20,000 h that we are aware of that has been monitored in this manner. When observing this apparently unreliable electrochemical data, a physical method of measuring hydrogen gas flow rate through the membrane using a bubble flow meter, was added to our diagnostics for this life test. At approximately 26,000 h, the life test was reported as failed when the volumetric flow rate of hydrogen through the membrane exceeded a value corresponding to 10 mA cm⁻² equivalent hydrogen cross-over current density. It is also of interest to comment that extrapolating the exponential fit for the hydrogen cross-over data determined electrochemically (0–22,000 h) predicted a membrane life of 25,200 h.

The electrical short resistance through the membrane was also monitored throughout this life test, by calculating the slope of the limiting current density plateau, measured in hydrogen cross-over experiment. The data showed no trend over time and
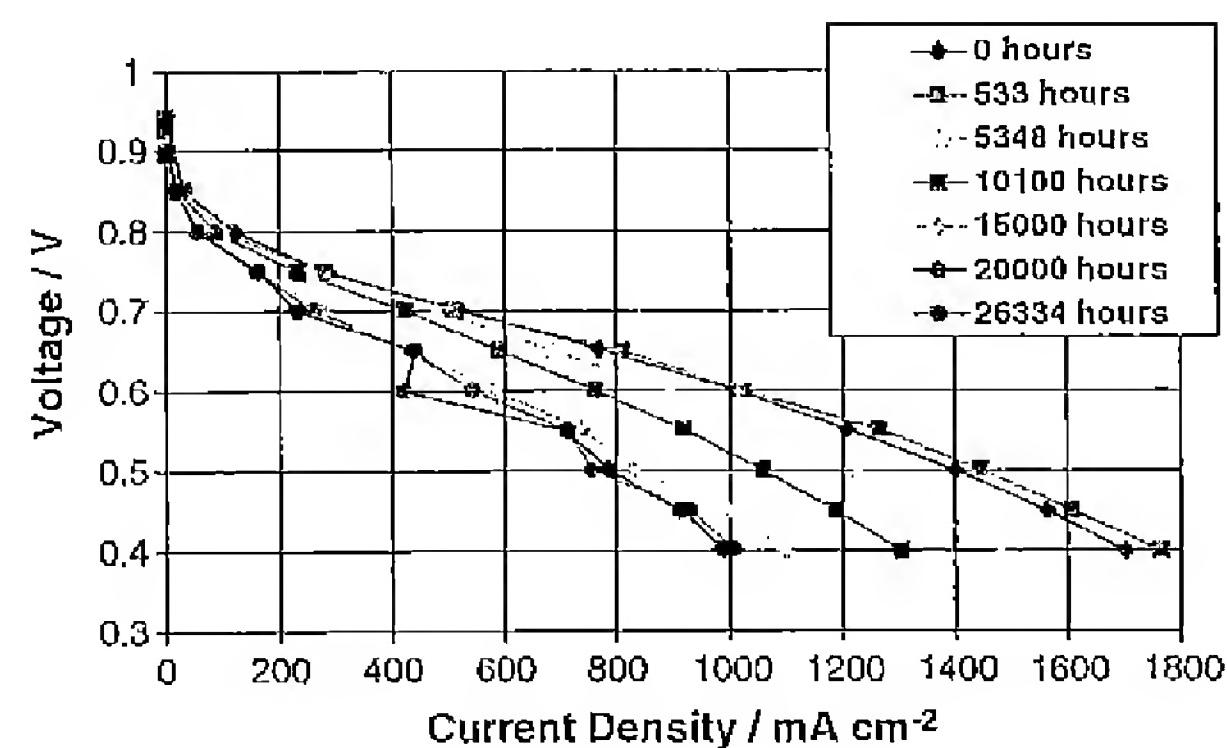
there was no evidence that electronic shorting was a concern in this test.

3.2.3. Polarization curves

Probably the most ubiquitous diagnostic performed in PEM-FCs is the polarization curve. Fig. 7 shows a sample of polarization curves recorded under potential control, at various times throughout the life test, on completion of the voltammetric experiments. The data demonstrates loss in fuel cell performance throughout the polarization curve, without any significant change in the overall characteristics of the curve.

The cell voltage, as a function of time at 200, 600 and 800 mA cm⁻², has been determined by interpolation of the polarization curves. A linear curve fit through this data was used as a further method to determine the voltage decay rate for the life test (Fig. 6). This is also considered to be durability decay rate. The calculated decay rates are reported in Table 1. As well as reporting an overall decay rate for the entire test at each current density, decay rates have also been calculated for the time period 0–12,000 h and from 12,000 to 26,300 h. There is an easily identifiable step in the data at 12,000 h. This is much more difficult to identify in the raw data (Fig. 1). At approximately 11,500 h, the cell was maintained under load with much reduced air feed for approximately 24 h. This caused the cell voltage to be reduced to approximately 0 V while the cell operated at 1× stoichiometric air flow. (It was postulated that this condition may have results in localized hydrogen evolution at the cathode.) This error in operation resulted in a 20–30 mV performance loss at 800 mA cm⁻² which was not recovered throughout the remainder of the life test.

Table 1
Voltage decay rates for the life test as a function of current density

| Current density (mA cm⁻²)	Decay rate 0–12,000 h (μV h⁻¹)	Decay rate 12,000–26,300 h (μV h⁻¹)	Overall decay rate (μV h⁻¹)
200	2	0.7	2
600	5	0.8	5
800	7	3	7

Fig. 8. Nyquist plot for the life-tested cell at the end of life (26,300 h) as a function of current density. Cell temperature 70 °C. Air: 2.0× stoichiometry, ambient pressure, 100% RH. Hydrogen: 1.2× stoichiometry, ambient pressure and 100% RH.

3.2.4. AC impedance

AC impedance was only performed on the life-tested cell on completion of the test after 26,300 h of operation. The impedance scans for fuel cell operated at a variety of current densities are shown from 8 kHz to 0.1 Hz (Fig. 8). This data has been compared to AC impedance data collected after break-in for a fuel cell built with the same hardware, as used in the life test, assembled with a new MEA from an identical lot as used in the life test (Fig. 9). The high-frequency resistance measured for the life-tested cell is approximately 75 mΩ cm^2 (at 1500 mA cm^{-2} the high-frequency resistance is increased to 85 mΩ cm^2). This resistance measured by impedance agrees very well with the cell resistance data measured by current interrupt shown in Fig. 1. The new cell has a slightly higher high-frequency resistance (between 94 and 99 mΩ cm^2), which is not significantly increased at 1500 mA cm^{-2}.

Considering the entire frequency scan at low current density (100 mA cm^{-2}), the impedance for the life tested and new cells appears very similar, with similar total impedance. It is expected that electron transfer resistance should dominate the impedance characteristic of the cell at this current density, and it is, therefore, implied that the electron transfer (or kinetic)

resistance of the life-tested cell is not significantly changed. This may be a surprising result, considering the large change in ECA measured in voltammetry. At moderate current density (600 mA cm^{-2}), where fuel cell processes are expected to be under mixed kinetic and diffusion control, and high-current density (1500 mA cm^{-2}), where diffusion processes should be in control, the new and life-tested cells demonstrate very different behavior. In these current density ranges, the total impedance of the life-tested cell is dramatically increased relative to the new cell. This data suggests that the resistance to transport, or diffusion processes, has significantly increased between the new cell and the life-tested cell. In fact, even at 600 mA cm^{-2} where the new cell shows features of both kinetic and transport resistance, the life-tested cell impedance is dominated by transport resistance. To understand the source of the increased transport resistance AC, measurements of the life-tested cell were recorded when the reactant RH was reduced. At 1500 mA cm^{-2}, this resulted in a significant reduction in the total impedance (430 mΩ) of the cell. This observation might be consistent with the presence of liquid water impeding transport of reactant gases to active catalyst sites.

AC impedance can also be a valuable tool, in the absence of faradic reactions, to elucidate any change in the ionic conductivity of the electrodes, which may provide evidence for changes in ionomer structure or ionomer degradation in the electrode layer. Fig. 10 shows the impedance spectra for the life-tested cell between 0.1 Hz to 20 kHz at 80 °C with nitrogen flowing on both sides of the cell at four different relative humidities. Impedance spectra using this technique have been previously described [23]. At higher frequencies the Nyquist plot shows a 45° slope characteristic of proton transport in the catalyst layer. Then an inflection in the curve occurs at lower frequency where the impedance becomes dominated by the electrode capacitance. We have defined this inflection as $R_i/3$, where R_i is the ionic resistance of the catalyst layer. The raw data demonstrates that the impedance of the electrode layer increases with decreased relative humidity. It is also evident that at lower frequency there
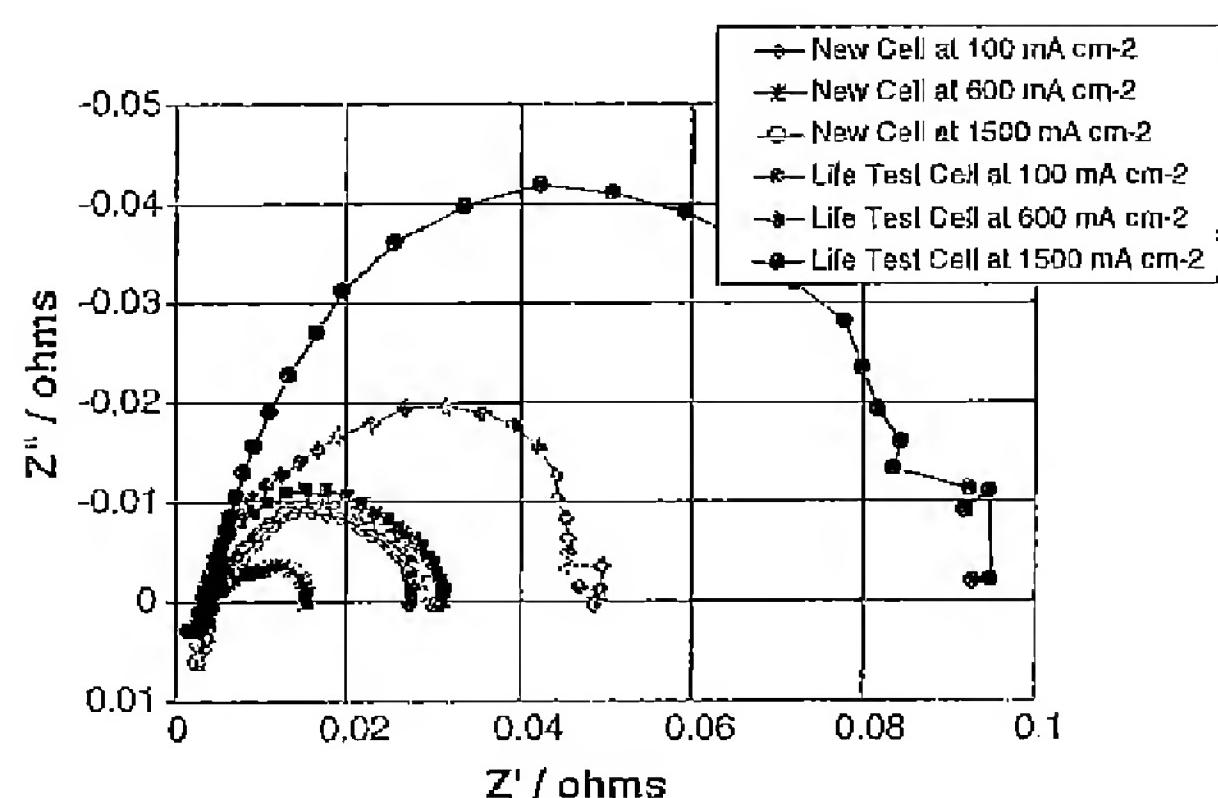
Fig. 9. Nyquist plot comparing the life-tested cell at the end of life (26,300 h) and a new cell at 100, 600 and 1500 mA cm^{-2}. Cell temperature 70 °C. Air: 2.0× stoichiometry, ambient pressure, 100% RH. Hydrogen: 1.2× stoichiometry, ambient pressure and 100% RH.
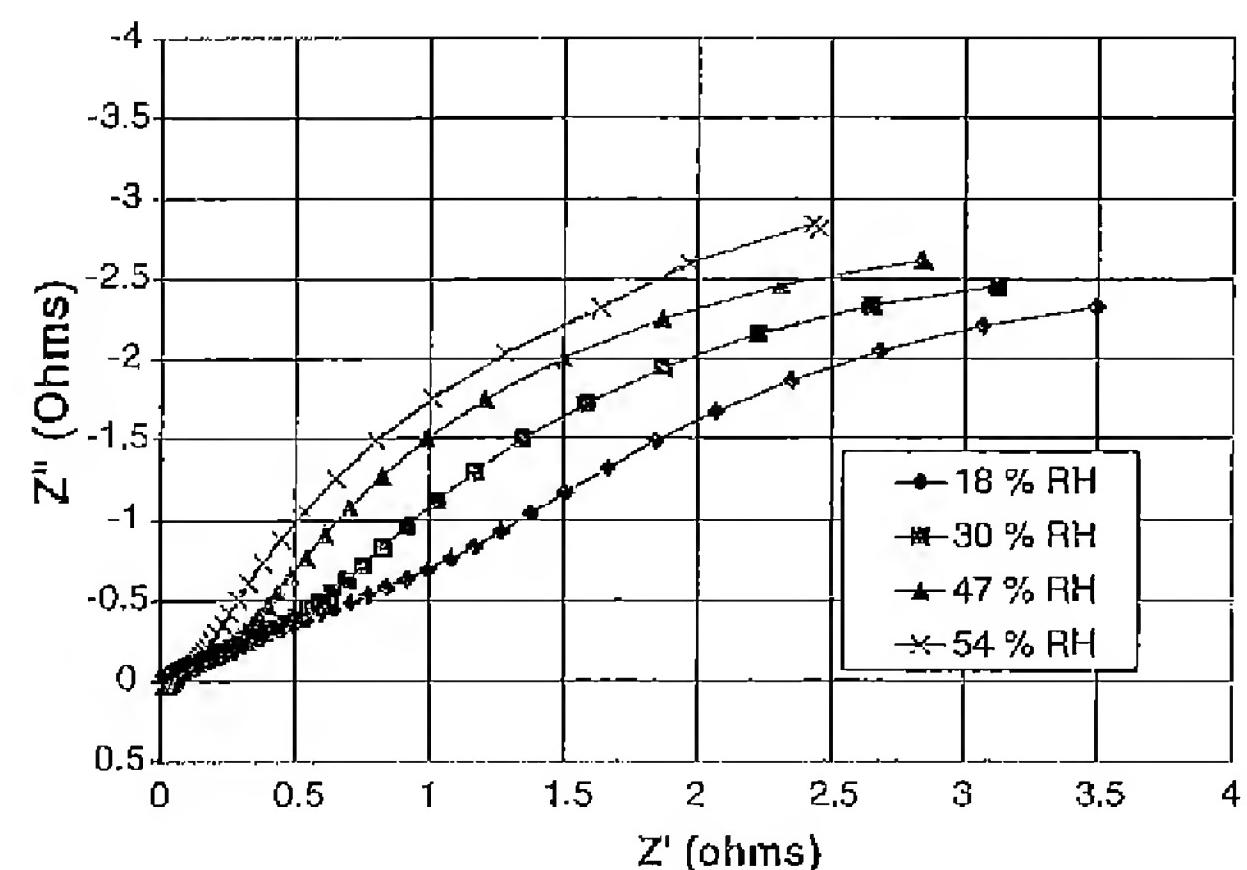

Fig. 10. Nyquist plot for the life-tested cell at the end of life (26,300 h) as a function of cell relative humidity (18, 30, 47 and 54%) in the presence of an inert gas. Cell temperature 70 °C. Nitrogen (provided to both cell compartments): flow rate 50 ml min^{-1}, ambient pressure.
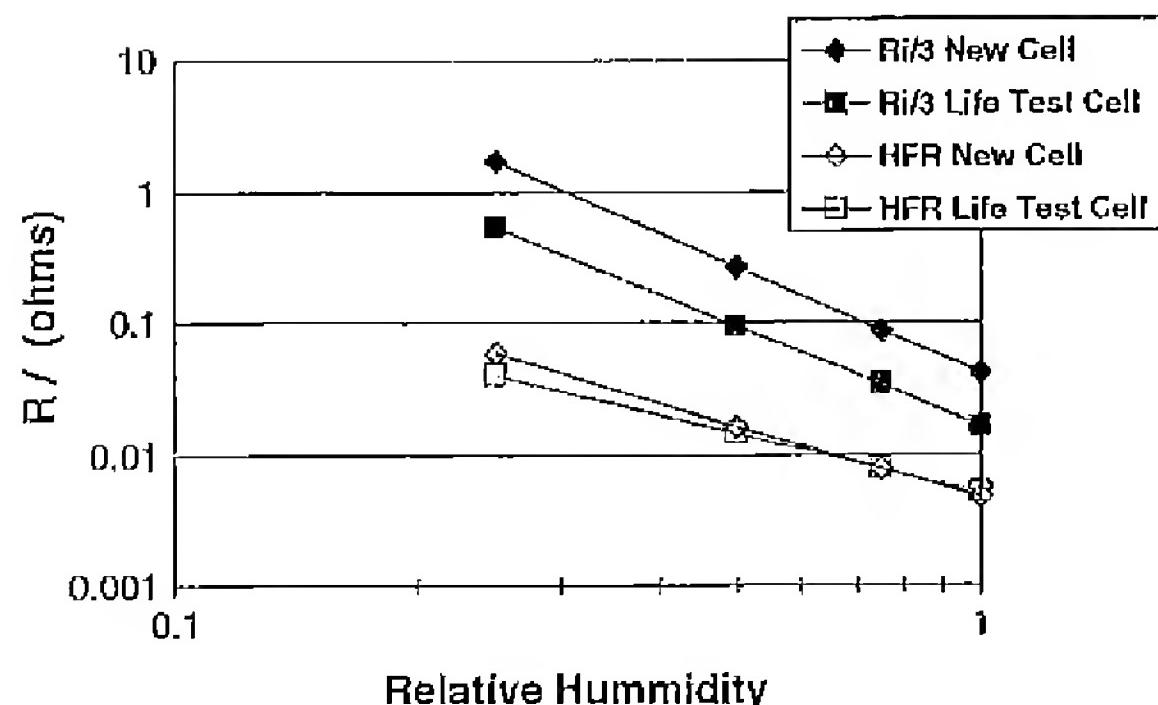
Fig. 11. High-frequency resistance (HFR) and ionic resistance of the electrode $(R_i/3)$ as a function of relative humidity for the life-tested cell at the end of life (26,300 h) and a new cell. Cell temperature 70 °C. Nitrogen (provided two both cell compartments): flow rate 50 ml min^{-1}, ambient pressure.

is a large deviation from the vertical behavior expected for a capacitive electrode. This data suggests there is some evidence of electric shorting in the cell at the reduced relative humidity in which these measurements were performed. (The DC measurements at fully saturated conditions did not indicate presence of electrical shorts.)

Again we have compared the impedance data collected in this experiment, with a new cell after break-in, as a function of RH (Fig. 11). Once again it was concluded that there is no appreciable difference in the HFR of the new and life-tested cells. There is, however, a difference in the electrode impedance between the new and used cells; the ionic resistance in the catalyst layer is determined to be significantly reduced in the life-tested MEA when compared to the new MEA. We have observed this behavior in a number of our life-tests and have several hypothesis which can account for this behavior. (1) Over the life of the test, ionic pathways in the electrode are improved compared to a new MEA (consider MEA break-in). (2) During the life-test, ionic conduction pathways have been cut as a result of ionomer degradation: the impedance technique is now only able to access to a reduced depth in the electrode, because a smaller fraction of the electrode is now accessible the apparent ionic resistance of the electrode layer is decreased.

3.3. Post mortem analysis

At 26,300 h the life test was concluded as a result of the hydrogen gas cross-over exceeding our pre-determined criteria for failure. Upon conclusion of the life test, the cell was disassembled and components analyzed.

3.3.1. Gasket

On disassembly of the cell, the only visual change in the cell was the apparent degradation of the silicone/glass re-enforced gasket. Upon measurement, the gasket thickness was typically reduced by approximately 25 μm. This silicone degradation was so severe at active area edges, that in these areas only the glass re-enforcement remained. Silicone particles from the gasket were also observed on the surface of the gas diffusion media. We have concluded that the gasket changes observed were the cause for the cell to loss compression during the test (the cell was re-torqued on several occasions). Gasket degradation may have several effects on fuel cell performance in this life test: (i) increase the load on the gas diffusion media, leading to decreased porosity and increase reactant transport resistance; (ii) increase hydrophilicity of the gas diffusion media; (iii) poisoning of the catalysts.

3.3.2. Gas diffusion media

On completion of the test, the CARBEL® CL gas diffusion media on both sides of the membrane were strongly adhered to the electrodes of the MEA. The gas diffusion layers were removed from the MEA, however, the micro-layer remained stuck to the electrodes. Because the electrochemical data suggests that the mass transport resistance of the cell was increase over the life of the test, we were interested to determine whether any change in the gas diffusion media could be observed. It has been observed in our lab and others [10] that the after life testing some gas diffusion media types will pick-up water when immersed in boiling water. On completion of the life test, both anode and cathode gas diffusion media were immersed in water at 80 °C for over 500 h, no observable water pick-up was observed for these materials, indicating no change in the material could be detected by this test. SEM of the gas diffusion media, after testing, also indicated no observable change.

3.3.3. Membrane electrode assembly

SEM analysis of the failed MEA was focused on two areas, the reactant inlet area and an edge area close to the reactant exits. The most obvious observation through both of these areas was the wide spread presence of silicon contamination, which was confirmed by EDS mapping. The silicon found in the MEA, at the end of the life test, was thought to have been introduced by degradation of the silicone gaskets that were used in this test. The presence of significant quantities of silicon made the SEM cross-sections very difficult to interpret; however, it was evident that severe membrane thinning had occurred and was observed in both areas of the MEA that were sectioned. It was found that ionomer loss was most severe at the cathode side of the membrane, although ionomer loss from the anode side was also observed. The cross-sectional analysis demonstrated no observable change in the electrodes: no electrode thinning was observed on either anode or cathode electrodes, which suggests that there was no evidence of carbon corrosion. The back-scatter electron images showed no evidence of platinum rearrangement in the electrode or dissolution of platinum into the membrane. Further EDS analysis provided no evidence of ruthenium migration to the cathode.

4. Conclusions

In this publication we have reported the results of a 26,300 h life-test, performed in single cell hardware, at test conditions relevant to a stationary fuel cell application. The fuel cell life was limited in this test by the failure of the membrane, due to increased hydrogen gas cross-over. In this experiment, the cell performance degraded at a rate of between 4 and 6×10^{-6} V h^{-1}

at the operating current density of $800\,\text{mA}\,\text{cm}^{-2}$, corresponding to a maximum total voltage loss of less than $150\,\text{mV}$ over the length of the test. The diagnostic experiments performed, during and on completion of the test, indicate that approximately 66% of the original cathode electrochemical area was lost. It was estimated that this loss in electrocatalytic surface area might only account for about $34\,\text{mV}$ of the total cell performance loss. It was concluded from the AC impedance analysis that the major contribution to cell performance loss was due to increased transport losses in the cell. We have been unable to completely explain the source of this increase in transport resistance from the experiments that were performed, however, we suspect that the detected presence of silicone contamination may have strongly influenced the performance of the cell.

Acknowledgements

References

[1] J.A. Kolde, B. Bahar, M.S. Wilson, T.A. Zawodzinski, S. Gottesfeld, Proton Conducting Membrane Fuel Cells, PV95-23, Electrochemical Society, Pennington, NJ, 1995.
[2] M.S. Wilson, S. Gottesfeld, J. Appl. Electrochem. 22 (1992) 1.
[3] M. Mathias, H.A. Gasteiger, Electrochemical Society Proceedings, vol. PV 2002-31, in: M. Murthy, T.F. Fuller, J.W. Van Zee, S. Gottesfeld (Eds.), Third International Symposium on PEM Fuel Cells, Salt Lake City, UT, 2002.
[4] D. Jollie, Fuel Cell Market Survey: Portable Applications, www.fuelcelltoday.com, 6 September 2005.
[5] F. Barbir, in: W. Vielstich, A. Lamm, H.A. Gasteiger (Eds.), Handbook of Fuel Cells, John Wiley & Sons Ltd., 2003, pp. 683–691 (Chapter 51).
[6] D.P. Wilkinson, J. St-Pierre, in: W. Vielstich, A. Lamm, H.A. Gasteiger (Eds.), Handbook of Fuel Cells, vol. 3, John Wiley & Sons Ltd., 2003, pp. 611–626 (Chapter 47).
[7] A.B. LaConti, M. Hamdan amd, R.C. McDonald, in: W. Vielstich, A. Lamm, H.A. Gasteiger (Eds.), Handbook of Fuel Cells, vol. 3, John Wiley & Sons Ltd., 2003, pp. 647–662 (Chapter 49).
[8] R. Baldwin, M. Pham, A. Leonida, J. McElroy, T. Nalette, J. Power Sources 29 (1990) 399–412.
[9] A.B. LaConti, Introduction to SPE Technology, in: Proceedings of Oronzio de Nora Symposium: Chlorine Technology, Venice Lido, Italy, May 15–18, 1979.
[10] J. St-Pierre, N. Jia, J. New Mater. Electrochem. Syst. 5 (2002) 263–271.
[11] O. Yamazaki, M. Echigo, T. Tabata, Abstracts from Fuel Cell Seminar 2002, Palm Springs, CA, November, 2002, pp. 105–108.
[12] M. Hicks, D. Ylitalo, Abstracts from Fuel Cell Seminar 2003, Miami Beach, FL, November, 2003, pp. 97–99.
[13] S.J.C. Cleghorn, J.A. Kolde, Abstract from Fuel Cell Seminar 2003, Miami Beach, FL, November, 2003, pp. 832–835.
[14] M. Takahashi, N. Kusunose, M. Aoki, A. Seya, Abstracts from Fuel Cell Seminar 2002, Palm Springs, CA, November, 2002, pp. 74–77.
[15] S.D. Knight, K.M. Colbow, J. St-Pierre, D. Wilkinson, J. Power Sources 127 (2004) 127–134.
[16] S.S. Kocha, in: W. Vielstich, A. Lamm, H.A. Gasteiger (Eds.), Handbook of Fuel Cells, vol. 3, John Wiley & Sons Ltd., 2003, pp. 538–565 (Chapter 43).
[17] T.E. Springer, T.A. Zawodzinski, M.S. Wilson, S. Gottesfeld, Electrochem. Soc. 143 (2) (1996) 587.
[18] D.A. Blom, J.R. Dunlap, A. Nolan, L.F. Allarda, J. Electrochem. Soc. 150 (4) (2003) A414.
[19] M.S. Wilson, F.H. Garzon, K.E. Sickafus, S. Gottesfeld, J. Electrochem. Soc. 140 (1993) 2872.
[20] C. Huang, K.S. Tan, J. Lin, K.L. Tan, Chem. Phys. Lett. 371 (2003) 80–84.
[21] B. Mattsson, H. Ericson, L.M. Torrell, F. Sundholm, Electrochim. Acta 45 (2000) 1405–1408.
[22] M. Murthy, D. Moore, Electrochemical Society Proceedings, vol. (in press), in: M. Murthy, K. Ota, J. W. Van Zee, S.R. Narayan, E. S. Takeuchi (Eds), Fourth International Symposium on PEM Fuel Cells, Honolulu, HI, 2004.
[23] M. Murthy, Electrochemical Society Proceedings, vol. PV 2002-31, in: M. Murthy, T.F. Fuller, J.W. Van Zee, S. Gottesfeld (Eds.), Third International Symposium on PEM Fuel Cells, Salt Lake City, UT, 2002, p. 257.
[24] S.J.C. Cleghorn, Abstracts from Fuel Cell Seminar 2000, Portland, OR, November, 2002, pp. 35–39.
[25] T. Patterson, Fuel Cell Technology; Oportunities and Challenges proceeding 2002 AIChE Spring National Meeting, New Orleans, LO, March, 2002, pp. 313–318.
[26] S.J.C. Cleghorn, J.A. Kolde, W. Liu, in: W. Vielstich, A. Lamm, H.A. Gasteiger (Eds.), Handbook of Fuel Cells, vol. 3, John Wiley & Sons Ltd., 2003, pp. 566–575 (Chapter 44).

- Cheng, X. et al; *A review of PEM hydrogen fuel cell contamination, . . .*; Journal of Power Sources; 165, 2, 739-756, (March 2007).

ScienceDirect

Home   Browse   Search   My Settings   Alerts   Help

Quick Search

🔍 search tips

All fields

Journal/book title

return to SCIrUS

Journal of Power Sources
Volume 165, Issue 2, 20 March 2007, Pages 739
IBA – HBC 2006 - Selected papers from the
INTERNATIONAL BATTERY ASSOCIATION & H
BATTERY CONFERENCE 2006 Waikoloa, Hawa
9-12 January 2006

▸ **Abstract**   Figures/Tables   Order Document

doi:10.1016/j.jpowsour.2006.12.012 **Article Toolbox**
⑦ Cite or Link Using DOI

Review

A review of PEM hydrogen fuel cell contamination: Impacts, mechanisms, and mitigation

🕐 E-mail
Article

🕐 Cited By

🕐 Save as
Citation Alert

📶 Citation
Feed

Export
Citation

Add to my
Quick Links

Add to 2collab

Permissions & Reprints

Cited By in
Scopus (53)

Relevant Terms extracted from this **Article**

See **Data Correlations, Clinical Trials** and more on:

Diseases | 3
poisoning   poisoning by
foreign materials

Compounds | 5
Platinum   nitrogen
ethanol   sodium

Xuan Cheng[a, b], Zheng Shi[a], Nancy Glass[a], Lu Zhang[b], Jiujun Zhang[a, ✉], Datong Song[a], Zhong-Sheng Liu[a], Haijiang Wang[a] and Jun Shen[a]

[a]Institute for Fuel Cell Innovation, National Research Council of Canada, Vancouver, BC V6T 1W5, Canada

[b]Department of Materials Science and Engineering, State Key Laboratory for Physical Chemistry of Solid Surfaces, Xiamen University, Xiamen, FJ 361005, PR China

Biogroups | 2

proton transportatio...   sulfur oxides

View more...

Scientific correlations by NextBio

Related Articles in ScienceDirect

- Development and demonstration of a higher temperature P...
  Journal of Power Sources
- PEM fuel cells operated at 0% relative humidity in the ...
  Electrochimica Acta
- A review of accelerated stress tests of MEA durability ...
  International Journal of Hydrogen Energy
- Effects of membrane electrode assembly components on pr...
  International Journal of Hydrogen Energy
- Analysis of proton exchange membrane fuel cell polariza...
  Electrochimica Acta
- View More Related Articles

View Record in Scopus

Abstract

This paper reviewed over 150 articles on the subject of the effect of contamination on PEM fuel cell. The contaminants included were fuel impurities (CO, CO_2, H_2S, and NH_3); air pollutants (NO_x, SO_x, CO, and CO_2); and cationic ions Fe^{3+} and Cu^{2+} resulting from the corrosion of fuel cell stack system components. It was found that even trace amounts of impurities present in either fuel or air streams or fuel cell system components could severely poison the anode, membrane, and cathode, particularly at low-temperature operation, which resulted in dramatic performance drop. Significant progress has been made in identifying fuel

cell contamination sources and understanding the effect of contaminants on performance through experimental, theoretical/modeling, and methodological approaches. Contamination affects three major elements of fuel cell performance: electrode kinetics, conductivity, and mass transfer.

This review was focused on three areas: (1) contamination impacts on the fuel cell performance, (2) mechanism approaches dominated by modeling studies, and (3) mitigation development. Some future work on fuel cell contamination research is suggested in order to facilitate the move toward commercialization.

Keywords: PEM fuel cells;
Contamination; Mechanism;
Modeling; Pt catalyst
poisoning; Fuel impurities
and air pollutants

Article Outline

Corresponding author. Tel.: +1 604 221 3087; fax: +1 604 221 3001.

Home   Browse   Search   My Settings   Alerts   Help

About ScienceDirect | Contact Us | Information for Advertisers | Terms & Conditions | Privacy Policy

- Molter, Trent M.; *The effects of impurities on fuel cell performance and durability*; (May 2007).

The Effects of Impurities on Fuel Cell Performance and Durability

Trent M. Molter

Research Scientist and Business Development Officer

The Connecticut Global Fuel Cell Center

The University of Connecticut

May 2007

Project ID
#FCP15

Hamilton Sundstrand
A United Technologies Company

FuelCell Energy

Overview

Timeline

- Start March 2007
- End February 2011
- New Start ~0% Complete

Budget

- Total project funding $2,335,725
  - DOE share $1,868,580
  - Contractor share $467,145
- No Funding Received in FY06
- Funding for FY07 - $70K

Barriers

- Establish Tolerance to Air, Fuel and System Derived Impurities

Partners

- United Technologies Hamilton Sundstrand – Historical Contaminant Data
- FuelCell Energy, Inc., – Contaminant Test Support
- UConn CGFCC – Project Management

Objectives

- **Overall Objective – Develop an Understanding of the Effects of Various Contaminants on Fuel Cell Performance and Durability**

- **Specific Task Objectives Shown Below**

Task	Objectives
1.0 Contaminant Identification	• Identify specific contaminants and contaminant families present in both fuel and oxidant streams.
2.0 Analytical Method Development	• Development of analytical methods to study contaminants. • Experimental design of analytical studies. • Novel *in situ* detection methods.
3.0 Contaminant Studies	• Develop contaminant analytical models that explain these effects. • Establish an understanding of the major contamination-controlled mechanisms that cause material degradation in PEM cells and stacks under equilibrium and especially dynamic loading conditions
4.0 Contaminant Model Development	• Construct material state change models that quantify that material degradation as a foundation for multiphysics modeling • Establish the relationship between those mechanisms and models and the loss of PEM performance, especially voltage decay
5.0 Contaminant Model Validation	• Validate contaminant models through single cell experimentation using standardized test protocols.
6.0 Novel Mitigation Technologies	• Develop and validate novel technologies for mitigating the effects of contamination on fuel cell performance.
7.0 Outreach	• Conduct outreach activities to disseminate critical data, findings, models, and relationships etc. that describe the effects of certain contaminants on PEM fuel cell performance.

CGFCC

Hamilton Sundstrand
A United Technologies Company

FuelCell Energy

Approach

- Initiate Studies by Leveraging Existing Database From Prior Work
  - DOE Sponsored Activity
  - USFCC Data
  - Prior Electrolysis Product Experience
- Focus on Specific Contaminants/Concentrations Identified by DOE/Others
- Use Standardized Test Protocols Where Appropriate to Investigate Contaminant Effects
- Develop Empirical Models Based on Our Findings

CGFCC — INNOVATION MADE SIMPLE

Diagram labels:
- CO, NH_3, H_2S, Trace Metals, Formic Acid, Hydro-carbons
- SO_2, NO_2, Dust, Ocean salt, Chlorides
- $2 H_2$, $4 e^-$, $4 H^+$, O_2, $2 H_2O$
- Proton Exchange Membrane, PEM
- anode, cathode, TPB

Hamilton Sundstrand — A United Technologies Company

FuelCell Energy

Project Work Plan/Deliverables

CGFCC
INNOVATIONS MADE TRUE

1.0 Contaminant Identification

2.0 Analytical Method Development

3.0 Contaminant Studies

Effects of Impurities on Fuel Cell Performance and Durability

4.0 Contaminant Model Development

5.0 Contaminant Model Validation

6.0 Novel Mitigation Technologies

7.0 Outreach

Outreach & Education

Novel Mitigation Technologies

Contaminant Modeling and Validation

Industrial Experience Base
Laboratory Experimentation
Literature Review

Deliverables
- Validated Contaminant Models
- New Mitigation Technologies
- Outreach: Papers, Workshops, Technical Interchange, Etc.

Hamilton Sundstrand
A United Technologies Company

FuelCell Energy

Future Work

Task	Yr 1 Q1	Q2	Q3	Q4	Yr 2 Q1	Q2	Q3	Q4	Yr 3 Q1	Q2	Q3	Q4	Yr 4 Q1	Q2	Q3	Q4
1.0 Contaminant Identification																
2.0 Analytical Method Devt.																
3.0 Contaminant Studies																
4.0 Contaminant Model Devt.																
5.0 Contaminant Model Validation																
6.0 Novel Mitigation Tech.																
7.0 Outreach																
8.0 Project Management and Reporting																

Task	Milestone	Date Year/Quarter
1.0 Contaminant Identification	• Contaminant Identification Review With DOE Sponsor & Industry Focus Group	Y1/Q2
2.0 Analytical Method Development	• Validate Analytical Methods For Studying Contaminants With Ersatz Gases	Y1/Q4
3.0 Contaminant Studies	• Establish an Understanding of the Major Contamination-Controlled Mechanisms that Cause Material Degradation	Y2/Q4
4.0 Contaminant Model Development	• Determine the Relationship Between Contaminant Mechanisms and the Loss of PEM Performance, Especially Voltage Decay.	Y3/Q4
5.0 Contaminant Model Validation	• Validate Contamination Models Through Single Cell Experimentation Using Standardized Test Protocols and a DOE Approved Test Matrix	Y4/Q1
6.0 Novel Mitigation Technologies	• Demonstrate Novel Technologies for Mitigating the Effects of Contamination on Fuel Cell Performance	Y4/Q4
7.0 Outreach	• Dissemination of Results Through Reports (DOE Approved), Papers and Workshops	Continuous
8.0 Project Management and Reporting	• Program Written Reports and Program Reviews	Continuous

- 4 Year Project
- Time Phased Milestones
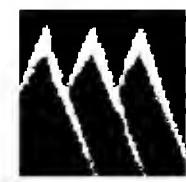
Activities and Expertise

CGFCC
INNOVATION MADE SIMPLE

Hamilton Sundstrand
A United Technologies Company

FuelCell Energy

Roles of Participants

The Universtiy of Connecticut
Connecticut Global Fuel Cell Center
Program Lead

United Technologies
Hamilton Sundstrand
Advise on Fate of Contaminants

- Electrolysis Contaminant Experience
- Prior Contaminant Studies

The University of Connecticut
Institute for Materials Science
Gas Analyses/Surface Studies

- Surface Studies/Equipment
- Gas Purity Analyses

The University of Connecticut
School of Engineering
Contaminant Testing
Modeling & Mitigation Strategies

- Fuel Cell Testing
- Modeling/Transport Expertise
- Industry Relationships

FuelCell Energy Inc.
Contaminant Identification
Fuel Cell Testing

- Gas Contaminant Experience
- Fuel Cell Test Experience

CGFCC
INNOVATION MADE SIMPLE
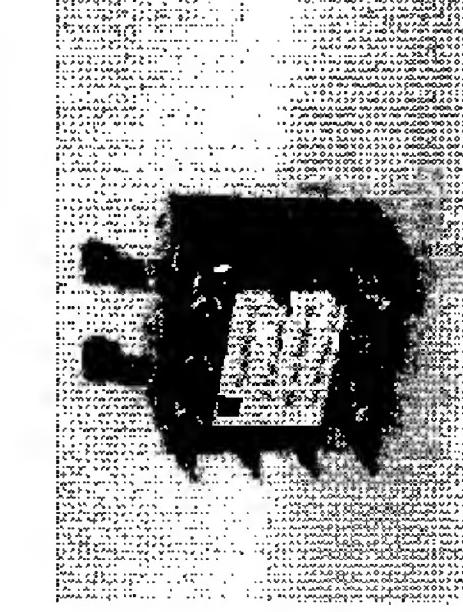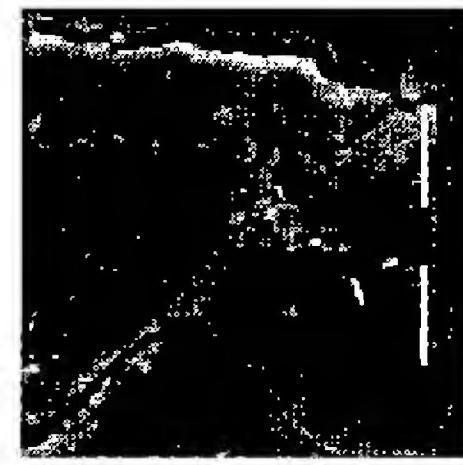
Hamilton Sundstrand
A United Technologies Company

FuelCell Energy

Project Summary

- **Relevance** - A Deeper Understanding of the Effects of Specific Contaminants on Fuel Cell Performance is Necessary for Successful Commercialization

- **Approach** - Our Experienced Team Will:
  - Leverage Existing Knowledge and Will Systematically Investigate Certain Fuel Contaminants of Interest
  - Create Empirical and Detailed Analytical Models to Predict the Fate of Specific Contaminants and Their Effect on Fuel Cell Performance

- **Technology Transfer** - Data Will Be Shared Through Papers, Workshops, Working Groups, Etc.

- **Collaboration** – Active Partnership with UTC and FCE
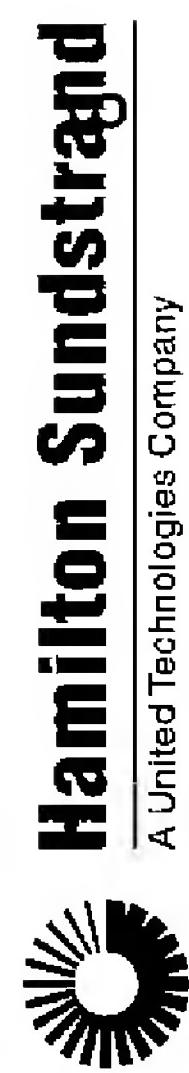
CGFCC
INNOVATION MADE SIMPLE

UNIVERSITY OF CONNECTICUT 1881

Hamilton Sundstrand
A United Technologies Company

FuelCell Energy

Effects of Impurities on Fuel Cell Performance and Durability

Trent M. Molter

Research Scientist and Business Development Officer

The Connecticut Global Fuel Cell Center

The University of Connecticut

CGFCC
INNOVATION MADE SIMPLE

UNIVERSITY OF CONNECTICUT 1881

Hamilton Sundstrand
A United Technologies Company
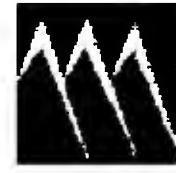
FuelCell Energy

Agenda

- Introduction
- Background/Technical Concept
- Project Objectives
- Project Work Plan/Deliverables
- Project Timetable
- Roles of Participants
- Facilities and Equipment
- Summary

CGFCC
INNOVATION MADE SIMPLE

UNIVERSITY OF CONNECTICUT 1881

Hamilton Sundstrand
A United Technologies Company

FuelCell Energy

SO_2
NO_2
Dust
Ocean salt
Chlorides

O_2

$2 H_2O$

$4 e^-$

$4 H^+$

Proton Exchange Membrane

PEM

TPB

cathode

TPB

anode

$2 H_2$

CO
NH_3
H_2S
Trace Metals
Formic Acid
Hydro-carbons
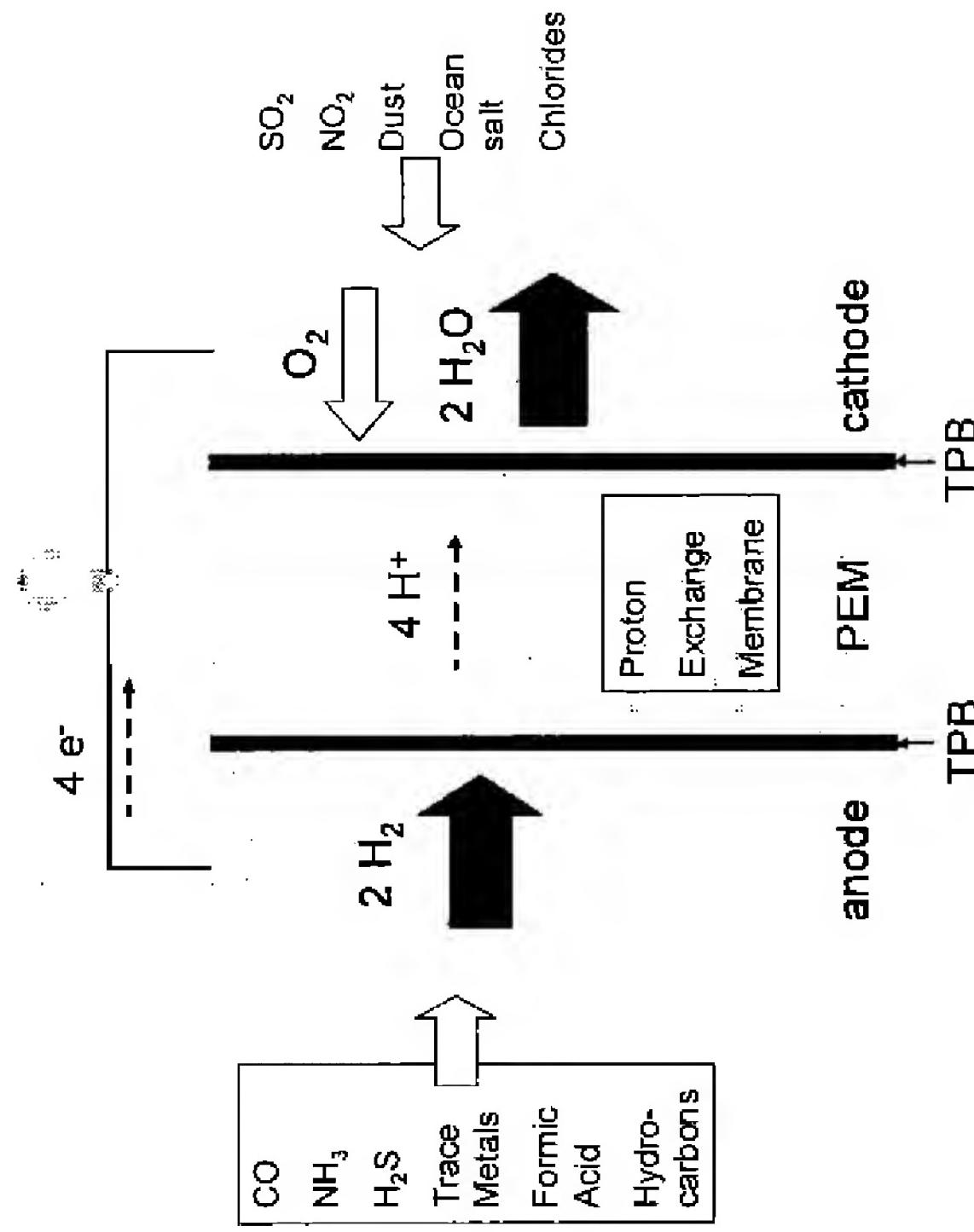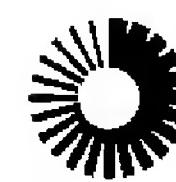
Introduction

- Cost and Durability of Fuel Cells are Important Barriers to Commercialization

- Contamination of Fuel Cells From Fuels/Oxidants Affects Both Cost And Durability

- General Effects of Certain Contaminants on Fuel Cell Performance and Durability are Known, But Empirical Relationships and Specific Performance Models are Not Well-Established

Contaminant Category	Examples	Fate of Contaminant	General Performance Effects
Large Cations	Fe, Cr, Ni	Broad Distribution Throughout Membrane	Increases Ionic Resistance
	Cu	Movement to Cathode/Membrane Interface During Operation	Contributes to Electrode Overvoltage
	Mg, Ca	Tends to Agglomerate in Membrane (Forms Rocks)	Increases Ionic Resistance, Causes Pinholing
Small Cations	Na+, Li+	Broad Distribution Throughout Membrane, Move to Cathode During Operation	Increases Ionic Resistance, Reduces Water Content at Cathode Surface
Anions	Cl-, SO_2--	Movement to Anode	Sometimes No Effect
Organics	HCOOH,	Some Adsorbs on Catalyst Surface	Reduces Catalyst Activity
Inerts	N_2, Ar	Some Adsorbs on Catalyst Surface	Functions as Diluent for Reactants

CGFCC
INNOVATION MADE SIMPLE

Hamilton Sundstrand
A United Technologies Company
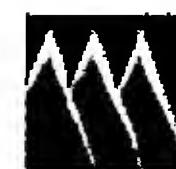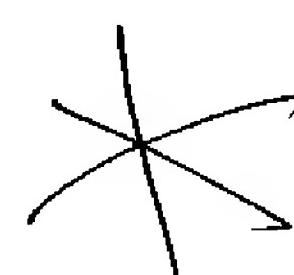
FuelCell Energy

Background/Technical Concept

- Initiate Studies by Leveraging Existing Database From Prior Work
  - DOE Sponsored Activity
  - USFCC Data
  - Prior Electrolysis Product Experience
- Focus on Specific Contaminants/Concentrations Identified by DOE/Others
- Use Standardized Test Protocols Where Appropriate to Investigate Contaminant Effects
- Develop Empirical Models Based on Our Findings

Contaminant	Affected Area			Contaminant Source
	Membrane (MEA)	Electrode	Assembly	
Stainless Steel				Gas Diffusion Layer (GDL) Screen and Bipolar Plates
• Cr				
• Ni				
• Fe				
Silicon	Pt Catalyst Formed Under Pt Oxides			Gasket and Cooling Fluid
Sulfur	Pt Catalyst			Vulcanized Carbon in Catalyst
Sodium	Membrane			Membrane Impurities
Copper Chloride	Membrane Conductivity			Coating for Aluminum Bipolar Plate
Ca^{2+}	Membrane			Membrane Impurity
Carbon Monoxide	Pt Catalyst			Gas Reactants
Sulfur Dioxide	Membrane			Air Near Battlefield
Benzene	Membrane			Air Near Battlefield
Ammonia	Membrane			Air Pollution
SO_2	Catalyst			Air Pollution
HCN	Catalyst			Air Near Battlefield
CNCl	Catalyst			Air Near Battlefield
Sarin	Catalyst			Air Near Battlefield
Sulfur Mustard	Catalyst			Air Near Battlefield
Acetaldehyde	Catalyst			Byproduct of Ethanol Fuel Source

Hamilton Sundstrand
A United Technologies Company

FuelCell Energy

Project Objectives

Task	Objectives
1.0 Contaminant Identification	• Identify specific contaminants and contaminant families present in both fuel and oxidant streams.
2.0 Analytical Method Development	• Development of analytical methods to study contaminants. • Experimental design of analytical studies. • Novel *in situ* detection methods.
3.0 Contaminant Studies	• Develop contaminant analytical models that explain these effects. • Establish an understanding of the major contamination-controlled mechanisms that cause material degradation in PEM cells and stacks under equilibrium and especially dynamic loading conditions
4.0 Contaminant Model Development	• Construct material state change models that quantify that material degradation as a foundation for multiphysics modeling • Establish the relationship between those mechanisms and models and the loss of PEM performance, especially voltage decay
5.0 Contaminant Model Validation	• Validate contaminant models through single cell experimentation using standardized test protocols.
6.0 Novel Mitigation Technologies	• Develop and validate novel technologies for mitigating the effects of contamination on fuel cell performance.
7.0 Outreach	• Conduct outreach activities to disseminate critical data, findings, models, and relationships etc. that describe the effects of certain contaminants on PEM fuel cell performance.

CGFCC
INNOVATION MADE SIMPLE

Hamilton Sundstrand
A United Technologies Company

FuelCell Energy

Project Work Plan/Deliverables

CGFCC
INNOVATION MADE SIMPLE

UNIVERSITY OF CONNECTICUT · 1881

Effects of Impurities on Fuel Cell Performance and Durability

- 1.0 Contaminant Identification
- 2.0 Analytical Method Development
- 3.0 Contaminant Studies
- 4.0 Contaminant Model Development
- 5.0 Contaminant Model Validation
- 6.0 Novel Mitigation Technologies
- 7.0 Outreach

Outreach & Education

Novel Mitigation Technologies

Contaminant Modeling and Validation

Industrial Experience Base
Laboratory Experimentation
Literature Review

Deliverables
- Validated Contaminant Models
- New Mitigation Technologies
- Outreach: Papers, Workshops, Technical Interchange, Etc.

Hamilton Sundstrand
A United Technologies Company

FuelCell Energy

Project Timetable

Task	Yr 1				Yr 2				Yr 3				Yr 4			
	Q1	Q2	Q3	Q4	Q1	Q2	Q3	Q4	Q1	Q2	Q3	Q4	Q1	Q2	Q3	Q4
1.0 Contaminant Identification																
2.0 Analytical Method Devl.																
3.0 Contaminant Studies																
4.0 Contaminant Model Devt.																
5.0 Contaminant Model Validation																
6.0 Novel Mitigation Tech.																
7.0 Outreach																
8.0 Project Management and Reporting																

- 4 Year Project
- Time Phased Milestones Activities and Expertise

Task	Milestone	Date Year/Quarter
1.0 Contaminant Identification	Contaminant Identification Review With DOE Sponsor & Industry Focus Group	Y1/Q2
2.0 Analytical Method Development	Validate Analytical Methods For Studying Contaminants With Ersatz Gases	Y1/Q4
3.0 Contaminant Studies	Establish an Understanding of the Major Contamination-Controlled Mechanisms that Cause Material Degradation	Y2/Q4
4.0 Contaminant Model Development	Determine the Relationship Between Contaminant Mechanisms and the Loss of PEM Performance, Especially Voltage Decay.	Y3/Q4
5.0 Contaminant Model Validation	Validate Contamination Models Through Single Cell Experimentation Using Standardized Test Protocols and a DOE Approved Test Matrix	Y4/Q1
6.0 Novel Mitigation Technologies	Demonstrate Novel Technologies for Mitigating the Effects of Contamination on Fuel Cell Performance	Y4/Q4
7.0 Outreach	Dissemination of Results Through Reports (DOE Approved), Papers and Workshops	Continuous
8.0 Project Management and Reporting	Program Written Reports and Program Reviews	Continuous

UNIVERSITY OF CONNECTICUT 1881

CGFCC
INNOVATION MADE SMART

Hamilton Sundstrand
A United Technologies Company

FuelCell Energy

Roles of Participants

The University of Connecticut
Connecticut Global Fuel Cell Center
Program Lead

United Technologies
Hamilton Sundstrand
Advise on Fate of Contaminants

The University of Connecticut
Institute for Materials Science
Gas Analyses/Surface Studies

The University of Connecticut
School of Engineering
Contaminant Testing
Modeling & Mitigation Strategies

FuelCell Energy Inc.
Contaminant Identification
Fuel Cell Testing

- Electrolysis Contaminant Experience
- Prior Contaminant Studies

- Surface Studies/Equipment
- Gas Purity Analyses

- Fuel Cell Testing
- Modeling/Transport Expertise
- Industry Relationships

- Gas Contaminant Experience
- Fuel Cell Test Experience

CGFCC
INNOVATION MADE SIMPLE

Hamilton Sundstrand
A United Technologies Company

FuelCell Energy

Task Participants

CGFCC
INNOVATION MADE SIMPLE

Program Lead
T. Molter
CGFCC/UConn

Task 1.0 Team Leader
Contaminant Identification and Characterization
Nigel Sammes
CGFCC/UConn

Hamilton Sundstrand
A United Technologies Company

Task 2.0 Team Leader
Analytical Method Development
Steven Suib
IMS/UConn

Task 3.0 Team Leader
X. Huang
Contaminant Studies
CGFCC/UConn

FuelCell Energy

Task 4.0 Team Leader
U. Pasaogulari
Contaminant Model Development
CGFCC/UConn

Task 5.0 Team Leader
K. Reifsnider
Contaminant Model Validation
CGFCC/UConn

FuelCell Energy

Task 6.0 Team Leader
B. Willhite
Novel Mitigation Methods
CGFCC/UConn

Task 7.0 Team Leader
T. Molter
Outreach

FuelCell Energy

**Hamilton Sundstrand**
A United Technologies Company

Hamilton Sundstrand
A United Technologies Company

Facilities and Equipment

- 16,000 Ft² Facility
- 4 – 24 Foot High Bay Test Areas With Air/Water/Ventilation, Overhead Doors and a 220/480 Electrical Bus
- 4 Physical Wet-Lab Areas With Air/Water/Ventilation and 110/220 Electrical Service
- 2 Classrooms
- Conference Room
- Administrative Offices
- Access to Main Campus Facilities Including the Institute for Materials Science

CGFCC
INNOVATION MADE SIMPLE

UNIVERSITY OF CONNECTICUT 1881

Hamilton Sundstrand
A United Technologies Company

FuelCell Energy

Facilities and Equipment

- **Analytical Capabilities at UConn's Institute for Materials Science Will Be Leveraged to Support This Activity**
  - Surface Studies
  - Gas Analysis
- **Additional Capabilities at FuelCell Energy/UTC Will Be Leveraged to Support Program Activities As Required**

Optical	Catalysis
Nicolet 750 FTIR, Near, Mid and Far Regions	In Situ Photoreactors
Spex Raman	Transient Reactor with Nuclide Mass Spec/GC
Spex Fluorolog	Batch and Flow Thermal Reactors
ISA/JY CCD Spectrometer	HP GCMS
Raman Imaging	

Thermal	Analytical
DuPont TGA	Inductively Coupled Plasma Mass Spec
DSC	Bomb Atom
Cahn Balance	Bomb hydrocalorimetric Spec
Home-Built Temperature Program Desorption/Reaction/Reaction	Binary Diffraction & Ray Analysis
Home-Bulk Microbalance	GCMS
	TOF Maldi MS
	Atomic Absorption

| Structural |
|---|
| Scintag XDS 2000 Diffractometer, In Situ Heating Stage |
| In Situ XRD |
| Thermo ARL/Anton Parr |

Morphological	Magnetic
JEOL 2010 FasTEM HRTEM	Varian E-3 EPR
Philips EM400T Transmission Electron Microscope	X/Q Band Bruker Spectrometer
Nikon Optical Metallurgical Microscope	Spin Echo NMR
AMRAY 1810 D SEM	Vibrating Sample Magnetometer
JEOL 6315F FESEM	
AMRAY 9800 EDX	

Chromatography
ISCO HPLC System -Single-Pump Ternary Gradient Programmer, Programmable Pump -V Variable UV/VIS Detector
HP6890 GC Equipped With TCD and FID Detectors
HP6890 GC With Sulphur Specific PPD

Hamilton Sundstrand — A United Technologies Company

FuelCell Energy

Summary

- Contaminants Affect Fuel Cell Performance in Many Ways

- A Deeper Understanding of the Effects of Specific Contaminants on Fuel Cell Performance is Necessary for Successful Commercialization

- Our Experienced Team Will Leverage Existing Knowledge and Will Systematically Investigate Certain Fuel Contaminants of Interest

- Empirical and Detailed Analytical Models Will Be Created to Predict the Fate of Specific Contaminants and Their Effect on Fuel Cell Performance

- Data Will Be Shared Through Papers, Workshops, Working Groups, Etc.

Hamilton Sundstrand
A United Technologies Company

FuelCell Energy

- Wu, J. et al; A review of PEM fuel cell durability: . . .; Journal of Power Sources; 184, 105-119, 107, (June 2008).
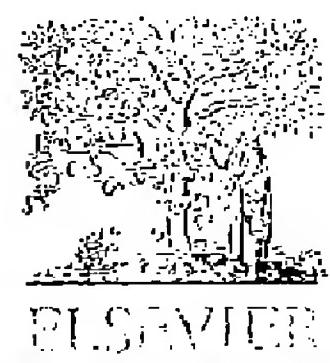
Review

A review of PEM fuel cell durability: Degradation mechanisms and mitigation strategies

Jinfeng Wu[a], Xiao Zi Yuan[a], Jonathan J. Martin[a], Haijiang Wang[a,*], Jiujun Zhang[a], Jun Shen[a], Shaohong Wu[a], Walter Merida[a,b]

[a] Institute for Fuel Cell Innovation, National Research Council of Canada, Vancouver, B.C., Canada V6T 1W5
[b] Department of Mechanical Engineering, University of British Columbia, Vancouver, B.C., Canada V6T 1Z4

ABSTRACT

This paper reviews publications in the literature on performance degradation of and mitigation strategies for polymer electrolyte membrane (PEM) fuel cells. Durability is one of the characteristics most necessary for PEM fuel cells to be accepted as a viable product. In this paper, a literature-based analysis has been carried out in an attempt to achieve a unified definition of PEM fuel cell lifetime for cells operated either at a steady state or at various accelerated conditions. Additionally, the dependence of PEM fuel cell durability on different operating conditions is analyzed. Durability studies of the individual components of a PEM fuel cell are introduced, and various degradation mechanisms are examined. Following this analysis, the emphasis of this review shifts to applicable strategies for alleviating the degradation rate of each component. The lifetime of a PEM fuel cell as a function of operating conditions, component materials, and degradation mechanisms is then established. Lastly, this paper summarizes accelerated stress testing methods and protocols for various components, in an attempt to prevent the prolonged test periods and high costs associated with real lifetime tests.

© 2008 Elsevier B.V. All rights reserved.

Contents

* Corresponding author. Tel.: +1 604 221 3038; fax: +1 604 221 3001.
  E-mail address: haijiang.wang@nrc-cnrc.gc.ca (H. Wang).

1. Introduction

To date, considerable effort has been devoted to the development of highly efficient and reliable polymer electrolyte membrane (PEM) fuel cells and stacks intended for many potential power source applications, including batteries for portable devices; fuel cell engines for automotive applications, displacing the internal combustion engine; and the residential stationary power market. Unquestionably, significant progress has been achieved over the past decade, especially in the areas of increasing volumetric and/or gravimetric specific power density and more effective materials utilization.

However, contrary to expectations held since the last decade that PEM fuel cells would be commercialized in stationary applications by 2001 and in transport applications as early as 2003 [1], technical challenges remain for the on-board storage and infrastructure for hydrogen fuel, as well as for the fuel cell system itself. With regard to the fuel cell system, one of the major hurdles is still its high cost; only when fuel cell costs are dramatically reduced to the US Department of Energy (DOE) target of $50 kW^{-1} will fuel cells be competitive for virtually every type of power application.

Another technical barrier for the acceptance of fuel cells as a practical power source is durability under a wide range of operational conditions [2]. For different applications, the requirements for fuel cell lifetime vary significantly, ranging from 5000 h for cars to 20,000 h for buses and 40,000 h of continuous operation for stationary applications. Although the life targets for automobiles are much lower than those for stationary applications, the operating conditions of dynamic load cycling, startup/shutdown, and freeze/thaw make this goal very challenging for current fuel cell technologies. Unfortunately, at present most PEM fuel cell stacks provided by manufacturers and research institutes cannot achieve these goals.

The performance of a PEM fuel cell or stack is affected by many internal and external factors, such as fuel cell design and assembly, degradation of materials, operational conditions, and impurities or contaminants. Performance degradation is unavoidable, but the degradation rate can be minimized through a comprehensive understanding of degradation and failure mechanisms. In order to clearly understand the concepts of PEM fuel cell lifetime and performance decay discussed in this review, we first clarify several relevant terms [3–5]:

- *Reliability*: The ability of a fuel cell or stack to perform the required function under stated conditions for a period of time. It includes failure modes that can lead to catastrophic failure and performance below an acceptable level.
- *Durability*: The ability of a PEM fuel cell or stack to resist permanent change in performance over time. Durability decay does not lead to catastrophic failure but simply to a decrease in performance that is not recoverable or reversible (i.e., due to loss of electrochemical surface area, carbon corrosion, etc.). This issue is related to ageing.
- *Stability*: The ability to recover power lost during continuous operation. Stability decay is always concerned with operating conditions (such as water management) and reversible material changes.

The overall fuel cell performance decay rate, measured during continuous and uninterrupted operation, is the sum of both the stability and durability decay rates. Normal degradation targets require less than 10% loss in the efficiency of the fuel cell system at

Table 1
Summary of steady state lifetime tests in the literature

Authors	Test time (h)	Degradation rate	Reference
Ralph	5,000	4 μV h^{-1}	[7]
St-Pierre et al.	5,000	1 μV h^{-1}	[8]
Washington	4,700	6 μV h^{-1}	[9]
	8,000	2.2 μV h^{-1}	
Endoh et al.	4,000	2 μV h^{-1}	[10]
Yamazaki et al.	8,000	2–3 μV h^{-1}	[11]
St-Pierre and Jia	11,000	2 μV h^{-1}	[12]
Fowler et al.	1,350	11 μV h^{-1}	[13]
Ahn et al.	1,800	>4 mV h^{-1}	[14]
Cheng et al.	4,000	3.1 μV h^{-1}	[15]
Scholta et al.	2,500	20 μV h^{-1}	[16]
Cleghorn et al.	26,300	4–6 μV h^{-1}	[4]

the end of life, and a degradation rate of 2–10 μV h^{-1} is commonly accepted for most applications [6].

In this paper, studies conducted by academic and industry researchers on the lifetime of state-of-the-art PEM fuel cells operated in steady state or accelerated conditions such as load or thermal cycles or fuel or oxidant starvation are summarized. The major findings from both experimental and theoretical studies of the degradation and failure modes of fuel cells and their components are introduced. Feasible strategies to mitigate the performance decay resulting from each degradation mechanism are discussed in detail. The existing methods for accelerated stress testing of different components are analyzed. From the viewpoint of practical applications, a statistical model based on the accelerated lifetime data of fuel cell components is proposed to estimate real lifetime under normal testing conditions.

2. Steady state and accelerated lifetime tests

Until now, while comprehensive experimental results and reviews have been published in an attempt to understand the degradation mechanisms of fuel cell components such as electrocatalysts, membranes, and bipolar plates, only a relatively small number of studies aimed at real PEM fuel cell lifetimes have been conducted, due to the high costs and prolonged testing periods required. For example, more than 4.5 years of uninterrupted testing is needed to reach the 40,000-h lifetime requirement for a fuel cell system for stationary applications. For testing a fuel cell bus system (275 kW) for 20,000 h, the fuel expense alone would be approximately US $2 million (3.8 billion liters of hydrogen at US $5.3 m^{-3}). To increase sample throughput and reduce the experimental time required, several fuel cell developers and companies, such as Ballard Power Systems, DuPont, Gore, and General Motors, have proposed and implemented different accelerated stress tests (ASTs) to determine the durability and performance of current fuel cell components. This study summarizes papers published in the last decade on PEM fuel cell degradation and lifetimes. Tables 1 and 2 present work on steady state and accelerated lifetime tests, respectively.

Although most experiments on fuel cell lifetime under steady state operation demonstrated acceptable results, with a degradation rate between 2 and 10 μV h^{-1}, they were conducted for much less than 40,000 h. As for ASTs, almost all degradation rates were greater than 10 μV h^{-1}. Prior to commercializing fuel cell technology, more thorough studies on components and the analysis of system failure modes are imperative.

Table 2
Summary of accelerated durability tests in the literature

Authors	Test time (h)	Degradation rate	Operating conditions	Reference
Sishtla et al.	5,100	$6 \mu V h^{-1}$	Reformate fuel	[17]
Nakayama	4,000	$4.3 \mu V h^{-1}$	Reformate fuel	[18]
Isono et al.	2,000	$10 \mu V h^{-1}$	Reformate fuel	[19]
Maeda et al.	5,000	$6 \mu V h^{-1}$	Reformate fuel	[20]
Sakamoto et al.		$50–90 \mu V$	Per start/stop cycles	[21]
Fowler et al.	600	$120 \mu V h^{-1}$	Humidity cycles	[22]
Cho et al.		$4200 \mu V$	Per thermal cycles	[23]
Knights et al.	13,000	$0.5 \mu V h^{-1}$	Methane reformate fuel	[6]
			Low humidification	
Oszcipok et al.		$22,500 \mu V$	Per cold start-up	[24]
Xie et al.	1,916	$60 \mu V h^{-1}$	Over-saturated humidification	[25]
	1,000	$54 \mu V h^{-1}$		
Yu et al.	2,700	$21 \mu V h^{-1}$	Low humidification	[26]
Endoh et al.	3,500	$3 \mu V h^{-1}$	High temperature	[27]
			Low humidification	
Du et al.	1,900	$70–800 \mu V h^{-1}$	Cold start and hot stop	[28]
Xu et al.	1,000	$<10 \mu V h^{-1}$	High temperature	[29]
			Low humidification	
Owejan et al.		$0.212 mV$	Per start/stop cycles	[30]

3. Major failure modes of different components of PEM fuel cells

3.1. Membrane

In a typical PEM fuel cell, the membrane is sandwiched between two catalyzed electrodes to transport the protons, support the anode and cathode catalyst layers, and more importantly, separate the oxidizing (air) and reducing (hydrogen) environments on the cathode and anode sides, respectively. Therefore, the requirements for an excellent membrane are manifold and stringent, including high protonic conductivity, flow reactant gas permeability, thermal and chemical stability, and so on [31]. The most commonly used and promising membranes for PEM fuel cells are perfluorosulfonic acid (PFSA) membranes such as Nafion® (Dupont™), Gore-Select® (Gore™), and Aciplex® and Flemion® (Asahi™). Extensive studies have been carried out on the mechanisms of membrane degradation and failure in the fuel cell environment. At present, however, unsatisfactory durability and reliability of the membrane is still one of the critical issues impeding the commercialization of PEM fuel cells.

3.1.1. Membrane degradation mechanisms

3.1.1.1. Mechanical degradation of the membrane. Membrane degradation can be classified into three categories: mechanical, thermal, and chemical/electrochemical [32,33]. Among them, mechanical degradation causes early life failure due to perforations, cracks, tears, or pinholes, which may result from congenital membrane defects or from improper membrane electrode assembly (MEA) fabrication processes. The local areas corresponding to the interface between the lands and channels of the flow field or the sealing edges in a PEM fuel cell, which are subjected to excessive or non-uniform mechanical stresses, are also vulnerable to small perforations or tears. During fuel cell operation, the overall dimensional change due to non-humidification [34], low humidification [6,26,35,36], and relative humidity (RH) cycling [37] are also detrimental to mechanical durability. The constrained membrane in an assembled fuel cell experiences in-plane tension resulting from shrinkage under low RH and in-plane compression during swelling under wet conditions. The migration and accumulation of the catalysts and the decomposition of the seal into the membrane, as described in Sections 3.2.1 and 3.5, also negatively affect membrane conductivity and mechanical strength, significantly reducing ductility. A physical breach of the membrane due to local pin-

holes and perforations can result in crossover of reactant gases into their respective reverse electrodes. If this happens, the highly exothermic direct combustion of the oxidant and reductant occurs on the catalyst surface and consequently generates local hot-points. A destructive cycle of increasing gas crossover and pinhole production is then established, which undoubtedly accelerates degradation of the membrane and the entire cell. The results of Huang et al. [37] suggested that mechanical failure of the membrane starts as a random, local imperfection that propagates to catastrophic failure.

3.1.1.2. Thermal degradation of the membrane. In order to maintain well-hydrated PFSA membranes, the most favorable working temperature of a PEM fuel cell is usually from 60 to 80 °C. Conventional PFSA membranes are subject to critical breakdown at high temperatures due to the glass transition temperatures of PFSA polymers at around 80 °C. However, rapid startup, stable performance, and easy operation in subfreezing temperatures are necessary capabilities for fuel cell technologies to achieve prior to commercialization in vehicles and portable power supply applications. On the other hand, much effort has been made recently to develop PEM fuel cells that operate above 100 °C, in order to enhance electrochemical kinetics, simplify water management and cooling systems, and improve system CO tolerance. Membrane protonic conductivity drops significantly with the decrease in water content when the fuel cell is operated at high temperatures [38] and under low humidity [39].

Several studies have addressed the issue of thermal stability and thermal degradation of PFSA membranes. The polytetrafluoroethylene (PTFE)-like molecular backbone gives Nafion membranes their relative stability until beyond 150 °C due to the strength of the C–F bond and the shielding effect of the electronegative fluorine atoms [40]. At higher temperatures, Nafion begins to decompose via its side sulfonate acid groups. The thermal stability of Nafion was investigated by Surowiec and Bogoczek [41] using thermal gravimetric analysis, differential thermal analysis, and Fourier transform infrared spectroscopy, and only water was detected below 280 °C. At temperatures above 280 °C, sulfonic acid groups were spilt off. In their studies on the effect of heating Nafion onto platinum (Pt) in air, Chu et al. [42] found that sulfonic acid groups were lost after heating at 300 °C for 15 min, while Deng et al. [43], measured small amounts of sulphur dioxide up to 400 °C. Detailed mechanisms for PFSA thermal degradation were proposed by Wilkie et al. [40] and Samms et al. [44], including initiative rupture of the C–S bond to produce

sulphur dioxide, OH• radicals, and a left carbon-based radical for further cleavage at higher temperatures.

In order for fuel cells to be successfully commercialized for automotive and portable applications, membranes must be able to tolerate freezing temperature as well as thermal cycling. Several studies on the state of water in PFSA membranes below freezing have been conducted. Kim et al. [45] suggested that three different states of water exist in the membrane and that the "free water", which was not intimately bound to the polymer chain, would freeze below 0°C. In addition, Cappadonia et al. [46] and Sivashinsky and Tanny [47] found that only a part of the water present in Nafion underwent freezing. Cho et al. [23] reported that the contact resistance between the membrane and the electrode increased after thermal cycles, whereas membrane ionic conductivity itself was not affected. However, McDonald et al.'s [48] results illuminated that, after 385 temperature cycles between +80 and −40°C, ionic conductivity, gas impermeability, and the mechanical strength of Nafion membranes were severely impaired, although no catastrophic failures were detected. The phase transformation and volume change of water due to freeze/thaw cycles has a detrimental effect on the membrane's lifetime. To avoid this, proposed mitigation strategies include gas purging and solution purging to remove residual water during fuel cell startup and shutdown, which will be described in Section 3.1.2.

3.1.1.3. Chemical/electrochemical degradation of the membrane.

The rates of hydrogen and air crossover to opposite sides of the membrane have been proved to be relatively slow and to result in only a 1–3% loss in fuel cell efficiency [49,50]. However, the aforementioned highly exothermal combustion between H_2 and O_2 can possibly lead to pinholes in the membrane, destroying the MEA and causing catastrophic problems. More severely, the chemical reaction on the anode and cathode catalysts can produce peroxide (HO•) and hydroperoxide (HOO•) radicals, which are commonly believed to be responsible for chemical attack on the membrane and catalysts [51,52]. Further investigation has also revealed that the generation of these radicals as well as the chemical degradation of the membrane is accelerated when the fuel cell is operated under open circuit voltage (OCV) and low humidity conditions [36]. Several mechanisms have been proposed, with conflicting views on whether the radicals are formed at the anode, at the cathode, or on both sides of the membrane. Some studies have shown that the loss of ionic groups begins at the anode side of the membrane and progresses towards the cathode [53,54], but Pozio et al. [55] and other researchers [56,57] have provided evidence of predominant cathode degradation. However, Mattsson et al.'s [58] observed no noticeable difference between the anode and cathode sides.

The presence of foreign cationic ions can significantly decrease cell performance by adsorbing on the membrane or catalysts. Possible sources of ultivalent ion contaminants include corrosion of stack components and impurities in the air stream, humidifier reservoirs, etc. [59]. Many cations showed stronger affinity than H^+ with the sulfonic acid group in PFSA membranes [60]. When the fuel cell was operating, more active sites were occupied by the ultivalent ions and, as a consequence, the membrane bulk properties, such as membrane ionic conductivity, water content, and H^+ transference numbers, changed proportionally to the cation ionic charge [61]. This effect is not normally serious unless the contamination concentration goes beyond 50% of sulfonic acid groups in the membrane [60]. The second possible mode of membrane deterioration due to contaminant ions comes from the altered water flux inside the membrane, and in this case, only 5% contaminant is sufficient. The displacement of H^+ with foreign cations also results in attenuated water flux and proton conductivity, and leads to much faster or more extensive membrane dehydration, especially near the anode

[2]. Contamination by trace metal ions originating from the corrosion of metal bipolar plates or end plates, such as Fe^{2+} and Cu^{2+}, can strongly accelerate membrane thinning and performance decay of a PEM fuel cell by catalyzing the radicals' formation reactions, as shown in following equations [49]:

$$H_2O_2 + Fe^{2+} \rightarrow HO• + OH^- + Fe^{3+} \tag{1}$$

$$Fe^{2+} + HO• \rightarrow Fe^{3+} + OH^- \tag{2}$$

$$H_2O_2 + HO• \rightarrow HO_2• + H_2O \tag{3}$$

$$Fe^{2+} + HO_2• \rightarrow Fe^{3+} + HO_2^- \tag{4}$$

$$Fe^{3+} + HO_2• \rightarrow Fe^{2+} + H^+ + O_2 \tag{5}$$
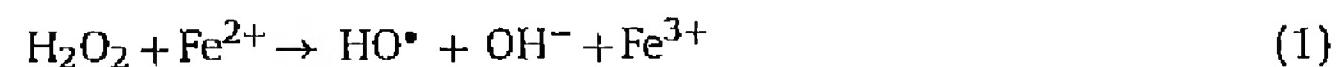
As described above, this mechanism can lead to membrane thinning or the formation of pinholes and eventually to the catastrophic failure of the fuel cell.

Depending on the type of membrane, the HO• and HOO• radicals generated during the reaction can attack the α-carbon of an aromatic group, the ether links, or the branching points of the polymer. As for the PFSA membranes, the small quantity of carboxylate end groups with H-containing terminal bonds, which are inevitably formed during the polymer manufacturing process, are regarded as the inducing agent for membrane chemical decay due to its susceptibility to radical attack. One generally accepted mechanism, the unzipping reaction, initiates the abstraction of hydrogen from the end groups, releases HF, CO_2 and forms new carboxylate groups at the chain ends [61]. An example of radical attack on an end group of $-CF_2COOH$ is shown below [62].

$$R_f - CF_2COOH + •OH \rightarrow R_f - CF_2• + CO_2 + H_2O \tag{6}$$

$$R_f - CF_2• + •OH \rightarrow R_f - CF_2OH \rightarrow R_f - COF + HF \tag{7}$$

$$R_f - COF + H_2O \rightarrow R_f - COOH + HF \tag{8}$$
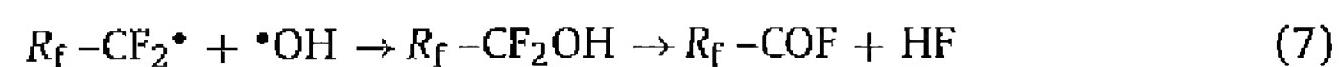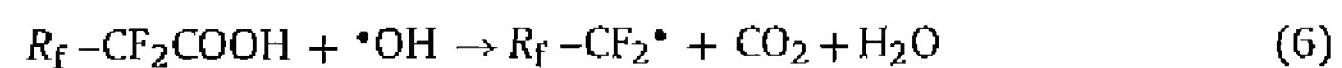
As the process repeats, the attack may propagate along the main chain, and eventually the polymer decomposes into low-molecular weight compounds. Another possible mechanism proposed by Endoh et al. [27] is the scission of the polymer main chains, in which the ether linkages are suggested to be the most susceptible side chain sites to radical attack, producing vulnerable $-COOH$ groups. As a result, the average molecular weight of the polymer decreases while the number of $-COOH$ groups increase with time. Even without susceptible end groups, under exposure to H_2, the polymer backbone of the PFSA membrane may preferentially react as follows [2]:

$$-CF_2- + 2H_2 \rightarrow -CH_2- + 2HF \tag{9}$$

Following this reaction, the radicals attack the resulting $-CH_2-$ groups. The rate of fluoride loss has been considered an excellent measurement of PFSA membrane degradation [63].

3.1.2. Mitigation strategies for membrane degradation

To prevent mechanical failure of the membrane, the MEA and flow field structure must be carefully designed to avoid local drying of the membrane [64,65], especially at the reactant inlet area [66]. A membrane reinforced with e-PTFE, developed by Gore Fuel Cell Technologies, exhibited a lifetime an order of magnitude longer than a non-reinforced membrane of comparable thickness [63], as shown in Fig. 1. Similar results for enhanced membrane mechanical strength were reported by Wakizoe et al. [67] and Xu et al. [29] using reinforced Aciplex® membranes and Nafion®–Teflon®–phosphotungstic acid composite membranes, respectively.

Several review papers [68–71] have covered the recent PEM development and fabrication approaches focusing on achieving
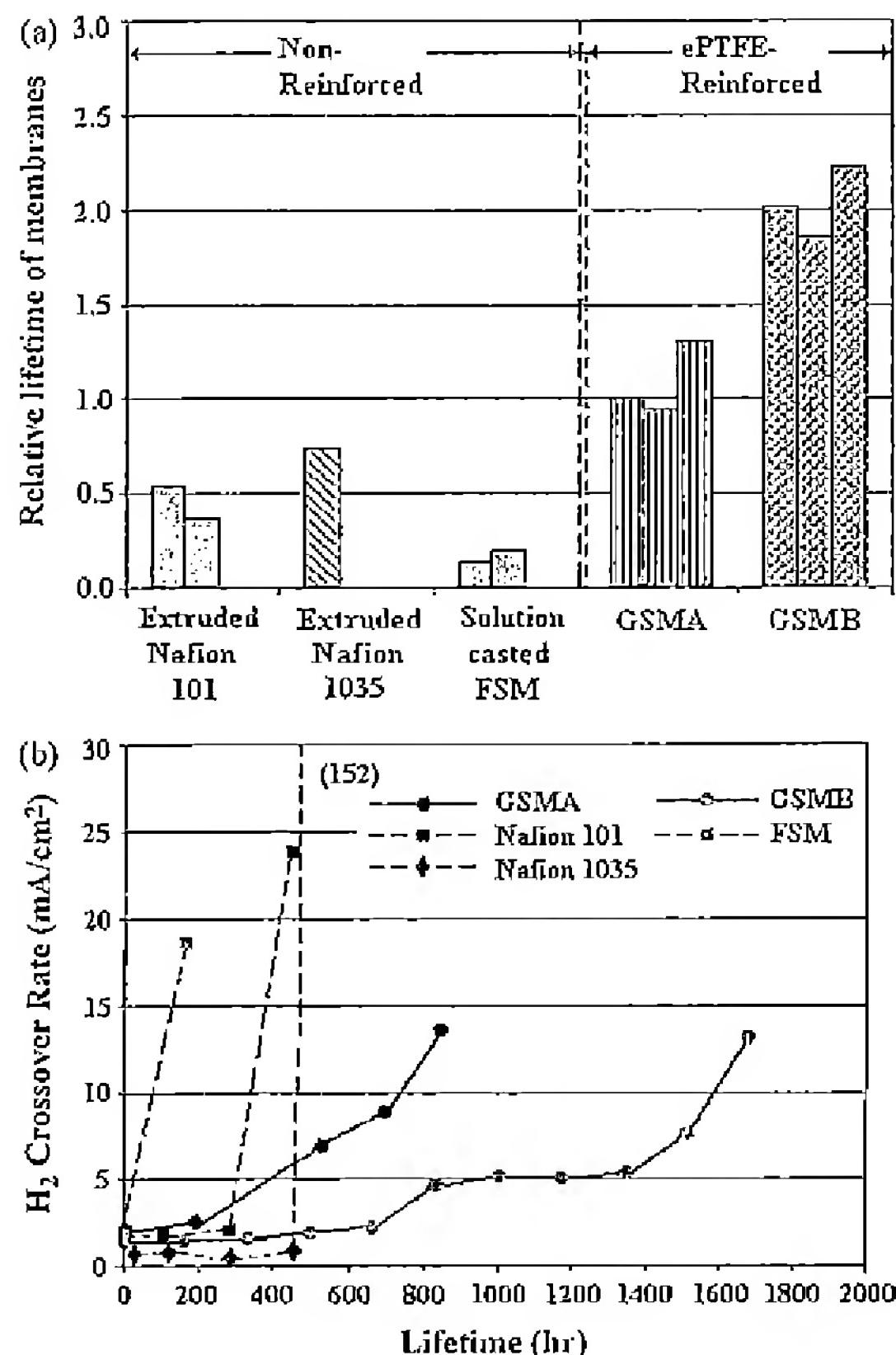
Fig. 1. Comparison of Gore reinforced membranes and non-reinforced membranes. (a) Lifetime of various membranes in accelerated fuel cell conditions; (b) H$_2$ crossover rate as a function of time. (Modified from [63] with permission.)

prolonged durability above 100 °C. The membranes developed so far can be classified into three groups: (1) modified PFSA membranes, which are swelled with nonvolatile solvents or incorporate hydrophilic oxides and solid inorganic proton conductors; (2) alternative sulfonated polymers and their composite membranes, such as SPSF, SPEEK, PBI, and PVDF; and (3) acid–base polymer membranes, such as phosphoric acid-doped Nafion®–PBI composite membranes.

With respect to the chemical and electrochemical degradation of the membrane, developing membranes that are chemically stable against peroxy radicals has drawn particular attention. Firstly, one solution is to develop novel membranes with higher chemical stability, such as a radiation-grafted FEP-g-polystyrene membrane [72,73], in which polystyrene was used as a sacrificial material owing to its low resistance to radicals [57]. Free-radical stabilizers and inhibitors such as hindered amines or antioxidants also have the potential to be mingled during membrane fabrication. Secondly, increased chemical stability can also be realized by modifying the structure of the available membrane. Curtin et al. [62] suggested that radical attack of the residual H-containing terminal bonds of the main chain of the PFSA membrane was the primary degradation mechanism. By eliminating the unstable end group, chemical stability was significantly enhanced [62]. Thirdly, the damage caused by hydrogen peroxide can be suppressed by redesigning the MEA. For example, a composite membrane suggested by Yu et al. [57], in which a thin recast Nafion membrane was bonded with a polystyrene sulfonic acid (PSSA) membrane, when positioned at the cathode of the cell could successfully prevent oxidation degradation of the PSSA membrane. Fourthly, introduction of peroxide-decomposition catalysts like heteropoly acids within

the membrane has proven to moderate or eliminate membrane deterioration due to peroxide [74,75]. However, the advantage of this approach would be partially counteracted by a decrease in membrane stability and conductivity caused by the mixture of the catalysts. Last but not least, the development and implementation of new metal coatings with improved corrosion resistance and of catalysts that produce less hydrogen peroxide are long-term goals for membrane durability enhancement.

3.2. Electrocatalyst and catalyst layer

Pt and binary, ternary, or even quaternary Pt-transition metal alloys, such as PtCo, Pt–Cr–Ni, and Pt–Ru–Ir–Sn, supported on conductive supports have been proposed and implemented as electrocatalysts in PEM fuel cells. Commonly used supports include high-surface-area carbon materials, such as Vulcan-XC 72, Ketjen black, or Black pearls BP2000. These catalysts are in principle able to meet the performance and cost requirements for high-volume fuel cell applications. However, from a catalyst durability viewpoint, the performance of currently known materials is still unsatisfactory under harsh operating conditions, including high humidity, low pH values, elevated temperature, and dynamic loads in combination with an oxidizing or reducing environment [59].

3.2.1. Electrocatalyst and catalyst layer degradation mechanisms

Considerable effort has been put into the detailed examination of the mechanism of Pt catalyst degradation under long-term operation. Firstly, a pure Pt catalyst may be contaminated by impurities originating from supply reactants or the fuel cell system [50]. Also, the catalyst may lose its activity due to sintering or migration of Pt particles on the carbon support, detachment and dissolution of Pt into the electrolyte, and corrosion of the carbon support. Several mechanisms have been proposed to explain the coarsening in catalyst particle size during PEM fuel cell operation: (1) small Pt particles may dissolve in the ionomer phase and redeposit on the surface of large particles, leading to particle growth, a phenomenon known as Ostwald ripening [76]. On the other hand, the dissolved Pt species may diffuse into the ionomer phase and subsequently precipitate in the membrane via reduction of Pt ions by the crossover hydrogen from the anode side, which dramatically decreases membrane stability and conductivity [77]; (2) the agglomeration of platinum particles on the carbon support may occur at the nanometer scale due to random cluster–cluster collisions, resulting in a typical log-normal distribution of particles sizes with a maximum at smaller particle sizes and a tail towards the larger particle sizes [78]; (3) the growth in catalyst particles may also take place at the atomic scale by the minimization of the clusters' Gibbs free energy. In this case, the particle size distribution can be characterized by a tail towards the smaller particle sizes and a maximum at larger particle sizes [79]. However, so far, there is still no agreement on which mechanism is dominantly responsible for the catalyst particle growth [80]. Coarsening of the catalyst due to movement of its particles and coalescence on the carbon support can cause the catalytically active surface area to decrease [81]. Lastly, the formation of metal oxides at the anode [15] or cathode [14] side probably leads to an increase in particle sizes and ultimately results in a decrease in catalyst activity.

Corrosion of the catalyst carbon support is another important issue pertaining to electrocatalyst and catalyst layer durability that has attracted considerable attention lately in academic as well as in industry research [6,82,83]. In PEM fuel cells and stacks, two modes are believed to induce carbon corrosion: (1) transitioning between startup and shutdown cycles and (2) fuel starvation due to the blockage of H$_2$ from a portion of the anode under steady state conditions. The first mode, referred to as air-fuel front, can

be caused by non-uniform distribution of fuel on the anode and crossover of oxygen through the membrane, which is likely to occur during startup and shutdown of the PEM fuel cell. For the second mode, fuel starvation in individual cells may result from uneven flow sharing between cells during high overall stack utilization or from gas flow blockage attributed to ice formation when fuel cells work in subfreezing temperatures. In both cases, the anode electrode is partially covered with hydrogen and, under the circumstances of hydrogen exhaustion, the anode potential will be driven negative until water and carbon oxidation takes place according to the following equations [2]:

$$2H_2O \leftrightarrow O_2 + 4H^+ + 4e^- \quad E^\circ = 1.229V_{RHE} \tag{10}$$

$$C + 2H_2O \rightarrow CO_2 + 4H^+ + 4e^- \quad E^\circ = 0.207V_{RHE} \tag{11}$$
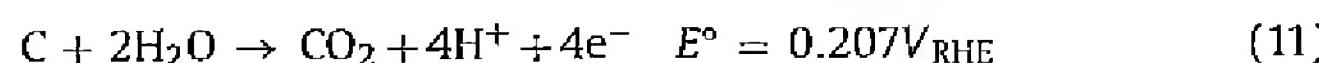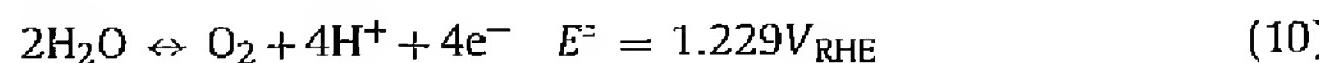
Despite the thermodynamic instability, carbon corrosion in a normal PEM fuel cell is negligible at potentials lower than 1.1 V vs. reversible hydrogen electrode (RHE) due to its slow kinetics. However, recent experiments have confirmed that the presence of electrocatalysts like Pt/C or PtRu/C can accelerate carbon corrosion and reduce the potentials for carbon oxidation to 0.55 V (vs. RHE) or lower [84]. When provided with sufficient water in the fuel cell, carbon is actually protected from corrosion by virtue of the H_2O oxidation process, unless the water in the electrode is depleted or the cell is subjected to a high current density not sustainable by water oxidation alone [28]. According to Eq. (8), cell reversal as a result of fuel starvation has a potential impact on the durability of the catalyst layer, the gas diffusion layer, or even the bipolar plate. As a consequence, the relative percentage of conductive material in the electrode may drop and the contact resistance with the current collector, as well as the internal resistance of the cell, will eventually increase. More seriously, the number of sites available to anchor the catalyst decreases with carbon corrosion, causing catalyst metal sintering [85], and in the extreme, a structural collapse of the electrode.

Another noteworthy hazard to PEM fuel cell durability at subzero temperatures is the influence of the phase transformation and volume changes of water on the physical properties of the membrane/electrode interface and electrode structure, in addition to the membrane. Cho et al. [23] observed a performance degradation rate of about 2.3% per freeze–thaw cycle from 80 to −10 °C. The cell performance degradation seen with thermal cycles was attributed to the physical damage of the electrode structure and MEA integrity resulting from ice expansion during freezing. The analytical results of McDonald et al. [48] demonstrated the relationship of temperature cycling between 80 and −40 °C to membrane structure, water management, ionic conductivity, gas permeability, and mechanical strength. A detailed summary of research on PEM fuel cell freeze and rapid startup can be found in Ref. [86].

Experimental results from Xie et al. [25] have also revealed the change in hydrophobic characteristics of the catalyst layer over time due to the dissolution of Nafion or PTFE, which detrimentally affects the water management and mass transport ability of the electrode.

3.2.2. Mitigation strategies for electrocatalyst and catalyst layer degradation

Recent research has proposed and successfully employed several strategies to enhance catalyst durability. First of all, fuel cell operating conditions play a major role in catalyst degradation. The dissolution of Pt from the carbon support is less favorable at low electrode potentials, which makes Pt catalysts more stable at the anode electrode than that at the cathode side. The experimental results of Mathias et al. [85] showed that the loss in Pt active surface area associated with an increase in testing time can be significantly decreased by operating the cell at low RH and low temperature,
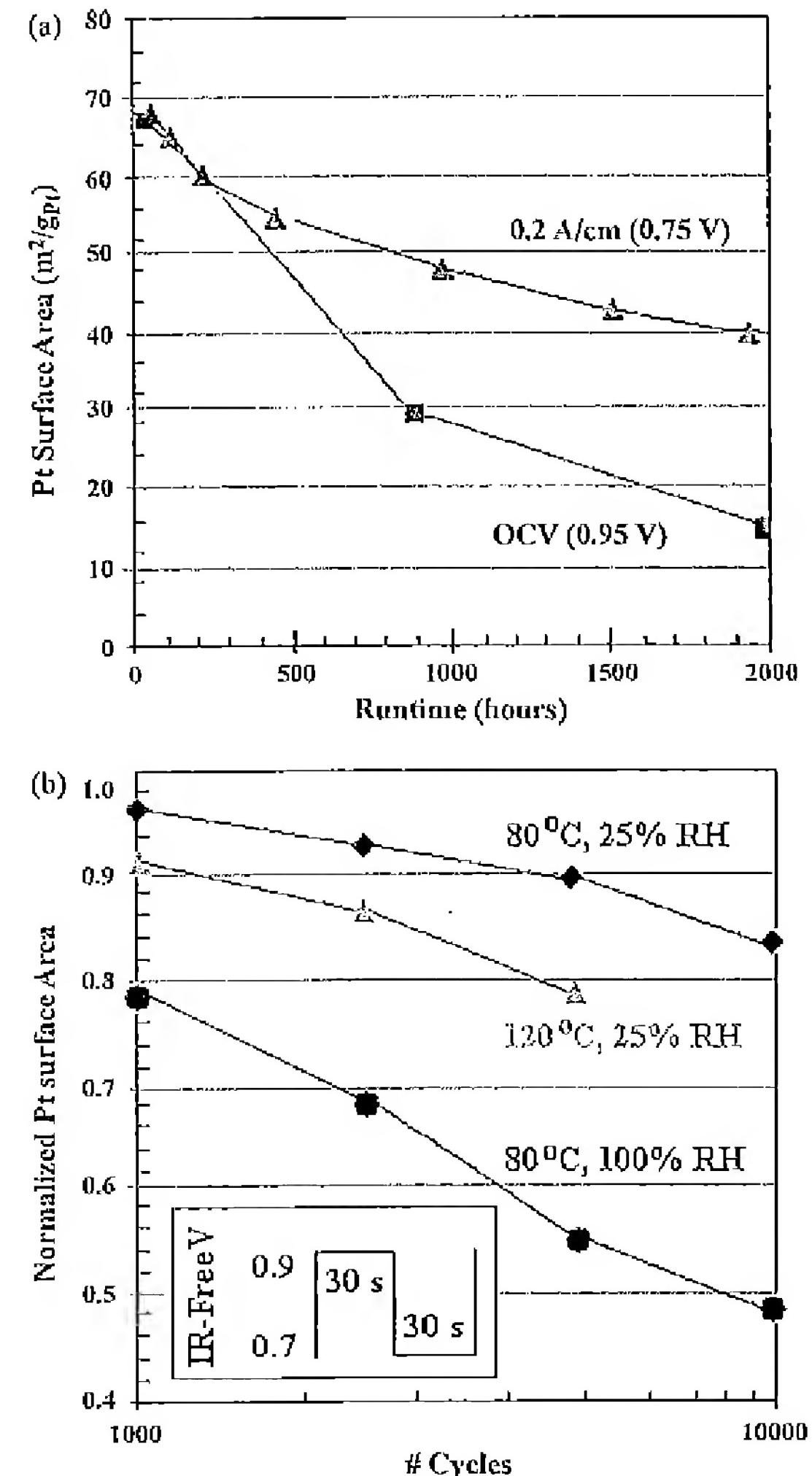

Fig. 2. Impact of operational conditions on catalyst active surface area loss. (a) Pt surface area as a function of stack runtime; (b) impact of RH and high temperature operation on Pt surface area loss of Pt/C as a function of potential cycles. (From [85] with permission.)

as shown in Fig. 2. However, carbon corrosion of the catalyst layer was recently found by Borup et al. [87] to increase with decreasing RH. They also revealed that the growth in cathode Pt particle size was much greater during potential cycling experiments than during steady state testing, and that it increased with an increase of potential, which was recently employed as an AST method to evaluate electrocatalyst stability.

Secondly, corrosion of the carbon support due to fuel starvation can be alleviated by enhancing water retention on the anode, such as through modifications to the PTFE and/or ionomer, the addition of water-blocking components like graphite, and the use of improved preferable catalysts for water electrolysis, as demonstrated by Knights et al. [6] in Fig. 3. With respect to PEM fuel cell freeze and rapid startup issues, two main strategies have been proposed to mitigate fuel cell performance degradation, based on whether the system uses extra energy during parking or startup. The first solution, the "keep-warm" method [88–90], is to consume power from a continuous or intermittent low-power energy source (from an extra battery or hydrogen fuel converter) to keep the system above a certain threshold temperature during the parking period. The other option is to heat the fuel cell system to raise its temperature above the freezing point of water at startup [91,92].
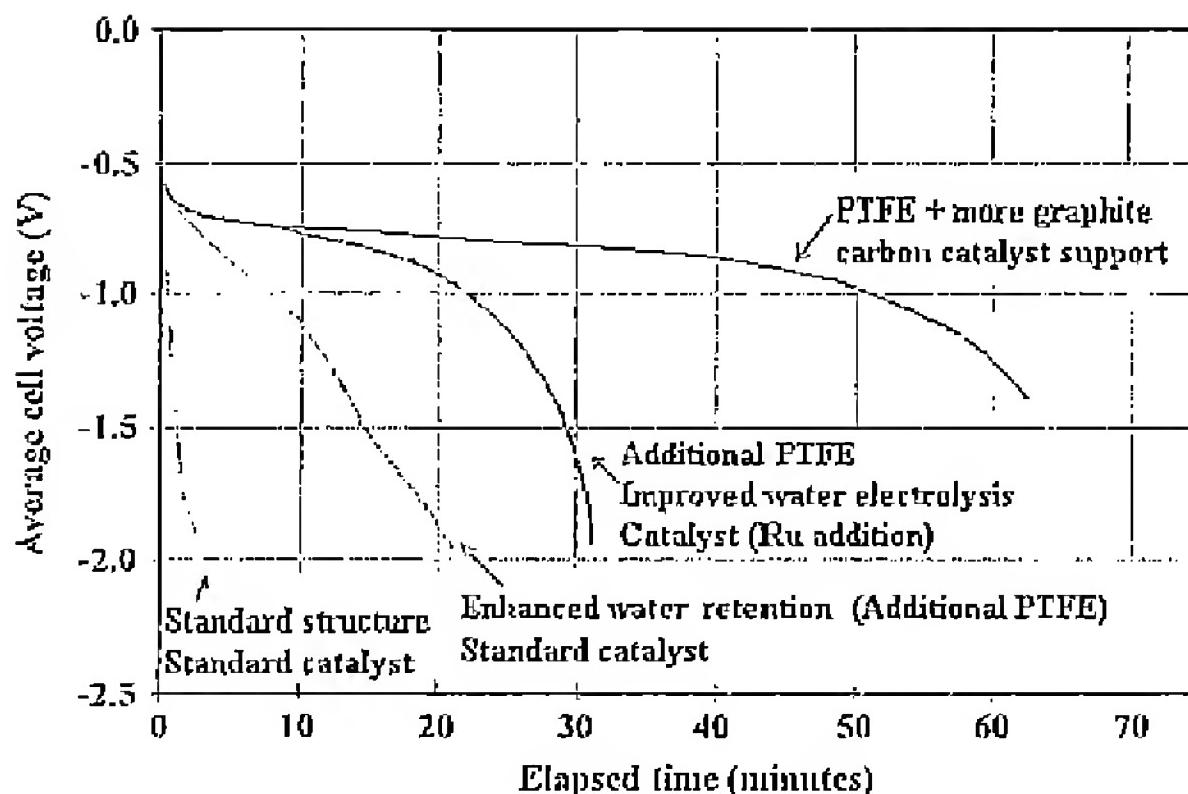
Fig. 3. Comparison of different anode structures in severe failure testing. Each cell has an equivalent cathode (~0.7 mg cm^{-2} Pt, supported on carbon). Testing conducted at 200 mg cm^{-2}, fully humidified nitrogen on anode. Anode loading at ~0.3 mg cm^{-2} Pt supported on carbon (varied materials and compositions). (Modified from [6] with permission.)

For this method, a higher power heat is required and it is strongly suggested that the method be combined with effective removal of residual water to save energy and alleviate physical damage to the MEA due to ice expansion. Possible methods for getting rid of the water include gas purging [6] or washing it away with an antifreeze solution [23] prior to fuel cell shutdown.

Thirdly, Pt-alloy catalysts such as PtCo, Pt–Cr–Ni have shown better activity and stability compared to pure Pt catalysts [93]. The increased sintering resistance offered by the alloying elements [93] or the larger alloy particle size [94] may explain the observed improvement. However, X-ray diffraction (XRD) analysis has revealed a skin consisting of a monolayer of pure Pt formed on the surface of the alloys after long-term testing [95–97]. This indicates that the non-noble metals in the Pt-transition metal alloy catalysts are more susceptible to dissolving in the ionomer phase, partially counteracting the advantage of Pt-alloy catalysts. Metals such as Co, Cr, Fe, Ni, and V have already proved to be soluble in a fuel cell operating environment; Pt–Co/C has drawn more attention recently due to its superior stability compared to that of the other Pt-transition alloy catalysts [94,98]. It is noteworthy that recently Adzic and co-workers [99] significantly improved the Pt stability against dissolution under potential cycling regimes by modifying Pt nanoparticles with gold (Au) clusters. There were no obvious changes in the activity and surface area of Au-modified Pt under oxidizing conditions and potential cycling between 0.6 and 1.1 V after over 30,000 cycles. The considerable improvement in the Au/Pt/C catalyst stability was mainly attributed to the existence of the non-dissolvable Au clusters. By strengthening the interaction between the metal particles and the carbon support, sintering and dissolution of the metal alloy catalysts can be alleviated. For example, Roy et al. [100] introduced nitrogen-based carbon functionality to the carbon support surface by chemical modification and, consequently, the ability of the treated support to anchor metal particles as well as its catalyst activity showed obvious improvement. Multiwalled carbon nanotubes (CNTs) have also demonstrated promise as catalyst supports in PEM fuel cell applications [101]. In a recent publication, Shao et al. [102] reported that the degradation rate of Pt/CNTs was nearly two times lower than that of Pt/C under the same accelerated durability testing conditions, which was attributed to the specific interaction between Pt and CNTs and to the higher resistance of the CNTs to electrochemical oxidation. In addition, the decrease in support surface area or graphitization of the carbon support can also enhance the support's resistance to oxidation and carbon corrosion [103,104]. However,

the number of active surface sites on which to anchor metal particles correspondingly decreases, which is a potential detriment to the deposition of metal on the carbon support.

3.3. Gas diffusion layer

3.3.1. Gas diffusion layer degradation mechanisms

The gas diffusion layer (GDL) is typically a dual-layer carbon-based porous material, including a macroporous carbon fiber paper or carbon cloth substrate covered by a thinner microporous layer (MPL) consisting of carbon black powder and a hydrophobic agent. In past studies of GDLs, the impact of GDL materials and design on PEM fuel cell performance, rather than durability, has been the focal point. However, increased GDL surface hydrophilicity has been clearly observed after 11,000 h of operation [12] and cold start conditions [24], which unquestionably indicates that further investigation of the GDL is warranted. To date, only a limited number of studies have focused on the degradation mechanisms of GDLs or on the relationship between GDL properties and fuel cell performance decay. Moreover, these studies have employed mainly ex situ GDL aging procedures in order to avoid the possible confounding effects from adjoining components such as the catalyst layer and bipolar plate.

The results of Borup et al. [105] showed that the loss of GDL hydrophobicity increased with operating temperature and when sparging air was used instead of nitrogen. Additionally, they concluded that changes in the GDL properties were attributed mostly to the MPL. Frisk et al. [106] aged GDLs by submerging the samples in 15 wt.% hydrogen peroxide at 82 °C. They found that weight loss and the MPL contact angle increased with the time of exposure and the increase was attributed to oxidation of the carbon in the MPL. Kangasniemi et al. [107] demonstrated the effect of electrochemical surface oxidation on GDL properties and found that the contact angle of the MPL surface decreased remarkably over time when the GDL samples were immersed in 1 M H_2SO_4 under potentiostatic treatment of 1.2 V vs. standard hydrogen electrode (SHE). Most recently, Lee and Mérida [108] comprehensively studied GDL properties, such as electrical resistivity, bending stiffness, air permeability, surface contact angle, porosity, and water vapor diffusion, after degradation tests under steady state (over 1500 h aging time at 80 °C and 200 psi) and freezing (54 freeze-thaw cycles between −35 and 20 °C) conditions. As the fuel cell operates, the PTFE and carbon composite of the GDLs are susceptible to chemical attack (i.e., OH• radical as electrochemical byproduct) and electrochemical (voltage) oxidation [106]. The loss of PTFE and carbon results in the changes in GDL physical properties, such as the decrease of GDL conductivity and hydrophobicity, which further lowers MEA performance and negatively affects the durability of the whole fuel cell. With regard to the quantitative correlation between performance loss and the changes in GDL properties, Schulze et al. [109] recently found that the decomposition of PTFE in the electrodes induced an approximately two times higher performance loss than that related to the agglomeration of the platinum catalyst after 1000 h of fuel cell operation. However, the effect of PTFE degradation in the catalyst layer and GDL was not separated in their paper and the decomposition mechanism of PTFE was not thoroughly discussed.

3.3.2. Mitigation strategies for GDL degradation

Little information about mitigating GDL degradation is available from the literature. To improve GDL oxidative and electrooxidative stability, Borup [110] suggested using graphitized fibers during GDL preparation. Borup also proposed that higher PTFE loading could benefit the water management ability of aged GDLs, as shown in Fig. 4. By incorporating graphitized carbon material Pureblack®
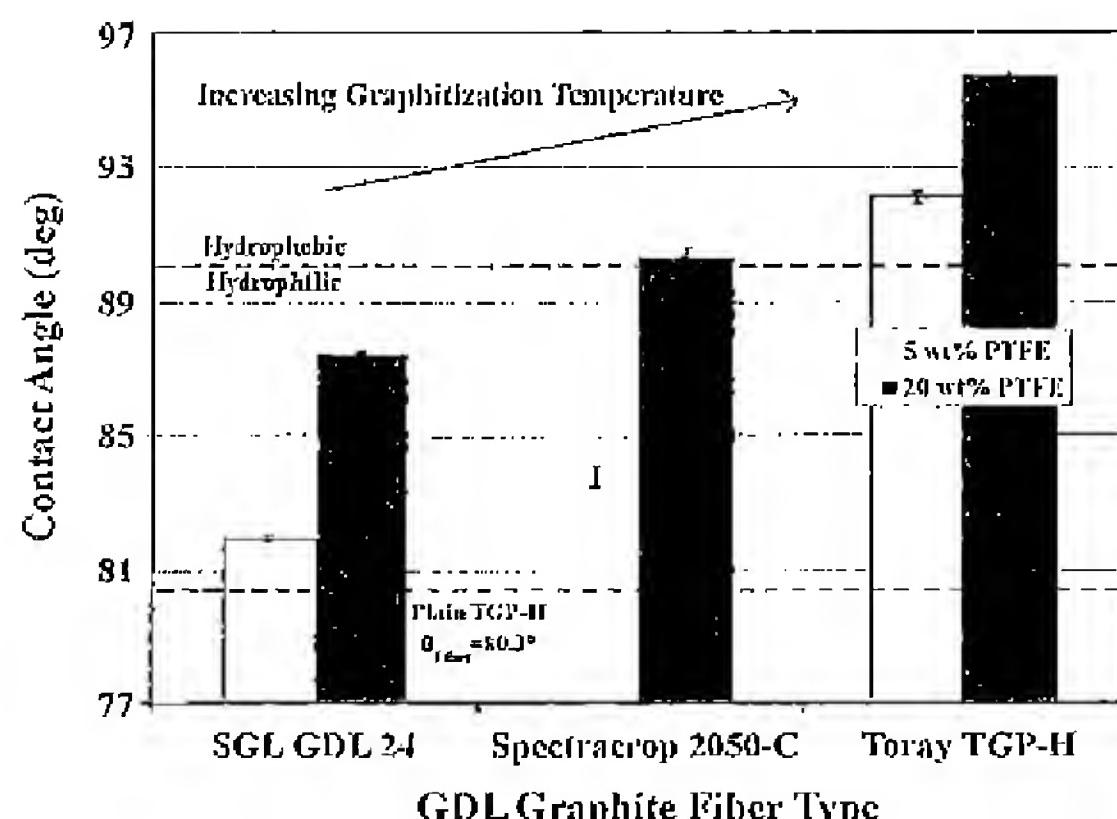
Fig. 4. Effect of GDL graphite fiber type and PTFE loading on contact angle. (Modified from [110] with permission.)

in the MPL, Owejan et al. [30] found a 25% improvement in the start/stop degradation rate at 1.2 A cm^{-2}.

3.4. Bipolar plate

3.4.1. Bipolar plate degradation mechanisms

The bipolar plate is a multifunctional component of the fuel cell stack, acting as a separator between the fuel, oxidant gases, and coolant; homogeneously distributing reactant and product streams; and collecting the current generated by the electrochemical reaction. A great deal of research and some literature reviews [111–114] related to bipolar plate studies have been published.

To fulfill all of the required functions, multiple properties are required for the materials to be acceptable for bipolar plates. These include, but are not limited to, high electrical conductivity, low gas permeability, high corrosion resistance, sufficient strength, low thermal resistance, and low cost, etc. In addition to graphite, materials such as metals, graphite/carbon-based composites, and polymer-based composites with conductive graphite/carbon fillers are currently being tested and evaluated by researchers [115–117]. The combination of high corrosion and chemical resistance, low density, and high electrical and thermal conductivity are attractive characteristics of graphite and graphite composites. However their durability under shock and vibration, permeability to hydrogen, and manufacturability are unfavorable when compared to metals, such that an increase in weight as well as volume is needed to overcome their shortcomings. Noble metals such as Pt, Ta, Nb, and Zr are highly corrosion resistant and are manufacturable as lightweight thin plates, but the raw material costs for these plates prohibit them from commercial applications [118]. As for other metallic bipolar plates, commercially available metals and their alloys such as Al, Ti, and Ni have exhibited inspiring potential in bipolar plates owing to their good electrical conductivity, excellent mechanical properties, and low cost. However, the major concern with these metallic bipolar plates is the contact resistance between the bipolar plate and the GDL, attributed to electrically resistant oxide films formed on the surfaces, which inevitably increase the internal electrical resistance of the fuel cell. Stainless steel has received considerable attention due to its wide range of alloy choices and applicability to mass production, but it is prone to corrosion in the aggressive acidic and humid environment inside a PEM fuel cell [119], which causes a further increase in contact resistance. Moreover, corrosion of metallic materials leads to the production of multivalent cations, which can seriously impair the durability of the membrane and catalyst [115], as discussed in Section 3.1.1. A chemical analysis of the MEA after 100 h of cell operation revealed that a large quan-

tity of Fe and Ni atoms, as well as traces of Cr, was released from untreated stainless steel 316L [120]. As a result, a voltage drop of up to 300 mV at a current of 700 mA cm^{-2} was measured due to the chemical corrosion of this bipolar plate material. By exposing eight commercial stainless steels to an acid solution, Shores et al. [121] carried out an ex situ experiment to study the corrosion of stainless steel. A controlled potential was applied and the gas (H_2 or air) was bubbled into the solution to simulate either anode or cathode conditions. After 72 h of aging, the dissolved metal cations (including Fe^{+3}, Cr^{+3}, Ni^{+2}) were detected in the solution [121].

3.4.2. Mitigation strategies for bipolar plate degradation

Current work in this key area is focused mainly on the use of graphite/polymer composites, metallic materials coated with noble metals, or various nitride- or carbide-based alloys to improve corrosion resistance in real or simulated PEM fuel cell environments [122]. The most up-to-date research on carbon-based and metal-based coatings for PEM fuel cell bipolar plates, in addition to the corresponding coating techniques, are compiled in Table 3. Various coating methods that have been developed and applied widely in other industrial areas, such as immersion coating, spraying, electroplating, electroless deposition, electrolytic anodization, and painting [115], are being evaluated for bipolar plate materials. Taking cost competitiveness for continuous high-volume production into consideration, research in recent years [115] has focused on physical vapor deposition (PVD) and chemical vapor deposition (CVD) processes, as illustrated in detail in Table 3.

However, a potential risk with protective coating methods is the deformation of the coating material when the PEM fuel cell operates under thermal cycling conditions. Woodman et al. [148] proposed a reasonable explanation that the coating material and the substrate might expand and contract at different rates due to the difference in their coefficients of thermal expansion (CTEs). The micro-pores and micro-cracks arising from deformation of the coating layer can lead to the direct exposure of the substrate metal to a highly corrosive environment and, subsequently, the dissolved metal ions diffuse into the membrane and get trapped in the ion exchange sites, resulting in considerable adverse effects on cell performance. The addition of intermediate coating layers with high bonding strength and gradient CTEs between adjacent layers of the coating and bipolar plate is one effective strategy for buffering the CTE differential.

Another common concern related to bipolar plates is the possible deformation or even fracture caused by the compressive forces that are used to ensure good electric contact and reactant sealing during fuel cell operation [149]. Some operational factors, such as thermal cycling, non-uniform current, or thermal misdistributions over the active area, can impair the mechanical properties of the bipolar plate materials. Hodgson and Farndon [150] and Lee et al. [151] subjected the surface of a metallic material, such as stainless steel or nickel-rich alloys, to an electrical current in the presence of an acidic electrolyte. After this treatment, the corrosion resistance of the metallic bipolar plate was improved, which was attributed to the modification of the surface composition and/or the surface morphology. This surface treatment method is particularly promising since the treatment is a modification to the surface rather than a coating procedure and therefore delamination is not an issue.

Table 4 presents research on composite bipolar plate materials, including carbon–polymer composites and carbon–carbon composites, with a summary of their advantages and disadvantages. As shown, carbon–carbon composites have many advantages, although their lack of mechanical strength in addition to the lengthy and expensive chemical vapor impregnation (CVI) process destines them to limited success. Recently, carbon–polymer materials, especially those with thermoset resins, are becoming competitive

Table 3
Practicable coated metallic bipolar plates proposed in the literature

Coating category	Coating method	Coating materials	Applicable base plate materials				Reference
			Al	Ti	Ni	Other	
Metal-based coating							
Noble metals	Pulse current electrodeposition	Gold over Ni over Cu	X				[123,124]
	Electrodeposition	Gold	X			Stainless steel (SS)	[125]
	DC magnetron sputtering	Ta	X			SS316	[120]
	Electroplating	Gold			X		[120]
Metal nitrides	PVD (e.g. magnetron sputtering) or CVD, and electrolessdeposition for Ni-Ph alloy	(1) Sublayer-Cr/Ni/Mo-rich SS or Ni-phosphorus alloy; (2) topcoat-Ti nitride	X	X		SS	[126]
	Radio frequency (RF)-planar magnetron (sputtering)	Ti–Al–nitride layer	X				[127]
	RF-diode sputtering	TiN layer		X			[127]
	Thermal nitridation	CrN/Cr₂N surface				Cr-bearing alloy	[128–132]
						Ferritic SS	[133,134]
						Austenitic SS	[132,135]
	PVD	NS				SS304	[136]
	PVD	TiN				SS410	[137]
	Electrodeposition	TiN				SS316	[138]
	NS	TiN				SS316	[121]
Metal carbides	Glow discharge decomposition and vapor deposition	(1) n-Type silicon carbide (SiC); (2) gold				SS	[127]
	Electro-spark deposition process	Cr carbide				SS310	[139]
Metal oxide	Electron beam evaporation	Indium doped tin oxide (Sn(In)O₂)		X			[127]
	Vapor deposition and sputtering	(1) Sublayer-lead; (2) topcoat-lead oxide (PbO/PbO₂)		X			[127]
Carbon-based coating							
Graphite	Painting or pressing	(1) Sublayer-sonicated graphite particles in an emulsion, suspension or paint (e.g. graphite particles in an epoxy resin thinned by an organic solvent, such as toluene); (2) topcoat-exfoliated graphite in the form of sheets of flexible, graphite foil	X	X	X		[140]
	PVD (closed-field, unbalanced, magnetron sputter ion plating) and chemical anodization/oxidation overcoating	(1) Sublayer-titanium over titanium-aluminum-nitride; (2a) overcoat-transient metal sublayer of Cr (Ti, Ni, Fe, Co) followed by sulphuric/chromic acid OR; (2b) topcoat-graphite	X	X	X	SS	[140]
Conductive polymer	NS	Organic self-assembled monopolymers	NS				[141]
	NS	Conductive polymers	NS				[141]
	Electrodeposition	Conductive polymers polyaniline (PANI) and polypyrrole (PPY)				SS304	[142]
	Plasma-polymer coating	Hexafluoropropylene (HFP)		X		SS304	[143]
	Electrodeposition	Multilayer coating (Ni, Au) conductive polymer (polyaniline)	X				[123]
	Spraying	(1) Sublay-conductive polymer (M2-48); (2) interlay- commercial graphite (TV-Koat); (3) topcoat-conductive polymer (M2-48)				SS316L	[144]
	NS	Coating comprised of carbon fibers contained within a polymer matrix				SS	[145]
Diamond or diamond-like carbon	NS	Diamond-like carbon	NS				[141]
	PVD	YZU001 diamond-like material	X			SS316	[146]
Organic self-assembled monoploymers	NS	Organic self-assembled monopolymers	NS				[147]

Note: Not specified (NS).

alternatives to bipolar plates in terms of bulk conductivity and dimensional tolerance. However, high carbon loadings are always necessary to obtain the required electrical conductivity, which eventually causes difficulties in processability. Another problem associated with carbon–polymer materials is the degradation of the resins in PEM fuel cell working environments due to the inherent properties of these polymers [111]. The heavy atoms released from these resins as a consequence, such as calcium, magnesium, or zinc, may diffuse into and contaminate the PEM, decreasing fuel cell durability.

Following principles of stack manufacturing and environmental impact, Cooper has identified 51 bipolar plate requirements and

Table 4
Practicable carbon composite bipolar plates proposed in the literature

Carbon composite	Polymer	Filler	Fiber	Reference	Advantages	Disadvantages
Carbon–polymer composite						
Thermoplastic	PVDF	Carbon/graphite particles		[152]	Injection molding lends itself to manufacturing automation	Low electrical conductivity when using standard thermoplastics
	PVDF	Carbon/graphite particles	Carbon/graphite fibers	[153]	Fast cycle time	Limited to low-temperature operation
	PVDF	Carbon black, graphite powder	Carbon/graphite fibers	[154]	Flow field introduced during molding	Injection molding difficult at high carbon loading
	PVDF	Carbon black	Carbon fibers	[155]	Low contact resistance	Generally less chemically stable than thermoset resins
	Liquid crystal polymer (LCP)	Carbon black		[156]		Difficult to increase carbon concentration
	Polyethylene terephthalate (PET)/PVDF	Carbon or CNT		[157]		
Thermoset	Mixture of epoxy resin and aromatic amine hardener	Graphite powder		[158]	Higher temperature operation than thermoplastic	Relatively low electrical conductivity
	Phenyl-aldehyde resol or novolac	Graphite powder	Graphite fibers	[159]	Flow field introduced during molding	Difficult to increase carbon concentration
	Phenyl-aldehyde resol or novolac	Coke-graphite particles		[160]	Low contact resistance	
	Reichhold 24-655 phenolic resin	Graphite powder	Cellulose fibers (not rayon or cellulose acetate)	[161]		
	Furan resin or phenolic resin	Graphite powder	Cellulose fibers (not rayon or cellulose acetate)	[162]		
	Vinyl ester	Graphite powder		[163,164]		
Carbon–carbon composites						
	Phenolic resin	Carbon fiber	Vapor-infiltrated carbon	[165,166]	High electrical conductivity	Long and expensive CVI process is necessary to deposit graphitic carbon and to pyrolize resins (bulk processing and automation set to lower price)
	Unsaturated polymer	Compound graphite powder	Vapor-infiltrated carbon	[167]	High thermal conductivity	Lack of mechanical strength
	Epoxy resin	Pan-based carbon fiber	Vapor-infiltrated carbon	[168]	Lightweight	
	Phenol-formaldehyde resin	Pan-based carbon fiber, carbon black		[169]	High temperature operation	
					High strength Highly corrosion and chemical resistance Flow field introduced during stamping of perform	

J. Wu et al. / Journal of Power Sources 184 (2008) 104–119
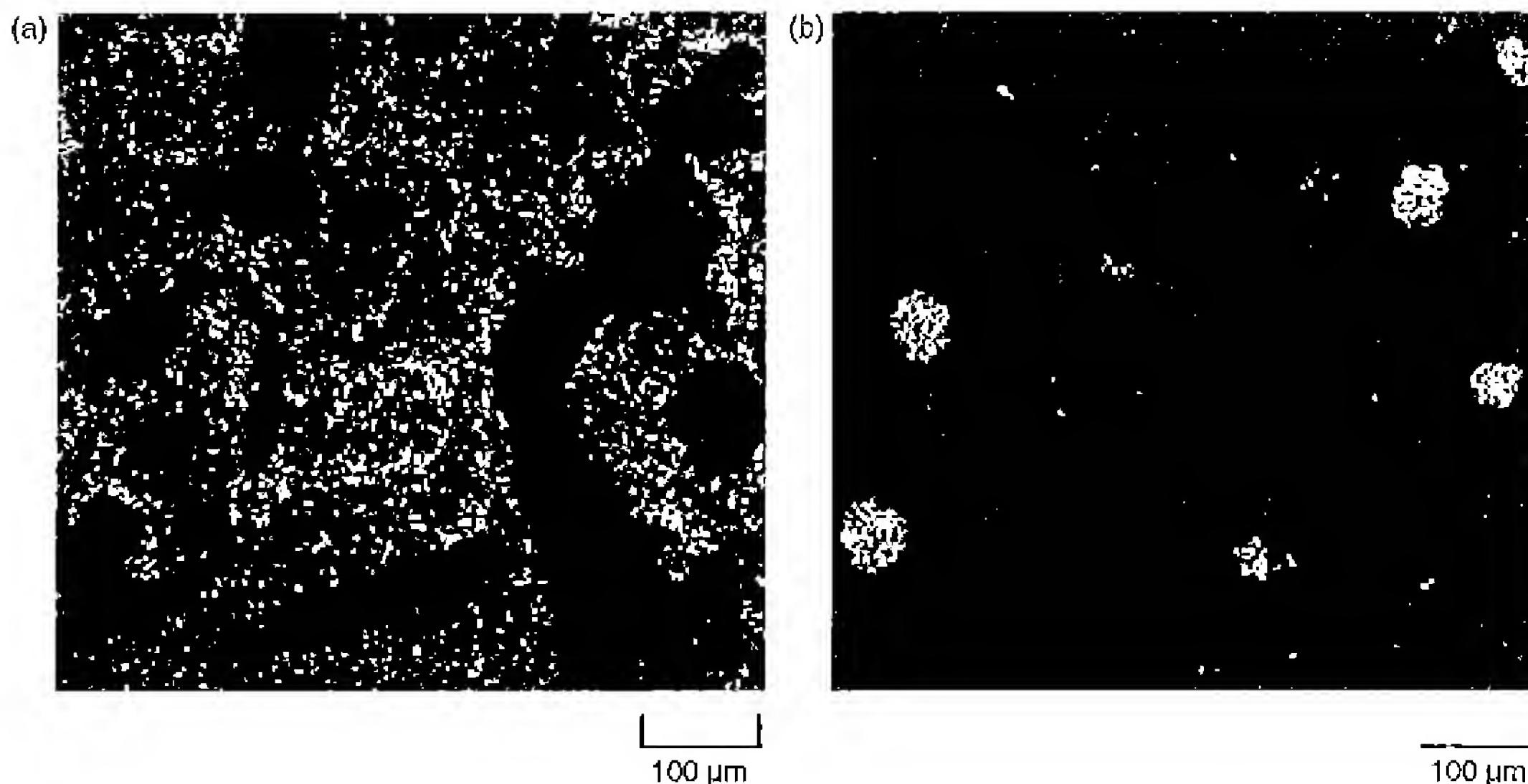
Fig. 5. SEM–EDX images of an embrittled membrane sample. The holes and tears resulted from reduced mechanical integrity caused by the crystallization of (a) silicon- and (b) calcium-containing particles from the degradation of incompatible sealing materials inside and on the surface of a membrane. (From [174] with permission.)

design rules for PEM fuel cells [170]. Among the state-of-the-art alternatives for bipolar plates, although no material has definitely established itself as capable of meeting all the desired target properties for commercial applications [131], each material has its specific advantages and disadvantages and, therefore, will find its specific application fields. The choice of material depends on the driving constraints of the application and is always a compromise between performance, efficiency, size, lifetime, cost, operational range flexibility, local climate, and so on.

3.5. Sealing gasket

Sealing material is placed between the bipolar plates to prevent gas and coolant leakage and crossover. Typical sealing materials utilized in PEM fuel cells include fluorine caoutchouc, EPDM, and silicone [171]. Tan et al. [172] reported their results from a recent ex situ investigation on the chemical degradation of four commercial gasket materials in simulated fuel cell environments. Cleghorn et al. [4] and St-Pierre and Jia [12] observed the degradation and dissolution of silicone in the active section of the stack during their lifetime experiments. Schulze et al. [171] detailed the degradation of silicon-based seals during long-term fuel cell operation. They

detected residues of the silicone in the anode catalyst layer and cathode GDL by XPS. The authors concluded that the direction of movement of the silicone traces was from the anode to the cathode due to the electrical field and that it was blocked by the PEM. However, traces of decomposition products of the sealing material in both the membrane and electrodes, as shown in Fig. 5, have been detected by Ahn et al. [14], Xie et al. [173], and Du et al. [174]. The acid character of the PEM, together with the thermal stressing [171] or hydrogen embrittlement [12], possibly induces the alteration of the sealing material. The degradation of the seals results in the loss of their force retention and can lead to compression loss, external leaks of coolant, gas crossover, or plate electrical shorting, eventually accelerating the performance degradation of the fuel cell. The migration and accumulation of the sealing materials within the electrodes will also negatively change the hydrophobic character of the electrodes and probably poison the Pt catalysts. Furthermore, the traces from the seal may diffuse into the membrane phase and consequently lead to a decrease in membrane conductivity and a reduction in the mechanical integrity of the membrane, both of which would severely impair the fuel cell lifetime [174]. Seal selection through ex situ and in situ screening processes should be based on the overall chemical and mechanical properties of the

Table 5
Major failure modes of different components in PEM fuel cells [3,175]

Component	Failure modes	Causes
Membrane	Mechanical degradation	Mechanical stress due to non-uniform press pressure, inadequate humidification or penetration of the catalyst and seal material traces
	Thermal degradation	Thermal stress; thermal cycles
	Chemical/electrochemical degradation	Contamination; radical attack
Catalyst/catalyst layer	Loss of activation	Sintering or dealloying of electrocatalyst
	Conductivity loss	Corrosion of electrocatalyst support
	Decrease in mass transport rate of reactants	Mechanical stress
	Loss of reformate tolerance	Contamination
	Decrease in water management ability	Change in hydrophobicity of materials due to Nafion or PTFE dissolution
GDL	Decrease in mass transport	Degradation of backing material
	Decrease in water management ability	Mechanical stress; Change in the hydrophobicity of materials
	Conductivity loss	corrosion
Bipolar plate	Conductivity loss	Corrosion; oxidation
	Fracture/deformation	Mechanical stress
Sealing gasket	Mechanical failure	Corrosion; mechanical stress

Table 6
General AST methods in PEM fuel cell lifetime analysis

Component	General criteria	Failure modes	Available protocols	Reference
Membrane/MEA	OCV at reduced RH for chemical stability; RH cycling for mechanical degradation	Chemical stability	Fenton's test: 30% H_2O_2, 20 ppm Fe^{+2}, 85 °C, 3 cycles with fresh reagent	[176]
		Chemical/electrochemical stability	OCV, 90 °C, with partially humidified H_2 and O_2 (both 30% RH) introduced to anode and cathode, respectively	[37]
			OCV, 80 °C, with dry air and fully humidified H_2 supplied to cathode and anode, respectively	[36]
			OCV, 90 °C, with partially humidified H_2 and air (both 30% RH) introduced to anode and cathode, respectively	[177]
			OCV, 95 °C, with partially humidified H_2 and air (both 50% RH) introduced to anode and cathode, respectively	[82]
			OCV, 90 °C, with partially humidified H_2 and O_2 (both 30% RH) introduced to anode and cathode, respectively	[178]
		Mechanical stability	65 °C, RH cycling from 30 to 80% or from 80 to 120% with 30 min/step, with air supplied to anode and cathode	[37]
			80 °C, RH cycling from 0 to 150% with 2 min/step, with air supplied to anode and cathode sides	[85]
		Chemical and mechanical stability	Humidity cycle: N_2/N_2, 80 °C, RH of inlet gases cycled between 0 and 100% RH every 30 min	[178]
			Load cycle: H_2/O_2, 50% RH, 80 °C, load cycled between 10 and 800 mA cm^{-2} (7 min/3 min)	[178]
Catalyst/catalyst layer	Potential cycling; acid washing; elevated temperatures; fuel or oxidant contaminants	Pt and/or Pt alloy chemical and electrochemical stability	80 °C, 100% RH, step change (30 s/step) in voltage from 0.6 to 0.96 V with air on cathode and H_2 on anode	[178]
			80 °C, 100% RH, 20 mV s^{-1}, linear sweep in voltage from 0.6 to 1.2 V with N_2 on cathode and H_2 on anode	[178]
			80 °C, 100% RH, with N_2 on cathode and H_2 on anode, 10 mV s^{-1}, from 0.1 to either 1.0 or 1.2 V	[179]
			80 °C, 100% RH, cathode 1.2 V relative to anode, with N_2 on cathode and H_2 on anode	[106]
			80 °C, H_2 with 226% RH at anode, Air with 100% RH at cathode, 10 mV s^{-1} potential cycling from 0.1 to 1.2 V	[110]
			80 °C, 100% RH, step change (30 s/step) in voltage from 0.6 to 0.9 V with N_2 on cathode and H_2 on anode	[177]
			20 °C, 0.5 M H_2SO_4, potentiostatic treatment 1.2 V (vs. RHE)	[102]
			40 or 80 °C, 1 M $HClO_4$, potential cycling between 0.85 V (vs. RHE) and 1.4 V (vs. RHE)	[180]
		Carbon support stability	80 °C, 100% RH, Potential hold at 1.2 V, with N_2 on cathode and H_2 on anode	[181]
			80 °C, 100% RH, Potential hold at 1.5 V, with N_2 on cathode and H_2 on anode	[181]
			OCV, 80 °C, with partially humidified H_2 and air (both 66% RH) introduced to anode and cathode, start/stop cycles between H_2/air (45/100 sccm) for 30 s and air/air (45/0 sccm) for 20 s.	[84]
			50 °C, with fully humidified 4% H_2/N_2 and He for anode and cathode respectively, 2 mV s^{-1} potential cycling between 0.04 V (vs. RHE) and 1.2 V (vs. RHE)	[84]
			95 °C, 80% RH, potential hold at 1.2 V, with N_2 on cathode and H_2 on anode	[177]
GDL	Chemical oxidation in hydrogen peroxide (H_2O_2); elevated potential; low humidity	Chemical/electrochemcial oxidation	DI water, 60 or 80 °C, purged with N_2 or air	[105]
			15 wt.% H_2O_2 at 82 °C	[106]
			1 M H_2SO_4, under potentiostatic treatment of 1.2 V (vs. RHE)	[107]
			80 °C, with fully humidified H_2 and N_2 for anode and cathode respectively, 1.2 V (vs. RHE)	[30]
		Mechanical stability	Compressive stress at 80 °C and 200 psi	[108]
			Freeze–thaw cycles between −35 and 20 °C	[108]

[156] H. Wolf, M. Willert-porada, J. Power Sources 153 (2006) 41–46.
[157] M. Wu, L.L. Shaw, J. Power Sources 136 (2004) 37–44.
[158] A. Pellegri, P.M. Spaziante, US Patent 4,197,178 (April 8, 1980).
[159] R.C. Emanuelson, W. Luoma, W. Taylor, US Patent 4,301,222 (November 17, 1981).
[160] W.A. Taylor, US Patent 4,592,968 (June 3, 1986).
[161] Jr. Stewart, C. Robert, US Patent 4,679,300 (June 2, 1987).
[162] T. Uemura, S. Murakami, US Patent 4,737,421 (April 12, 1988).
[163] M.S. Wilson, D.N. Busick, US Patent 6,248,467 (June 19, 2001).
[164] H.C. Kuan, C.C.M. Ma, K.H. Chen, S.M. Chen, J. Power Sources 134 (2004) 7–17.
[165] T.M. Besmann, J.W. Klett, J.J. Henry Jr., E. Lara-Curzio, J. Electrochem. Soc. 147 (2000) 4083–4086.
[166] T.M. Besmann, J.J. Henry Jr., E. Lara-Curzio, J.W. Klett, D. Hack, K. Butcher, Mater. Res. Soc. Symp. Proc. 756 (2003) FF7.1.1–FF7.1.8.
[167] E.A. Cho, U.S. Jeon, H.Y. Ha, S.A. Hong, I.H. Oh, J. Power Sources 125 (2004) 178–182.
[168] H.J. Li, X.H. Hou, Y.X. Chen, Carbon 38 (2000) 423–427.
[169] S.K. Ryu, T.S. Hwang, S.G. Lee, S.A. Lee, C.S. Kim, Carbon Sci. 2 (2001) 165–169.
[170] J.S. Cooper, J. Power Sources 129 (2004) 152–169.
[171] M. Schulze, T. Knöri, A. Schneider, E. Gülzow, J. Power Sources 127 (2004) 222–229.
[172] J. Tan, Y.J. Chao, J.W. Van Zee, W.K. Lee, Mater. Sci. Eng. A 445/446 (2007) 669–675.
[173] Z. Xie, N. Titichai, K. Shi, S. Holdcroft, Fuel Cell Durability Conference, Washington, DC, USA, December 8–9, 2005.
[174] B. Du, Q. Guo, R. Pollard, D. Rodriguez, C. Smith, J. Elter, J. Met. Miner. Mater. Soc. 58 (2006) 45–49.
[175] J.F. Wu, X.Z. Yuan, J.J. Martin, H.J. Wang, X.T. Bi, P.C. Pei, H.Y. Huang, Proceedings of Hydrogen & Fuel Cell 2007, Vancouver, BC, Canada, May, 2007, pp. 448–458.
[176] T.G. Benjamin, High Temperature Membrane Working Group Meeting, Washington, DC, USA, May 14, 2007.
[177] DOE cell component accelerated stress test protocols for PEM fuel cells, at: http://www1.eere.energy.gov/hydrogenandfuelcells/fuelcells/components .html (accessed December 2007).
[178] S. Knights, 4th Annual International Fuel Cell Testing Workshop, Vancouver, BC, Canada, September 12–13, 2007.
[179] K.L. More, 2005 DOE H₂ Program Review Proceedings, May 2005.
[180] V.A.T. Dam, F.A. de Bruijn, J. Electrochem. Soc. 154 (2007) B494–B499.
[181] T. Rockward, 2007 DOE H₂ Program Review Proceedings, May 2007.
[182] R. Hornung, G. Kappelt, J. Power Sources 72 (1998) 20–21.
[183] J.S. Kim, W.H.A. Peelen, K. Hemmes, R.C. Makkus, Corros. Sci. 44 (2002) 635–655.
[184] S.J. Lee, J.J. Lai, C.H. Huang, J. Power Sources 145 (2005) 362–368.
[185] S.J. Lee, Y.P. Chen, C.H. Huang, J. Power Sources 145 (2005) 369–375.

- *Effects of fuel and air impurities on PEM fuel cell performance*; 2008 DOE Hydrogen Program Review; presented by Fernando Garzon, Los Alamos National Laboratory, (June 2008).

2008 DOE Hydrogen Program Review:

Effects of Fuel and Air Impurities on PEM Fuel Cell Performance

- *Presented by:Fernando Garzon*

- Los Alamos National Laboratory

- June 12, 2008

Project ID
#FC30

Los Alamos
NATIONAL LABORATORY

Technical Staff

Los Alamos

Rod Borup
Eric Brosha
John Davey
Fernando Garzon
Bryan Pivovar
Tommy Rockward
Tom Springer
Francisco Uribe
Idoia Urdampilleta
Judith Valerio

Case Western Reserve University

Thomas Zawodzinski
Brian Kienitz

Overview

Timeline

- Project start - FY07
- Status - ongoing

Budget

- Funding in FY08: $1000 K
- Funding for FY07: $1200 K
- Non-cost shared

Barriers

- Fuel cell systems must cost less than $50/kw
  - Fuel and air purifications systems add cost
  - Higher Pt loading required to maintain performance in presence of impurities increases cost
- 5000 hr lifetime needed. Durability may decrease in the presence of impurities

Near Term Targets:
- *5000 hrs durability*
- *30$/kW by 2010*
- *55% energy conversion efficiency*
- *0.3g/kW Pt loading*

Partners

Case Western Reserve University

xradia

Los Alamos

3
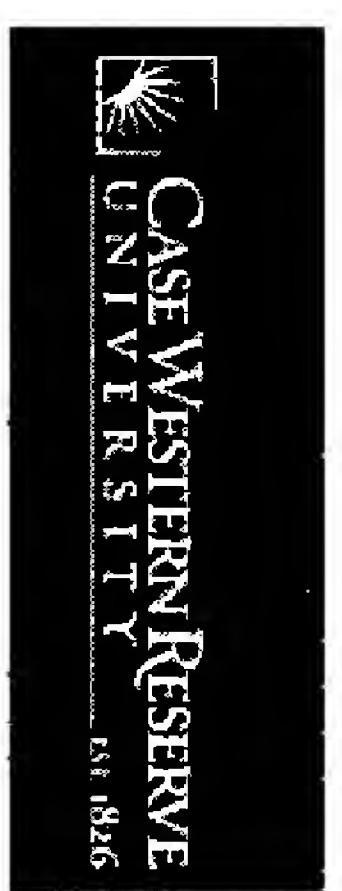
Technical Approach
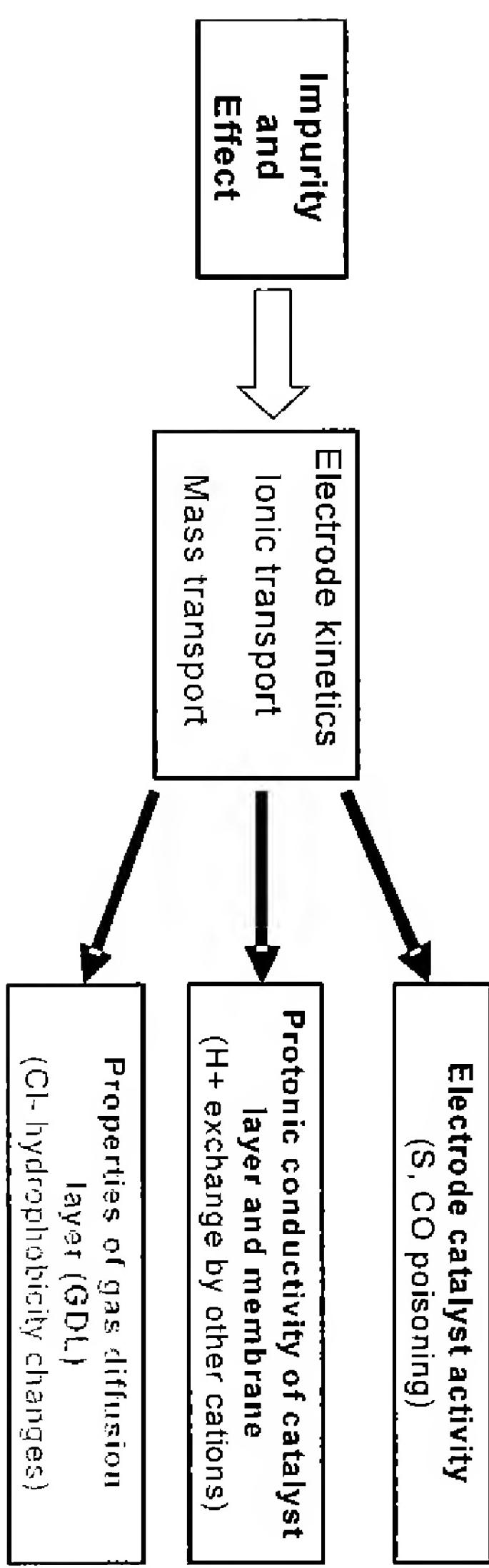
- Fabricate and operate fuel cells under controlled impurity gases
  - Multi-gas mixing manifolds and FC test stations
  - Pre-blend impurity gases
  - Measure performance
  - Steady state and *cycling* conditions
    - Understand degradation mechanisms
    - Study mitigation approaches
- Design supporting experiments to measure fundamental parameters needed for modeling
  - *Electroanalytical experiments*
  - *Adsorption studies*
  - *Permeation studies*
- Analyze and model data
  - Impurity impact on catalysis
  - Impurity impact on transport

```
          ┌──────────┐
          │ Impurity │
          │   and    │
          │  Effect  │
          └──────────┘
               │
               ▼
   ┌────────────────────┐
   │ Electrode kinetics │
   │  Ionic transport   │
   │  Mass transport    │
   └────────────────────┘
        │    │    │
        ▼    ▼    ▼
```

Electrode catalyst activity (S, CO poisoning)

Protonic conductivity of catalyst layer and membrane (H+ exchange by other cations)

Properties of gas diffusion layer (GDL) (Cl- hydrophobicity changes)

- Impurities affect fuel cells in many ways:
  - Electrocatalyst poisoning e.g. H_2S, CO and SO_2 adsorption onto Pt catalysts
  - Reduce ionomer conductivity- Na^+, Ca^{++}, NH_3
  - Block proton access to electrochemically active interface
  - GDLs become hydrophilic and flood at high current densities

Los Alamos

Objectives

Overall Objective: Contribute to the scientific understanding of the effects of fuel and air impurities on fuel cell performance and how it affects DOE fuel cell cost and performance targets.

Specific Objectives:

• Investigate effects of impurities on catalysts and other FC components

• Understand the effect of catalyst loadings on impurity tolerance

• Investigate the impacts of impurities on catalyst durability

• Develop methods to mitigate negative effects of impurities

• Develop models of fuel cell-impurity interactions

• Collaboration with USFCC, Fuel Cell Tech Team, Industry and other National Laboratories to foster a better understanding of impurity effects

Los Alamos

Milestones

Month/Year	Milestone or Go/No-Go Decision
Mar-08	Milestone: report on the performance degradation due to H$_2$S anode poisoning as a function of catalyst loading (0.1 and 0.05 mg Pt/cm^2). Completed
Apr-08	Milestone: Modeling and validation of impurity effects in PEMFCs. We have developed a model for understanding the effects of alkali contaminants on fuel cell response and experimentally validated the results using novel experimental methods. Completed
May-08	Milestone: Determination of multiple contaminant effects carbon monoxide and hydrogen sulfide, on fuel cell response. Completed

Los Alamos
NATIONAL LABORATORY

Exposure to 1.5 ppm H_2S for 2, 4 and 6 hour

Cell Voltage normalized / V

H_2S on

H_2S off

H_2S off

(a)

(b)

(c)

- ○ 2 h poisoning (a)
- ● 4 h poisoning (b)
- △ 6 h poisoning (c)

Time / hours

Cell Current / A

— Neat H2
— — 2 h poisoning
······ 4 h poisoning
– – 6 h poisoning

Cell Voltage / V
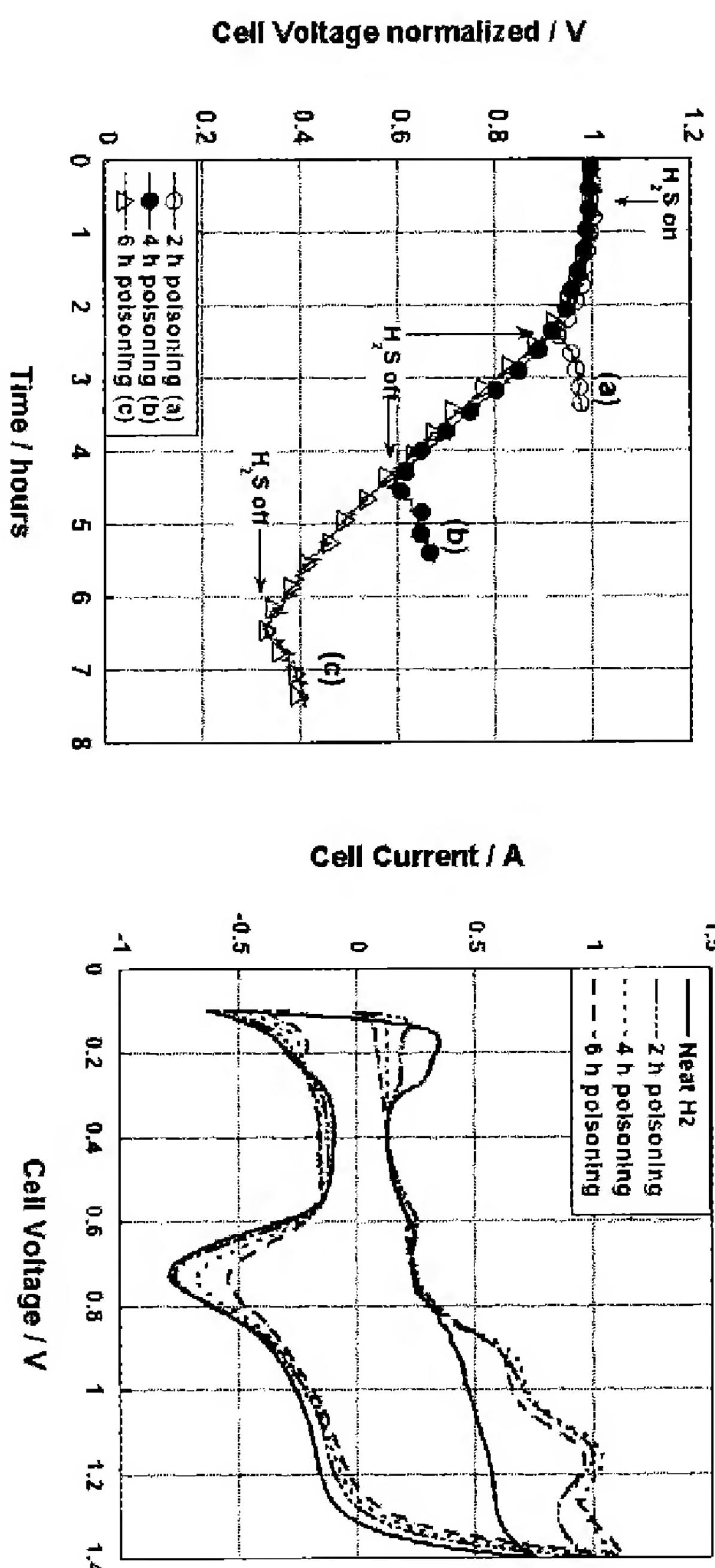
- **Performance degradation is more severe for larger dosages**
- **Catalyst poisoning is cumulative**

Basic Degradation Mechanism

H₂ → H_2 ... Pt

Anode CV / 3 ppm H₂S

Current / mA cm⁻²

- - - - Before exposure
———— After exposure

Potential / V vs. HRE
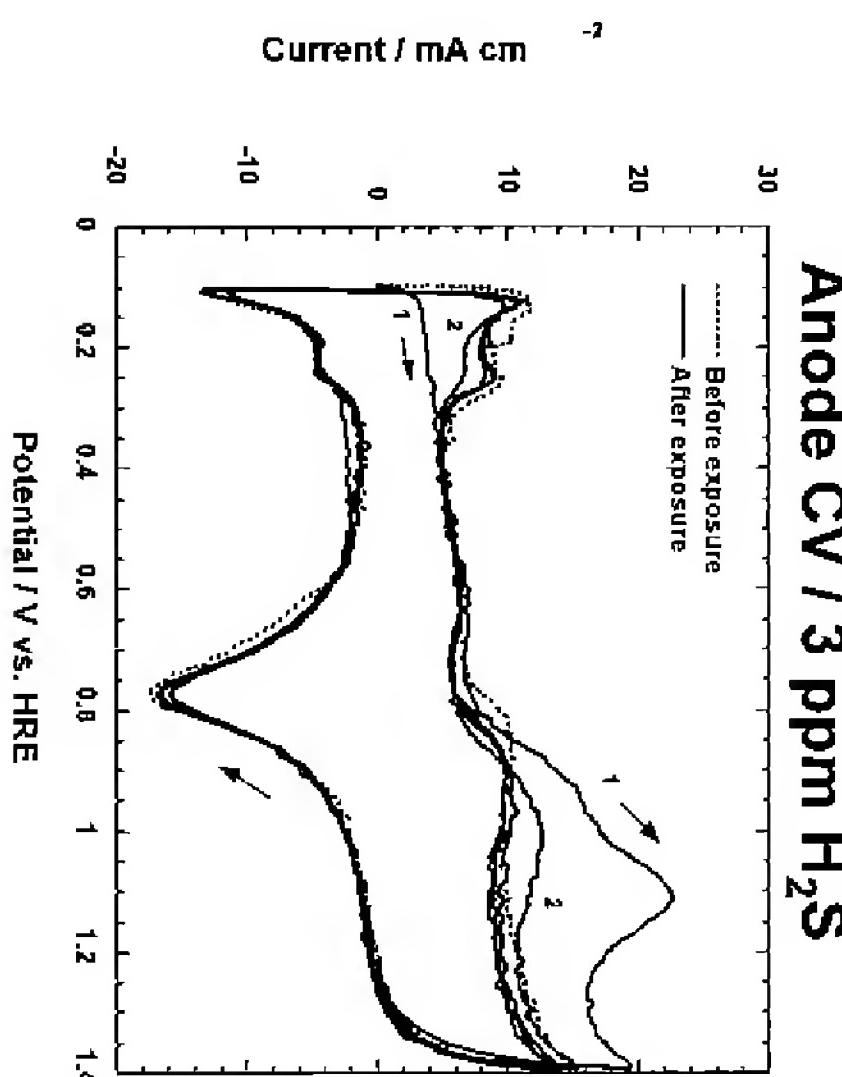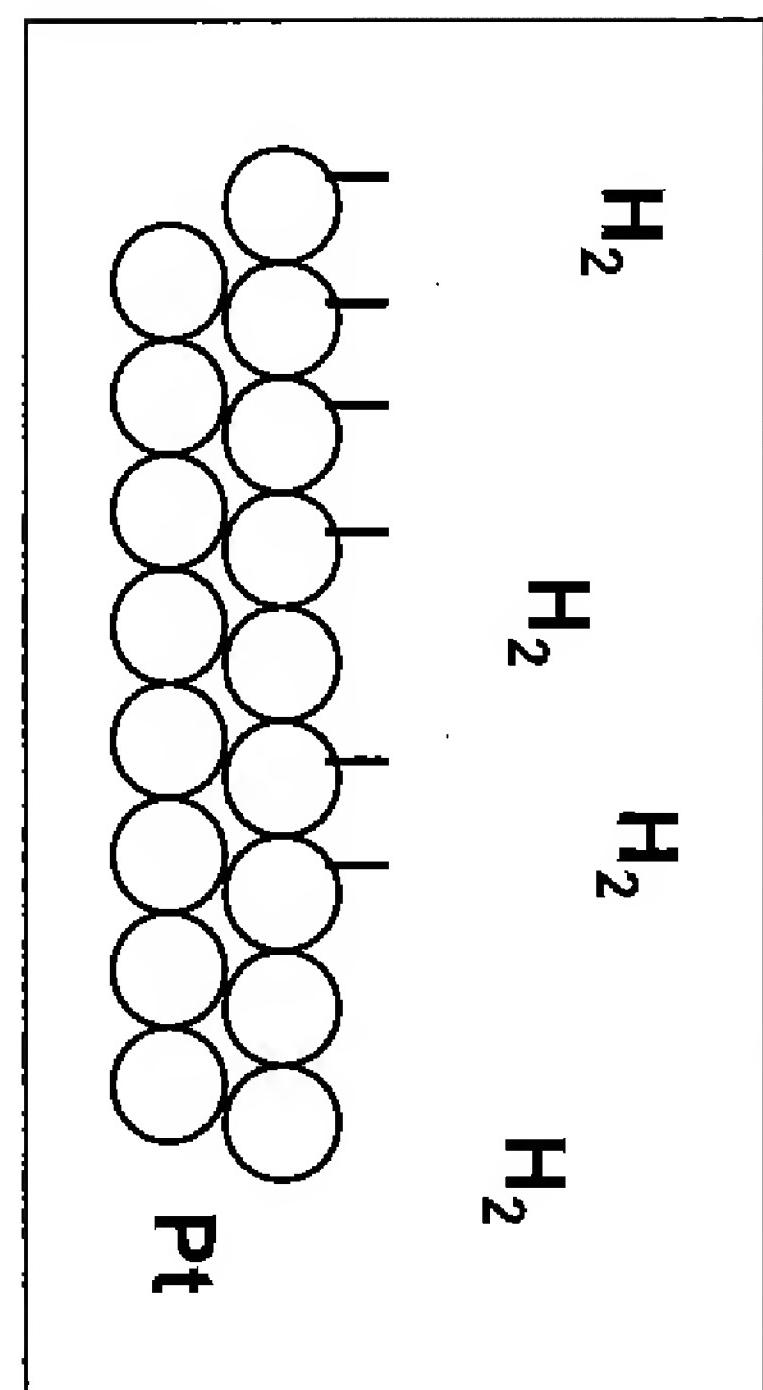
Deactivation: Pt + H₂S □ Pt-S + H₂

$$Pt + H_2S \square Pt\text{-}S + H_2 \quad \text{(heterogeneous catalysis)}$$

$$Pt + H_2S \square Pt\text{-}S + 2H^+ + 2e^- \quad \text{(eletrochem. conditions)}$$

Cleaning: Pt-S + 4H₂O □ Pt + SO₄²⁻ + 8H⁺ + 6e⁻

$$Pt\text{-}S + 4H_2O \square Pt + SO_4^{2-} + 8H^+ + 6e^-$$

- *Strong sulfur chemisorption onto Pt deactivates the catalyst*
- *Pt-coverage: more than one monolayer of sulfur*
- *PtS may form under severe conditions*

1. T. Loucka, *J. Electroanal. Chem.,* **31,** 319 (1971)
2. R. Mohtadi et al., *Electrochem. Solid State Lett.,* **6,** A272(2003
3. Garzon, et al., *ECS Trans.* 3, (1) 695 (2006))
4. W. Shi et al., *Journal of Power Sources,* **164,** 272 (2007)
5. Z. Shi et al., *J. Electrochem. Soc.,* **154,** B609 (2007)

Technical Results: H₂S Temperature Effects

Poisoning with 2ppm H2S for 3h 15 min
400/2100sccm

Cell Voltage / V

Time / hours

Legend:
- 90°C
- 80°C
- 70°C
- 60°C
- 50°C

50 cm² / 40 A / 80 °C

- *As T increases so does
- *the degradation rate
- *and extent.
- *Relative recovery after
- *returning to neat H₂
- *is higher at the higher T
- *but less total recovery

Los Alamos
NATIONAL LABORATORY

Technical Results: Co-adsorption of CO and H$_2$S

- CO and H$_2$S often times occur together though CO concentration typically higher

- Both strong adsorpates CO peak 0.6-0.8V, S above 0.9V

- CO gas phase transport low water solubility; H$_2$S high water solubility

- Wet environment shows relatively more CO/H$_2$S

- Mix both gasses at 10:1 CO:H$_2$S ratio at concentrations for nearly complete poisoning

Baseline CVs for H$_2$S and CO at 60°C

Voltage/ V vs HRE

— 500 ppm CO (12min)
— 50 ppm H2S (12min)
— Baseline CV

50 cm^2 cells / N112, 20 mV/s
Loadings: 0.2 mg Pt at each electrode
Cell Temperature: 80 °C, PSIG: 3.7/3.7

Los Alamos
NATIONAL LABORATORY

Technical Results: Co-adsorption of CO and H₂S

- *CV indicates a larger presence of CO during short term exposure*

- *H₂S eventually replaces CO on the electrode surface*

- *CO kinetics are faster, H₂S has a higher adsorption strength H₂S suppresses CO adsorption*

Wet environment shows more relatively more CO/H₂S
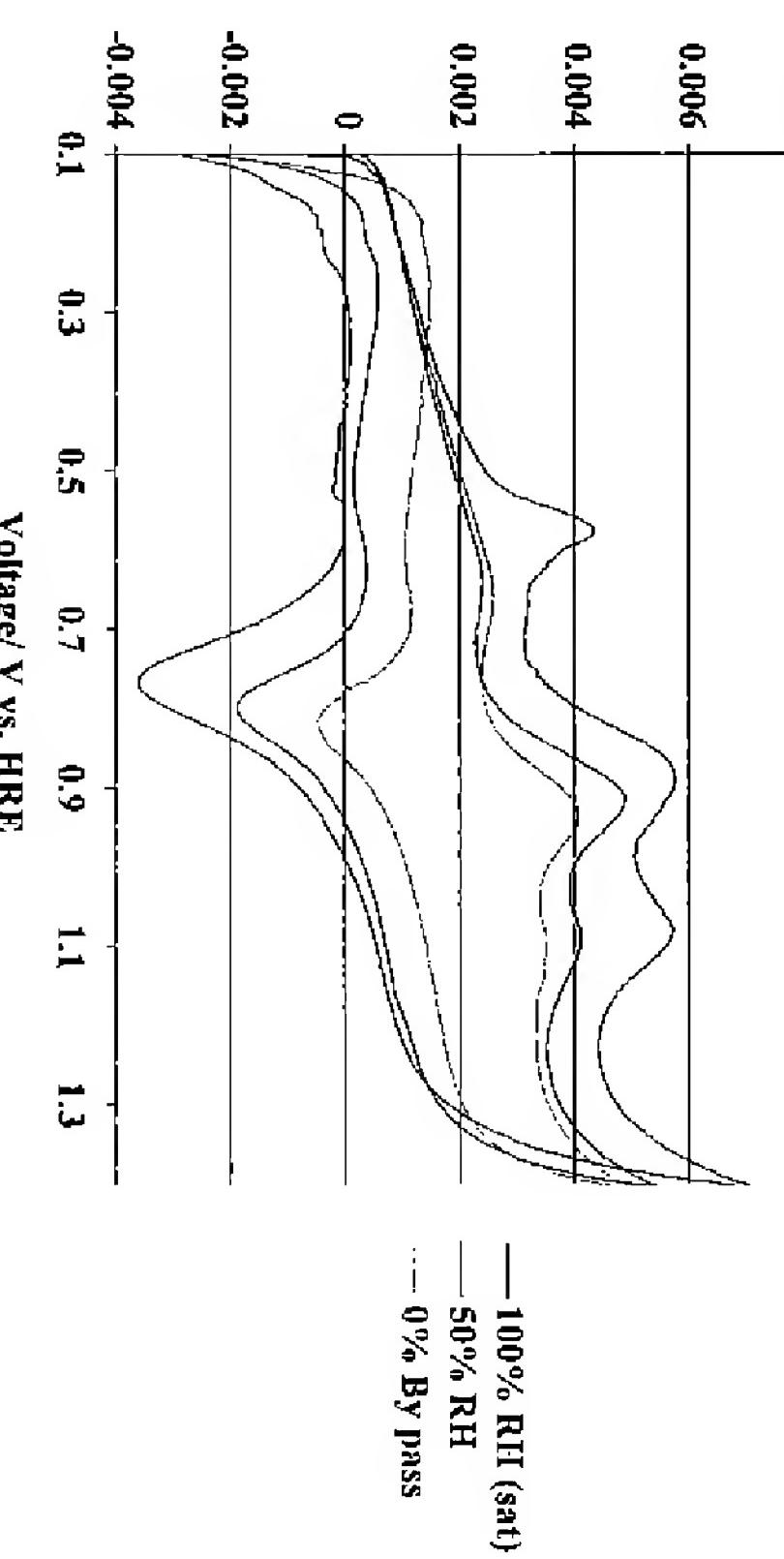
Co-Adsorption between CO and H₂S
on Pt Electrode(10:1)at 80°C
-Effects of RH

— 100% RH (sat)
— 50% RH
-- 0% By pass

Co-Adsorption between CO and H₂S
on Pt Electrode(10:1)at 60°C

— 10 min
— 8 min
— 6 min
— 4 min
— 2 min

Co-Adsorption between CO and H2S
on Pt Electrode(10:1)at 80oC
-Poisoning Order

— H2S then CO
— CO then H2S
— CO and H2S

Los Alamos
NATIONAL LABORATORY
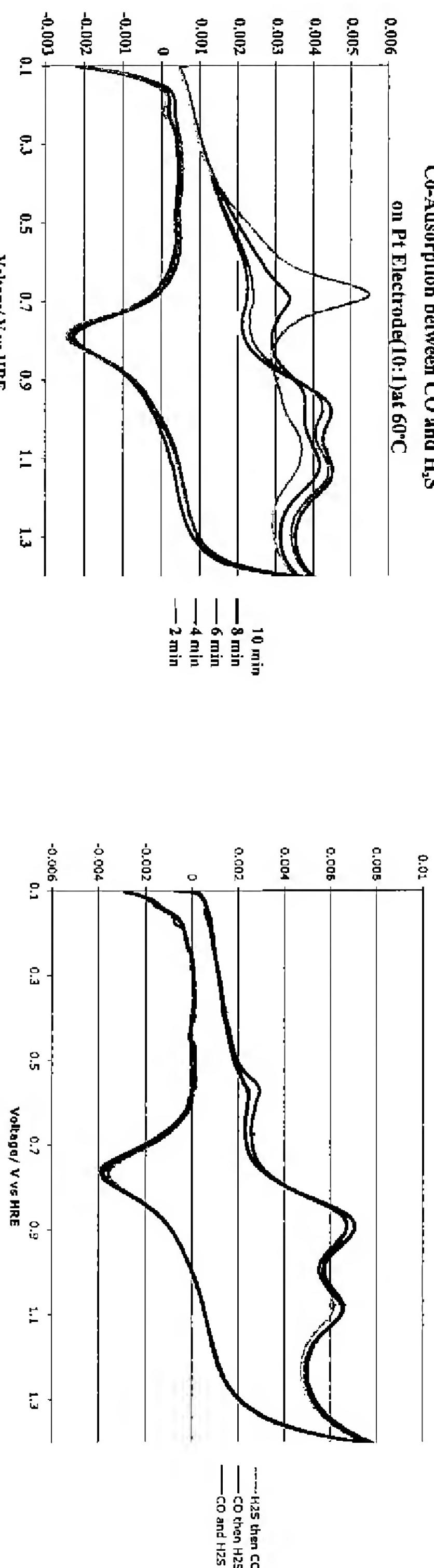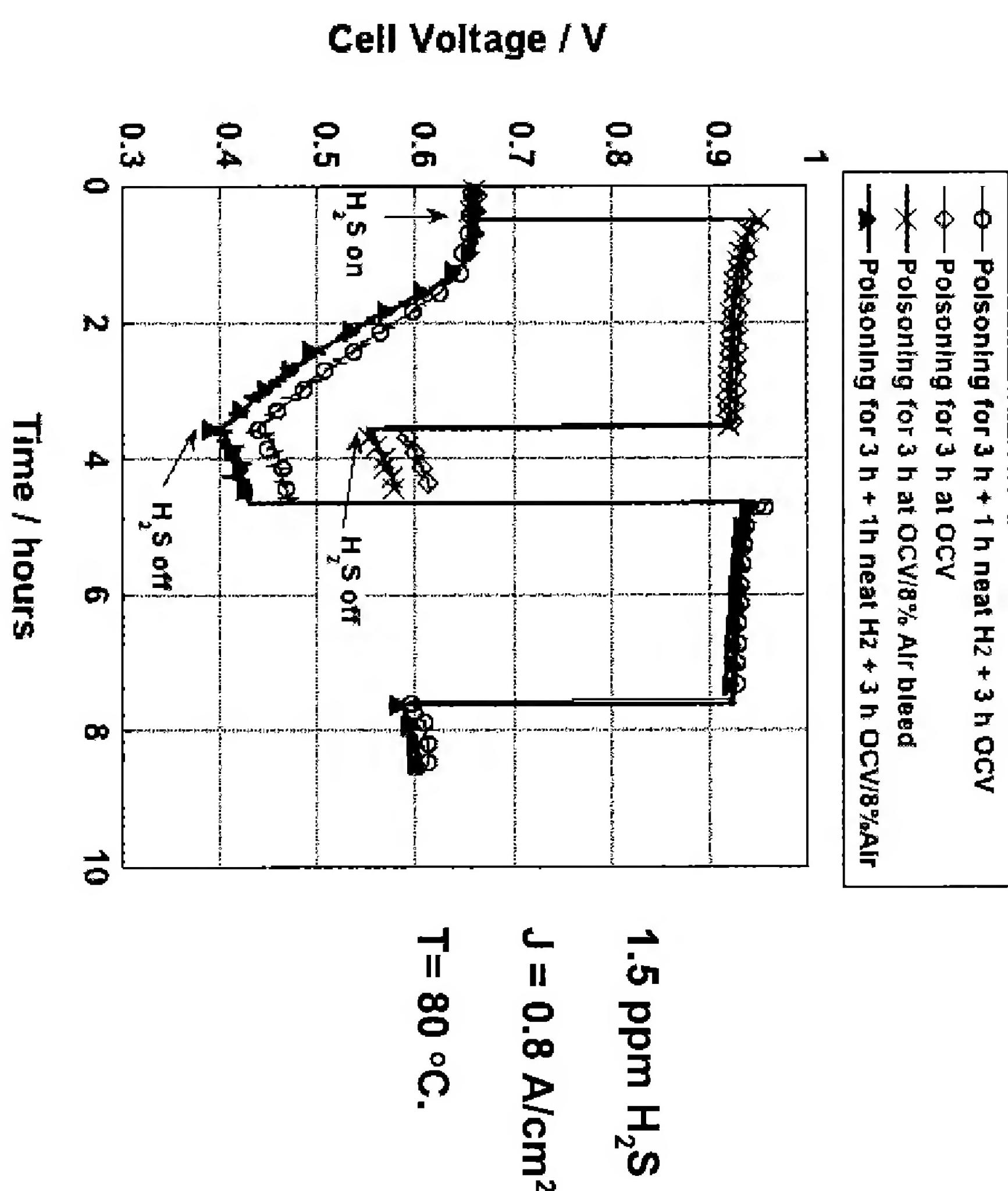
In contrast to CO mitigation, Anode *air bleed does not have any significant benefit* on poisoning or recovery for H_2S

H$_2$S crossover from anode to cathode ?

EVIDENCE:

1. Open circuit will allow chemical oxidation of sulfur by O$_2$ at the cathode

   1. Possible reaction: Pt-S + 3/2O$_2$ + H$_2$O⬜ Pt + SO$_4^{2-}$ + 2H$^+$ (slow)

2. FC operation at high voltage will induce partial electrochemical

3. oxidation of sulfur, only at the cathode

4. Diffusion of H$_2$S observed across the Nafion membrane

5. Injected H$_2$S at the cathode produces performance degradation

- Hydrogen sulfide state in membrane is a polar molecule
- No ionic dissociation at low pH
- High solubility:3.4 g/l-atm at 25°C

MECHANISMS:

- **Dry membrane permeation:**
  - Permeation by diffusion
  - Rate proportional to concentration gradient
- **Wet membrane permeation:**
  - co-permeation with water gradient
  - Rate proportional to water activity and conc
- **Proton drag:**
  - moves with proton across cell
  - Rate proportional to current density
  - Need hydrogen pumping cell to study (avoids oxidation of H$_2$S)

13

Los Alamos

Technical Results: H₂S crossover, cont'd

1 ppm H₂S injected at the cathode

Current at 0.5 V / A

H₂S on

Time / hours

50 cm² cell

50 cm² cell / scan rate: 20 mV/s

Current / A

Clean cathode Pt surface
After poisoning with 1 ppm H2S for 2.5 h

Potential / V vs. RHE
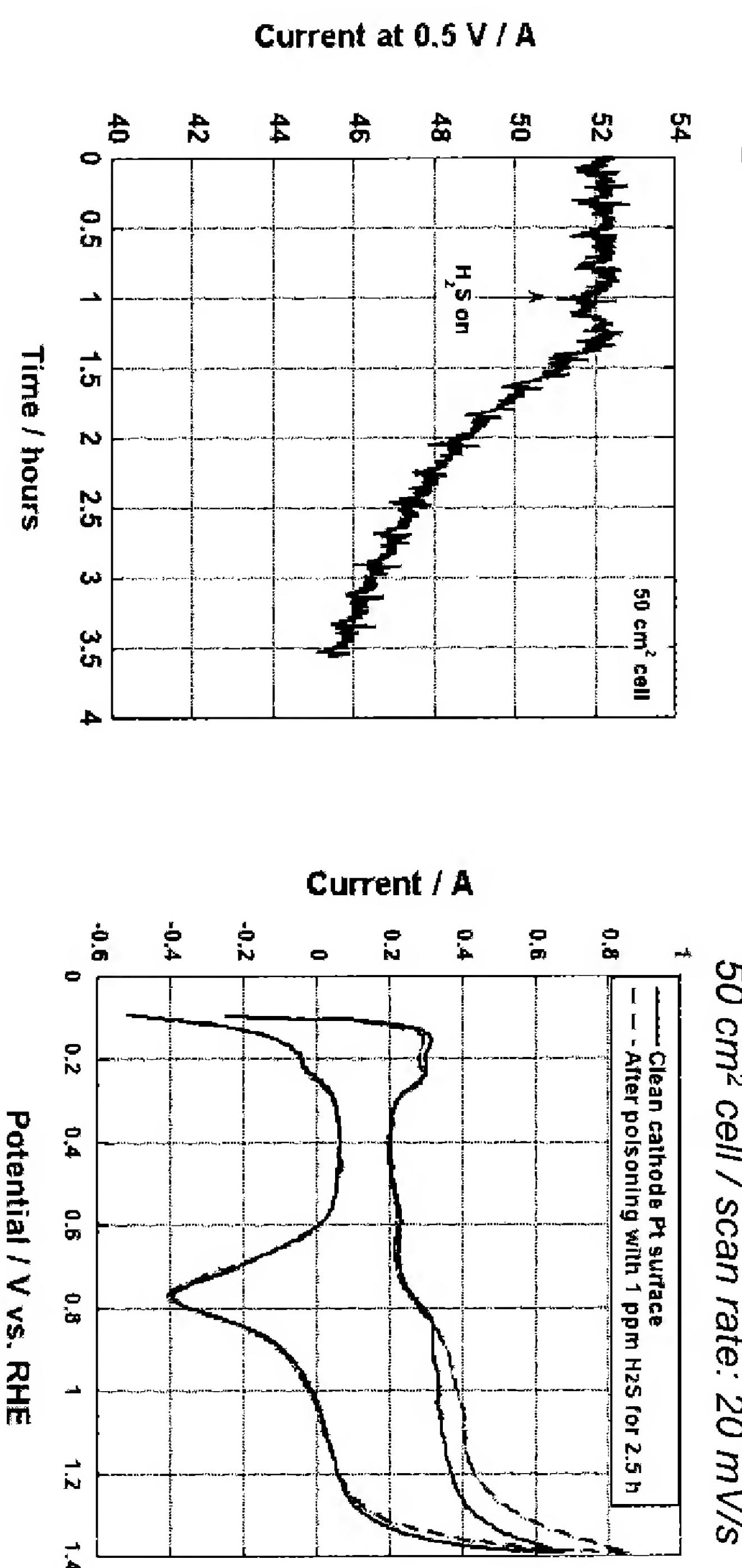
- *H₂S at the cathode degrades cell performance*
- *Similar effect observed when SO₂ is injected at the cathode*

Los Alamos
NATIONAL LABORATORY

14

Technical Results: Wet Versus Dry Gas Permeation for Hydrogen Sulfide

- 1030 ppm of H_2S (wet/dry) and 6% H_2 (wet/dry) were flowed across the sides of a 117 membrane 50 cm² for 72 hours.
- The H_2S trap was placed in line after sufficient H_2S crossed over to passivate GDL and flow fields.
- Trapping experiment was run between 500 and 1300 min alternating between humidified and dry membrane state.

- Dry : 3.2e-8g/min H_2S crossover
- Wet: 5.9e-7g/min H_2S crossover

- Gas humidification greatly increases rate of crossover
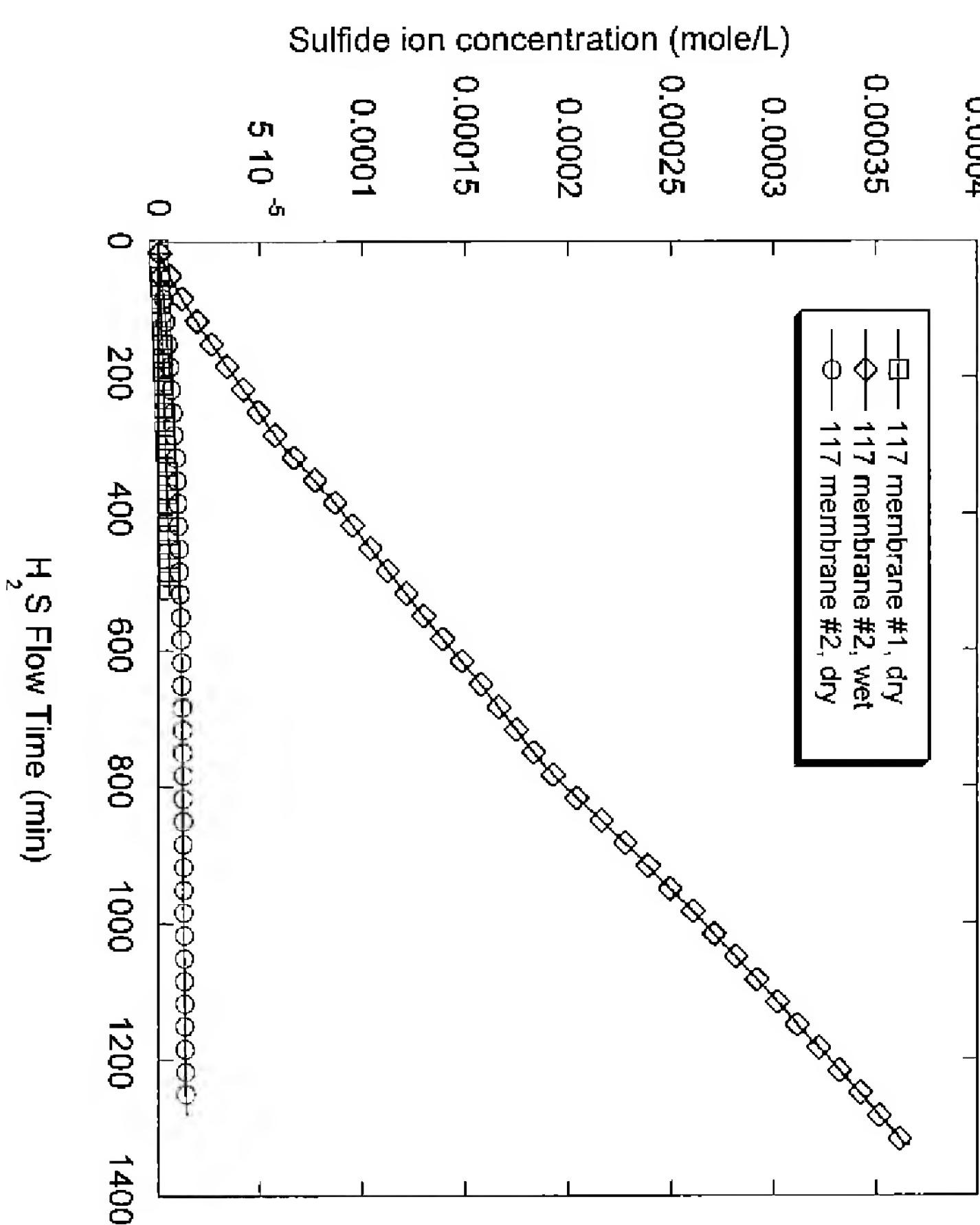
Rate of H$_2$S crossover in wet 212 membrane is 1.8e^{-6} g/min.
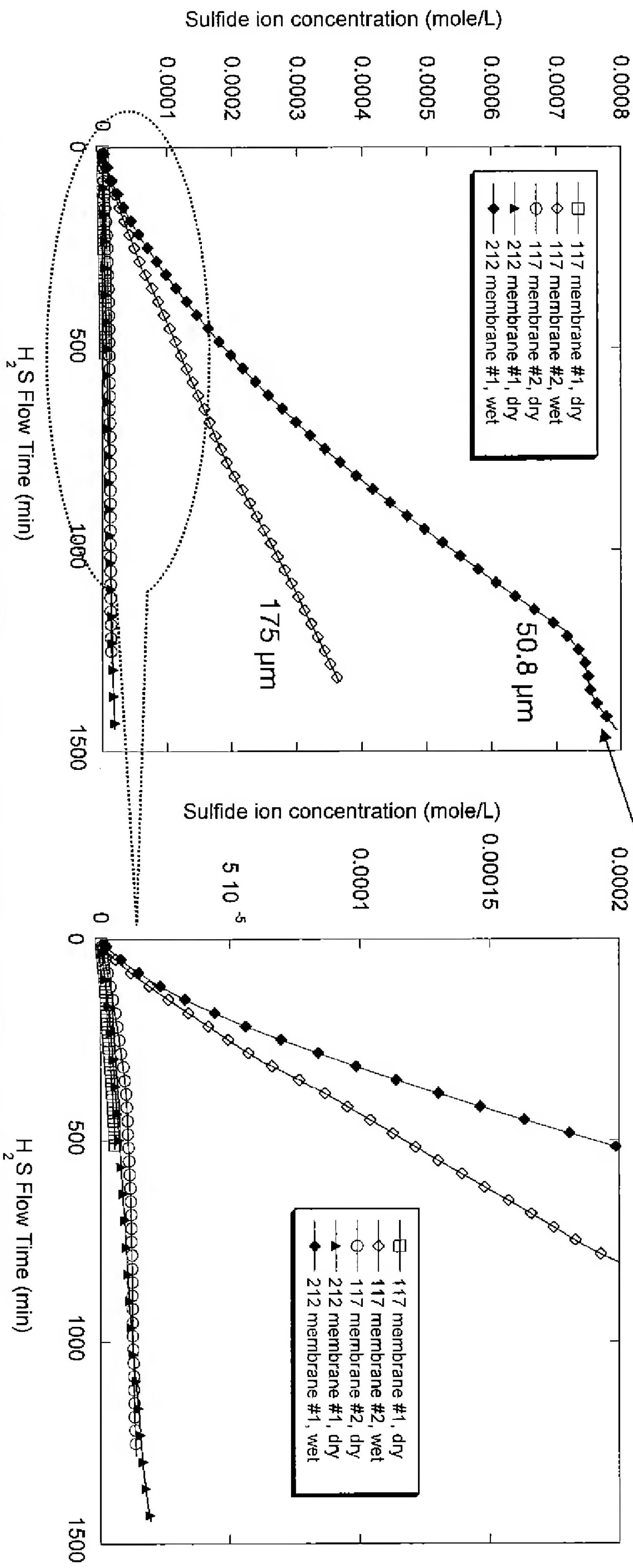
- Thinner membranes show higher crossover rates; scales with thickness
- Wet membranes show higher permeation rates
- however humidification decreases H$_2$S concentration reaching electrode

Technical Results: Hydrogen Pump Cell

- Use hydrogen pump cell to study anode poisoning and crossover

  - Measure polarization behavior before and after poisoning from either the anode or cathode compartment

  - Compare to fuel cell behavior

- 0.5 PPM H₂S in humidified H₂

hydrogen pump after anode exposure to hydrogen sulfide

baseline for anode H2S
0.5 ppm H2S anode,1 hr,anode
0.5 ppm H2S,2.5hr,anode

hydrogen pump after cathode hydrogen sulfide exposure

Baseline
0.5 ppm H2S(1hr,cathode)
0.5 ppm H2S(2.5hr,cathode)
baseline Xposed

Fuel cell Performance after hydrogen sulfide exposure

Voltage (0 hrs)FC mode
Voltage(1 hr) FC mode
Voltage (2.5 hrs)FC mode

Significant voltage losses created by H₂S in hydrogen pump mode

- Surface/speciation model pH Temp and *S* concentrations

  - Predominate sulfur species are H_2S, $S-Pt$, PtS, PtS_2 and HSO_4^-

  - SOx species are not stable in acid fuel cells

    – Explains similarity in poisoning results from using H_2S, SO_2 or Na_2S

  – CANNOT be displaced by hydrogen or CO

- Pt sulfur coverage at -0.15 volts with increasing coverage as anode potential is raised for 1 ppb H_2S

- At higher potentials transition from S adsorbed on Pt to PtS with surface reconstruction

- Oxidation cleaning mechanism is inhibited by kinetics not thermodynamics @ 0.450 mV

- Surface speciation model coupled to fuel cell electro-kinetics model

  – Activity coefficient corrections for strong electrolytes (Pitzer model)

  – nanoparticle free energies data (+ than bulk Pt)

  – Surface thermodynamics for nanoparticles
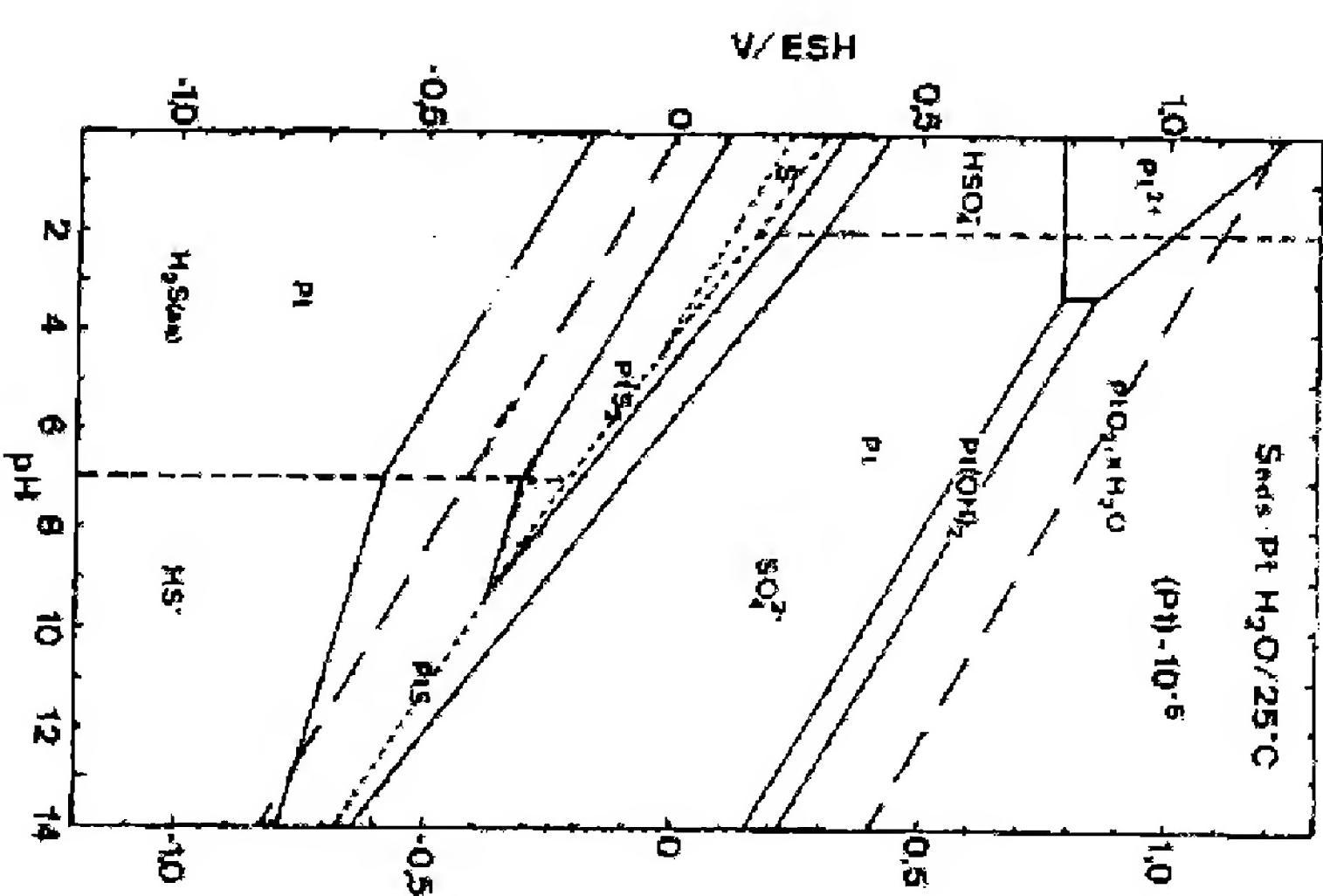
P. Marcus, E. Protopopoff, *Comptes Rendus de L Academie Des Sciences Serie Ii* **308**, 1685 (1989).

Cation Contamination

Cationic contaminants

- Displace protons in the ionomer phase
- Have higher affinity for the membrane
- Have a lower conductivity than protons
- Originate from aerosols or corrosion
- Have been shown to affect fuel cell performance
- Removal mechanism poorly understood
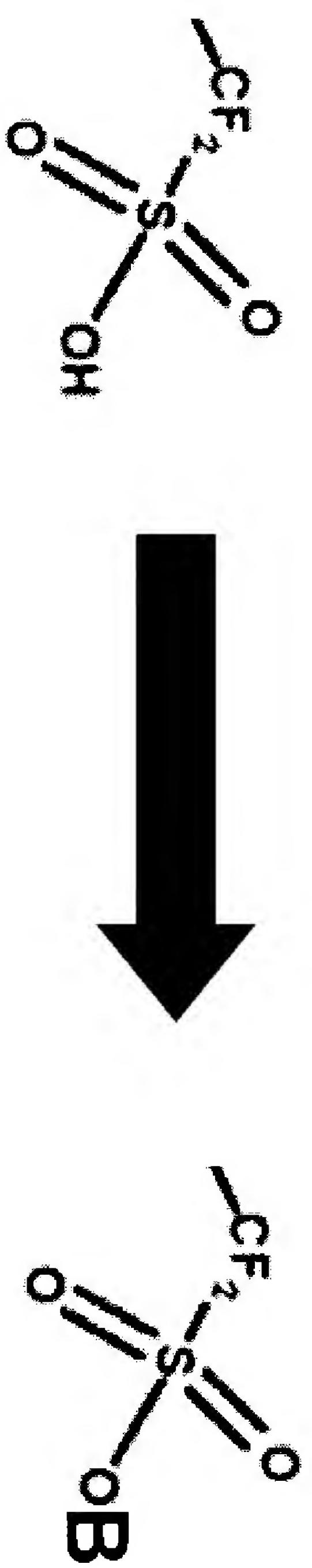

Protonated SO_3^- site

Contaminated SO_3^- site

$B = Na^+, NH_4^+, Cs^+, Ni^{2+}, Fe^{3+}, ...$

Technical Results: Membrane Contaminant Profiles

- Cations move due to electro-migration and chemical diffusion:

$$j_i = -D_i \frac{dC_i}{dx} + u_i C_i \frac{d\Phi}{dx}$$

- Contaminants build up near the cathode

- Novel strip cell was used to show concentration profiles exist

- Contaminate concentration measured by XRF

anode   ref1   ref2   cathode

2 mm   15 mm

Nafion

Pt wire

Pt/C/Nafion Catalyst

y_Φ

1.00   0.75   0.50   0.25   0.00

0.00   0.25   0.50   0.75   1.00

Increasing Current Density

i (A/cm²)
— 0.0
— 0.5
— 1.0
— 1.5
— 2.0

y_{Cs}

1.0   0.8   0.6   0.4   0.2   0.0

0.0   0.2   0.4   0.6   0.8   1.0

dimensionless position
(0=cathode)

Los Alamos
NATIONAL LABORATORY
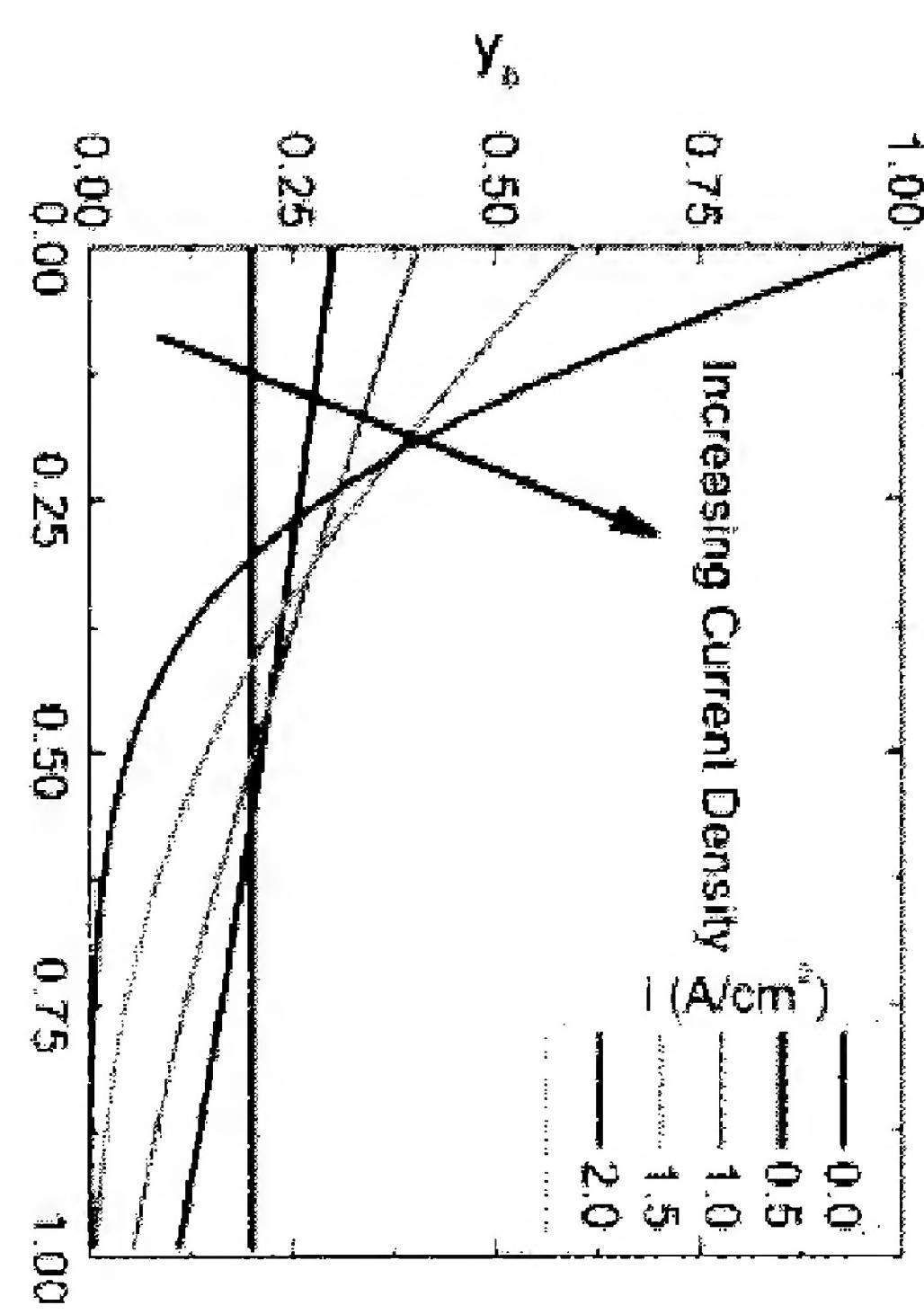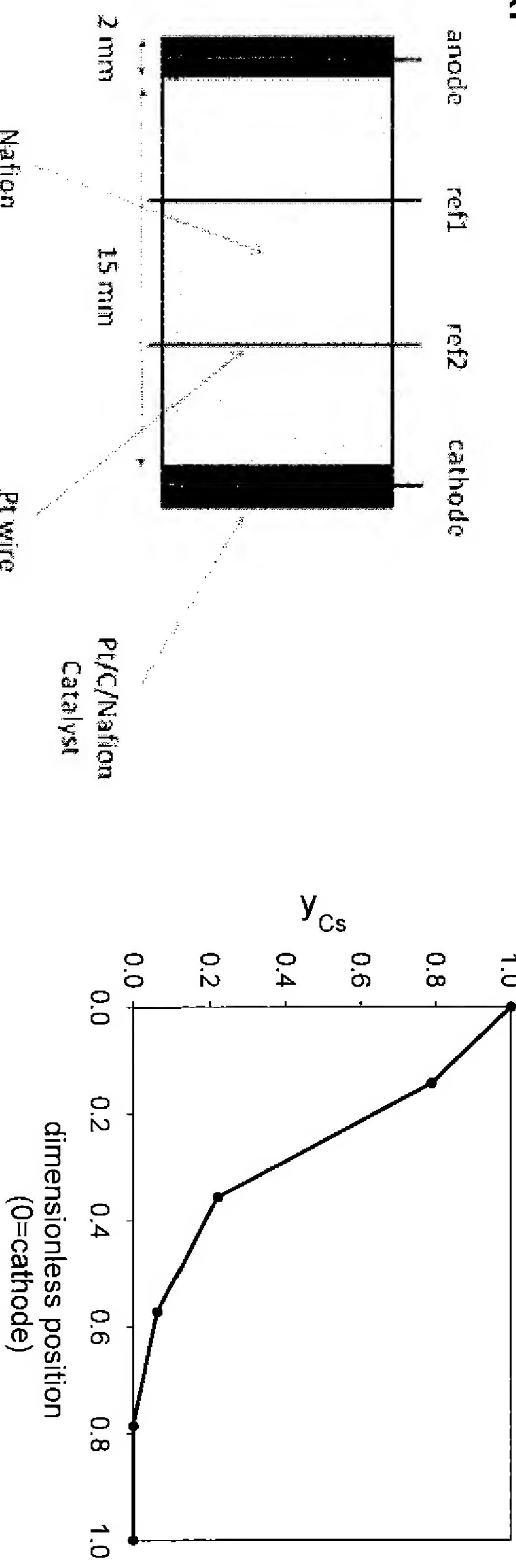
Technical Results: Effects Electrode Effects Model

- Contaminants replace protons in the electrode
- Cathode overpotential increases account for most performance loss
- Lack of protons leads to proton limited currents
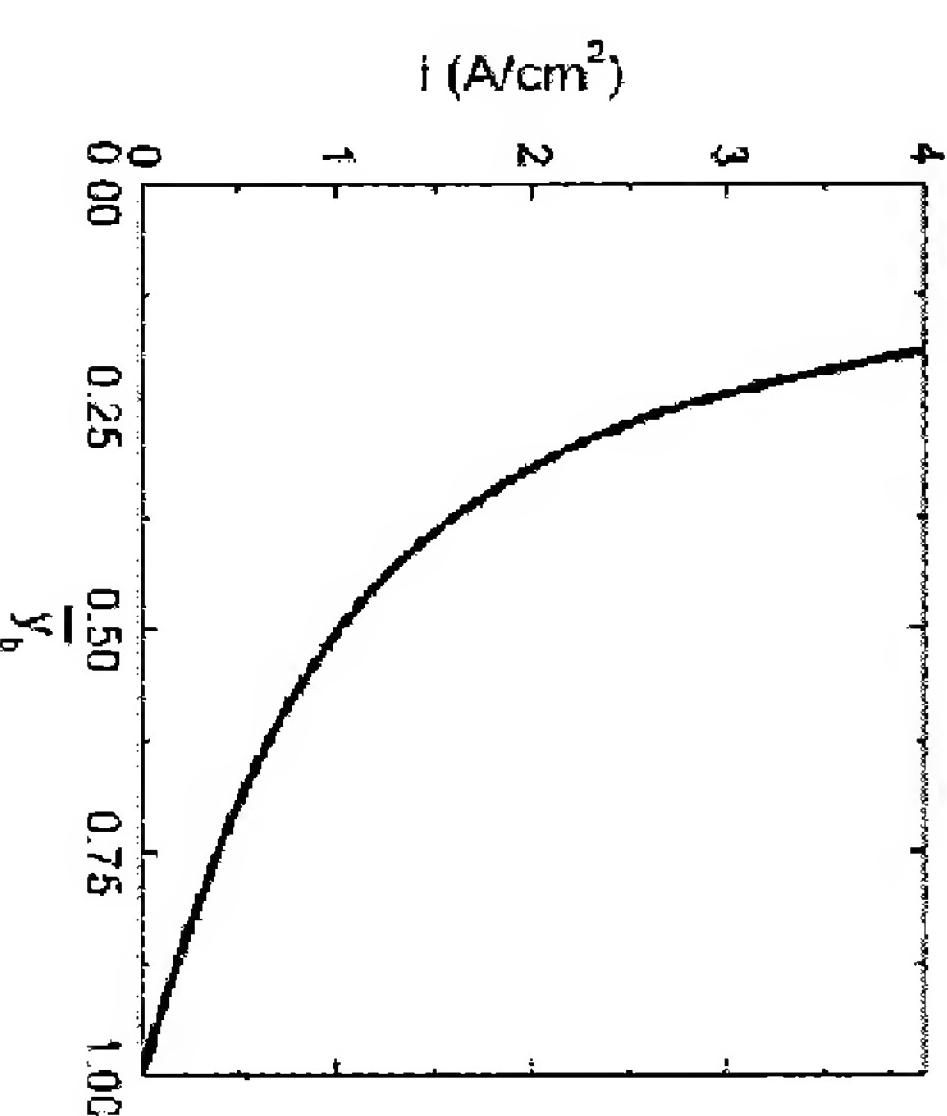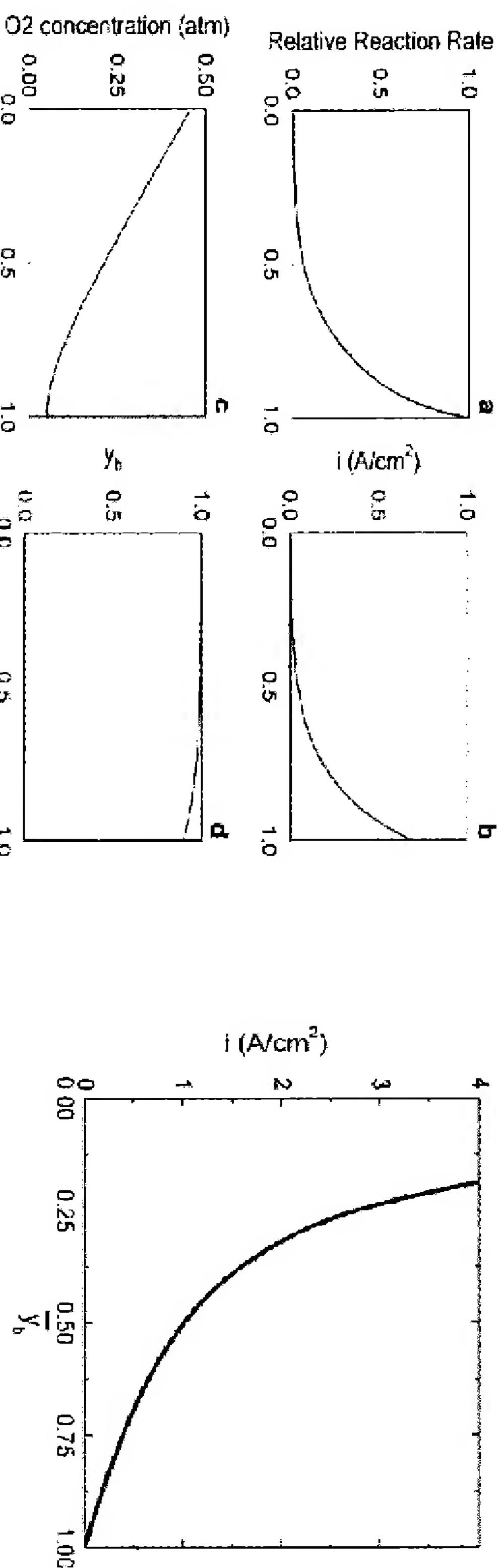
Species and reaction rate profiles across the electrode near proton limitation

Proton limited current for base case parameters

Technical Results: Alkali Contamination

- *We are using Cs^+ as a model alkali cation (behaves like Na^+, K^+)*
- *Very low detection limits with X-ray fluorescence Spectroscopy*

Legend (fraction of sites contaminated): 0.0, 0.13, 0.29, 0.33, 0.72, 1.00
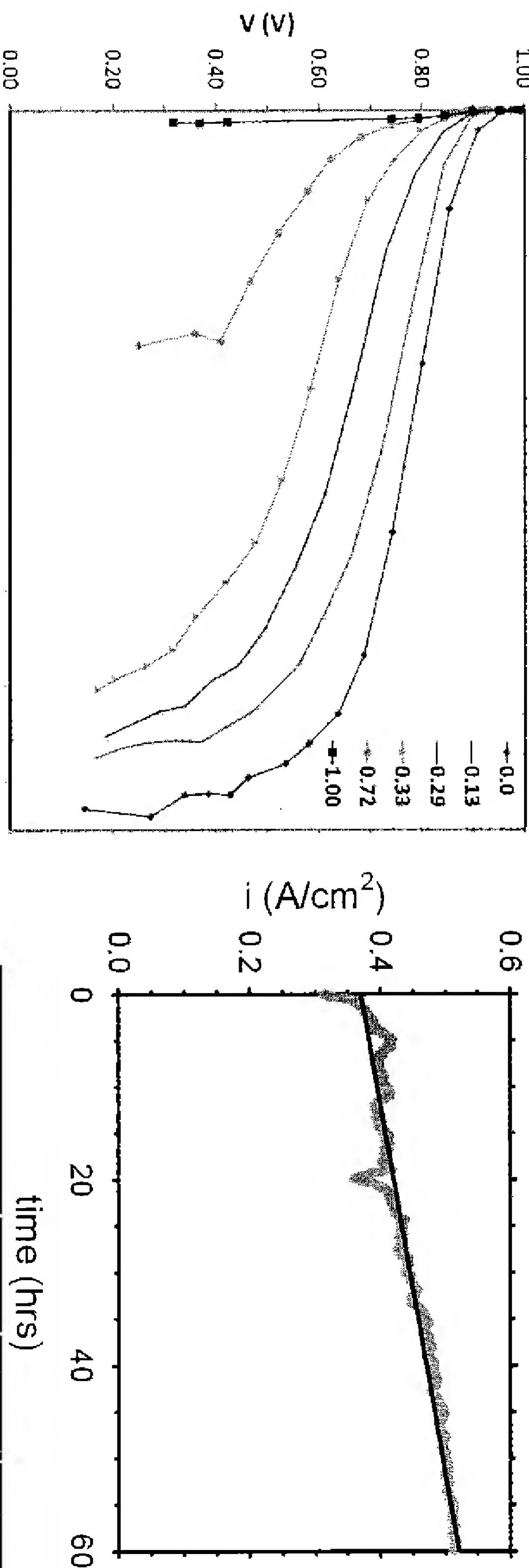
H2/Air 30 PSI Temp A/C/Cell 85/80/85

Legend represents fraction of sites contaminated

Increasing contamination
- Decreases ionomer conductivity
- Lowers limiting current
- Affects kinetics

	level	i @ 0.5 V	HFR
Clean	0	1.31	0.048
Contaminated	0.716	0.37	0.114
After 60 hours	0.567	0.53	0.104

Cs^+ ions leave the membrane slowly (2.5 µg/cm²/hr) but other cations show no recovery

Los Alamos

Cationic Contamination Summary

- Fuel cell cationic contamination
  - Decreases ionomer conductivity
  - Lowers limiting current
  - Affects kinetics
- Modeling shows the mechanisms of performance degradation
  - Greatly increases cathodic overpotential due to loss of protons in the ionomer phase
  - Can lead to proton limited current
- Fuel cell recovery
  - 50% of Cs can leave in 2 days of operation
  - Some other ions also show recovery
  - Rate of recovery is still small compared to proton flux

Los Alamos
NATIONAL LABORATORY

Technical Achievements

- Measurement of increased degradation of fuel cell performance by H_2S with increasing temperature

- Measurements of H_2S membrane crossover for wet and dry membranes

- CO and H_2S co-adsorption kinetic studies

    - fast adsorption kinetics for CO but eventually displaced by H_2S

- H_2S anode poisoning studied by H_2 pump cells

- Model development and measurement of alkali cation contaminant behavior in perfluorosulfonic acid membranes

- Experimental measurement of fuel cell losses due to alkali cation contamination- good agreement with model

Future Work

- Continued contaminant crossover studies: Proton drag of H_2S

- Fundamental electrokinetic measurements of poisoned electrodes

- Lower cathode loading impurity studies

- Impurity effects on durability studies
  - New commercial MEAs with 2010 loadings

- Refine and validation of electrode impurity modeling efforts

- Studies of the effect of divalent cations on Fuel Cell performance

- Air contaminate studies: hydrocarbons and particulates

- Zhang, X. et al; *Contamination of membrane-electrode assemblies by ammonia . . .*; presentation preprint for 216th ECS Meeting, Vienna Austria, (October 2009).

Contamination of Membrane-Electrode Assemblies by Ammonia in Polymer Electrolyte Fuel Cells

Xiaoyu Zhang[1,2], Mustafa Fazil Serincan[1,2],
Ugur Pasaogullari[1,2 *], Trent Molter[1]

[1] Connecticut Global Fuel Cell Center
[2] Department of Mechanical Engineering,
University of Connecticut, 44 Weaver Rd, Unit 5233,
Storrs, CT 06269-5233, USA

Contamination of polymer electrolyte fuel cell (PEFC) membranes and catalyst layers with ammonia (NH₃) is studied experimentally and computationally. Cyclic voltammetry (CV) scans and electrochemical impedance spectroscopy (EIS) analyses show that trace amounts of ammonia can significantly contaminate both the polymer electrolyte membrane (PEM) and the catalyst layers. The results show that the catalyst layer contamination can be reversed under certain conditions, while the membrane recovery tends to be much slower, and permanent effects of ammonia contamination is observed.

We have also developed a model that predicts the transport and distribution of ammonium (formed upon reaction of ammonia with proton) and the impact of ammonium on the cell performance due to the apparent decrease in membrane proton conductivity. The model incorporates the Nernst-Planck equations to describe the multi-component cation transport through the membrane. With the model predictions, we are able to differentiate between the performance loss due to increased internal resistance and that due to the poisoning of the catalyst layers. Mechanisms of contamination of the polymer electrolyte and catalyst layers, and performance degradation of the PEFC are also postulated.

Figure 1 shows the performance of a PEFC with 25 cm² active area during contamination and recovery with 25 ppm NH₃. It is clearly visible that a trace amount of NH₃ in H₂ can cause a serious decay of the cell performance, which makes agreement with the findings before. [1-3] However, the cell internal resistance increase can only contribute little to the total performance loss. EIS performed during the contamination process shows that the electrodes might be seriously poisoned by NH₃ or NH₄⁺ (shown in Figure 2).

Contamination tests at non-running conditions were also performed to further elucidate the poisoning mechanism on the electrodes. In these tests, the anode was continuously fed with 25 ppm NH₃/H₂, and the cathode was fed with pure N₂. Cyclic voltammetry (CV) was used to characterize the changes in the cathode catalyst layer. Figure 3 shows that the hydrogen absorption peaks of the cathode greatly decreased during the contamination, which means that the catalyst surface may be covered by adsorbents, which decrease the electrochemical active area (ECA) of the cathode.

* Corresponding Author: ugur.pasaogullari@uconn.edu
Tel: +1 860 486-9441 Ph: +1 860 486-8378
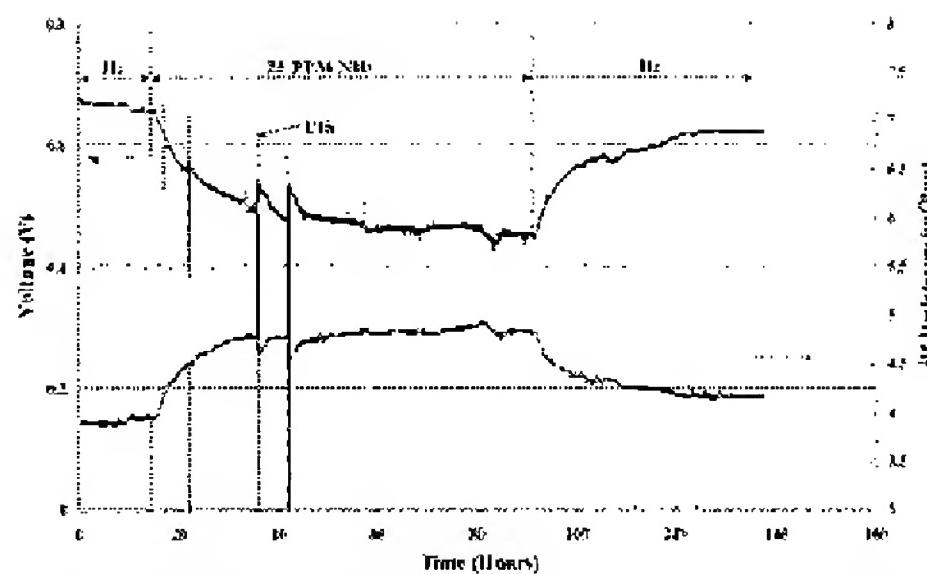
Figure 1. Contamination and recovery of a PEFC (25 cm² active area) with 25 ppm NH₃. The cell was running at 0.6 A/cm² at 52°C with dew point at 50°C. NH₃ was started at 18 hours and shut down at 94 hours, followed by pure H₂.
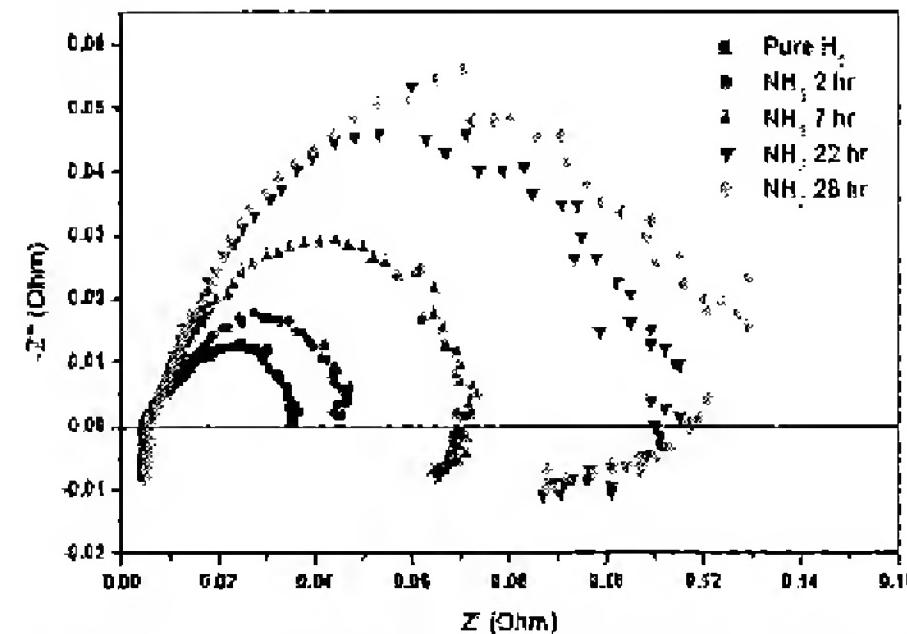

Figure 2 Electrochemical impedance spectroscopy performed during contamination with 25 ppm NH₃ (as shown in Figure 1). Sweep frequency: 10K-0.1 Hz.
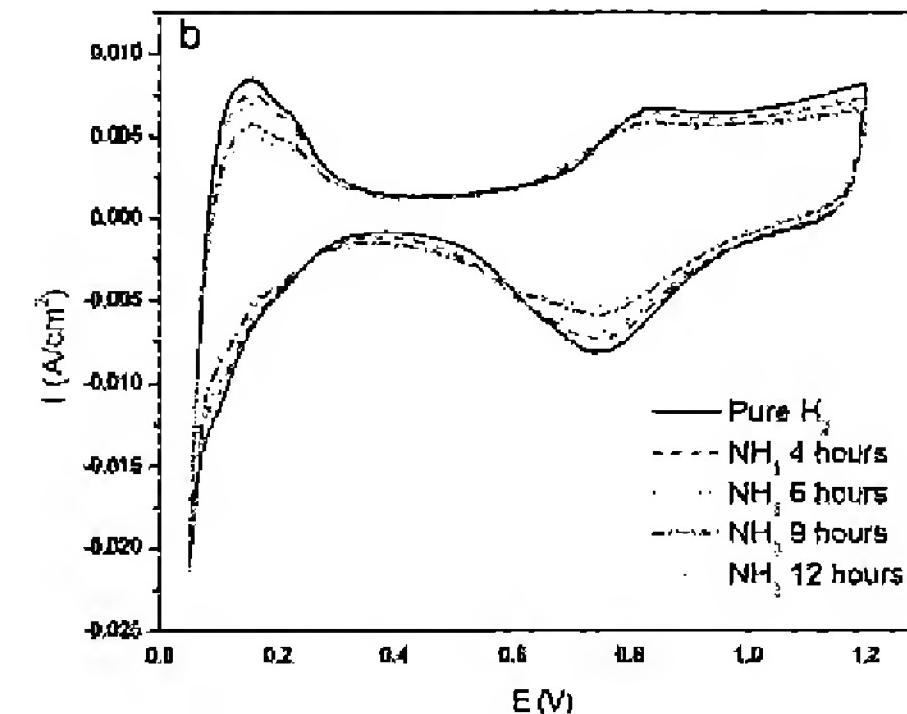

Figure 3 Cyclic voltammetry (CV) scans at 49% relative humidity. CVs were obtained with N₂ flowing at the cathode and H₂ or NH₃+H₂ at the anode. Cell was kept at 65°C and scan rate was 20 mV/sec.

REFERENCES

1. F. Uribe, S. Gottesfeld, and T. Zawodzinski, Jr., *J. Electrochem. Soc.*, **149**, A293 (2002)
2. H. Soto, W. Lee, J. Van Zee, and M. Murthy, *Electrochem. Solid-State Lett.*, **6**, A133 (2003)
3. R. Halseid, P. Vie, and R. Tunold, *J. Power Sources*, **154**, 343 (2006)

- Garzon, F.H. et al; *The impact of impurities on long term PEMFC performance*; presentation preprint for 216th ECS Meeting, Vienna Austria, (October 2009).

The Impact of Impurities On Long Term PEMFC Performance

Fernando H. Garzon[a],Thiago Lopes[a,b], Mark Nelson[a]
David Wood[a],Tommy Rockward[a], Rangachary
Mukundan[a], Thomas Springer[a], and Eric Brosha[a]
[a]Los Alamos National Laboratory
Los Alamos NM 87545/USA
[b]Instituto de Quimica de Sao Carlos
Universidade de Sao Paulo
Sao Carlos SP 13566-970/Brazil

Optimal PEMFC performance occurs when they are supplied with ultrapure hydrogen, air, and water. Fuel and air impurities such as common sulfur compounds, adsorb very strongly to the electrode surfaces blocking surface sites for catalytic splitting of diatomic hydrogen on the anode and diatomic oxygen on the cathode. The adsorption of some impurities is so strong that part per billion impurity levels can substantially degrade fuel cell performance. Unfortunately the cost of removing these common impurities rises rapidly with increasing purity requirements [1].

Another class of impurities is cationic impurities primarily arising from corrosion and salt aerosols from natural and anthropogenic sources [2]. These impurities such as sodium, magnesium and calcium form ions in the presence of water and ion exchange for mobile protons in the ionomer membrane. These foreign positively charged ions are more strongly bound to the membrane than protons and are recognized to impede proton transport.

The approach we use to understand impurity effects in fuel cells is threefold [3,4]. The first method is direct measurements of fuel cell performance subjected to controlled amounts of impurities directly introduced into the fuel cells. These measurements include the direct injection of sulfur compounds, carbon monoxide, nitrogen oxides, ammonia and salts into working fuel cells. After performance measurements are completed, the fuel cell materials are subsequently analyzed for trace quantities of impurities by various methods. The second method is the use of carefully designed experiments to measure the interactions of impurities on fuel cell components. An example of this is impurity permeation studies of hydrogen sulfide to measure gas crossover rates in the ionomer. These are important, as fuel cell cathodes may be poisoned by anode fuel impurities crossing over the membrane into the cathode compartment. The third method we use is the theoretical first principles modeling of impurity effects on the important physiochemical reactions required for fuel cell operation. An example of this approach is the modeling of the effect of a slowly diffusing cation impurity on fuel cell performance.

Past fuel cell experiments determined that hydrogen sulfide exposure lowered the fuel cell operation voltage for constant current operation. We performed hydrogen pump experiments to help determine the anode polarization losses for hydrogen sulfide exposure (0.5ppm, 1hr) at a given current density. Our results show that significant anode overpotentials ~75 mV at 1A/cm^2 occur after short-term hydrogen sulfide exposure. These anode overpotentials do not normally occur in standard fuel cell operation and result in fuel cell performance losses.

Our previous work has demonstrated that very small amounts of hydrogen sulfide can also affect the kinetically slower oxygen reduction reaction on Pt surfaces. As the membranes are highly permeable to water, hydrogen sulfide permeation is a possibility. Three types of transport mechanisms may occur; dry membrane permeation, copermeation with water, and electro-osmotic drag with the proton flux. We successfully measured the hydrogen sulfide crossover rate at differing relative humidities and membrane thicknesses. The permeation rate across wet membranes was many times greater than that for dry membranes [5].

Cation impurity behavior was successfully studied using fuel cell measurements, AC impedance spectroscopy, novel combined electrochemical/X-ray fluorescence spectroscopy cells and by electrochemical modeling. Cesium was chosen as a model cation as it is easily measured *in situ* by X-ray fluorescence spectroscopy and imaged using micro-X-ray tomography. Perfluorosulfonic acid membranes were partially ion exchanged with Cs and then subjected to a flux of protons. The concentration profile measured was in excellent agreement with the ion impurity model. The build up of foreign cations at the cathode effectively blocks access of protons to Pt cathode sites limiting the reaction current density. This affects fuel cell performance more than the loss in overall proton conductivity. The change in local ionomer water content may also degrade fuel cell performance in the mass transport dominated region.

References:

1- F. Garzon and F. Uribe, in *Handbook of Fuel Cells, Vol 5*, H. Gaistiger, Editor, J. Wiley and Sons, London, UK (2008).

2- B. S. Pivovar, B. L. Kienitz, T. Rockward, F. Uribe and F. Garzon, in *Handbook of Fuel Cells, Vol 5*, H. Gaistiger, Editor, J. Wiley and Sons, London (2008).

3- T. Rockward, I. G. Urdampilleta, F. A. Uribe, E. L. Brosha, B. S. Pivovar and F. H. Garzon, *ECS Transactions*, 11, 821 (2007).

4- I. G. Urdampilleta, F. A. Uribe, T. Rockward, E. L. Brosha, B. S. Pivovar and F. H. Garzon, *ECS Transactions*, 11, 831 (2007).

5- E. L. Brosha, T. Rockward, F. A. Uribe and F. H. Garzon, *ECS Transactions*, 16, 1205 (2008).

- *Fuel cell basics*; http://www.fctec.com/fctec_basics.asp (August 2009)

About the FC*Tec* | Fuel Cell Basics] Capabilities | Projects | Resource Center | What's New | Take a T

Home

View Our:

Types of Fuel Cells

How does it work?

History
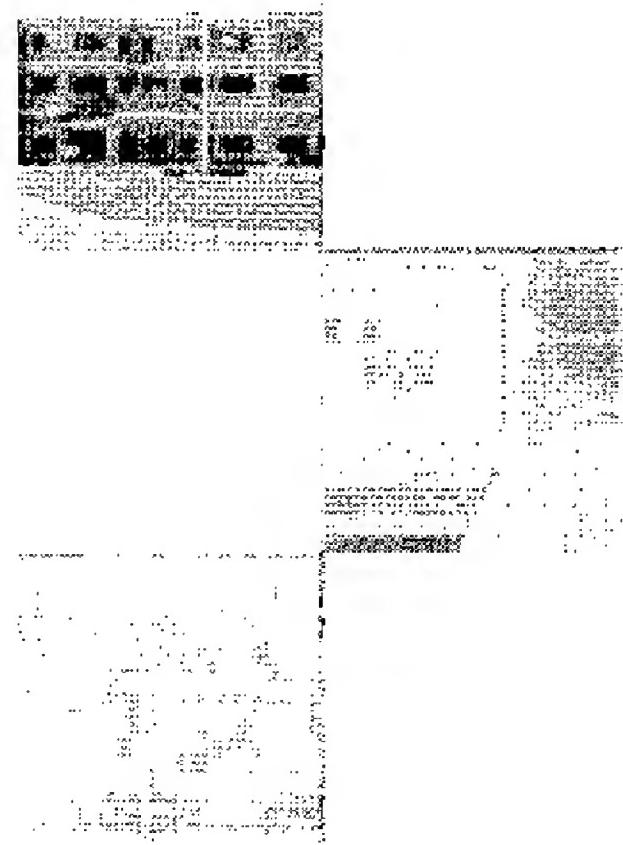
What is a fuel cell?

A fuel cell is a device that converts the chemical energy of a fuel (hydrog gas, methanol, gasoline, etc.) and an oxidant (air or oxygen) into electricit principle, a fuel cell operates like a battery. Unlike a battery however, a fu not run down or require recharging. It will produce electricity and heat as fuel and an oxidizer are supplied.

Both batteries and fuel cells are electrochemical devices. As such, both ha\ positively charged anode, a negatively charged cathode and an ion-conduct material called an electrolyte. Fuel cells are classified by their electrolyte n Electrochemical devices generate electricity without combustion of the fuel oxidizer, as opposed to what occurs with traditional methods of electricity

Fuel cell construction generally consists of a fuel electrode (anode) and an electrode (cathode) separated by an ion-conducting membrane. Oxygen pa one electrode, and hydrogen over the other, generating electricity, water a Fuel cells chemically combine the molecules of a fuel and oxidizer without having to dispense with the inefficiencies and pollution of traditional combu

Basic Characteristics

Some of the general characteristics of fuel cells have been introduced abo\ however, to understand the difference between types of fuel cells, several characteristics must be explained.

Charge Carrier

The *charge carrier* is the ion that passes through the electrolyte, and for s types of fuel cells, the charge carrier is a hydrogen ion, H+, which is simp proton. The charge carrier differs between different types of fuel cells.

Poisoning by Contamination

Fuel cells can be "poisoned" (experience severe degradation in performanc(different types of molecules. Because of the difference in electrolyte, opera temperature, catalyst and other factors, different molecules can behave dif different fuel cells. The major poison for all types of fuel cells is sulfur-con compounds such as hydrogen sulfide (H_2S) and carbonyl sulfide (COS). Su compounds are naturally present in all fossil fuels, and small quantities rer normal processing and must be almost completely removed prior to enterir cell.

Fuels

Hydrogen is the current fuel of choice for all fuel cells. Some gases, such from the air, have only a dilution effect on the performance of the fuel cel gases, such as CO and CH_4, have different effects on fuel cells, depending type of fuel cell. For example, CO is a poison to fuel cells operating at rel: temperatures, such as the Proton Exchange Membrane Fuel Cell (PEMFC).